TRANSDERMAL AND TRANSBUCCAL DRUG DELIVERY: ENHANCMENT USING IONTOPHORESIS AND CHEMICAL ENHANCERS

by

LONSHENG HU

A Dissertation submitted to the

Graduate School-New Brunswick

Rutgers, The State University of New Jersey

in partial fulfillment of the requirements

for the degree of

Doctor of Philosophy

Graduate Program in Pharmaceutical Science

written under the direction of

Bozena Michniak-Kohn

and approved by

_____

_____

_____

_____

New Brunswick, New Jersey

October, 2010

ABSTRACT OF THE DISSERTATION

TRANSDERMAL AND TRANSBUCCAL DRUG DELIVERY:

ENHANCMENT USING IONTOPHORESIS AND CHEMICAL ENHANCERS

By LONSHENG HU

Dissertation Director:
Professor Bozena Michniak-Kohn

Transdermal and transbuccal routes offer attractive alternatives for systemic delivery of drugs due to their distinct advantages: non-invasive, avoidance of first-pass effect, improved bioavailability and reduction of systemic side effects. However, only a few drugs have been successfully delivered into blood stream to reach therapeutic levels without causing notable skin irritation or damage. Transbuccal drug delivery systems are still at research stage. The major barriers to transdermal and transbuccal drug delivery are stratum corneum of skin and epithelium of buccal tissue. The objective of this work was to overcome these barriers to significantly enhance transdermal and transbuccal delivery of hydrophilic drugs without causing major damage to skin and buccal tissue. In this work, iontophoresis, chemical enhancers and their combination were investigated for their enhancement effects on transdermal and transbuccal delivery of hydrophilic drugs with different indications: lidocaine HCl (LHCl) for pain management, nicotine hydrogen tartrate (NHT) for smoking cessation, diltiazem HCl (DHCl) for anti-hypertension and ondansetron HCl (ODAN HCl) for anti-vomiting. Low toxic chemical enhancers used

were dodecyl 2-(*N*, *N*-dimethyl amino) propionate (DDAIP), its HCl salt dodecyl-2-(*N*, *N*-dimethylamino) propionate hydrochloride (DDAIP HCl), N-(4-bromobenzoyl)-*S*,*S*-dimethyliminosulfurane (Br-iminosulfurane). Their enhancement effects were evaluated using *in vitro* Franz cell diffusion model via porcine skin and buccal tissue. The results demonstrated that iontophoresis alone significantly enhanced transdermal and transbuccal delivery of LHCl, NHT, DHCl and ODAN HCl. DDAIP HCl alone significantly enhanced transbuccal delivery of these four drugs. DDAIP and Br-iminosulfurane significantly enhanced transdermal delivery of LHCl and ODAN HCl. Synergistic enhancement effects were observed on transdermal delivery of LHCl and NHT, ODAN HCl when using DDAIP or Br-iminosulfurane in combination with iontophoresis. A light microscopy, DSC and SEM studies showed that treatment with chemical enhancers and iontophoresis did not cause major morphological changes in the skin and buccal tissue. EpiOral™ MTS cytotoxicity study demonstrated that DDAIP HCl at less than 5% (w/v) in water did not have significant detrimental effects on buccal tissue. In conclusions, iontophoresis and chemical enhancer and their combined treatment are feasible approaches to enhance transdermal and transbuccal delivery of LHCl, NHT, DHCl and ODAN HCl.

DEDICATION:

To My Family

ACKNOWLEDGEMENTS

I would like to thank all people who have helped and inspired me during my doctoral study.

First of all, I would like to express my sincere gratitude to my advisor Dr. B. Michniak-Kohn for her enormous support throughout the entire period of my Ph. D study since Sept. of 2003. I am grateful that she gave me the opportunity to join her drug delivery lab to explore my scientific curiosity. Her technical guidance, unwavering commitment to research excellence played an integral role in the success of this project. I also thank my thesis committee members: Dr. Tamara Minko, Dr. Guofeng You and Dr. Nava Dayan for their insightful comments and suggestions for my research proposal. Without their support, it would be impossible for me to complete my research work.

I extend gratitude to my management at Pfizer and Johnson & Johnson: Josephine Minerva, Susan Wendling, Virginia Goldman and Dan Fagan for their encouragement and strong support throughout the entire period of my Ph. D study.

I acknowledge technical assistance and support from colleagues at Dr. Michniak-Kohn's Laboratory of Drug Delivery. Special thanks to Peter Zhang for his help with synthesizing Br-iminosulfurane and to Sergio Silva for assistance in running permeation studies and to Vishwas Rai for help with cell culture of human skin fibroblast and keratinocytes. Also I would like to express my thanks to Matthew Laughland and Dr. Sanjeeva Murphy at Dr. Joachim Kohn's instrumentation lab for their assistance with the use of Differential Scanning Calorimetric, Milijana Dukovic in Biomaterial Center of New Jersey, Hui Pung and Dr. Ah-Ng Tong Kong, College of Pharmacy, Rutgers

University for their administrative support. I also like extend my gratitude to Mr. Val Starovoytov at Division of Life Sciences, Electron Imaging Facility at Rutgers University for his technical assistance in taking SEM photos.

I would like to acknowledge Iomed, Inc. for their generosity to donate their PM series of Phoresor power devices for my research work. Special thanks go to Bob Hause at Iomed, Inc. for his technical support of how to use these devices.

I would also like to acknowledge Tara McNulty at UMDNJ and Lindsay Hodgson at Ethicon of Johnson & Johnson for their help to harvest porcine skin and buccal tissue. Without their help, it will probably take me many more years to complete this work. I am also very much thankful for the support and encouragement from my friends both in the US and back home in China: Yan Wang, Steve Wallace, Jinbai Young, Yan Liu, Mylene Enriquez, John Highton, Art Love, Norman Richardson, Zoe Paleocostas, Shongxi Fang and Fan Wang.

Most of all, I owe my deepest gratitude to my family closest to me: my lovely daughter Rebecca, my mother, brothers, sisters, nieces and nephews for their unconditional love and support throughout this long journey.

TABLE OF CONTENTS

4 *IN VITRO* TRANSDERMAL EXPERIMENTAL METHODOLOGY

5 *IN VITRO* TRANSBUCCAL EXPERIMENTAL METHODOLOGY

LIST OF TABLES

LIST OF FIGURES

LIST OF SYMBOLS AND ABBREVIATIONS

ANOVA - Analysis of variance

BR – Br-Iminosulfurane

CMC - Carboxymethyl Cellulose

CRM – Confocal Raman Microscropy

DDAIP – Dodecyl 2-(*N*,*N*-dimethyl amino) propionate (DDAIP)

DDAIP HCL – Dodecyl-2-(N,N-dimethylamino) propionate hydrochloride (DDAIP HCl)

DHCL – Diltiazem HCL

DSC - Differential scanning calorimetry

FDA - Food and Drug Administration

GRAS - Generally Recognized As Safe

HPLC – High Pressure Liquid Chromatography

LHCL – Lidocaine Hydrogen Chloride

NHT – Nicotine Hydrogen Tartrate

NRT – Nicotine Replacement Therapeutic

ODAN HCL – Ondansetron Hydogen Chloride

PBS - Phosphate buffered saline

PG – Propylene Glycol

Q_8 – Accumulated amount permeated within 8 hours

Q_{24} – Accumulated amount permeated within 24 hours

TEWL - Transepidermal Water Loss

TDDs - Ttransdermal Drug Delivery System

SC – Stratum Corneum

CHAPTER 1. INTRODUCTION

Transdermal drug delivery is a method of applying a drug to intact skin. The drug is absorbed continuously through the skin and enters the bloodstream. This route of drug administration has a long history dating back to the use of plasters and poultices and was most often used for drug delivery to local skin sites or directly underlying tissue. The development of mustard plaster or ointment, applied as a home remedy for severe chest congestion, may be considered one of the early example for transdermal delivery of medications [1]. The use of the mustard plant for medicinal purposes goes back several millennia. Mustard was used as both a condiment and medicine by the ancient Egyptians, Sumerians and Chinese. During the first century CE, the Romans combined ground mustard seed with vinegar to make an ointment for snakebites and scorpion stings and chewed the seed to relieve toothaches. Stronger Mercurial Ointment was perhaps the most amazing modern transdermal medication [1]. It was used as a treatment for syphilis when Salvarsan and other arsenicals were in use, before the discovery of penicillin. Stronger Mercurial Ointment was normally applied and rubbed into areas where the skin is thinnest: the groin and the bends of the elbows and knees.

Compared to other conventional routes of drug delivery such as oral, injection and inhaler, transdermal delivery has a variety of advantages. Transdermal systems are non-invasive, convenient, inexpensive and can be self-administered. They can provide sustained plasma concentration profile for long periods of time. The systems can greatly improve patient compliance through avoidance of first-past metabolism, improved bioavailability, reduction of systemic side effects and dosing schedule. In the past three decades, transdermal drug delivery has been developed to the stage where transdermal systems become a feasible way of delivering

clinically effective drugs particularly those drugs with significant first-pass effect of the liver that can prematurely metabolize drugs. The first prescription patch was approved by the U.S. Food and Drug Administration in December 1979. These patches administered scopolamine with indication for motion sickness [2]. At the beginning of 1992, the FDA approved nicotine patches for smoking prevention. Later transdermal patch products of nitroglycerin for angina, clondine for hypertension, and estradiol for estrogen deficiency were successfully commercialized. The worldwide transdermal market is currently exceeding more than 4 billion US $ and the annual US market for transdermal patches is more than 3 billion US $ [3]. However, in spite of the variety of advantages of transdermal delivery systems, there are some challenges to extend its application in more therapeutic areas [4,5,6,7]. Some of the greatest disadvantages to transdermal drug delivery are local irritation at the site of application, erythema, itching, and local edema caused by the drug, the adhesive, or other excipients in the patch formulation. So far only limited number of small molecules (Da <500) were able to be delivered into blood stream transdermally. Using buccal area to delivery ingredients systematically goes back to early 19th century. Sobrero first attempted use of buccal mucosa for drug absorption in 1847, the discoverer of nitroglycerin [8]. In the early 1880s, two brothers, Henry and Frank Fleer, began experimenting with chicle, the sticky substance found inside a sapodilla tree, and put together a recipe to make the world's first bubble gum, originally called "Blibber Blubber Bubble Gum." [9].

Similar to skin, buccal route offers another attractive alternative for systemic delivery of drugs. Buccal route drug delivery involves the administration of the desired drug through the buccal mucosal membrane. Unlike oral drug delivery, which presents a hostile environment for drugs, especially proteins and polypeptides, due to acid hydrolysis and the hepatic first-pass effect, the mucosal lining of buccal tissues provides a much milder environment for drug absorption. It is

richly vascularized and more accessible for the administration and removal of a dosage form. Avoidance of acid hydrolysis in the gastrointestinal (GI) tract and the first-pass effect in the liver are some of the advantages of this route of drug delivery. Moreover, a rapid onset of drug action, improved patient compliance and rapid cellular recovery are among the other advantages of this route of drug delivery [12,13]. The disadvantages associated with this route of drug delivery are the low permeability of the buccal membrane [14,15]. The total surface area of the buccal membrane available for drug absorption is about 50 cm^2. The continuous secretion of saliva (0.5–2 l/day) leads to subsequent dilution of the drug. Swallowing of saliva can also potentially lead to the loss of dissolved or suspended drug and, ultimately, the involuntary removal of the dosage form. These are some of the problems associated with buccal drug delivery. Moreover, the hazard of choking by involuntarily swallowing the delivery system is a concern, in addition to the inconvenience of such a dosage form when the patient is eating or drinking. Nevertheless, the advantages and recent progress in delivering a variety of compounds, specifically peptides and proteins, render the disadvantages of this route less significant. Fortunately, the enzyme activity in the buccal mucosa is relatively low compared to other mucosal routes. Furthermore, the buccal mucosa offers several advantages for controlled drug delivery for extended periods of time. The mucosa is well supplied with both vascular and lymphatic drainage and is well suited for a retentive device and appears to be acceptable to the patient. With the right dosage form design and formulation, the permeability and the local environment of the mucosa can be controlled and manipulated in order to accommodate drug permeation. Buccal drug delivery is a promising area for continued research with the aim of systemic delivery of orally inefficient drugs as well as a feasible and attractive alternative for non-invasive delivery of potent peptide and protein drug molecules. However, the need for safe and enhanced efficiency of buccal

permeation/absorption is a crucial component for a prospective future in the area of buccal drug delivery.

The major barriers to transdermal and transbuccal drug delivery are stratum corneum of skin and epithelium of buccal tissue. It remains a great challenge to enhance transdermal and transbuccal drug delivery without compromising safety concerns and expand their applications into wide therapeutic areas.

Over the years, different physical and chemical enhancement methods have been studied for enhancing transdermal and transbuccal delivery of hydrophilic and hydrophobic drugs. Typical physical enhancement methods include iontophoresis, electroporation, sonophoresis, stratum corneum ablation, microneedles. Chemical enhancement methods involve the use of various chemical enhancers such as organic solvents and surfactants, etc.. The objective of this work was to develop enhanced transdermal and transbuccal delivery systems for hydrophilic drugs: LHCl, NHT, DHCl and ODAN HCl without causing major damage to skin and buccal tissue using iontophoresis and chemical enhancer and their combined treatment.

To achieve this goal, it was important to understand biology of skin and buccal tissue. The structures and chemical compositions of skin and buccal tissue under normal physiological conditions are described in Chapter 2. A literature review of the historical perspectives, principles and mechanisms of transdermal and transbuccal drug delivery systems were performed in Chapter 2. Iontophoresis and chemical enhancer were two most studied methods to enhance transdermal and transbuccal drug delivery. However, their clinical application has been very limited. Chapter 2 discussed in details about these two enhancement methods: their characteristics and mechanism of action. Iontophoresis is a promising technique to deliver ionic compounds across the skin and buucal tissue with an applied electric current to overcome the

low permeability of skin and buccal tissue [10,11]. Enhancers offer several to more than a hundred times higher drug penetration in terms of the flux, depending on the properties of the penetrants and enhancers as well as the other additional ingredients of the formulations [12]. It is believed that some of the chemical enhancers can increase permeability of the SC and epithelium by acting as solvents to dissolve the skin and buccal lipid or to denature skin proteins. Their combination has demonstrated synergistic enhancement effect in transdermal drug delivery of sumatriptan and midodrine hydrochloride through human skin [13,14].

In this work, low toxic chemical enhancers used were dodecyl 2-(*N*, *N*-dimethyl amino) propionate (DDAIP), its HCl salt dodecyl-2-(*N, N*-dimethylamino) propionate hydrochloride (DDAIP HCl), N-(4-bromobenzoyl)-*S,S*-dimethyliminosulfurane (Br-iminosulfurane) [15,16]. Azone was chosen to be as a control. Iontophoresis at 0.1, 0.2 and 0.3 mA (<0.5 mA/cm^2) were selected to enhance transdermal and transbuccal drug delivery of LHCl, NHT, DHCl and ODAN HCl. Chapter 3 described the background information on the four selected hydrophilic drugs including rationales for selecting these drugs for transdermal and transbuccal delivery systems. Their physical and chemical properties, indications, pharmacokinetic, pharmacodynamic, and gel formulations were also discussed.

In this work, *in vitro* Franz cell diffusion model was used to evaluate effects of iontophoresis and chemical enhancer as well as their combination treatment on transdermal and transbuccal drug delivery through porcine skin and buccal tissue. In Chapter 4 and 5, the experimental methodologies for transdermal and transbuccal drug delivery were described. Evaluations of integrity of skin and buccal with and without treatments were performed using DSC, SEM and histological analysis. The results demonstrated that iontophoresis alone significantly enhanced transdermal and transbuccal delivery of LHCl, NHT, DHCl and ODAN HCl. DDAIP HCl alone

significantly enhanced transbuccal delivery of these four drugs. DDAIP and Br-iminosulfurane significantly enhanced transdermal delivery of LHCl and DHCl. Synergistic enhancement effects were observed on transdermal delivery of LHCl and NHT when using DDAIP or Br-iminosulfurane in combination with iontophoresis. A light microscopy, DSC and SEM studies showed that treatment with chemical enhancers and iontophoresis did not cause major morphological changes in the skin and buccal tissue. EpiOral™ MTS cytotoxicity study demonstrated that DDAIP HCl at less than 5% (w/v) in water did not have significant detrimental effects on buccal tissue. In conclusions, iontophoresis and chemical enhancer and their combined treatment are feasible approaches to enhance transdermal and transbuccal drug delivery and to potentially deliver the therapeutic levels of LHCl, NHT, DHCl and ODAN HCl. Iontophoresis was more effective in enhancing transdermal drug delivery and DDAIP HCl was more effective in enhancing transbuccal drug delivery.

In Chapter 6 described preparation of DHCl and ODAN HCl patch formulations incorporating DDAIP and DDAIP HCl for proof of concept purpose. Then enhancement effects of iontophoresis and chemical enhancers were evaluated using Franz diffusion cells via porcine skin and buccal. The results demonstrated that patch formulation was a viable option for both enhanced transdermal and transbuccal delivery systems of DHCl and ODAN HCl using either iontophoresis or chemical enhancer. Chapter 7 concluded that iontophoresis was a feasible approach to enhance both transdermal and transbuccal drug delivery. Iontophoresis was more effective in enhancing transdermal drug delivery than transbuccal drug delivery. Depending on drugs being delivered, chemical enhancers can be effective in enhancing transdermal and transbuccal drug delivery.

Chapter 2. BACKGROUND

2.1. Skin

Skin is the largest organ of the body with a significant surface area for application of drugs. It consists of several layers: the cellular outermost layer, epidermis, and the inner connective tissue layer, dermis. Lying between these two layers is the basal lamina or basement membrane zone (Figure 1).

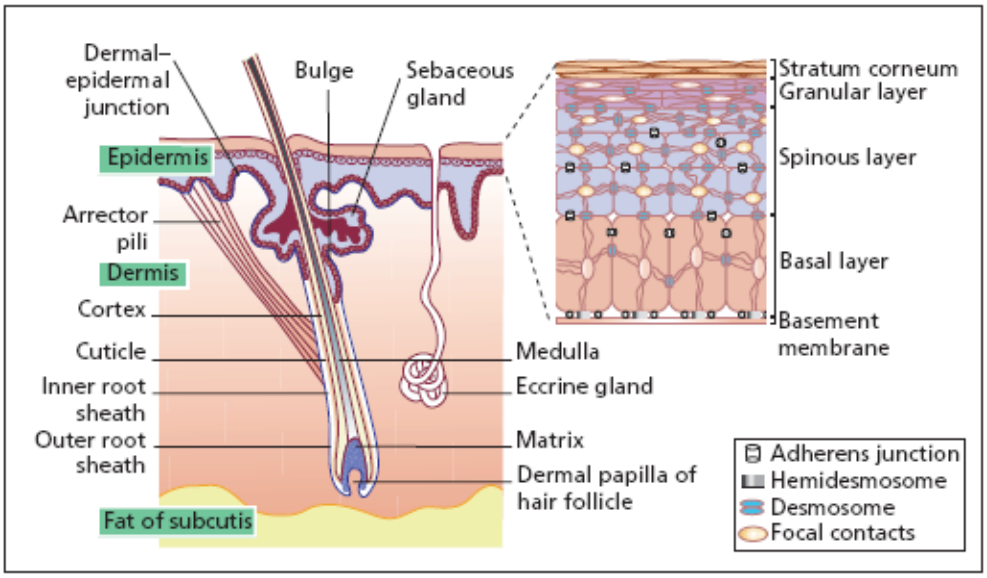

Figure 1. Schematic representation of the skin. Reproduced from reference [17].

The epidermis is composed of two parts: the living cells of the Malpighian layer and the dead cells of the stratum corneum commonly referred to as the “horny” layer. The viable cells of the epidermis move progressively upward though the skin from the basal layer to the top through a process of differentiation, eventually generating the barrier layer of the stratum corneum. The

epidermis is a continually self-differentiating, stratified squamous epithelium covering the entire outer surface of the body (Figure 1). Over most of the body the epidermis ranges in thickness from 0.06 to 0.1 mm [18]. The major cell of the epidermis is the keratinocyte and other important cellular elements include the melanocyte (the source of melanin pigment), the Langerhans cell (part of the immune system), and the Merkel cell functioning as a mechanoceptor for the sensation of touch [18]. The stratum corneum is the final product of epidermal differentiation and consists of 10 to 25 compressed cell layers with 10 to 25 μm in thickness [19]. The dead corneocyte is the largest cell in the stratum corneum, approximately 0.5 μm in thickness and 20 to 40 μm in width [20]. It contains no organelles but is filled with protein, 80% of which is high molecular-weight keratin. The intercellular space is majorily composed of lipids organized into multiple bilayers and these lipids are of a unique composition. Approximately 14 % of the stratum corneum (SC), by weight, is lipids. In addition, this layer has very low water content of about 7% [21]. Formation of the stratum corneum is also accompanied by the deposition of a 15 nm thick band of protein on the inner surface of the plasma membrane, the cornified cell envelope, a structure unique to keratinocytes [20]. The natural function of the skin is to protect the body against exogenous material, dehydration, and environmental stress. The major barrier against inward and outward diffusion of compounds is the outermost layer of the skin, SC. SC consists of lipid-depleted and keratinized cells (corneocytes) embedded in a lamellar lipid-rich interstitium. Unique lipid arrangements within the SC are mainly responsible for establishing the barrier function and maintaining cohesion between corneocytes. These lipids are extruded into the intercellular spaces where it undergoes enzymatic processing to produce a lipid mixture consisting of 41% ceramides, 27% cholesterol, 10% cholesteryl esters, and 9% fatty acids [22]. These are the main lipid components of SC. The minor lipid components are polar lipids:

glucosylceramides and cholesterol sulfate. The lipid bilayer containing these components greatly reduces skin permeability [23,24,25,26]. The functions of these important lipids in SC are discussed as follows:

Ceramides: SC ceramides located in the intercellular spaces form the ordered structures of bilayers with cholesterol, free fatty acids, and cholesterol sulfate. These ceramides represent a unique, heterogeneous group of at least six ceramides (CER(1–6)). They differ from each other mostly by the head group architecture and by the mean fatty acid chain length (Figure 2). The fatty acid chain length varies from 16 C atoms in CER 5 to C30–C34 atoms in CER 1. CER 1, a ceramide contains linoleic acid linked to the long chain (C30) *v*-hydroxy fatty acid and is critical for proper SC barrier function [27]. Ceramide 2 contains normal mostly 24-, 26- and 28-carbon fatty acidsamide-linked to sphingosine and dihydrosphingosine bases. The bases range from 16 through 20 carbons in length. Ceramide 3 contains the same normal fatty acids found in ceramide 2, but the base component is a phytosphingosine. Ceramides 4 and 5 both consist of a-hydroxyacidsamide-linked to sphingosine and dihydrosphingosine bases. The more mobile ceramide 4 contains mainly 24- through 28-carbon a-hydroxyacids, whereas ceramide 5 contains almost exclusively a-hydroxypalmiticacid. The most polar ceramide, found in fraction 6, ceramide 6 consists of a-hydroxyacids amide-linked to phytosphingosines [28]. The differences in chemical structure of the ceramides are assumed to be important for the characterisitic organization of SC lipids [29]. Therefore, ceramides play an essential role in structuring and maintaining the water permeability barrier function of the skin. They form highly ordered structures with other stratum corneum lipids. An essential factor is the physical state of the lipid chains in the nonpolar regions of the bilayers. The stratum corneum intercellular lipid lamellae,

the aliphatic chains in the ceramides and the fatty acids are mostly straight long-chain saturated compounds with a high melting point and a small polar head group.

Cholesterol: Cholesterol is a ubiquitous membrane lipid. The role of cholesterol in the epidermal barrier is probably to provide a degree of fluidity to what could otherwise be a rigid, possibly brittle membrane system. i.e., cholesterol can regulate the mobility of hydrocarbon chains of natural SC lipid bilayer, which is primarily responsible for SC barrier properties [28].

Cholesteryl esters:

Free fatty acids: Fatty acids are substrates for the formation of sphingolipids which are important constituents of the stratum corneum permeability barrier and cutaneous antimicrobial defense [30]. Fatty acids are derived from phospholipase-mediated hydrolysis of phospholipids during cornification [30].

Acylglucosylceramide: Acylglucosylceramide associated with the internal lamellae of the lamellar granules undergoes deglycosylation when it is extruded into the intercellular space and passes into the stratum corneum as acylceramide. It has been suggested that the acylceramide plays a major role in determining the state of organization of the intercellular lamellae [31].

Cholesterol sulfate: Cholesterol sulfate plays an important role in the desquamation process of SC. It increases the stability of the lamellar phases in the deeper layers of the SC due to its capacity to enhance the solubility of cholesterol in the lamellar phases of SC. Meanwhile, its absence in the superficial layers of SC might destabilize the lipid lamellae and therefore facilitate the desquamation process [32].

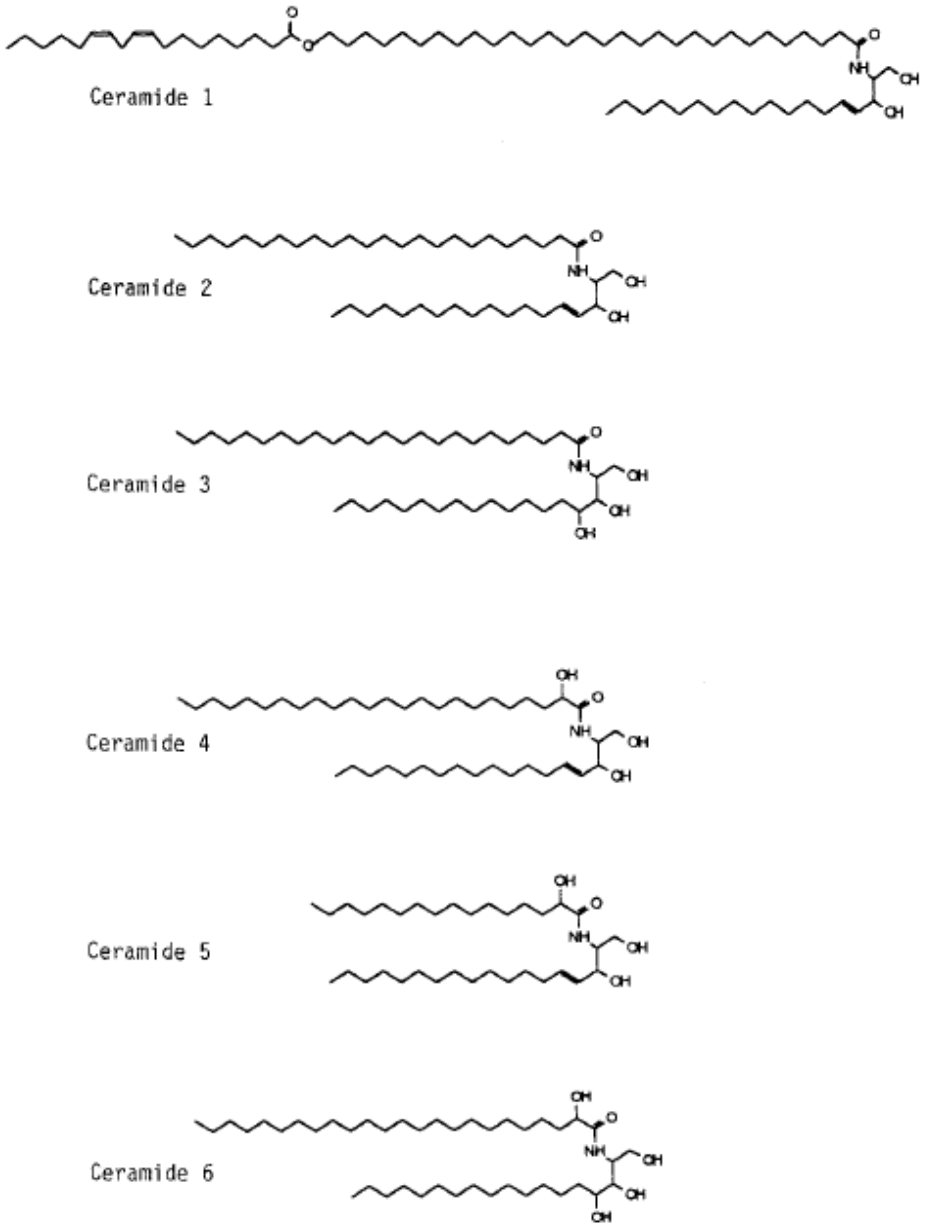

Figure 2. The molecular structures of pig ceramides published by Wertz and Downing [33].

It is well documented that pig skin has similar physiological and anatomical characteristics of human skin [34,35,36,37,38]. Comparative studies designed to predict skin permeation in man concluded that similar permeation values were obtained between pig and human skin when tested under identical conditions in vitro [39]. It was also noted that the morphology of the epidermis and upper dermis vasculature in the pig was similar to that in man and functions of the endothelial cell, such as plasminogen activator, were also similar [40]. Investigation of the synthesis and turnover of membrane glycoconjugates in pig and human epidermal cells suggested that the results for human epidermal cells closely matched those for pig epidermal cells, indicating that pig cells can be used as a model for human cells [34]. Pig skin is much more accessible than human skin. Therefore, in this study, pig skin was used in place of human skin.

2.2. Buccal Mucosa

Buccal mucosa refers to the mucous membrane tissues located on the inside of the cheek (Figure 1). It contains non-keratinized stratified squamous epithelium, basement membrane, lamina propria and the submucosa as the innermost layer [41]. The epithelium advances through a number of differentiating intermediate layers to the superficial layers, where cells are shed from the surface of the epithelium. The epithelium of the buccal mucosa is about 40-50 cell layers with thicknesss of 200-400 μm [42]. The combination of the lamina propria and submucosa is also referred to as the connective tissue [43].

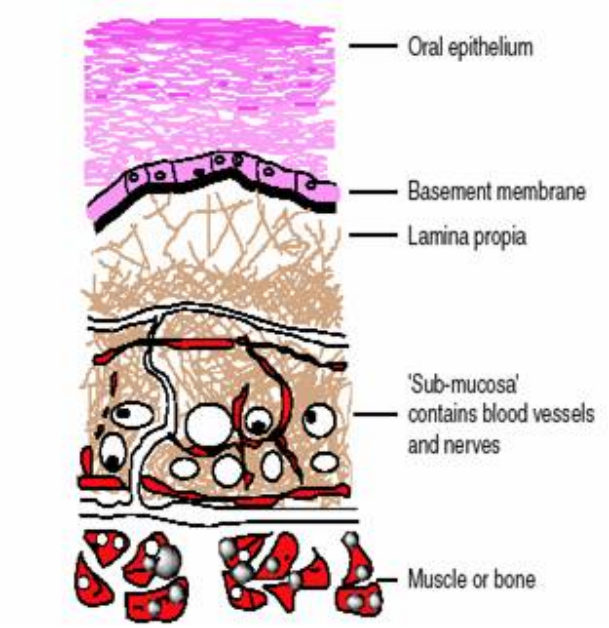

Figure 3. Structure of the oral mucosa [43]

The epithelial cells increase in size and become flatter as they migrate from the basal to the superficial layers. The turnover time for the buccal epithelium has been estimated at 5-6 days [41]. The thickness of buccal mucosa measures at 500-800 μm. The mucosa of areas subject to mechanical stress (the gingival and hard palate) is keratinized similar to the epidermis of the skin. The mucosa of the soft palate, the sublingual, and the buccal regions are not keratinized. The keratinized epithelia contain neutral lipids such as ceramides and acylceramides which have been associated with the barrier function. These epithelia are relatively impermeable to water. In contrast, non-keratinized epithelia, such as the floor of the mouth and the buccal epithelia do not contain acylceramides and only have small amounts of ceramide. Buccal epithelia contain small amounts of neutral but polar lipids, mainly cholesterol sulfate and glucosylceramides (Table 1). The permeability of the buccal mucosa is estimated to be 4-4000 times greater than that of the

skin [44,45]. The buccal mucosa does not have the intercellular lamellar bilayer structure to the same extent found in the stratum corneum of the skin. The intercellular lipids provide the physical barrier properties of the buccal mucosa because the extraction of these lipids has been shown to result in a highly permeable tissue [46,47]. The most abundant lipids from the superficial barrier region of porcine buccal epithelium are phospholipids, cholesterol and glycolipids; however, there are also small proportions of ceramide and saturated fatty acids [33,46]. Since the plasma membrane and internal organelles survive to the surface in buccal epithelium, these membranous structures may account for the bulk of the lipids present in this epithelial region. These intercellular lamellae are composed of ceramides, saturated fatty acids and cholesterol. This is similar to the lipid mixture that comprises the intercellular lamellae of epidermal stratum corneum [33]. These lipids could form highly ordered gel phase membrane domains that could provide barrier properties for buccal tissue. There are essentially no differences between human and pig buccal mucosa in terms of lipid content and composition, membrane morphology and permeability barrier function [33,47,48]. Therefore, porcine buccal mucosa was selected for this *in vitro* permeation study. In this work, since porcine skin was selected for transdermal permeability study, the comparison between transdermal and transbuccal drug delivery was also conducted using porcine skin vs porcine buccal tissue.

Table 1. Water permeability and lipid content of porcine skin and oral mucosa [33]

	Skin	Gingiva	Palate	Buccal Mucosa	Floor of Mouth
Water Permeability K_p x 10^{-7}	62±5 [a]	364±18 [a]	412±27 [a]	634±19 [a]	808±523 [a]
Epidermal/epithelial lipid content mg/g tissue (±SEM)					
Sphingomyelin	9.5±0.30	6.2±0.48	5.7±0.83	9.6±0.38	10.7±0.35
Phosphatidylcholine	16.7±1.58	12.5±1.05	16.2±1.85	14.0±0.80	24.1±1.47
Phosphatidylserine	1.1±0.83	1.1±0.83	16.2±1.85	14.0±0.80	24.1±1.47
Phosphatidylinositol	2.1±0.26	0.8±0.15	1.1±0.81	1.6±0.19	2.1±0.26
Phosphatidylethanolamine	8.4±0.38	6.4±0.95	6.9±0.98	14.9±0.57	19.5±0.45
Total phospholipids	37.8	27.0	30.5	42.7	57.6
Cholesterol sulphate	1.1±0.15	3.0±0.07	1.3±0.15	8.8±0.35	4.2±0.61
Glycosylceramides	3.6±0.45	1.4±0.15	1.4±0.19	18.4±0.88	7.5±0.30
Acylglucosylceramide	4.9±0.60	1.4±0.17	2.2±0.26	0	0
Total glycosylceramides	8.5	2.8	3.6	18.4	7.5
Ceramides[b]	25.3	4.8	2.7	0.9	1.0
Cholesterol	24.4±1.47	14.1±0.85	26.2±1.32	15.1±0.59	25.4±1.32
Fatty acids	21.2±1.07	3.3±0.45	1.0±0.7	1.8±0.11	0.8±0.15
Cholesterol esters	4.1±0.45	0.7±0.15	0.2±0.04	6.6±0.71	19.5±0.41
Triglycerides	38.7±1.39	11.4±0.32	12.4±1.02	17.6±0.87	14.5±0.57
Hydrocarbons	2.5±0.87	1.3±0.15	0	1.0±0.18	0.8±0.18
Total nonpolar lipids	49.7	18.1	27.4	23.5	45.7
Total lipids	122.4	55.1	65.5	94.3	116.0

a – All values significantly different ($p<0.05$) from one another except for gingival and palate.

b – Ceramides represent the sum of several chromatographically distinct ceramide types previously identified in porcine epidermis.

2.3. Transdermal Drug Delivery Systems

Transdermal delivery of drugs serves to circumvent the degradation of drugs in the gastrointestinal (GI) tract and their subsequent metabolism due to hepatic first pass effects. It also allows controlled drug delivery to the target tissues, thereby reducing the potential adverse effects. The skin is a multilayered organ, and the outermost layer, the stratum corneum is the rate limiting step to drug permeation as it hosts dead protein-filled corneocytes intercalated by a complex lipid structure that together form a strong permeation barrier. This permeation barrier provided by the stratum corneum effectively regulates transepidermal water loss and maintains homeostasis, but greatly limits the range and the type of molecules that can be therapeutically delivered by the otherwise accessible and large surface area of the skin. This resulted in only a small number of drugs commercially available using transdermal systems with limited daily drug dosage to about 10 mg via an acceptable sized patch. Moreover, transdermal drug delivery is not suited to all drugs. Currently most of drugs transdermally administered have been small in molecular weight (≤500 Da), highly lipophilic and require small dosages (Table 2).

Table 2. Formulation considerations for passive transdermal delivery and ideal limits [5]

Aqueous solubility	> 1 mg / ml
Lipophilicity	10 < Ko/w < 1000
Molecular weight	< 500 Da
Melting point	< 200 ^{o}C
pH of saturated aqueous solution	pH = 5 - 9
Dose deliverable	< 10 mg / day

Abbreviation: Ko/w, oil–water partition coefficient.

It has been even more challenge to exploit the transdermal route to deliver hydrophilic drugs and large molecules such as peptides and macromolecules into blood circulations, including new genetic treatment of DNA or small-interfering RNA (siRNA). So far FDA only approved eighteen - small active agents (Table 3): scopolamine, nitroglycerin, clonidine, estradiol-norethindrone, fentanyl, nicotine, testosterone, ethinyl estradiolnorelgestromin, oxybutynin, 17-estradiol, lidocaine, lidocaine-epinephrine, estradiol-levonorgestrel, lidocaine-tetracaine, fentanyl HCl, methylphenidate, selegiline, rotigotine, and rivastigmine.

Table 3. Transdermal drugs approved by the US FDA[a] [49]

Approval year	Drug	Indication	Product Name	Marketing company
1979	Scopolamine	Motion sickness	Transderm-Scop	Novartis Consumer Health (Parsippany, NJ)
1981	Nitroglycerin	Angina pectoris	Transderm-Nitro	Novartis (East Hannover, NJ)
1984	Clonidine	Hypertension	Catapres-TTS	Boehringer Ingelheim (Ridgefield, CT)
1986	Estradiol	Menopausal symptoms	Estraderm	Novartis (East Hannover, NJ)
1990	Fentanyl	Chronic pain	Duragesic	Janssen Pharmaceutica (Titusville, NJ)
1991	nicotine	Smoking cessation	Nicoderm, Habitrol, ProStep	GlaxoSmithKline (Philadelphia, PA), Novartis Consumer Health (Parsippany, NJ) Elan (Gainesville, GA)
1993	Testosterone	Testosterone deficiency	Testoderm	Alza, Mountain View, CA
1995	Lidocaine/epinephrine (iontophoresis)	Local dermal analgesia	Iontocaine	Iomed (Salt Lake City, UT)
1998	Estradiol/norethidrone	Menopausal symptoms	Combipatch	Novartis (East Hannover, NJ)
1999	Lidocaine	Post-herpetic neuralgia pain	Lidoderm	Endo Pharmaceuticals (Chadds Ford, PA)
2001	Ethinyl estradiol/norelgestromin	Contraception	Ortho Evra	Ortho-McNeil Pharmaceutical (Raritan, NJ)
2003	Estradiol/levonorgestrel	Menopausal symptoms	Climara Pro	Bayer Healthcare Pharmaceuticals (Wayne, NJ)
2003	Oxybutynin	Overactive bladder	Oxytrol	Watson Pharma (Corona, CA)
2004	Lidocaine (ultrasound)	Local dermal anesthesia	SonoPrep	Echo Therapeutics (Franklin, MA)
2005	Lidocaine/tetracaine	Local dermal analgesia	Synera	Endo Pharmaceuticals (Chadds Ford, PA)
2006	Fentanyl HCl (iontophoresis)	Acute postoperative pain	Ionsys	Alza, Mountain View, CA
2006	Methylphenidate	Attention deficit hyperactivity disorder	Daytrana	Shire (Wayne, PA)
2006	Selegiline	Major depressive disorder	Emsam	Bristol-Myers Squibb (Princeton, NJ)
2007	Rotigotine	Parkinson's disease	Neupro	Schwarz Pharma (Mequon, WI)
2007	Rivastigmine	Dementia	Exelon	Novartis (East Hannover, NJ)

[a] This list includes transdermal patches and delivery systems approved by the FDA. Only the first approved product for a given drug or drug combination administered by a given delivery method is shown. Topical creams, ointments, gels and sprays are not included.

To develop enhanced transdermal drug delivery systems, it is critical to understand the pathways. In general, drug molecules in contact with the skin surface can penetrate by three potential pathways: through the sweat ducts, *via* the hair follicles and sebaceous glands (collectively called the shunt or appendageal route), or directly across the stratum corneum (Figure 4). The relative importance of the shunt or appendageal route versus transport across the stratum corneum has been debated by scientists over the years [50] and is further complicated by the lack of a suitable experimental model to permit separation of the three pathways. *In vitro* experiments tend to involve the use of hydrated skin or epidermal membranes so that appendages are closed by the swelling associated with hydration. A follicular shunt route was responsible for the presteady-state permeation of polar molecules and flux of large polar molecules or ions that have difficulty diffusing across the intact stratum corneum [50]. However it is generally accepted that as the appendages comprise a fractional area for permeation of approximately 0.1%, their contribution to steady state flux of most drugs is minimal [19]. This assumption has resulted in the majority of skin penetration enhancement techniques being focused on increasing transport across the stratum corneum rather than via the appendages. Exceptions are iontophoretic drug delivery which uses an electrical charge to drive molecules into the skin primarily via the shunt routes as they provide less electrical resistance, and vesicular delivery. In order to understand how the physicochemical properties of the diffusing drug and vehicle influence permeation across the stratum corneum and thereby optimize delivery, it is essential to determine the predominant route of drug permeation within the stratum corneum. Traditionally it was thought that hydrophilic

chemicals diffuse within the aqueous regions near the outer surface of intracellular keratin filaments (intracellular or transcellular route) whilst lipophilic chemicals diffuse through the lipid matrix between the filaments (intercellular route) (Figure 5). However, this is an oversimplification of the situation as each route cannot be viewed in isolation. A molecule traversing via the transcellular route must partition into and diffuse through the keratinocyte, but in order to move to the next keratinocyte, the molecule must partition into and diffuse through the estimated 4-20 lipid lamellae between each keratinocyte. This series of partitioning into and diffusing across multiple hydrophilic and hydrophobic domains is unfavourable for most drugs. Consequently, the intercellular route is now considered to be the major pathway for permeation of most drugs across the stratum corneum. As a result, the majority of techniques to optimize permeation of drugs across the skin are directed towards manipulation of solubility in the lipid domain or alteration of the ordered structure of this region [50].

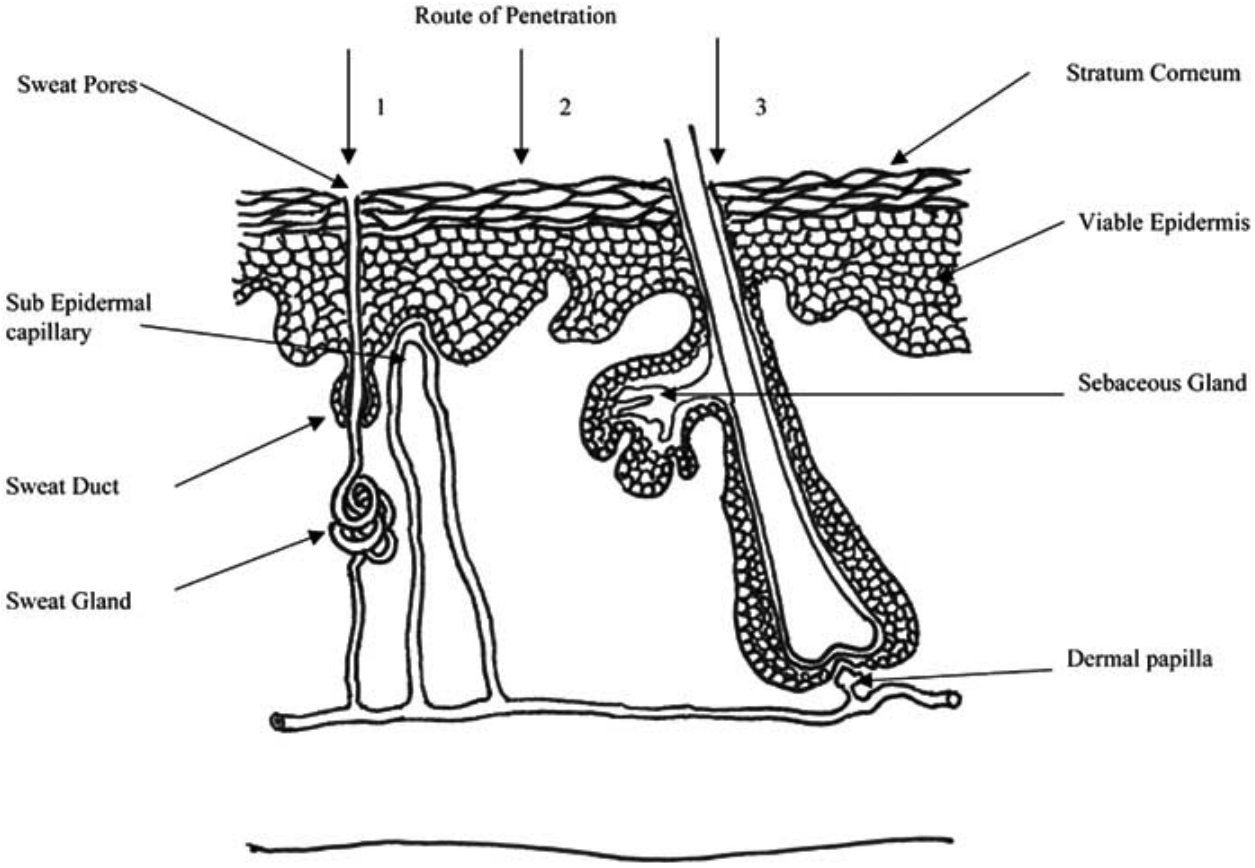

Figure 4. Simplified representation of skin showing routes of penetration: 1. through the sweat ducts; 2. directly across the stratum corneum; 3. via the hair follicles. [50].

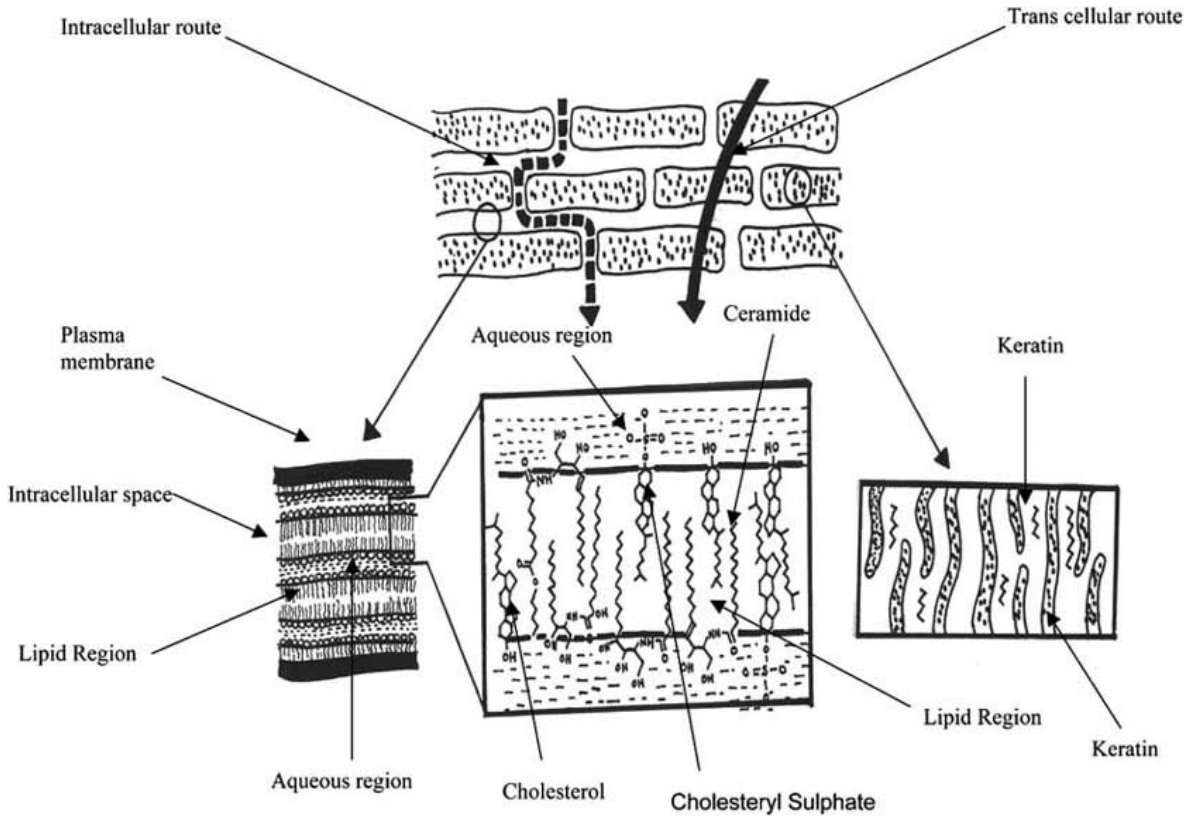

Figure 5. Diagrammatic representation of the stratum corneum and the intercellular and transcellular routes of penetration [50].

In order to extend the application of transdermal delivery to more agents encompassing different therapeutic areas, various penetration enhancement techniques have been investigated over the years. Several different strategies have been explored to increase permeability of the skin. Various physical and chemical enhancement methods or their combination have been investigated to enhance efficiency of transdermal drug delivery [51]. Physical methods include iontophoresis, electroporation, sonophoresis, stratum corneum ablation, microneedles. Chemical enhancement methods involve the use of various chemical enhancers such as organic solvents, surfactants, etc.. These techniques, broadly classified as chemical and physical enhancement

techniques, are reversible methods that aid to alter the skin barrier in order to increase the permeation of compounds through skin and achieve therapeutically effective concentrations in the tissues. Chemical enhancement methods have been widely studied and they work to increase the drug flux by one or a combination of the following mechanisms: i) disruption of the lipid structure in the stratum corneum, ii) opening up the dense protein structure in the corneocytes or iii) altering the chemical environment in the stratum corneum, thereby increasing the partitioning of a second active agent into skin. However, the type and amount of chemical enhancers that can be used in transdermal applications is restricted by their skin irritation potential. Physical enhancement methods constitute electrically assisted methods (iontophoresis, electroporation), mechanical methods (microneedles), velocity-based techniques such as jet-propulsion, or other methods such as ultrasound, laser and photomechanical waves [52,53]. Of the various enhancement methods, transdermal iontophoresis, which uses low level electric current (~0.5 mA/cm^2) to enhance the transdermal delivery of charged substances through skin, has been extensively studied in the past years and devices for drug delivery and for non-invasive blood monitoring have been developed and successfully commercialized**.** Iontophoresis has also demonstrated great value for delivery of macromolecules like proteins and peptides as it enhances their transdermal permeation while protecting them from the harsh proteolytic environments encountered with oral delivery [54,55,56].

In this thesis, iontophoresis, chemical enhancer and their combination treatment were investigated to enhance transdermal drug delivery of hydrophilic drugs. Also the impact of these treatments on the integrity of skin was evaluated.

2.4. Transbuccal Drug Delivery Systems

The oral mucosa in general is the epithelia intermediate between that of the epidermis and intestinal mucosa. The permeability barrier in the oral mucosa is believed to be the result of intercellular material derived from the so-called 'membrane coating granules'(MCG) [41]. MCGs start forming through cell differentiation and at the apical cell surfaces they fuse with the plasma membrane. Then their contents are pushed into the intercellular spaces at the upper layer of the epithelium. This barrier is present in the outermost 200 μm of the superficial layer. Permeation studies have been performed using a number of very large molecular weight tracers, such as horseradish peroxidase and lanthanum nitrate [57]. After being applied to the outer surface of the epithelium, these tracers penetrate only through outermost layer or two of cells. When applied to the submucosal surface, they permeate up to the top cell layers of the epithelium [57]. The MCGs of keratinized epithelium are composed of lamellar lipid stacks, whereas the non-keratinized epithelium contains MCGs that are non-lamellar [57]. While the basement membrane may present some resistance to permeation, the outer epithelium is considered to be the rate limiting step to mucosal penetration [58].

Compared to the sublingual mucosa, the buccal mucosa is a more preferred route for systemic transmucosal drug delivery [58]. There are two permeation pathways for passive drug transport across the oral mucosa: paracellular and transcellular routes [59]. Permeants can use these two routes simultaneously, but one route is usually preferred over the other depending on the physicochemical properties of the drug. Since the intercellular spaces and cytoplasm are hydrophilic in character, lipophilic compounds would have low solubilities in this environment. The cell membrane is lipophilic in nature and hydrophilic solutes will have difficulty permeating

through the cell membrane due to a low partition coefficient. Therefore, the intercellular space is the major barrier to permeation of lipophilic compounds and the cell membrane acts as the major transport barrier for hydrophilic compounds. Since the oral epithelium is stratified, solute permeation may involve a combination of these two routes.

Similar to any other mucosal membrane, the buccal mucosa as a site for drug delivery has limitations as well. One of the major disadvantages associated with buccal drug delivery is the low flux which results in low drug bioavailability. Various chemical enhancerss have been investigatedto increase the flux of drugs through the buccal mucosa [60].

Other than the low flux associated with buccal mucosal delivery, a major limitation of the buccal route of administration is the lack of dosage forms that can be retained at the site of absorption. Consequently, bioadhesive polymers have extensively been employed in buccal drug delivery systems [61]. Polymers which can adhere to either hard or soft tissue have been used for many years in surgery and dentistry [62]. Diverse classes of polymers have been investigated for their potential use as bioadhesive polymers / mucoadhesives. These include synthetic polymers such as monomeric a cyanoacrylate, polyacrylic acid, hydroxypropyl methylcellulose, and poly methacrylate derivatives as well as naturally occurring polymers such as hyaluronic acid and chitosan [63,64].

In general, dosage forms designed for buccal administration should not cause irritation and should be small and flexible enough to be accepted by the patient. These requirements can be met by using hydrogels.

Anders *et al*. [65] designed a bilayer patch (polytef-disk) consisting of protirelin for thyroid gland diagnosis. The patch had a backing layer of teflon and mucoadhesive layer of protirelin dispersed in hydroxyethylcellulose. Veillard *et al*. [66] designed a unidirectional buccal patch which consisted of three layers: an impermeable backing layer, a rate limiting center membrane containing the drug, and a mucoadhesive layer containing bioadhesive polymer polycarbophil. The bioadhesive polymer swells, creating a flexible network through which diffusion of drug takes place. This patch was tested in dog buccal mucosa and was shown to remain in place for up to 17 hours without any obvious discomfort.

Considering that in general buccal mucosa has higher permeability than skin, all substances administrated by transdermal iontophoresis may be potentially delivered by buccal iontophoresis. This type of electric enhancement in buccal delivery may be useful for local and also systemic drug delivery. The current density limitation may be more restrictive than for skin because buccal tissue is more sensitive to pain. The localization of the mucosa allows location of the electrodes set on the same surface or only the donor electrode may be positioned in a mouth and the acceptor one may be on the external side of cheek. This opposite location may increase the current efficiency of drug transfer. Giannola *et al.* [67] reported that iontophoresis at 2 mA/cm^2 enhanced permeation of naltrexone hydrochloride in a tablet formulation through buccal mucosa by 2-fold using human saliva as medium. Jacobsen [68] investigated the impact of current density on the in vitro buccal delivery of atenolol HCl using a three-chamber permeation cell. Their study found that as current density increased from 0.1, 0.2, 0.3, to 0.4 mA/cm^2 increased enhancement ratios of 6, 18, 36, and 58, respectively were recorded.

In this study, the enhancement effects of iontophoresis, chemical enhancers and their combined treatment on transbuccal drug delivery. Nonionized cellulose gum and hydroxymethyl propylecellulose were used to make hydrogel formulations of the tested drugs. The results were compared to that of transdermal drug delivery.

2.5. Iontophoretic Enhancement

2.5.1. History and Development of Iontophoresis

The history of iontophoresis has been detailed by Banga and Chien [69] and the concept of application of electric current to increase skin penetration is postulated to be described as early as the 1700s. One of the earliest and most well documented experiments in this field were however conducted by Ludec at the beginning of the 20th century where he demonstrated the importance of polarity when using direct current to administer strychnine and cyanide into two rabbits placed in series [70]. Though iontophoresis was significantly explored in the 1930s and 1940s, its use declined in the subsequent years. Nevertheless investigators investigated this technique for various applications such as sweat testing for diagnosis of cystic fibrosis (pilocarpine), hyperhidrosis (tap water, atropine), local anesthesia (lidocaine with epinephrine) and for ulcers (histamine, zinc oxide) [71]. Over the last decades iontophoresis has come to be used as a technique researched primarily for its use in delivery of charged ions and macromolecules through skin into the systemic circulation. A wide range of drugs such as propanolol hydrochloride [72] apomorphine [73,74], busiprone hydrochloride [75], insulin [55,76], thryrotropin releasing hormone [77], nafarelin and LHRH (luteinizing hormone-

releasing hormone) [56] have been investigated for their delivery potential by iontophoresis alone or in conjunction with other physical and chemical enhancement techniques [78].

2.5.2 Advantages and Limitations of Iontophoresis

Iontophoresis provides a non –invasive method for delivery of a wide variety of agents at therapeutically significant levels due to its enhancement effects on skin permeation. When used transdermally, it shares the benefits associated with transdermal drug administration, primarily the circumvention of the hepatic first pass effects and the harsh environment present in the gastrointestinal tract. These benefits are especially significant for the administration of proteins and peptides, which do not achieve therapeutically significant concentrations by the oral delivery route. Iontophoresis also allows the effective delivery of drugs with short biological half lives as it shortens the time frame from administration to delivery to the target tissues. Also, patient compliance is significantly improved due to infrequent dosing, and the treatment can be terminated when desired. This technique also enables a great degree of programmability as therapy can be monitored and tailored at pre-programmed rates that may be custom to the patient's condiction. This programmability in conjunction with the direct dependence of drug delivery to the applied current, results in significant reduction in the variability in the drug levels achieved.

Advantages of the iontophoresis technique are accompanied by limitations of the procedure, the most obvious being the potential for irritation and pain on application of the electric current. Although the technique is considered safe, increase in the intensity of applied current can lead to skin irritation, burning, blisters, necrosis and erythema [79,80]. In addition, iontophoresis is usually restricted to compounds that can be formulated in their ionic form. The design of the

system may further limit the range of molecules, as the effect of pH changes (from 4 to 7.3) encountered during transdermal transport may lead to ineffective iontophoresis for some molecules due to their effect on ionization. This phenomenon may be especially relevant for proteins and peptides where charge is an important factor in their delivery and stability. Effective iontophoretic transport of charged species may also be affected by an ion-competition factor due to the presence of other charged moieties. Also degradation or adsorption of drug under electrode has been a major concern. Lastly, the formulation of a device that is inexpensive, safe, convenient and ensures therapeutically relevant concentrations may be a challenge, although more devices today are nearing commercialization than before.

2.5.3 Iontophoretic delivery Principles and System components

Iontophoresis is based on the simple principle of any electrically based system, that is, like charges repel while opposite charges attract. A set of electrode systems is used to create these repulsive and attractive forces that provide the external energy to drive the ions through the skin leading to enhancement of drug permeation. These principles have led to the development of two types of primary systems: anodal and cathodal iontophoresis, both consisting of a basic iontophoretic setup with a set of electrodes (anode and cathode), drug and salt reservoirs and a current source. Thus positively charged ions can be delivered by placing them under the positive electrode (anode) creating repulsion and at the same time creating an attractive force by placing the negative electrode at a distal site on the skin. At the same time, negatively charged ions from the body (primarily Cl^-) move toward the anode. This system is called anodal iontophoresis, and a typical setup is illustrated in Figure 6. For cathodal iontophoresis, the electrodes are reversed so that a negatively charged drug is delivered through skin. Figure 1 illustrates a system that

comprises of silver-silver chloride (Ag/AgCl) electrodes, the most commonly used electrodes used till date in iontophoretic systems. The Ag^+ and Cl^- react at the anode-solution interface to form insoluble AgCl which is deposited at the electrode. In order to maintain electroneutrality, either a cation moves out of this compartment into the skin or an anion from the skin is taken up in this chamber. Similarly, in the cathodal compartment, reduction of the AgCl to Ag^+ at the electrode leads to release of a Cl^- ion into solution, which necessitates the uptake of a cation from the skin or loss of an anion from the chamber [81].

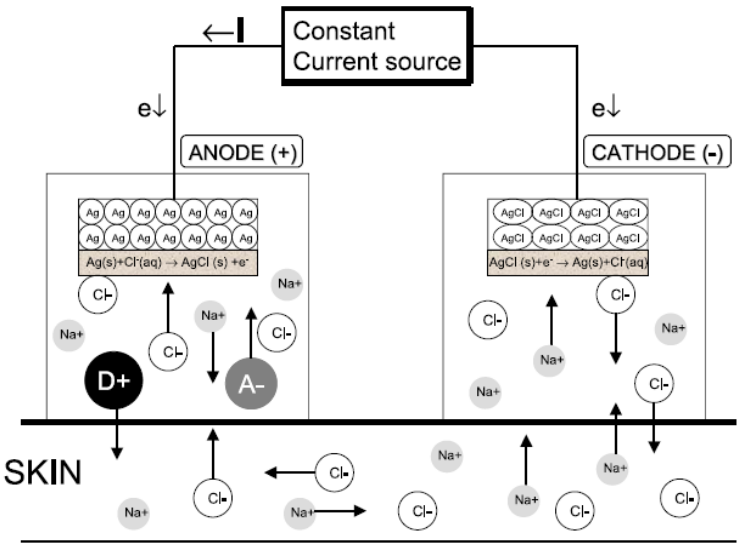

Figure 6: Basic setup of an iontophoretic system using a Ag/AgCl electrode [81].

On application of an electric current, the ionizable drug (D^+) is transported from the anodal compartment into the skin, while endogenous ions such as Cl^- move out of the skin. In the

cathodal compartment, the AgCl electrode releases Cl^- ions into the compartment, which may transport into the skin, or a cation may be transported into the chamber from the skin [81]. Several reasons make the Ag-AgCl system the most preferred electrode system. First, this pair of electrodes resists changes in pH, one of the primary requirements in the efficiency of iontophoresis. Since the AgCl/Cl pair are reversible electrodes, the electrochemical reactions that occur do so at voltages that are lower than those required for electrolysis of water, preventing pH changes and increasing the drug delivery efficiency. A reusable iontophoresis electrode device was invented to avoid release of metal from electrode into the body. It also claims no change in pH and any fluctuation in voltage/current during operation. This electrode component can include one of said depolarizers (potassium iodide, sodium sulfite, thioglycolicacid, ascorbic acid, etc.), pH regulators (calcium oxide, zeolite, hydroxyapatie, etc.) and water as electrolyte without generation of oxygen.

2.5.4 Drug Transport in Iontophoresis

A large portion of iontophoretic permeation enhancement occurs due to the effect of the applied electric current on the migration of charged molecules across the skin, a phenomenon called electromigration or electrorepulsion. The applied electric current also gives rise to a water transport phenomenon, called electroosmosis, which also contributes to iontophoretic transport of molecules. While electrorepulsion occurs due to repulsion of similarly charged molecules, electroosmosis is a facet of the cation permselectivity that occurs as a result of the net negative charge on the skin at physiological pH (7.4) [79]. This cation permselectivity can facilitate cation transport, present an electrostatic barrier to anion transport and enhance the transport of neutral or polar solutes. This results in a net volume flow, called electroosmosis, in the direction of

movement of the positive ions, and neutral molecules, such as water can be transported by this process. Electroosmostic flow is favored in the anode to cathode direction while catholic delivery is retarded.

Iontophoretic transport is primarily driven by electrorepulsion and electroosmosis, and to a smaller extent by passive diffusion. Thus the total iontophoretic flux, J Total [82] can be described as:

J Total = Je + Jc + Jp (1)

Where Je = flux contribution due to electrorepulsion, Jc= flux contribution due to electroosmosis and Jp= flux contribution due to passive diffusion

It has been considered that in all practical iontophoretic applications, Jp will form a negligible fraction of J Total with the contribution becoming even smaller with increasing molecular weight of agents.

$$J_e = \left(\frac{1}{Z_X F}\right)\frac{z_X u_X c_X}{\sum_{n=0}^{i} z_i u_i c_i} I_D \qquad (2)$$

where z_X, u_X and c_X refer to the charge, mobility and concentration of the drug in the membrane, respectively, F is the Faraday's constant and I_D is the applied current density, while the denominator is a summation of the products of the charge, mobility and the concentration for each ion in the system.

$$J_c = vC_X \qquad (3)$$

where Cx is the concentration of the compound and v is the electroosmotic solvent velocity. While the quantification of the contributions of each of these processes is difficult, it has been suggested that electrorepulsion enhances the transport of small cations such as Na^+ and then falls off sharply with increasing molecular weight of the species, and electroosmosis becomes the

more dominant mechanism, especially with bulkier cations of higher molecular weights (≥ 1000 daltons) [82,83]. Similarly, for anions, there will be a point where the increase in molecular weight will lead to the effects of electrorepulsion and electroosmosis cancelling out and the cathodal delivery will cease to be efficient.

The contribution that each component makes to the total flux is depends on several factors such as the physiochemical properties of the permeant including the degree and type of charge, the properties of the solution and the properties of the membrane. Merino et al [84] measured the *in vitro* iontophoretic delivery of a small negatively chargeable compound 5-fluorouracil (5-FU, pKa~8) through excised porcine skin as a function of the pH of the solutions in contact with both sides of the skin. They found that at pH of 8.5, when 5-FU was predominantly negatively charged, the electrorepulsive transport (cathode to anode) overwhelmed the electroosmotic convective flux in the opposite direction. At pH of 3, when 5-FU was almost completely unionized and the skin carried a net positive charge, the transport was primarily electroosmostic and was higher in the cathode to anode direction, while at pH 4, the anodal and the cathodal fluxes were equal due to neutralization of the skin at this pH (skin PI~ 4). However at pH 7.4, about 25% of 5-FU was ionized and the cathodal electrorepulsive forces carrying the ionized compound were about equal to the electroosmostic flow which carried the uncharged species in the opposite anodal direction. Just as they influence the mechanism of iontophoretic transport, the properties of the drug and the vehicle also influence the route of penetration in iontophoretic drug delivery [85] and the effect of these factors on the iontophoretic flux and the permeation routes will be discussed in the following sections.

2.5.5 Pathways for Iontophoretic Transport

There are three primary routes of passive skin permeation are transcellular, paracellular or transappendageal pathway (Figure 5). Iontophoretic transport is said to occur primarily through the transappeandageal (shunt pathway) and the paracellular route, however the appendageal pores such as the hair follicles and the sweat glands are most efficient in iontophoresis and major transport occurs through this route [86,87]. The dominance of this transappendageal iontophoretic transport has been determined by several techniques such as vibrating probe electrodes and visualization techniques such as transmission electron microscopy (use of mercuric chloride) and laser confocal microscopy [86,87]. Iontophoresis can also enhance skin delivery by a potential-dependant pore formation in the stratum corneum attributed to a "flip flop" gating mechanism that occurs due to the restructuring of the polypeptide helices on application of electric current. Though iontophoretic transport is capable of producing a 100 fold enhancement relative to passive diffusion (for a cation having a relative molecular size equal to unity), the efficiency of iontophoretic transport is frequently below 100% due to several variables influencing the transport efficiency, predominantly the properties of the permeant, the vehicle and other formulation factors, the membrane and components of the system.

2.5.6 Factors Affecting Iontophoretic Transport

Properties of the drug/ion: concentration, competing ions and molecular size

Increase in drug concentration has resulted in an increase in iontophoretic flux in various studies conducted, though the concentration-flux profile often shows a curvilinear pattern and plateaus off as the concentration is further increased. Van der geest, *et al*., [73] demonstrated a plateau in the flux profile during the iontophoretic delivery of apomorphine through human stratum

corneum, a factor of attainment of maximum solubility concentration of apomorphine in the donor and a postulated skin resistance caused by increasing concentrations of apomorphine. The effect of drug concentration on the flux is also negatively influenced by the presence of competing ions, either co-ions (same charge) or counter-ions (opposite charge) from the formulation itself, from the presence of a buffer added to maintain pH or from endogenous ions. This competition from other ions results in reduction of the transport number of the primary drug ion, especially if the competing ions are more mobile, such as those present in buffers [88]. Another important constituent in determination of iontophoretic flux is the molecular size of the permeant, where a decrease in the permeability coefficients with increasing molecular size has been established for positively charged, negatively charged and for uncharged solutes. This phenomenon is also complicated by the contribution of electroosmosis to the iontophoretic flux with increasing size of the molecules.

Properties of the Tontophoretic System: pH and Current

pH plays a very critical role in iontophoresis and functions to keep a large proportion of the drug in its ionized form. The importance of pH in the efficiency of iontophoretic transport has been clearly demonstrated in several studies. Siddiqui, *et al*., [89] showed that the passive diffusion flux of lignocaine was highest and iontophoretic flux low when it was in the unionized form. However at pH values of 5.2 and 3.4 where the drug is increasingly ionized, the iontophoretic flux increased by 4 and 8.5 times respectively relative to that occurring without iontophoresis. pH also plays an important role in the iontophoretic delivery of proteins and peptides, as it can control the net charge on these molecules based on their isoelectric points. In addition, the pH of

the membrane (skin) also regulates the flux as it determines the electromigration and electroosmotic contributions to the flux.

Iontophoretic flux has shown direct dependence on the strength of the applied current, with the flux values increasing linearly for several compounds such as lithium, verapamil [90], apomorphine [73], methylphenidate HCl [91], Thyrotropin Releasing Hormone (TRH) [77] with increases in current density. The application of higher current densities is however limited by a saturation phenomenon observed with higher current and also by the concern for causing skin discomfort and irritation [92]. Cazares-Delgadillo, *et al*., [93] used constant current iontophoresis for transdermal delivery of cytochrome C across porcine skin. While studying the impact of increasing current density from 0.15 to 0.5 mA/cm^2, they found that although the flux increased linearly with the applied current at lower current densities, the flux values of cytochrome C at 0.3 and 0.5 mA/cm^2 were not statistically different, probably due to a saturation phenomenon observed after a limiting transport number is achieved. Typically no more than 0.5 mA/cm^2 is recommended to be the current intensity level for human tolerance [90].

Iontophoretic devices employ either constant or pulsed current systems and both systems have been used with success in *in vitro* and *in vivo* transdermal studies [93,94]. Though comparisons have been made, the advantage of one type of current profile over the other has not been confirmed. Pulsed direct current profile was shown to be more efficient in transporting LHRH and Nafarelin across the human epidermis as compared to constant direct current (dc) and alternating current (ac). On the other hand, Tiwari, *et al*. [78] found constant direct current to be more effective than pulsed current for the transdermal permeation of ketorolac through rat skin. However it has been widely discussed by groups that the time between two pulses in a pulsed

current setup may allow the skin to depolarize and return to its original state, leading to more efficient transport (less buildup of charge) and safer delivery (minimal accumulation of charges). In order to account for a range of determinants for iontophoretic transport, models developed for iontophoretic delivery have strived to describe the relationship of iontophoretic transport to various factors that influence the delivery. Some models characterize limited variables such as the relationship of the solute structure and size to the iontophoretic transport (Stokes-Einstein and free volume models) [95] while other recent models such as the ionic mobility-pore model are more comprehensive. This model incorporates a range of important factors such as the solute size, mobility and concentration, applied current, presence of extraneous ions, the conductivity of the solvent, interaction of the solute molecules with the pore walls and the subsequent restriction of the pore size, the epidermal permselectivity and electroosmosis, and is described in detailed by Roberts, *et al*., [96,97].

2.6. Chemical Enhancement

2.6.1 Chemical Enhancers

Ideally, penetration enhancers reversibly reduce the barrier resistance of the stratum corneum without damaging viable cells. Some of the more desirable properties for penetration enhancers acting within the skin have been given as follows [98]:

- Compatibility with drug and other formulation excipients.
- Immediate permeation-enhancing action after administration of formulation.
- Reduction of barrier functions of the absorbing surface in one direction only.
- Pharmacologically inert, nontoxic and inexpensive.
- Rapidly reversible effect on barrier layer.

2.6.2 Mechanisms of Action of Chemical Enhancers

Many studies have investigated the mechanisms of action of chemical enhancers and the following have been suggested as possible explanations for activity [98,99]: (1) interaction with intercellular lipids of the SC resulting in disorganization of the highly ordered structures thus enhancing the paracellular diffusivity through the SC; (2) interaction with intracellular proteins of the corneocytes to increase transcellular permeation; and (3) increasing partitioning of the drug into the SC.

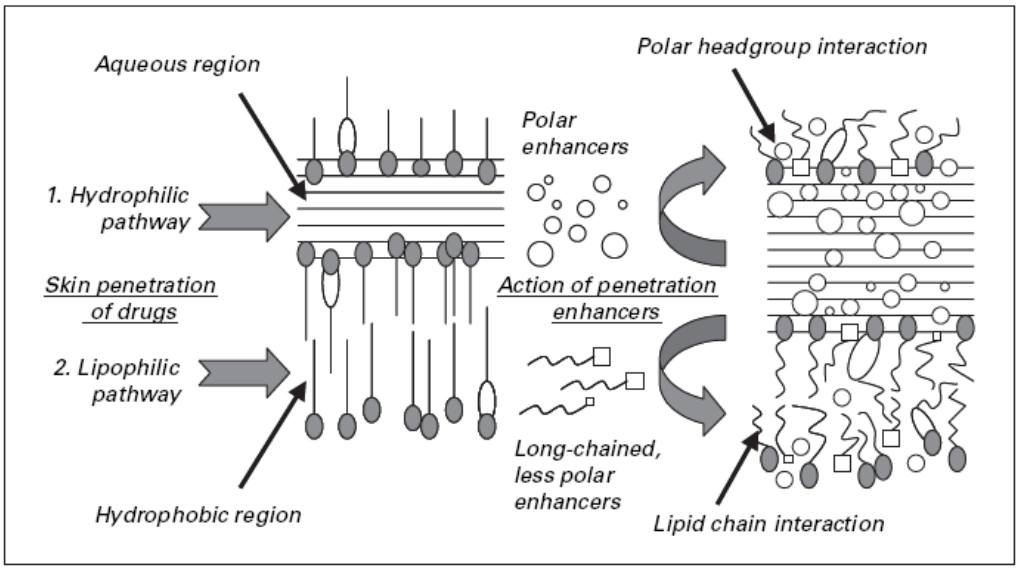

Figure 7. Hydrophilic and lipophilic pathways of drug penetration and action mode of penetration enhancers [99]

A penetration enhancement of drugs after topical application can be achieved by several compounds which are able to promote the transport of actives across the skin barrier. There are a variety of mechanisms for penetration enhancement by these substances [98,99,100]. One possibility is that the interaction of the enhancers with the polar headgroups of the lipids disturbs

the highly packing ordered structure of the lipids. The result is the facilitation of the diffusion of hydrophilic drugs. Simple hydration can be used in structure modification which results in changes to drug penetration [101]. Water is one of the most effective and safest penetration enhancers. By hydration of the stratum corneum, the penetration of most drugs can be increased.

Normally in the stratum corneum the water content is 5–10%. The water content can be increased up to 50% under occlusive conditions (e.g. by application of occlusive vehicles) [18]. Furthermore, moisturizers such as urea can be used to increase the hydration of the stratum corneum and in consequence to improve the diffusion of hydrophilic drugs. The headgroup disturbance of lipids by polar enhancer substances can also affect the hydrophobic parts of the lipids and leads to rearrangements in these bilayer areas. This also explains the penetration improvement for lipophilic drugs by use of lipid headgroup-influencing hydrophilic penetration enhancer. Another possibility is the interaction of lipophilic penetration enhancers with the hydrocarbon chains of the bilayer lipids. The penetration of lipophilic drugs is facilitated by disturbing the packing order of the bilayer lipids due to an increased fluidization of the hydrocarbon chains. These changes also influence the order of the polar headgroups which possibly results in the penetration enhancement of hydrophilic drugs by use of a lipophilic enhancer substance. Figure 7 illustrates the influence of penetration enhancers on both the lipophilic pathway and the hydrophilic pathway of drug penetration.

Some of the chemical enhancer substances need suitable vehicles or cosolvents (e.g. propylene glycol) to reach the polar lipid parts and exert their functions [102]. The increased drug solubility and the improvement of its partition coefficient (skin/vehicle) is another mechanism explaining the action of penetration enhancers. Additionally, the stratum corneum can be made more

permeable for drug substances by the extraction of its lipids as the result of an interaction with chemical penetration enhancers [22].

2.6.3 Chemical Enhancers for Transdermal Drug Delivery Systems

The most studied chemical enhancers for transdermal drug delivery systems are discussed as follows:

Sulphoxides and Similar Chemicals

Dimethyl sulphoxides (DMSO) is one of the earliest and most widely studied penetration enhancers [99]. It is a colourless, odourless, hydroscopic and powerful aportic solvent which hydrogen bonds with itself rather than with water. The effect of the DMSO as an enhancer is concentration-dependent and generally cosolvents containing > 60% DMSO are needed for optimum enhancement efficacy. However, at these relative high concentrations, DMSO can cause erythema and wheal of the stratum corneum. DMSO may also extract lipids, making the horny layer more permeable by forming aqueous channels. The mechanism of DMSO as a penetration enhancer is widely believed to denature protein and, on application to human skin, has been shown to change the intercellular keratin conformation from α-helical to ß sheet.

Azone and Derivatives

Azone (laurocapram) and its derivatives are the first molecules which were specifically designed as penetration enhancers. Azone is a highly lipophilic liquid with an octanol/water partition coefficient of 6.21 [99]. It is a chemically stable compound and an excellent solvent for many drugs. The substance has a low irritating potential, a very low toxicity and nearly no pharmacological activity. They can be used as penetration enhancers for hydrophilic and

lipophilic substances and for peptide molecules as well. Azone and derivatives are reported to be effective penetration enhancers when used in low concentrations (1–5%) [99]. Their activity can be increased by the addition of co-solvents like propylene glycol or ethanol. Azone derivatives are soluble in and compatible with most organic solvents. The penetration-enhancing effects of these compounds are probably due to an intercalation into the structured lipids of the stratum corneum and the disturbance of the lipid packing order. The dimensions of this chain are comparable with the dimensions of the cholesterol skeleton. Azone derivatives possibly decrease the cholesterol-cholesterol interferences and the cholesterol-ceramide interactions. Thus the fluidity of the hydrophobic stratum corneum regions is increased. Therefore, the permeation resistance of the horny layer against drug substances is reduced. Among the large number of investigated azone derivatives, the compounds with a chain length of 12 carbon atoms were the most effective ones independent of the ring dimensions [99].

Fatty Acids

Percutaneous drug absorption has been increased by a wide variety of long-chain fatty acids. The most popular one is oleic acid. Shin, *et al*., [103] studied various penetration enhancers like glycols [104] (diethylene glycol and tetraethylene glycol), fatty acids (lauric acid, myristic acid and capric acid) and nonionic surfactant (polyoxyethylene-2-oleyl ether, polyoxy ethylene-2-stearly ether) on the release of triprolidone. Lauric acid in propylene glycol enhanced the delivery of highly lipophilic antiestrogen. Oleic acid greatly increased the flux of many drugs such as increasing the flux of salicylic acid 28-fold and 5-flurouracil flux 56-fold through human skin membrane in vitro. The enhancer interacts with and modifies the lipid domains of the

stratum corneum as would be expected for a long chain fatty acid with cis- configuration [104,105].

Essential oil, Terpenes and Terpenoids

Terpenes are found in essential oils, and are compounds comprising of only carbon, hydrogen and oxygen atoms, but which are not aromatic. The essential oils of eucalyptus, chenopodium and ylang-ylang have been found to be effective penetration enhancers for 5-flouorouracil transversing human skin in vivo [106]. Cornwell, *et al*., [107] investigated the effect of 12 sesquiterpenes on the permeation of 5-flurouracil in human skin. Pretreatment of epidermal membranes with sesquiterpene oil or using solid sesquiterpenes saturated in dimethyl isosorbide increased the absorption of 5- flurouracil. One mechanism reported in the literature is to modify the solvent nature of the stratum corneum, thus improving drug partitioning into the tissue [107]. Many terpenes permeate human skin well and large amounts of terpene have been found in the epidermis after application from a matrix-type patch. Terpenes may also modify drug diffusivity through the membrane. It was found that during steady state permeation experiments terpene treatment reduced the lag time for permeation, indicating some increase in drug diffusivity through the membrane [106].

Surfactants

Surfactants are found in many existing therapeutic, cosmetic and agro-chemical preparations. Usually, surfactants are added to formulations to solubilise lipophilic active ingredients, and so they have potential to solubilise lipids within the stratum corneum. Typically surfactants are composed of a lipophilic alkyl or aryl fatty chain, together with a hydrophilic head group.

Anionic surfactants include sodium lauryl sulphate (SLS), cationic surfactants include cetyltrimethyl ammonium bromide, the nonoxynol surfactants are non-ionic surfactants and zwitterionic surfactants include dodecyl betaine. Anionic and cationic surfactants have potential to damage human skin; SLS is a powerful irritant and increased the transepidemeral water loss in human volunteers in vivo and both anionic and cationic surfactants swell the stratum corneum and interact with intercellular keratin [108]. Non-ionic surfactants are widely regarded as safe. Surfactants generally have low chronic toxicity and most have been shown to enhance the flux of materials permeating through biological membranes [101]. Most studies evaluating enhancement activity have focussed on the use of anionic and non-ionic surfactants. Anionic materials themselves tend to permeate relatively poorly through human stratum corneum upon short time period exposure (for example when mimicking occupation exposure) but permeation increases with application time [101]. Watkinson, *et al*., [99] reported that around 0.5% of the applied dose of nonoxynol surfactant materials traversed human skin after 48 h exposure in vitro. Surfactant facilitated permeation of many materials through skin membranes has been researched, with reports of significant enhancement of materials such as chloramphenicol through hairless mouse skin by SLS, and acceleration of hydrocortisone and lidocaine permeating across hairless mouse skin by the non-ionic surfactant Tween 80 [109].

2.6.4 Enhancers Transbuccal Drug Delivery Systems

Since the buccal epithelium is similar in structure to other stratified epithelia of the body, enhancers used to improve drug permeation in other absorptive mucosae have been shown to be effective in improving buccal drug penetration [110]. As discussed in Section 2.6.3, sulphoxides, azone and derivatives, essential oil, terpenes and terpenoids, propylene glycol and surfactants

have been used in enhancing transdermal drug delivery. Similar chemical enhancers have been studied for enhancing transbuccal drug delivery, and it was believed that the mechanisms of action of enhancers for transbuccal drug delivery were similar to those for transdermal drug delivery [110,111]. Small molecules such as butyric acid and butanol, ionizable low molecular weight drugs such as acyclovir, propranolol, and salicylic acid, large molecular weight hydrophilic polymers such as dextrans, and a variety of peptides including octreotide, leutinizing hormone releasing hormone (LHRH), insulin, and a-interferon have all been studied [112,113,114,115,116,117]. A series of studies [111,118] also demonstrated that di- and tri-hydroxy bile salts enhanced buccal penetration of buserelin and fluorescein isothiocyanate (FITC) labelled dextrans. Their results demonstrated that using the bile salts increased the permeability of porcine buccal mucosa to FITC by a 100-200 fold compared to FITC alone. The mechanism of penetration enhancement of FITC-labelled dextrans by sodium glycocholate (SGC) was shown to be concentration dependent. Below 10 mM SGC, buccal permeation was increased by increasing the intercellular transport and at 10 mM and higher concentrations by opening up a transcellular route. Gandhi and Robinson [116] investigated the mechanisms of penetration enhancement of transbuccal delivery of salicylic acid. They used sodium deoxycholate and sodium lauryl sulfate as penetration enhancers, both of which were found to be effective in increasing the permeability of salicylic acid across rabbit buccal mucosa. Their results also supported that the superficial layers and protein domain of the epithelium may play critical roles in maintaining the barrier function of the buccal mucosa. Literature review [119] have indicated the feasibility of buccal mucosal delivery of insulin using various enhancers in different animal models for in vivo studies. Aungst, *et al*., [110] enhanced insulin bioavailability

from about 0.7% (without enhancer) to 26-27% through rat buccal mucosa using sodium glycocholate (5% w/v) and sodium lauryl sulfate (5% w/v) as enhancers.

Skin Irritancy and Toxicity Due to Chemical Penetration Enhancers

Chemical penetration enhancers increase skin permeability by reversibly damaging or altering the physicochemical nature of the stratum corneum to reduce its diffusional resistance. One of the problems associated with many chemical penetration enhancers is that they cause irritancy in the skin. This is not surprising in chemicals that disrupt organized lipid structures, cell membranes and components. The toxicity associated with many chemical penetration enhancers has limited their usefulness for clinical application.

The search for an ideal skin and buccal tissue penetration enhancer has been the focus of a considerable research effort over the last decades. Unfortunately, no chemical enhancer has yet been found to possess ideal properties; furthermore, many enhancers are toxic, acting as skin irritants or allergens at some level (depending on their concentration and the frequency of their treatment). Generally, the toxicity of a potent enhancer is associated with its enhancement effect, indicating that its mechanism of action is related to chemical interaction with skin components or structures.

In this study, low toxic Dodecyl 2-(*N*,*N*-dimethyl amino) propionate (DDAIP) and dodecyl-2-(N,N-dimethylamino) propionate hydrochloride (DDAIP HCl), and Br-iminosulfurane with proved transdermal enhancement effects were chosen as chemical enhancers for enhancing both transdermal and transbuccal drug delivery, and Azone was chosen as a control chemical enhancer.

Dodecyl 2-(*N*,*N*-dimethyl amino) propionate (DDAIP) and dodecyl-2-(*N*,*N*-dimethylamino) propionate hydrochloride (DDAIP HCl)

As long chained alcohols, disubstituted aminoacetates were introduced as skin penetration enhancer substances [120]. Representatives of this group of penetration enhancers are dodecyl-*N,N*-dimethylaminoacetate and dodecyl-2-methyl-2-(*N,N*-dimethylaminoacetate) (DDAIP). These substances are not soluble in water, but soluble in most of the organic solvents and in water and alcohol mixtures. The skin penetration promotion potential of these substances is in the same dimension as Azone or even higher. The penetration enhancing activity is decreased by the increase in the *N,N*-dialkyl carbon chain. The skin-irritating potential of the aminoacetates is very low. This is due to the biological decomposition of these enhancers by the skin enzymes to *N,N*-dimethylglycine and the corresponding alcohols [108]. They enhance skin penetration by the interaction with stratum corneum keratin and the increase in the hydration efficiency resulting from these interactions [121].

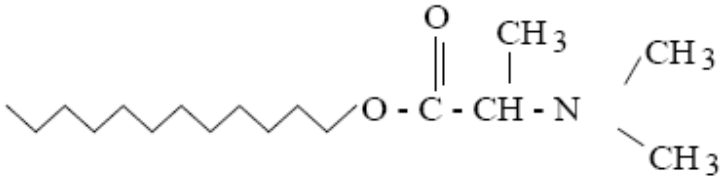

Figure 8. Chemical structure of DDAIP [122]

The penetration fluxes of indomethacin increased linearly as the concentration of DDAIP increased from 2.5 to 15% [123]. Snake skin pretreatment experiments indicated that the application of DDAIP significantly increased skin permeability [124]. Electron micrograph studies showed clearly that the enhancer was able to interact with both lipid rich layers and keratin-rich layers. Later, the effectiveness of DDAIP was tested using snake skin, rabbit pinna

skin and human skin for penetration experiments with the drugs indomethacin, 5-fluorouracil and propranolol-HCl. With all skins and all model drugs, DDAIP increased drug permeability at least as well as Azone [123]. In most cases it was the more effective penetration enhancer. The electrochemical investigation of human cadaver skin by impedance spectroscopy with and without penetration enhancers (DDAIP and Azone were used) revealed new insights into the mechanism of action of the enhancers [108]. The enhancers appeared to open new penetration routes and increased the ohmic resistance, capacity properties and fractal dimension of the skin. By fluorescence spectroscopic studies DDAIP was shown to alter molecular movement on the surface of the bilayers, resulting in a decrease in anisotropy of 19% [127]. By use of DDAIP as an enhancer in penetration studies of miconazole through shed snake skin, the permeation increased 11-fold compared with that of the suspension without DDAIP pretreatment [125]. The concentration of the miconazole in the skin increased 8-fold, indicating that the enhancement effect is connected with high partition of miconazole into the skin. Wolka, *et al.*, [122] studied the interaction of DDAIP with a phospholipid model membrane by differential scanning calorimetry for further clarification of the mechanism of action of this skin penetration enhancer. The results suggested that drug transport is enhanced by DDAIP by interaction with the polar regions of the phospholipid bilayers and also by increasing the motional freedom of lipid hydrocarbon chains. It also has been reported that the biodegradable skin permeation enhancer, DDAIP, improved the permeation of several anti-inflammatory drugs, as well as clonidine, hydrocortisone, etc. [123].

The clinical and mycological efficacy of different terbinafine HCl nail solutions (TNS) formulated with or without DDAIP HCl was evaluated using a guinea pig model of Trichophyton mentagrophytes dermatophytosis. The vehicle and 0.5% DDAIP HCl treated groups showed

minimal clinical efficacy (only 11% and 5%, respectively). Addition of 0.5% DDAIP HCl to 5% and 10% TNS significantly enhanced the clinical and mycological efficacy [124]. These DDAIP and DDAIP HCl have never been reported on enhancing transbuccal drug delivery.

Br-iminosulfurane

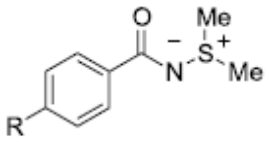

1: R = F
2: R = Br
3: R = I
4: R = *n*-butyl
5: R = *n*-hexyl

Figure 9. Chemical structure of iminosulfuranes.

Br-iminosulfurane is a small, polar molecule (Figure 9). It may interact with lipids in the SC with the aromatic ring lying in the plane of the lipid polar head groups [15,126]. These groups would then be forced apart, which not only efficiently disrupts the lipid packing at the head group region but also in the acyl chain region. The penetration of Br-iminosulfurane was examined by confocal Raman microscopy. The results indicated that compound Br-iminosulfurane penetrates through the SC and the enhancer remained primarily in the SC without any significant penetration into the viable epidermis. The pilot QSAR analysis was conducted with compounds 1Y5 and other iminosulfuranes previously studied. Results revealed that enhancement activity was paralleled by hydrophobicity of the iminosulfuranes and the number of hydrogen bonding acceptors in the molecules. The enhancement activity of Br-iminosulfurane is not accompanied by cytotoxic effect at a concentration of no more than than 0.2 M [15]. It was believed that the

mechanisms of action of dimethyliminosulfuranes probably included the solvent effect that increases drug partitioning in the SC, interaction with lipids in the SC, and interaction with protein in the SC [15]. Sintov, et al., [127] investigated the role of the skin's metabolism of Br-Iminosulfurane on its enhancement activity. They found that Br-Iminosulfurane hydrolyzed very fast in physiological buffer to 4-bromobenzamide (BBA), and even faster and almost completely in the presence of skin tissue. Thus it was proposed that a new mechanism of action by which a non-irritant and powerless "enhancer" (i.e., a pro-enhancer) was activated by its own metabolism in the skin tissue and proved that this biotransformation was essential for its enhancement activity. This enhancer was not researched in enhancing transbuccal drug delivery.

2.7 Combination Approaches

2.7.1. Combination Strategies to Improve Transdermal Iontophoretic Drug Delivery

Over the last 20 years, a tremendous amount of work has been directed toward developing various enhancement techniques to improve transdermal iontophoretic drug delivery. The major enhancement techniques include electroporation, microneedles, chemical enhancer, sonophoresis and ion-exchange materials [128]. In this study, combination approach using iontophoresis and chemical enhancer was used to enhance both transdermal and transmucosa drug delivery. Enhancers offer several to more than a hundred times higher drug penetration in terms of the flux, depending on the properties of the penetrants and enhancers as well as the other additional ingredients of the formulations. Sole chemicals, however, sometimes offer limited enhancements of skin permeability. The combined enhancers and iontophoresis have demonstrated synergistic effects in enhancing drug penetration as well as reduce the side effects such as irritation caused by high concentration of enhancers or stronger electric forces. Most commonly studied

enhancers in combination with iontophoresis are fatty acids, terpenes, surfactants, Azone, and diethyl acetamide [129]. A. Femenía-Font *et al*. [14] studied the effects of Azone® pretreatment followed by 0.5 mA/cm^2 iontophoresis on transdermal absorption of sumatriptan through human skin. Using the combination provided synergistic effects by increasing the drug flux by 5-fold compared with Azone® alone or 2-fold iontophoresis alone respectively. Similarly, fatty acids and iontophoresis were found to provide synergistic effects in promoting the delivery of midodrine hydrochloride through human skin [130]. Using the enhancer - 5% oleic acid in combination with iontophoresis resulted in more than 15-fold drug flux increase in comparison with 5% oleic acid alone, with the authors concluding that the combination of 5% oleic acid pretreatment followed with the electrical current offset at 0.1 mA/cm^2, the daily delivery of midodrine hydrochloride can provide an adequate clinical application.

In this study, combination approaches of iontophoresis and chemical enhancers: DDAIP HCl in water and PG, DDAIP in PG, and Br-iminosuflurane in PG were used to enhance transdermal and transbuccal drug delivery. These specific combined treatments were not previously reported on both transdermal and transbuccal drug delivery.

CHAPTER 3. DRUG SELECTION

3.1 Background

Transdermal and transbuccal delivery have been considered as alternative routes to oral dosing of drugs with low bioavailability due to significant degradation in the gastro-intestinal tract or hepatic first-pass metabolism. Ideally drug candidates need to possess following properties (Table 4) in order to be successfully delivered into blood stream transdermally or transbuccally.

Table 4. Formulation considerations for passive transdermal and transbuccal delivery and ideal limits (modified from Reference [5])

Aqueous solubility	> 1 mg / ml
Lipophilicity	10 < Ko/w < 1000
Molecular weight	< 500 Da
Melting point	< 200 ^{o}C
pH of saturated aqueous solution	pH = 5–9
Required dose deliverable	< 10 mg / day
No irritation to skin/buccal tissue	

Abbreviation: Ko/w, oil–water partition coefficient.

Also an ideal drug candidate for transdermal delivery must possess both lipoidal and aqueous solubility. When the drug is too hydrophilic, it will not be able to transfer with ease into the stratum corneum. On the other hand, if it is too lipophilic, the drug will tend to remain in the SC

layers [5]. In summary, there are many challenges involved in delivering therapeutic amounts of a hydrophilic drug transdermally and transbuccally. However, in general, a hydrophilic drug is easier to formulate than a hydrophobic drug because of its water solubility property. For this study we selected four hydrophilic drugs: two established drugs (lidocaine hydrochloride and nicotine hydrogen tartrate) and two other drugs (diltiazem HCl and ondrasetron HCl) were selected for this study. With the established drugs the experimental methodologies and parameters were explored for both transdermal and transbuccal routes of drug delivery. Then the permeation studies were conducted for the two "new" drugs diltiazem HCl and ondansetron HCl using the established systems.

3.1.1 Lidocaine HCl (LHCl)

Indications and usage for lidocaine

Lidocaine hydrochloride is indicated for prevention and control of pain in procedures involving the male and female urethra for topical treatment of painful urethritis, and as an anesthetic lubricant for endotracheal intubation (oral and nasal) [131]. A mixture of two topical local anesthetics: lidocaine and prilocaine periodontal (gingival) gel is used on the gums to cause numbness or loss of feeling during dental procedures through deadening the nerve endings in the gum [132]. Lidocaine hydrochloride injection, USP is a sterile, nonpyrogenic solution of an antiarrhythmic agent administered intravenously by either direct injection or continuous infusion [133]. LIDODERM® (lidocaine patch 5%) is used to relieve the pain of post-herpetic neuralgia, also referred to as after-shingles pain and applied only to intact skin with no blisters [134]. LidoSite™ System (Vyteris, NJ) [135] is a topical local anesthetic iontophoretic delivery system with indication for use on normal intact skin to provide local analgesia for superficial

dermatological procedures such as venipuncture, intravenous cannulation, and laser ablation of superficial skin lesions.

Chemical and physical properties [131]

Lidocaine hydrochloride, a local anesthetic, is chemically designated as:

2-(Diethylamino)-2′, 6′-acetoxylidide mono-hydrochloride, monohydrate, is a white crystalline powder freely soluble in water, with a molecular weight of 288.81, pKa = 7.8. Its molecular formula is C14H22N2O•HCl and its structural formula is (Figure 10):

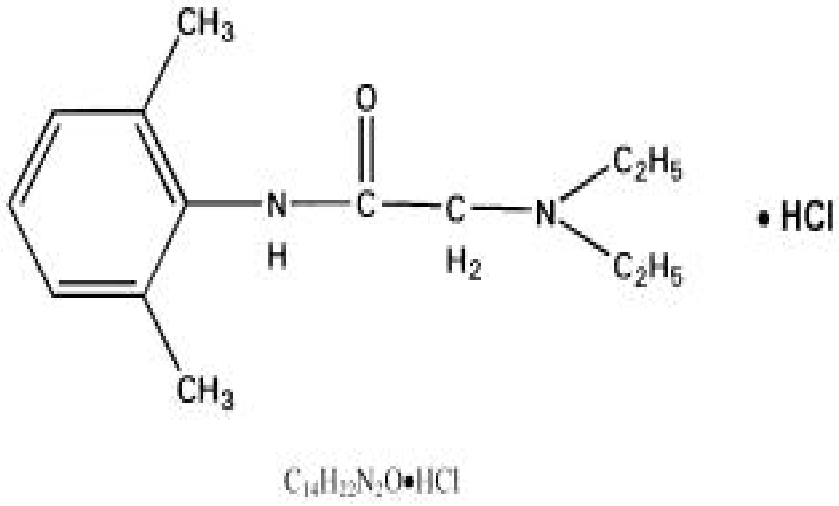

Figure 10. LHCl Molecular Structure.

Clinical pharmacology [131]

Mechanism of action

Lidocaine stabilizes the neuronal membrane by inhibiting the ionic fluxes required for the initiation and conduction of impulses, thereby effecting local anesthetic action.

Therapeutic plasma concentration is 1.5 to 5 μg/ml and epidural test dose is 45 – 75 mg.

Pharmacokinetics and metabolism

Lidocaine is usually absorbed following topical administration to mucous membranes. Its rate and extent of absorption varies depending upon concentration, total dose administered, the specific site of application and duration of exposure.

Lidocaine is well-absorbed from the gastrointestinal tract, but little intact drug may appear in the circulation because lidocaine is metabolized rapidly by the liver. Biotransformation includes oxidative N-dealkylation, ring hydroxylation, cleavage of the amide linkage, and conjugation. N-dealkylation, a major pathway of biotransformation, yields the metabolites: mono-ethylglycinexylidide and glycinexylidide. The pharmacological / toxicological actions of these metabolites are similar to, but less potent than, those of lidocaine. Approximately 90% of lidocaine administered is excreted in the form of various metabolites, and less than 10% is excreted unchanged. The primary metabolite in urine is a conjugate of 4-hydroxy-2, 6-dimethylaniline.

Elimination

Lidocaine and its metabolites are excreted by the kidneys. Following an intravenous bolus injection, the elimination half-life of lidocaine is typically 1.5 to 2.0 hours. Approximately 90%

of administered lidocaine is excreted in the form of various metabolites, and less than 10% is excreted unchanged.

In the literature, iontophoresis and chemical enhancers have been utilized to enhancer both topical and transdermal delivery of lidociane. Sintov, *et al*. [136], used the combination of a short-term iontophoresis and microemulsion formulations to enhance the skin penetration of lidocaine. The *in vitro* and *in vivo* studies showed that the combination of a microemulsion formulation of lidocaine with 10 min of iontophoresis (1.13 mA/cm^2) shortened lag times, significantly increased flux , and resulted in accumulation of a large skin drug depot compared to control, an aqueous lidocaine solution.

Lee, *et al*. [137], investigated the effect of various classes of chemical enhancers on the transdermal delivery of lidocaine across pig and human skin *in vitro*. The results demonstrated that chemical enhancers: oleic acid, oleyl alcohol, butenediol, and decanoic acid by themselves or in combination with isopropyl myristate (IPM) exhibited no significant flux enhancement. However, the binary system of IPM/*n*-methyl pyrrolidone (IPM/NMP) enhanced drug transport (flux) by 4-fold over NMP alone and 25-fold over IPM alone, respectively, at the same drug concentration ($p < 0.001$). At 2% lidocaine, this synergistic enhancement peaked at 25:75 (v/v) IPM:NMP with a resulting steady state flux of 57.6 ± 8.4 $\mu g/cm^2$ *h through human skin.

In 2004, Vyteris, NJ gained FDA's approval of its LidoSite™ System [135] - a topical local anesthetic iontophoretic delivery system with indication for providing local analgesia for superficial dermatological procedures such as venipuncture, intravenous cannulation, and laser ablation of superficial skin lesions. The LidoSite™ Topical System consists of a LidoSite™ Patch and a LidoSite™ Controller, a portable microprocessor-controlled battery-powered DC

current source. The LidoSite™ System delivers lidocaine and epinephrine simultaneously by topical iontophoresis to achieve dermal analgesia on intact skin. The LidoSite™ Controller is designed with a battery that provides up to 99 drug applications at 1.77 mA for 10 minutes (17.7 mA-min). The LidoSite™ Patch is for single use only and is disposable. The patch contains a 5cm^2 circular drug reservoir that delivers lidocaine and epinephrine to the skin and an elongated return reservoir containing electrolytes to complete the electrical circuit (Figure 11).

Figure 11. LidoSite™ System [135]

3.1.2 Nicotine Hydrogen Tartrate (NHT)

Indication and usage for NHT

Cigarette smoking is the single most preventable cause of death in modern society. It causes one in every five deaths in Britain and in the US nearly 500,000 deaths a year [138]. Smoking is the major cause of lung cancer, ischaemic heart disease and chronic obstructive airways disease.

When smoking a cigarette, a dose of nicotine, the major pharmacologically active component in tobacco, is rapidly delivered to receptors in the brain and then a pleasurable sensation is generated. This repeated experience can be easily developed into physiological and psychological addiction reinforced by pronounced withdrawal symptoms. Tobacco smoking also significantly increases the risk of preoperative and postoperative complications [139].

The therapeutic indication for NHT includes restraining the desire for cigarette smoking and eliminating the addiction gradually through delivering small and controlled doses of nicotine into the bloodstream by transdermal or transbuccal systems, but without consuming other toxic and dangerous chemicals present in cigarette smoke. This is easy, simple and no pain way to allow a person to enjoy double treatment effects to both physical and psychological smoking addictive.

Physical and chemical properties [140]

Nicotine hydrogen tartrate is a white powder and soluble in water. Its molecular weight is 462. Every 3 grams of nicotine hydrogen tartrate is equivalent to about 1 gram of Nicotine -(1-methyl-2(3-pyridyl) pyrrolidine) (Figure 12).

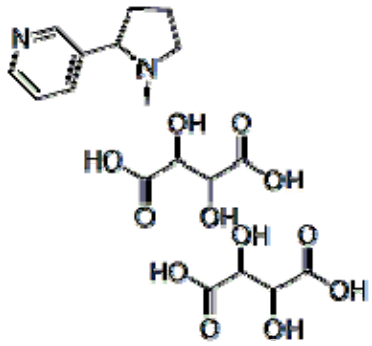

Figure 12. Chemical Structure of nicotine hydrogen tartrate

Therapeutic blood level of nicotine is 10 – 15 ng /ml and bioavailability is 60%.

The most widely used smoking cessation program is nicotine replacement therapy (NRT) [141]. A number of commercial NRT products are available. Nicotine products such as chewing gum, sublingual tablets, adhesive transdermal patches, nasal spray and (oral mucosal) inhalers are available on the market in different strengths. Nicorette gum contains nicotine-resin complex, the primary ingredient in tobacco products. Other ingredients may include chewing gum base, xylitol, sorbitol, peppermint oil, haverstroo flavor, menthol, sodium carbonate anhydrous, magnesium oxide, and glycerol. The gum is available in two strength levels: the 4 mg strength is recommended for smokers who use 20 or more cigarettes per day, and the 2 mg strength is for those who smoke less than 20 cigarettes daily [142]. It provided nicotine levels lower than those associated with smoking [143]. Nicorette patch (3.6cmx4.9cm) [144] is a typical transdermal system to deliver 10 to 15 mg of nicotine over 24 hours. The nicotine in the patches is absorbed continuously from the patches, through the skin and into the bloodstream. This produces a lower level of nicotine in the blood than smoking, but the continuous level is enough to help minimize the withdrawal symptoms and cravings when quitting smoking. The nasal spray nicotine formulation can give a rapid and short lived peak plasma level of nicotine. The chewing gum, sublingual tablets, and transdermal patch nicotine formulation can provide slow onset but prolonged plasma nicotine levels. The level of nicotine in the blood rises rapidly and reaches the brain within 10–20 sec. via the internal carotid arteries after inhalation of cigarette smoke. Plateau blood nicotine levels can be reached within 30 min from nicotine chewing gum, sublingual tablets and (oral mucosal) inhalers [145]. The nicotine peak plasma level can be reached within 10 min from nicotine nasal spray formulation. Nicotine is absorbed rather slowly from transdermal adhesive patches, taking hours to reach a plateau. The commercially available

products of NRT have been shown to be effective in promoting smoking cessation. However, none of the current dosage forms can provide the smoker with both the high and rapid peak arterial nicotine levels and subsequent rapid pharmacological effect similar to what can be obtained from cigarette smoking. In general, therefore, the presently marketed NRT products are not entirely satisfactory. To aid smoking cessation, there is a significant need for improved nicotine replacement formulations which should not only provide an initial rapid release and absorption of nicotine (the pulse effect) but also a sustained release and absorption of nicotine. The pulse effect would provide an initial rapid peak in plasma nicotine levels, which gives the pleasant feeling of smoking a cigarette, and a sustained release profile that provides a more gradually increased and maintained high plasma level of nicotine. This should result in easier and more effective smoking cessation. Iontophoresis and chemical enhancer pretreatment combination approaches are well fitted in this case to meet the need.

Conaghey, *et al*., [10] studied the iontophoretic delivery of nicotine across artificial and human skin membranes from heterogeneous gel vehicles comprised of mixtures of ion exchange resins - Amberlite IRC50, to which the nicotine had been bound, and agar hydrogel with a nicotine concentration range of 7.8 to 39.5 mg / ml at a current intensity of 0.5 mA/ cm^2. The nicotine release rates were found to show a plateau as the concentration of nicotine reached to 20 mg / ml.

Nolan, *et al*. [146], found that a combination of a fatty acid and anodal iontophoresis treatment synergistically enhanced the *in vitro* transport of nicotine across murine skin, and oleic acid increased both the iontophoretic and post-iontophoretic nicotine transport. The combined enhancement of drug delivery was greater than that caused by the current alone [146].

3.1.3 Diltiazem HCl (DHCl)

Indication [147]

Diltiazem hydrochloride (Dilacor XR®, Watson) is a calcium ion influx inhibitor (slow channel blocker or calcium antagonist). Dilacor XR® is indicated for the treatment of hypertension. Diltiazem hydrochloride may be used alone or in combination with other antihypertensive medications, such as diuretics. Dilacor XR® is also indicated for the management of chronic stable angina.

Physical and chemical properties [147]

Diltiazem hydrochloride is 1, 5-Benzothiazepin-4(5H) one, 3-(acetyloxy)-5-[2-(dimethylamino) ethyl]-2, 3-dihydro-2-(4-methoxyphenyl)-, monohydrochloride, (+)-cis-. Its molecular formula is $C_{22}H_{26}N_2O_4S$•HCl and its molecular weight is 450.98. Its structural formula is provided below (Figure 13):

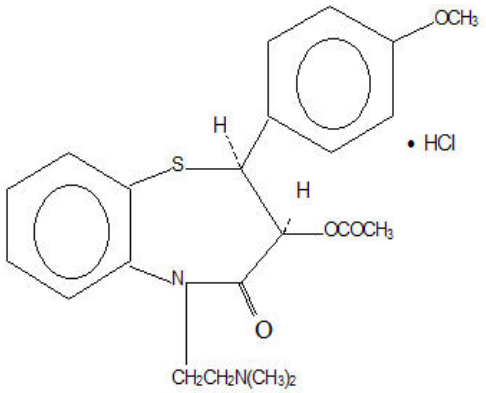

Figure 13. Chemical Structure of Diltiazem HCl

Diltiazem hydrochloride is a white to off-white crystalline powder with a bitter taste. It is soluble in water, methanol, and chloroform and light sensitive.

Dilacor XR® capsules have different dosage strengths such as 120 mg, 180 mg, or 240 mg that allows for the controlled release of DHCl over a 24-hour period.

Clinical pharmacology [147]

Mechanism of Action

The therapeutic effects of DHCl are believed to be related to its ability to inhibit the influx of calcium ions during membrane depolarization of cardiac and vascular smooth muscles.

Hypertension: Dilacor XR produces its antihypertensive effect primarily by relaxation of vascular smooth muscle with a resultant decrease in peripheral vascular resistance. The magnitude of blood pressure reduction is related to the degree of hypertension; thus hypertensive individuals experience an antihypertensive effect.

Angina: DHCl has been shown to increase exercise tolerance, probably due to its ability to reduce myocardial oxygen demand. This is accomplished through reductions in heart rate and systemic blood pressure at submaximal and maximal workloads.

Diltiazem has been shown to be a potent dilator of coronary arteries, both epicardial and subendocardial. Spontaneous and ergonovine-induced coronary artery spasms can be inhibited by diltiazem. In animal models, diltiazem interferes with the slow inward (depolarizing) current in excitable tissue. It causes excitation-contraction uncoupling in various myocardial tissues without changes in the configuration of the action potential. Diltiazem produces relaxation of

coronary vascular smooth muscle and dilation of both large and small coronary arteries at drug levels which cause little or no negative inotropic effect. The resultant increases in coronary blood flow (epicardial and subendocardial) occur in ischemic and nonischemic models and are accompanied by dose-dependent decreases in systemic blood pressure and decreases in peripheral resistance.

Pharmacokinetics and metabolism

Diltiazem is well absorbed from the gastrointestinal tract, and is subject to an extensive first-pass effect. When given as an immediate release oral formulation, the absolute bioavailability (compared to intravenous administration) of diltiazem is approximately 40%. Diltiazem undergoes extensive hepatic metabolism in which 2% to 4% of the unchanged drug appears in the urine. In vitro binding studies show DHCl is 70% to 80% bound to plasma proteins. The plasma elimination half-life of diltiazem is approximately 3.0 to 4.5 hours. Desacetyl diltiazem, the major metabolite of diltiazem, which is also present in the plasma at concentrations of 10% to 20% of the parent drug, is approximately 25% to 50% as potent a coronary vasodilator as diltiazem. Therapeutic blood levels of DHCl appear to be in the range of 40-200 ng/ml.

In the literature, L.M.A. Nolan, J. Corish [146] studied the combined effects of iontophoretic and chemical enhancement on drug delivery of DHCl, nicotine, and salbutamol. Their data suggested that diltiazem was not primarily electrically driven across the skin during iontophoresis but rather that the drug transport was the result of diffusion where the iontophoretic process had increased the skin permeability. In contrast, when oleic acid was incorporated into the delivery vehicle, the iontophoretic transport of diltiazem was increased by a factor of approximately 2.6 ($P \leq 0.02$). After cessation of the current, the rate of drug transport was identical to that observed

in the control experiment. Thus the fatty acid facilitated the increased participation of the drug in the conductive process during iontophoresis application. The increased iontophoretic transport of the drug may be a reflection of the interaction between the ionised oleic acid and buffer cations within the vehicle. An interaction of this nature would reduce the extent to which the current is carried across the vehicle and the skin by the extraneous ions. As a result, the participation of the drug ion in the conduction process should increase. The data relevant to the iontophoretic transport of salbutamol and nicotine indicate that the incorporation of oleic acid into the vehicle can affect drug transport during post iontophoresis. However, this was not the case for diltiazem. Six hours after cessation of the current no further transport of the drug across the tissue was evident in either the control experiment or that involving the fatty acid. The result indicated that passive diffusion of DHCl the skin was minimal.

Lee, *et al*. [148], developed a microemulsion composed of water, ethanol and IPM and Tween 80 (a nonionic surfactant), and transdermal enhancers such as n-methyl pyrrolidone (NMP) and oleyl alcohol. The effects of the oil-in-water microemulsion (O/W ME) system on transdermal delivery of DHCl, lidocaine free base, lidocaine HCl, and estradiol through human skin were investigated. The results demonstrated that enhancement of drug permeability from the O/W ME system was 520-fold for DHCl, 17-fold for lidocaine free base, 30-fold for lidocaine HCl, and 58-fold for estradiol over controls, indicating that the novel microemulsion systems potentially offered many beneficial characteristics for transdermal delivery of both hydrophilic and hydrophobic drugs.

Limpongsa, *et al*. [149], developed DHCl transdermal drug delivery systems using polymeric hydroxypropyl methylcellulose (HPMC) and ethylcellulose (EC) as hydrophilic and hydrophobic film formers, respectively. Their study found that the moisture uptake and initial release rates (0–

1 h) of DHCl films decreased with increasing the EC / HPMC ratio. DHCl films (10:0 and 8:2 HPMC/EC films) showed the comparable permeation-time profiles, and had higher flux values and shorter lag time as compared to 6:4 HPMC/EC films. Addition of enhancers IPM, IPP or Tween 80 could enhance the in vitro permeation fluxes of DHCl approx. three fold while Tween 80 shortened the lag time through pig ear skin. It was concluded that the film composed of HPMC/EC at the ratio of 8:2, 30% DBP and 10% IPM, IPP or Tween 80 as the permeation enhancer loaded with 25% DHCl formed the optimal formulation that should be selected for manufacturing a transdermal patch.

3.1.4 Ondansetron HCl (ODAN HCl)

Indication [150]

Ondansetron hydrochloride is a selective blocking agent of the serotonin $5\text{-}HT_3$ receptor type. ZOFRAN® (Glaxo Wellcome SmithKline, Ondansetron Hydrochloride) Tablets, ZOFRAN ODT® (Ondansetron) Orally Disintegrating Tablets, and ZOFRAN® (Ondansetron Hydrochloride) Oral Solution.

Chemical and physical properties [150]

The active ingredient in ZOFRAN® Tablets and ZOFRAN® Oral Solution is ondansetron hydrochloride (HCl) as the dihydrate, the racemic form of ondansetron. Chemically it is (±) 1, 2, 3, 9-tetrahydro-9-methyl-3-[(2-methyl-1H-imidazol-1-yl) methyl]-4H-carbazol-4-one, monohydrochloride, dihydrate. It has the following structural formula:

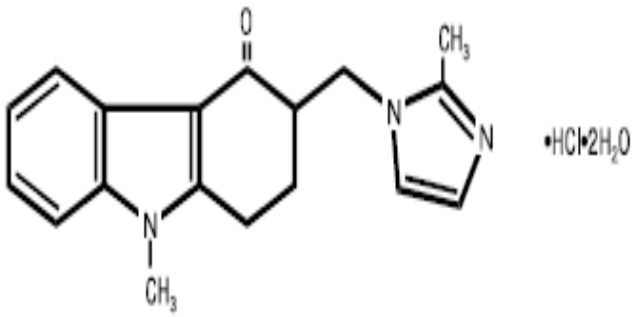

Figure 14. Chemical Structure of ODAN HCl

The empirical formula is $C_{18}H_{19}N_3O$•HCl•$2H_2O$, representing a molecular weight of 365.9. Ondansetron HCl dihydrate is a white to off-white powder that is soluble in water and normal saline.

Required therapeutic plasma levels are 30 – 100 ng/ml for treatment of postoperative nausea and vomiting. For prevention of post-operative nausea and vomiting ondansetron may be administered as a single dose of 16 mg given orally 1 hour prior to anesthesia. Alternatively, a single dose of 4 mg may be given by slow i.v. injection at induction of anesthesia. For the treatment of established postoperative nausea and vomiting, a single dose of 4 mg given by slow i.v. injection is recommended.

Each 4-mg ZOFRAN® Tablet for oral administration contains ODAN HCl dihydrate equivalent to 4 mg of ondansetron. Each 8-mg ZOFRAN® Tablet for oral administration contains ODAN HCl dihydrate equivalent to 8 mg of ondansetron. Each 4-mg ZOFRAN® ODT Orally Disintegrating Tablet for oral administration contains 4 mg ondansetron base. Each 8-mg ZOFRAN® ODT Orally Disintegrating Tablet for oral administration contains 8 mg ondansetron

base. Each 5 ml of ZOFRAN® Oral Solution contains 5 mg of ODAN HCl dihydrate equivalent to 4 mg of ondansetron.

Antiemetic action and clinical pharmacology [150]

Ondansetron is a selective antagonist of the serotonin receptor subtype, 5-HT3. Its precise mode of action in the control of chemotherapy-induced nausea and vomiting is not known. Cytotoxic chemotherapy and radiotherapy are associated with the release of serotonin (5-HT) from enterochromaffin cells of the small intestine, presumably initiating a vomiting reflex through stimulation of 5-HT3 receptors located on vagal afferents. Ondansetron may block the initiation of this reflex. Activation of vagal afferents may also cause a central release of serotonin from the chemoreceptor trigger zone of the area postrema, located on the floor of the fourth ventricle. Thus, the antiemetic effect of ondansetron is probably due to the selective antagonism of 5-HT3 receptors on neurons located in either the peripheral or central nervous systems, or both.

Pharmacokinetics [150]

Pharmacokinetic studies in human volunteers showed peak plasma levels of 20 to 30 ng/ml at around 1 1/2 hours after an 8 mg oral dose of ondansetron. An 8 mg infusion of ondansetron reached peak plasma levels of 80 to100 ng/ml. Repeat dosing of an 8 mg tablet every 8 hours for 6 days increased the peak plasma value to 40 ng/ml. A continuous i.v. infusion of 1 mg/hour after the initial 8 mg loading dose of ondansetron maintained plasma levels over 30 ng/ml during the following 24 hour period. The absolute bioavailability of ondansetron in humans was approximately 60% and the plasma protein binding was approximately 73%.

Following oral or i.v. administration, ondansetron is extensively metabolized and excreted in the urine and feces. In humans, less than 10% of the dose is excreted unchanged in the urine. The major urinary metabolites are glucuronide conjugates (45%), sulfate conjugates (20%) and hydroxylation products (10%).

The half-life of ondansetron after either an 8 mg oral dose or i.v. dose was approximately 3 to 4 hours and may be extended to 6 to 8 hours in the elderly.

In the literature, a few articles have been published regarding ODAN HCl transdermal as well as iontophoretic drug delivery. Gwak, *et al.* [151], investigated the effects of vehicles and penetration enhancers on the *in vitro* permeation of ODAN HCl across dorsal hairless mouse skins. Various types of vehicles (ester, alcohol, and ether) and their mixtures were used, and a number of fatty acids and fatty alcohols were employed as enhancers. Among pure vehicles used, water and ethanol showed high permeation fluxes, which were 48.2±23.7 and 41.9±17.9 mg/cm^2 per h, respectively. Propylene glycol monocaprylate (PGMC) alone did not increase permeation rate, but the skin permeability was increased by the addition of diethylene glycol monoethyl ether (DGME) and the highest flux was achieved when 40% of DGME was added. The combination of PGMC and ethanol (80:20) or PGMC and propylene glycol (PG) (60:40) increased the permeation flux by six- and two-fold, respectively, compared to PGMC alone. The synergistic enhancement was also obtained by using PG-oleyl alcohol (OAl) cosolvent. The combination of unsaturated fatty acids at 3% concentration to PG provided the greatest flux. The enhancement factors with the addition of oleic acid or linoleic acid to PG were about 1250 and 450, respectively. However, saturated fatty acids did not show significant enhancing effects. When the PGMC-DGME (60:40) cosolvent system was used as a vehicle, all fatty acids, including unsaturated fatty acids, failed to show significant enhancing effects. The results

indicate that the combinations of oleic acid, linoleic acid, or oleyl alcohol with PG, or PGMC-DGME (60:40) cosolvent could be potentially used to enhance transdermal delivery of ODAN HCl. Din, *et al.* [152], investigated the effects of current density and pH on the iontophoretic delivery of ODAN HCl through full thickness mouse skin. It was found that the steady state influx of ODAN HCl increased proportionally with current density from 0.05-0.3 mA/cm^2. The profile of the relationship between the state influx and the pH was an "S" shape, indicating that change of pH could affect skin permeation rate of ODAN HCl through changing its ionization degree.

In summary, no literature has been reported about enhanced transdermal or transbuccal delivery systems for these four drugs using pretreatment of chemical enhancers DDAIP, DDAIP HCl and Br-iminosulfurane alone or their combination with iontophoretic treatment.

3.2. Drug Formulations

3.2.1 2.5 % Lidocaine HCl (LHCl) Gel

Ingredients	% (w/w)
Cellulose gum (CMC)	2.0
Water	95.5
Lidocaine HCl	2.5

pH = 6.0

Viscosity (LV/#3/2 min) = 9000 cps

At room temperature, nonionized cellulose gum (CMC) 2% (w/w) was uniformly dispersed using lightning mixer in deionized water to obtain a gel. Then 2.5% (w/w) LHCl was added into CMC gel to form a 2.5% LHCl gel.

3.2.2 20 mg/ml Nicotine Hydrogen Tartrate (NHT) Gel

Ingredients	% (w/w)
CMC	2.0
Water	96.0
NHT	2.0

pH = 3.5

Viscosity (LV/#3/2 min) = 9200 cps

At room temperature, nonionized cellulose gum (CMC) 2% (w/w) was uniformly dispersed using lightning mixer in deionized water to obtain a gel. Then 2.0% (w/w) NHT was added into CMC gel to form a 20 mg/ml NHT gel.

3.2.3 2% Diltiazem HCl (DHCl) Gel

Ingredients	% (w/w)
CMC	1.0
Water	97.0
DHCl	2.0

pH = 5.5

Viscosity (LV/#3/2 min) = 8000 cps

At room temperature, nonionized cellulose gum (CMC) 1% (w/w) was uniformly dispersed using lightning mixer in deionized water to obtain a gel. Then 2% DHCl gel was added into CMC gel to form a 2.0% DHCl gel.

2.2.4 0.5% Ondansetron HCl (ODAN HCl) Gel

Ingredients	% (w/w)
CMC	1.0
Water	98.49
Citric Acid	0.01
ODAN HCl	0.5

pH = 3.6

Viscosity (LV/#3/2 min) = 3000 cps

At room temperature, nonionized cellulose gum (CMC) 1% (w/w) was uniformly dispersed using lightning mixer in deionized water to obtain a gel. Then 0.5% (w/w) ODAN HCl dihydrate was added into CMC gel together with 0.01% citric acid to form a 0.5% ODAN HCl gel.

CHAPTER 4. *IN VITRO* TRANSDERMAL EXPERIMENTAL METHODOLOGY

4.1 Materials and Equipment

4.1.1 Materials

ODAN HCl dihydrate was obtained from Polymed, Inc., Houston, TX, USA. Dodecyl-2-*N,N*-dimethylaminopropionate (DDAIP) and dodecyl-2-*N,N*-dimethylaminopropionate hydrochloride (DDAIP HCl) were provided by NexMed (San Diego, CA, USA). Azone and Br-iminosulfurane were synthesized at New Jersey Center for Biomaterials, Rutgers-The State University of New Jersey, Piscataway, NJ. Silver wire, propylene glycol (PG) (ReagentPlus®, 99%) and citric acid were purchased from Sigma Aldrich, Saint Louis, MO, USA. Phosphate buffer saline tablets were purchased from MP Biomedicals, LLC, Solon, OH, USA. Cellulose gum (CMC) was provided by TIC Gums, Belcamp, MD, USA. Tissue-Tek® compound was purchased from Sakura Finetek USA, Inc., Torrance, CA. Formalin 10% was purchased from Fisher Scientific. MTS - CellTiter 96® AQueous One Solution Reagent was purchased from Promega Corp., Madison, WI, USA. DMEM and EpiLife® mediums were purchased from Invitrogen Corp., Carlsbad, CA. Gelva ® GMS 3083 adhesive - ethyl acetate was provided by CYTEC Products, Inc., Elizabethtown, KY, USA. 3M Scotchpak™ 9732 Backing - polyester film laminate and 3M Scotchpak™ 9741 Release Liner – fluoropolymer coated polypropylene film were provided by 3M, Inc., St. Paul, MN, USA.

4.1.2. Equipment

Franz diffusion cells (PermeGear, Inc., Hellertown, PA, USA), Phoresor II Auto – Iontophoresis Power Device (Donated by Iomed, Inc.), HPLC system (model: Agilent or HP 1100 series),

Scanning Electron Microcopy (SEM) Model AMARY – 18301, (AMARY, Inc., Menlo Park, CA), Differential Scanning Calorimetry (DSC) Model 823_e (Mettler, Toledo, OH).

4.2 Methodology

4.2.1 Experimental Procedures

Porcine Skin Sample Preparation

Porcine skin obtained from young Yorkshire pigs (3 - 4 months old; 25 – 30 kgs, University of Medicine and Dentistry of ***New*** Jersey, Newark, NJ) was excised and dermatomed using Padgett® Model B Electric Dermatome (Integra LifeSciences, Plainsboro, NJ). The thickness of the dermatomed skin ranged 500-600 μm. The dermatomed skin was then cut into appropriate size of 1.0 cm^2 and stored at – 80 °C no more than 3 months prior to use. Prior to an experiment, the skin was thawed at room temperature and hydrated in Phosphate Buffer Saline (PBS) solution for one hour before the skin was placed on the donor compartment of Franz diffusion cells.

Preparation of Ag and AgCl Electrodes

Pure silver (Ag) wire with 0.5 mm in diameter was used as the anodal electrode. A AgCl electrode was prepared by dipping silver chloride powder coated silver wire and a pure silver wire into 0.1N HCl solution, and connecting them to a power source 3 mA for 12 hours. The purple layer coated silver wire – AgCl electrode was later used as a cathodal electrode in the iontophoretic experiment.

Chemical Enhancer Solution Preparation

All enhancer solutions were prepared at 2.5% and 5% w/v in water or propylene. The DDAIP HCl solutions were prepared in either water or propylene glycol (PG). The Br-iminosulfurane, DDAIP and Azone solutions were prepared in PG only due to their low aqueous solubilities.

***In Vitro* Transdermal Permeation Study**

Franz Diffusion Cells

The Franz diffusion cell was an in vitro model that is used as a standard for measuring the permeability of compounds into and across skin or other biological membranes. The major components of a diffusion cell included a donor chamber, a receptor chamber, a sampling port, a cell clamp, and a jacket that was connected to a water source. Figure 15 shows the schematic of the Franz diffusion cell [153].

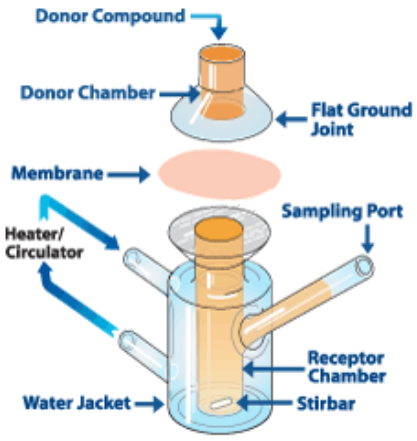

Figure 15. Schematic of Franz diffusion cell

The receiver chamber contained 5.1mL of phosphate buffer saline solution that was of physiological pH of approximately 7.4. The selected drug formulation was placed in the donor chamber and the top was sealed with Parafilm® to reduce evaporation. The membrane was held

between the receiver and donor chamber by the cell clamp. The water jacket surrounded the receiver chamber and was heated at a constant temperature of 37°C.

Phoresor II Auto (Model 850, Iomed, Inc.)

Phoresor II Auto (Model 850, Iomed, Inc.) was used to provide current for the iontophoresis studies (Figure 16).

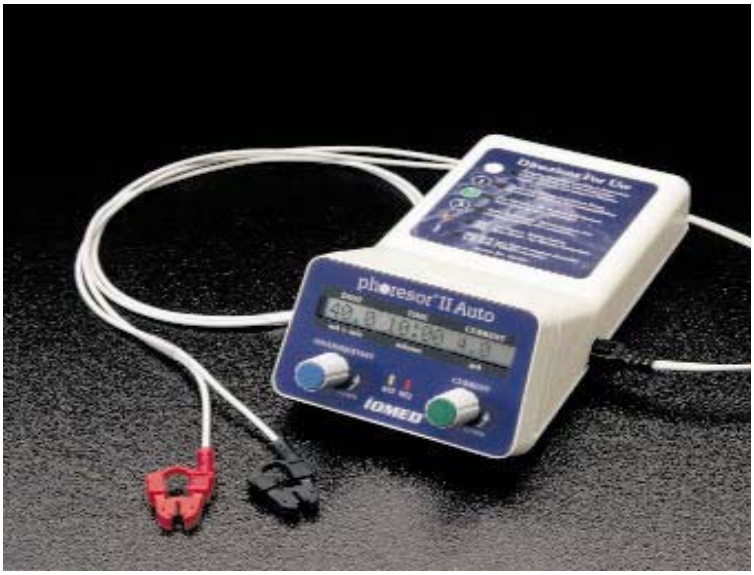

Figure 16. Phoresor II Auto (Model 850, Iomed).

***In Vitro* Transdermal Permeation Study**

Franz diffusion cells were used for all i*n vitro* permeation studies using buccal tissue under varying conditions: passive (control), 1.0 hr or 3.0 hr enhancer pretreatment, 8.0 hrs of iontophoretic treatment (0.1, 0.2 and 0.3 mA), and combined treatment of 1.0 hr enhancer pretreatment and 8.0 hrs iontophoresis at 0.3 mA, and then passive only up to 24 hrs. All experiments were performed at 37°C.

For the passive permeation study, Franz cell receptor compartment was filled with PBS solution and stirred at 600 rpm. The skin tissue was placed in between the donor and receptor compartments with the dermal side facing the donor compartment. The available diffusion area was 0.64 cm^2. 0.3 ml of the drug formulation was added into the donor compartment at the beginning of the experiment. At different time points (0.0, 0.5, 1.0, 3.0, 5.0, 8.0, 12, 20.0, 24.0 hrs), 300 µl sample was withdrawn from receptor compartment for HPLC analysis and immediately replaced with 300 µl of PBS (pH =7.4).

For enhancer pretreatment, the same procedures described above for passive permeation were followed except that the skin tissue was pretreated for 1 hr by adding 30 µl of chemical enhancer solution on top of buccal tissue in the donor compartment prior to the application of 0.3 ml drug formulation.

For iontophoresis, Phoresor II Auto (Model PM 850) provided 0.1, 0.2 and 0.3 mA for 8 hrs of treatment as well as 0.1 mA for 24 hrs (Figure 3). The anodal electrode (Ag) was placed in the gel formulation in the donor compartment about 2 mm above the buccal tissue membrane. The cathode (AgCl) was inserted into the receptor compartment. After 8 hours, iontophoresis was discontinued and then the passive-only permeation experiment continued for 16 hrs. The sampling method and time points were the same as for passive and chemical enhancer pretreatment permeation experiments.

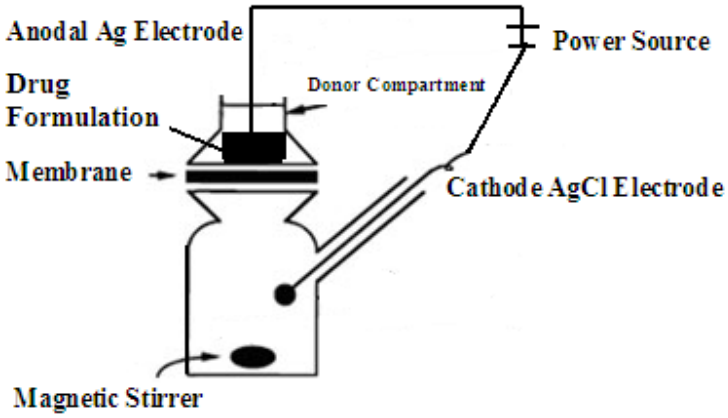

Figure 17: Placement of electrodes for iontophoresis

HPLC Assay Methods

HPLC system (model: Agilent or HP 1100 series) included degasser, pump, auto-sampler, and VWD detector (model# G1314A).

Lidocaine HCl [154]

a. Mobile phase preparation: Add 35 ml of glacia acetic acid (99%) into 930 ml of deionized water and mix until uniform. Then adjust its pH = 3.4 using 1 N NaOH solution. In the end, mix 4 volume of the above solution with 1 volume of acetonitrile until uniform.

b. HPLC operational parameter: mobile phase flow rate was1.5 ml/min;

column temperature was 25 °C; UV wavelength was254 nm; column used wasWaters Column Part No. WAT011695); injection volume was 15 µl.

Nicotine Hydrogen Nitrate (modified from [155])

a. Mobile phase preparation of 1500 ml: 5 Phosphate buffer saline (PBS) tablets were added into 1000 ml of water, mix until uniform; add 7.5 ml of Triethylamine and mix until uniform; then add glacial acetic acid (99%) to adjust pH=6.8. In the end, add 500 ml of methanol and mix until uniform.

b. HPLC operational parameters: Flow rate was1.4 ml/min; column temperature was 25 °C; UV was 256 nm; injection volume was 20 µl; column used was 150 x 4.6 mm C18 (2) 100 A Luna 5µm, Phenomenex.

Diltiazem HCl (modified from [156])

a. Mobile phase preparation of 1000 ml: Add glacial acetic acid to 200 ml of deionized water and mix well until pH = 3.1; then add 800 ml of methanol and mix until uniform; in the end adjust pH = 6.8 using triethylamine.
b. HPLC operational parameters: Flow rate was 1.2 ml/min; column temperature was 25 °C; UV wavelength was 236 nm; injection volume was 20 µl; column used was 150 x 4.6 mm Luna 5µm Phenyl-Hexyl, Phenomenex

Ondansetron HCl (modified from [157])

a. Mobile phase preparation of 1500 ml: 5 Phosphate buffer saline (PBS) tablets were added into 600 ml of water, mix until uniform; then add 900 ml of methanol and mix until uniform
b. HPLC operational parameters: Flow rate was1.0 ml/min; column tempaerature was 25 °C; column used was 150 x 4.6 mm C18(2) 100 A Luna 5µm, Phenomenex UV wavelength was 310 nm; injection volume was20 µl.

4.3 Data Analysis

The *in vitro* transdermal permeation data obtained was plotted as the cumulative corrected amount of drug penetrated into the receptor as a function of time.

The steady state flux at time t (J, μg cm $^{-2}$ hr^{-1}) was calculated from the slope of the linear portion of the profile of cumulative drug amounts permeated *vs*. time. The cumulative drug amount in the receptor compartment after 8 hrs and 24 hrs was defined as Q_8 and Q_{24} (μg cm $^{-2}$), respectively. The enhancement ratio (ER) for flux was calculated as follows:

$$ER = \frac{\text{Flux for treated sample with enhancer or iontophoresis or their combination}}{\text{Flux for untreated sample}}$$

Results were presented as mean±standard error (n) where n represented the number of replicates. Data analysis of flux was performed for treated tissue against control by the unpaired Student's t-test. ANOVA was used to compare fluxess among different treated tissues. A probability of less than 5% ($p<0.05$) was considered significant.

4.4 Evaluation of Skin Integrity

4.4.1 Scanning Electron Microscope (SEM)

It was reported in the literature that SEM can be used to investigate the effect of iontophoresis and chemical enhancer on the surface as well as cross sections of skin. Wang, *et al*., [13] used SEM to investigate the effect of pretreatment with fatty acids in PG on human SC. They found that the pretreatment caused the opening up of the tightly packed human SC cell layers and

particularly 10% oleic acid pretreatment for 1 h resulted in detachment and separation of the corneocytes on the surface of the skin. In this study, the same approach was taken to evaluate the morphological changes in both untreated and treated skin tissues.

SEM Experiment Procedures

Skin samples were embedded in OCT Compound (Tissue-Tek®, 4583) under dry ice, and then the cross-sections of the frozen samples were cut using a microtome (Leica Model CM 1850, Leica Microsystems, Inc. Bannockburn, IL, USA). The samples were defrosted and fixed with 4% formaldehyde for 1.5 hour and then washed with water at room temperature for 2 hours before being dehydrated with 30%, 50%, 75%, and 95% ethanol in water for 25 minutes each, respectively, and then with two exchanges of absolute ethanol for 2 hours at room temperature. After the dehydration, the samples were dried with a critical-point drier (model CPD 020) and coated with gold Sputter Coater: SCD 004. Surfaces and cross-sections of the samples were pictured using SEM (model AMARY-18301).

4.4.2 Differential Scanning Calorimetry (DSC)

The unique composition of the skin SC and buccal epithelium lipids and their complex structural arrangement is believed to play a major role in the barrier function of skin SC and buccal epithelium lipids [22,158]. Data obtained from infrared, thermal, and fluorescence spectroscopic examinations of the SC and its components imply that enhancer improved drug permeation through the SC is associated with alterations involving the hydrocarbon chains of the skin SC and buccal epithelium lipids [22]. DSC as a valuable tool has been used to characterize transition temperatures of SC lipids through heating the SC samples to high temperatures (100 to

250 °C) to evaluate the integrity of lipids within skin SC and buccal epithelium lipids [158,159,160]. Therefore, in this study, DSC was used to monitor thermo behavioral change of skin SC and buccal epithelium lipids from enhancer or iontophoresis treatment.

Differential Scanning Calorimetry (DSC) Procedures

Pig skin samples with / without iontophoretic and chemical enhancer treatment were first washed with deionized water, then soaked in 0.25% Trypsin solution (GIBCO™, Nitrogen Corp.) overnight. The stratum corneum (SC) was isolated from underlying epidermis by trypsin digestion. The SC samples were then washed under deionized water for at least15 minutes prior to DSC run [161]. Buccal epithelium was separated from the buccal tissue by soaking the buccal tissue in 60 ^{o}C water for 5 mins.

Untreated and treated (with / without iontophoresis and chemical enhancer) pig stratum corneum sample was placed in an aluminum pan, weighed and sealed with an aluminum cover. The reference was an empty sample pan. Nitrogen was passed through the cell with a constant flow rate of 60 ml/min. Thermograms were measured by heating the samples from 25 to 250^{o} C at a heating rate of 10^{o} C / min using DSC 823$_{e}$ (Mettler Toledo). Transition temperatures of pig stratum corneum were recorded from the thermograms.

4.5. Skin Cytotoxicity Study

MTS 3-(4, 5-dimethylthiazol-2-yl)-5-(3-carboxymethoxyphenyl)-2-(4-sulfophenyl)-2H-tetrazolium, inner salt) assay was used to evaluate enhancer cytotoxicity in buccal tissues. MTS assay is based on the ability of a mitochondrial dehydrogenase enzyme derived from viable cells to cleave the tetrazolium rings and form purple color formazan crystals that are largely impermeable to cell membranes, thus resulting in their accumulation within healthy cells [162].

The number of surviving cells is directly proportional to the level of the formazan. The color can then be quantified at 490 nm using Microplate Power Wave X Scanning Spectrophotometer (Bio-TEK Instruments, Inc., Winooski, VT, USA). MTS cell proliferation assays on human dermal fibroblast (HDF) and in human keratinocytes cells (HK) were performed after cells were seeded at 8000 cells/well in appropriate media (DMEM and EpiLife® respectively) and left in an incubator (37 ^{o}C, 5% CO_2) for 24 hours in 96-well plates. 1 µl of each enhancer solution (DDAIP HCl in water and DDAIP in PG) at several concentrations: 18.0 µM, 1.8 µM, 0.018 µM, 0.0018 µM for DDAIP HCl in water and 16.0 µM, 1.6 µM, 0.16 µM and 0.0016 µM for DDAIP HCl in propylene glycol (n=6), were applied to the cells along with 99 µl of DMEM medium for HDF and 99 µl of EpiLife® medium for HK, and then placed in the incubator for another 24 hours. Sterilized water was used as a negative control. After that 100 µl of premixed MTS solution (CellTiter 96® AQueous One Solution; ratio of MTS reagent : assay medium = 1:4) was added to each of the wells. The 24-well plate was then returned to the incubator for 2 hours. After this, 100 µl of the reacted MTS solutions from each well was pipetted into a marked 96-well microtiter plate for spectrophotometer reading (SPR) at 490 nm using the scanning spectrophotometer. 100µl of assay medium was used as a blank. All SPR readings were deducted from the SPR reading of blank.

% Cell Viability = 100 x [SPR for Treated Sample/ SPR for Negative Control] [162]

4.6 Results and Discussion

4.6.1. Lidocaine HCL Transdermal Delivery

4.6.1.1 Enhancement Using Iontophoresis

Table 5. Effect of 8.0 hr iontophoresis treatment on transdermal delivery of LHCl [a]

Treatment	Flux (μg/cm^2*h)	Q_8 (μg/cm^2)	Enhancement Ratio (ER)
Control	7.4±5.8	59.7±43.4	1
0.1	61.7±20.8	494.0±152.0	8.3
0.2	251.5±57.3 [b]	1924.8 ±425.7	33.9
0.3	375.6±69.44 [b]	2879.2±531.1	50.8

[a] Data are presented as means ± S.D. ($3 \leq N \leq 8$).

[b] Statistically significantly higher than control and 0.1 mA ($p < 0.05$).

Control – untreated passive; 0.1 mA – 0.16 mA/cm^2; 0.2 mA – 0.31 mA/cm^2;

0.3 mA – 0.47 mA/cm^2

Q_8 – drug cumulative amount permeated within 8 hrs; ER – enhancement ratio

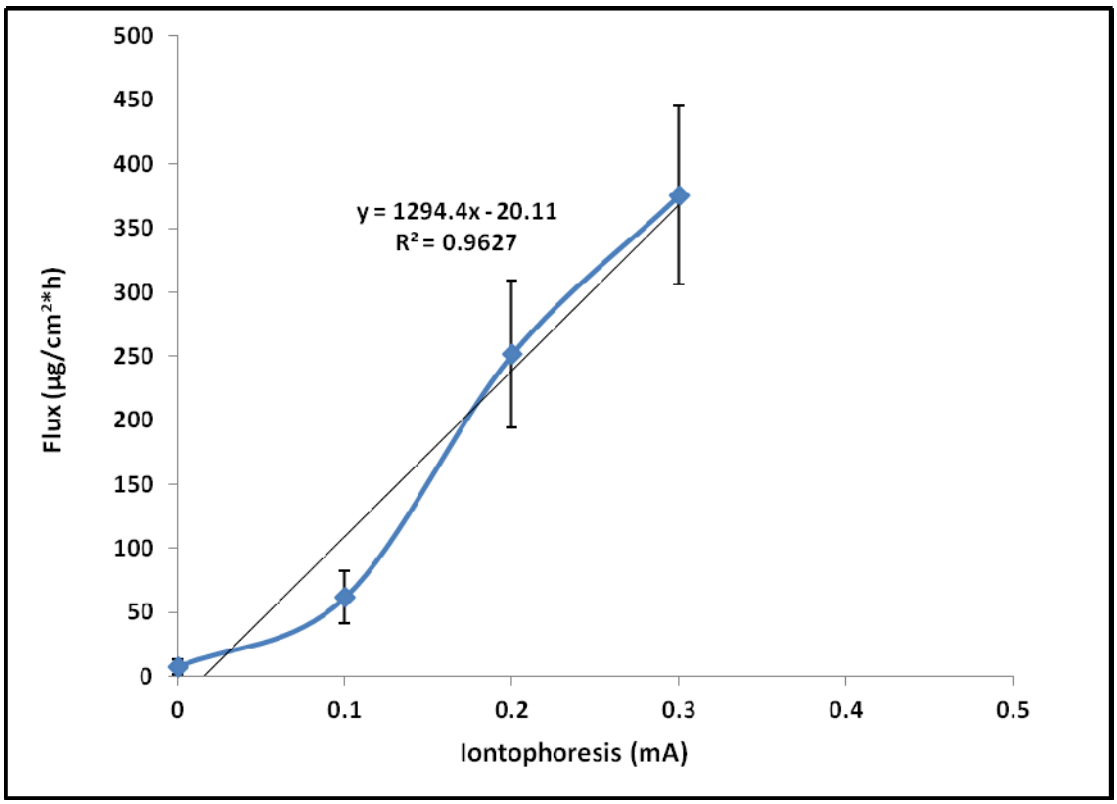

Figure 18. The effect of current intensity on flux of LHCl through porcine skin

Effect of iontophoresis at 0.1, 0.2 and 0.3 mA on transdermal delivery of LHCl through porcine skin was performed using *in vitro* Franz cell diffusion model. Table 5 showed that when compared to control, significant enhancement effect was achieved using iontophoresis at 0.1, 0.2, and 0.3 mA, and increasing current intensity linearly increased the enhancement effects (Figure 18). Both 0.2 mA and 0.3 mA had significantly higher enhancement effects than that of 0.1 mA. However, the enhancement effect from 0.3 mA and 0.2 mA was not significantly different. When a 10 cm^2 patch is used for 24 h, 0.3 mA iontophoresis can potentially deliver 3 x Q_8 x 10 = 3 x 2879 x 10 = 86 mg / day, i.e., a therapeutic level: an epidural dose of LHCl can be reached.

4.1.2 Enhancement Using Chemical Enhancers

Effect of enhancer concentration and pretreatment duration on transdermal delivery of LHCl

The effects of enhancer concentration and pretreatment duration were evaluated using *in vitro* Franz cell diffusion model on porcine skin. Results from Table 6 demonstrated that within 8 hrs of permeation study, when compared to control, 1.0 h pretreatment of 5.0% (w/v) Br-iminosulfurane demonstrated significant enhancement effect, and 5.0% (w/v) DDAIP 1.0 hpretreatment provided directional enhancement effect, but DDAIP HCl and Azone at both 2.5% (w/v) and 5.0%, DDAIP and Br-iminosulfurane at 2.5% (w/v) did not show enhancement effect. Increasing concentration of enhancers did directionally increase the enhancement effect for enhancers DDAIP and Br-iminosulfurane, indicating that enhancer concentration was an important factor for enhancering transdermal delivery of LHCl. However, it was opposite for Azone because directionally 2.5% Azone was more effective than 5.0% Azone, which was in line with results from literature [98]. A. C. Williams, *et al*., [98] indicated that Azone was most effective at low concentrations between 1.0 – 3.0%.

Tables 7 and 8 demonstrated that increasing enhancer pretreatment duration of 5.0% DDAIP and 5.0% Br-iminosulfurane from 1.0 h to 3 h, almost 4-fold increase in enhancement effect was achieved. However, increasing enhancer pretreatment duration of 5.0% Azone and 5% DDAIP HCl did not impact the enhancement effect significantly. This further demonstrated that the mechanisms of enhancement effects from DDAIP and Br-iminosulfurane were not identical to those of Azone that was in agreement with the discussion provided in Section 2.6.3 of Chapter 2. Azone is believed to be an effective enhancer due to its ability to interact with / fluidizing the

puckered lipid domains of the stratum corneum [98]. DDAIP was reported to enhance drug transport by interacting with the polar region of the phospholipid bilayer and promoting the motional freedom of lipid hydrocarbon [122]. The mechanisms of action of Br-iminsulfurane was reported to include its solvent effect that increased drug partitioning in the SC, interaction with lipids in the SC, and interaction with protein in the SC [15]. It was noticed that DDAIP was more effective than DDAIP HCl. It may be explained as that due to hydrophobic characteristic of skin, hydrophobic DDAIP had more interactions with skin lipids than hydrophilic DDAIP HCl. In addition, when compared to iontophoresis, enhancement effects from the tested chemical enhancers were significantly smaller than that obtained from 0.2 mA and 0.3 mA iontophoresis treatment ($p<0.05$), indicating that iontophoresis was more effective in enhancing transdermal delivery of LHCl.

Table 6. Effect of 1.0 h enhancer pretreatment on transdermal delivery of LHCl [a]

Treatment	Flux ($\mu g/cm^2*h$)	Q_8 ($\mu g/cm^2$)	ER
Control	7.4±5.8	59.7±43.4	1
Propylene Glycol (PG)	8.4±11.4	74.11±97.9	1.1
2.5% Azone in PG	9.6±2.8	87.3±23.2	1.4
5.0% Azone in PG	4.0±6.2	17.7±36.4	1
2.5% DDAIP in PG	7.4±5.5	57.7±42.6	1
5.0% DDAIP in PG	15.0±9.6	113.9±73.8	2.1
2.5% DDAIP HCL in Water	8.5±10	66.2±75.3	1.1
5.0% DDAIP HCL in water	9.8±7.1	79.9±57.8	1.3
2.5% DDAIP HCL in PG	3.6±7.9	30.5±68.1	1
5.0% DDAIP HCL in PG	7.0±3.3	66.8±31.7	1
2.5% Br-Iminosulfurane in PG	10.4±22.3	80.2±167.0	1.4
5.0% Br-Iminosulfurane in PG	35.4±8.8 [b]	266.5±69.4	4.8

[a] Data are presented as means ± S.D. ($3 \leq N \leq 8$).

[b] Statistically significantly higher than control ($p < 0.05$).

Table 7. Effect of 3.0 h enhancer pretreatment on transdermal delivery of LHCl at 8 h [a]

Treatment	Flux ($\mu g/cm^2*h$)	Q_8 ($\mu g/cm^2$)	ER
Control	7.4±5.8	59.7±43.4	1
PG	7.1±6.6	61.9±49.8	1
5.0% Azone in PG	1.8±1.3	16.6±10.4	1
5.0% DDAIP in PG	46.0±8.9 [b]	357.2±77.6	6.2
5.0% DDAIP HCL in water	7.9±6.6	71.5±69.0	1
5.0% DDAIP HCL in PG	14.7±13.6	113.2±105.2	2
5.0% Br-Iminosulfurane in PG	68.6±13.5 [b]	515.5±108.7	9.3

[a] Data are presented as means ± S.D. ($3 \leq N \leq 8$).

[b] Statistically significantly higher than control and the other enhancers ($p < 0.05$).

Table 8. Effect of 3.0 h enhancer pretreatment on transdermal delivery of LHCl at 24 h [a]

Treatment	Flux ($\mu g/cm^2*h$)	Q_{24} ($\mu g/cm^2$)	ER
Control	10.0±6.5	234.33±145.0	1
PG	11.8±8.2	269.6±187.7	1.2
5.0% Azone in PG	9.4±5.0	221.8±118.0	1
5.0% DDAIP in PG	46.1±12.4 [b]	1074.5±279.6	4.6
5.0% DDAIP HCL in PG	10.1±10.5	238.0±250.8	1
5.0% Br-Iminosulfurane in PG	55.8±78.6 [b]	1360.0±1894.6	7.8

[a] Data are presented as means ± S.D. ($3 \leq N \leq 8$).

[b] Statistically significantly higher than control and the other enhancers ($p < 0.05$).

Q_{24} – cumulative amount permeated within 24 hrs

4.1.3 Combined Enhancement Effect

Combined treatments of iontophoresis and chemical enhancers were conducted to investigate their synergistic enhancement effects on transdermal delivery of LHCl using *in vitro* Franz cell diffusion model on porcine skin.

Table 9 demonstrated that combined effect of iontophoresis (0.3 mA for 8.0 h) and chemical enhancer pretreatment (1.0 h) significantly enhanced transdermal delivery of LHCl and iontophoresis (0.3 mA for 8.0 h) was the dominated contributor for the combined enhancement effects. It was observed that only the combined treatment of 2.5% (w/v) and 5.0% (w/v) Br-iminosulfurane and 0.3 mA 8.0 h of iontophoresis provided synergistic enhancement effect. Again similar observations were obtained: except for Azone, increasing enhancer concentration of DDAIP and Br-iminosulfurane from 2.5% to 5.0% at least directionally increased their enhancement effects. It also clearly demonstrated that increasing hydrophilic DDAIP HCl concentration from 2.5% to 5.0% decreased the combined enhancement effect. This may be explained as: positive charges from DDAIP HCl compound were competing with LHCl for iontophoresis. Figure 19 shows that values for cumulative LHCl permeated through skin transdermally exhibited the same trend as for flux values.

Table 9. Effect of combined treatment of 1.0 hr enhancer pretreatment and 8.0 hr iontophoresis (0.3 mA) on transdermal delivery of LHCl [a]

Treatment	Flux ($\mu g/cm^2*h$)	Q_8 ($\mu g/cm^2$)	ER
Control	7.4±5.8	59.7±43.4	1
0.3 mA	375.6±69.44 [b]	2879.2±531.1	50.8
PG+0.3 mA	455.4±64.1 [b]	3602.8±500.3	61.5
2.5% Azone in PG+0.3 mA	430.0±99.4 [b]	3407.0±790.0	61.5
5.0% Azone in PG+0.3 mA	359.5±32.1 [b]	2826.7±244.6	48.6
2.5% DDAIP in PG+0.3 mA	456.6±82.0 [b]	3602.9±709.1	61.7
5.0% DDAIP in PG+0.3 mA	376.1±51.4 [b]	2975.6±388.9	50.8
2.5% DDAIP HCL in Water+0.3 mA	410.6±51.9 [b]	3224.3±407.9	55.5
5.0% DDAIP HCL in water+0.3 mA	293.5±41.8 [b]	2336.1±317.1	39.7
2.5% DDAIP HCL in PG+0.3 mA	395.7±133.9 [b]	3076.6±1054.5	53.5
5.0% DDAIP HCL in PG+0.3 mA	187.4±53.9 [b]	1543.3±418.3	25.3
2.5% M Br-Iminosulfurane in PG+0.3 mA	490.1±156.1 [b]	3944.1±1170.9	66.2
5.0% Br-Iminosulfurane in PG+0.3 mA	630.8±124.5 [b]	4896.5±954.8	85.2

[a] Data are presented as means ± S.D. ($3 \leq N \leq 8$).

[b] Statistically significantly higher than control ($p < 0.05$).

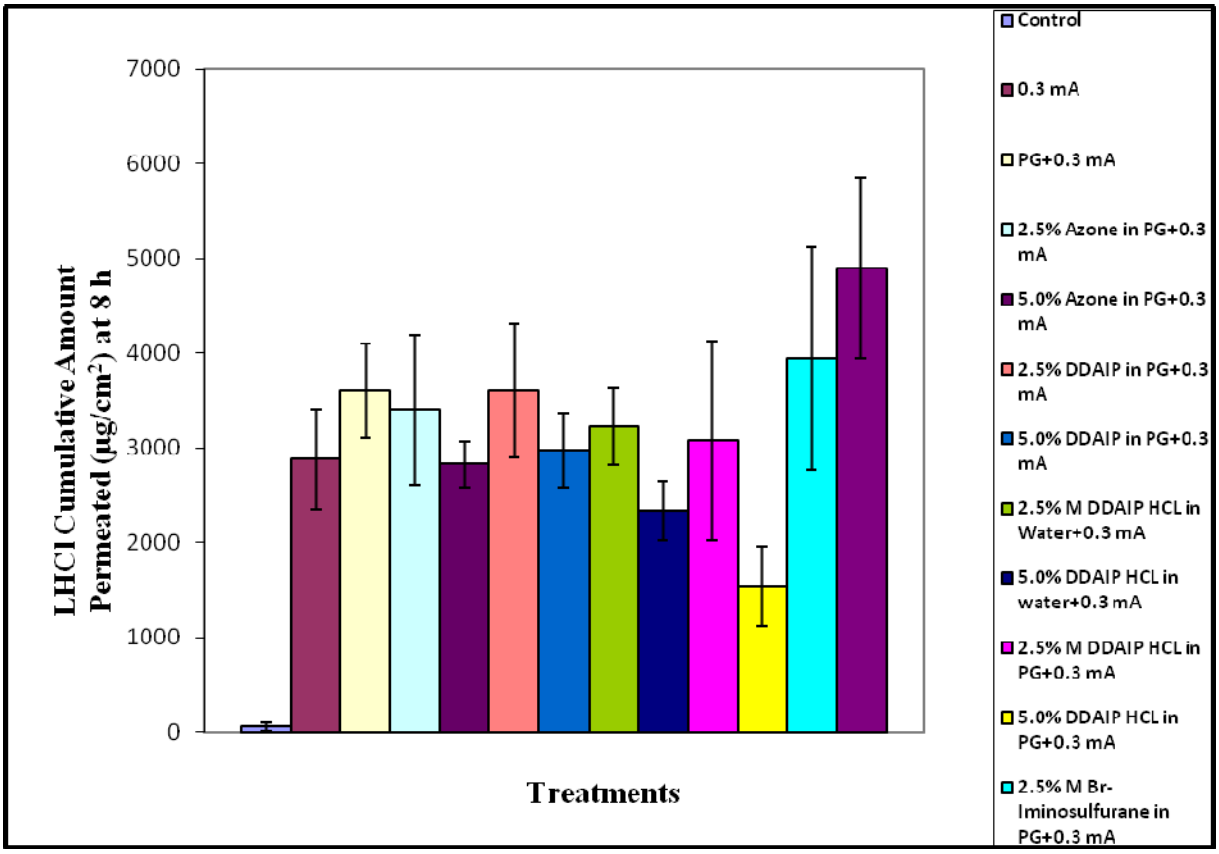

Figure 19. Combined effect of iontophoresis and enhancer on transdermal delivery of LHCl

To evaluate the effect of enhancer pretreatment duration and current intensity on the combined enhancement effect of iontophoresis and enhancer on transdermal delivery of LHCl, different pairs of combined enhancer and iontophoresis treatments were applied on porcine skin. 1.0 hr enhancer pretreatment plus 8.0 h 0.3 mA iontophoresis, 3.0 h enhancer pretreatment plus 8.0 h 0.1 mA iontophoresis, 3.0 h enhancer pretreatment plus 8.0 hrs 0.3 mA were chosen for the study. The results (Table 9, 10 and 11) demonstrated that for the same enhancer pretreatment duration of 3 h, for all tested enhancers, increasing current intensity of iontophoresis from 0.1 mA to 0.3 mA significantly increased the combined enhancement effects ($p<0.05$); for the same

iontophoresis treatment (0.3 mA for 8.0 h), increasing enhancer pretreatment duration from 1.0 hr to 3.0 h had no significant impact on their combined enhancement effects. This further indicated that iontophoresis was the dominating force for enhancing transdermal delivery of LHCl when used in combination with enhancement pretreatment.

In addition, it was found (Table 10 and 11, Figure 7) that when the total iontophoresis "dosing" was the same: from Table 10, it was: 0.3 mA x 8 h = 2.4 mA*h; from Table 10, it was: 0.1 mA x 24 h = 2.4 mA*h, for all tested enhancers, 0.3 mA for 8 hrs iontophoresis always demonstrated significantly higher enhancement effect ($p<0.05$). However, combined treatment of 0.1mA for 24 h of iontophoresis and enhancer seemed to deliver higher total drug accumulated amount permeated than the combined treatment of 0.3 mA 8.0 h of iontophoresis and enhancer. Therefore, depending on purpose, higher current intensity can dramatically increase the mode of action while low current intensity can be more suitable for sustained drug release.

Table10. Effect of combined treatment of 3.0 h enhancer pretreatment and 8.0 h iontophoresis (0.1 mA) on transdermal delivery of LHCl[a]

Treatment	Flux ($\mu g/cm^2*h$)	Q_8 ($\mu g/cm^2$)	ER
Control	7.4±5.8	59.7±43.4	1
0.1 mA	61.7±20.8[b]	494.0±152.0	8.3
PG+0.1 mA	133.3±23.7[b]	1040.9 ±180.7	12.6
5.0% Azone in PG +0.1 mA	103.2±11.3[b]	823.3±83.6	10.3
5.0% DDAIP in PG +0.1 mA	168.8±33.4[b]	1334.6±260.8	22.8
5.0% DDAIP HCL in PG+0.1 mA	61.7±20.8[b]	494.0±152.0	8.3
5.0%% Br-Iminosulfurane in PG+0.1 mA	138.1±23.8[b]	1086.2±183.3	18.7

[a] Data are presented as means ± S.D. ($3 \leq N \leq 8$).

[b] Statistically significantly higher than control ($p < 0.05$).

Table 11. Effect of combined treatment of 3.0 h enhancer pretreatment and 8.0 h iontophoresis (0.3 mA) on transdermal delivery of LHCl [a]

Treatment	Flux ($\mu g/cm^2*h$)	Q_8 ($\mu g/cm^2$)	ER
Control	7.4±5.8	59.7±43.4	1
0.3 mA	375.6±69.4 [b]	2879.2±531.1	50.8
5.0% Azone in PG+0.3 mA	283.1±48.7 [b]	2241.1±377.7	38.3
5.0% DDAIP in PG+0.3 mA	429.7±42.1 [b]	3412.8±303.4	58.1
5.0% DDAIP HCL in PG+0.3 mA	286.1±71.6 [b]	2277.6±559.9	38.7
5.0% Br-Iminosulfurane in PG+0.3 mA	608.6±93.9 [b]	4765.8±694.7	82.2

[a] Data are presented as means ± S.D. ($3 \leq N \leq 8$).

[b] Statistically significantly higher than control ($p < 0.05$).

Table 12. Effect of combined treatment of 3.0 h enhancer pretreatment and 24 h iontophoresis (0.1 mA) on transdermal delivery of LHCl [a]

Treatment	Flux ($\mu g/cm^2*h$)	Q_{24} ($\mu g/cm^2$)	ER
Control	10.0±6.5	234.33±145.0	1
0.1 mA	105.2±17.6 [b]	2605.1±441.8	10.5
PG+0.1 mA	167.1±23.1 [b]	4006.9 ±549.2	16.7
5.0% Azone in PG+0.1 mA	132.5±9.8 [b]	3121.8±241.8	13.3
5.0% DDAIP in PG+0.1 mA	192.6±29.5 [b]	4538.1±699.2	19.3
5.0% DDAIP HCL in PG+0.1 mA	101.5±16.0 [b]	2453.3±520.4	10.1
5.0% Br-Iminosulfurane in PG+0.1 mA	180.1±20.0 [b]	4228.0±481.9	18.1

[a] Data are presented as means ± S.D. ($3 \leq N \leq 8$).

[b] Statistically significantly higher than control ($p < 0.05$).

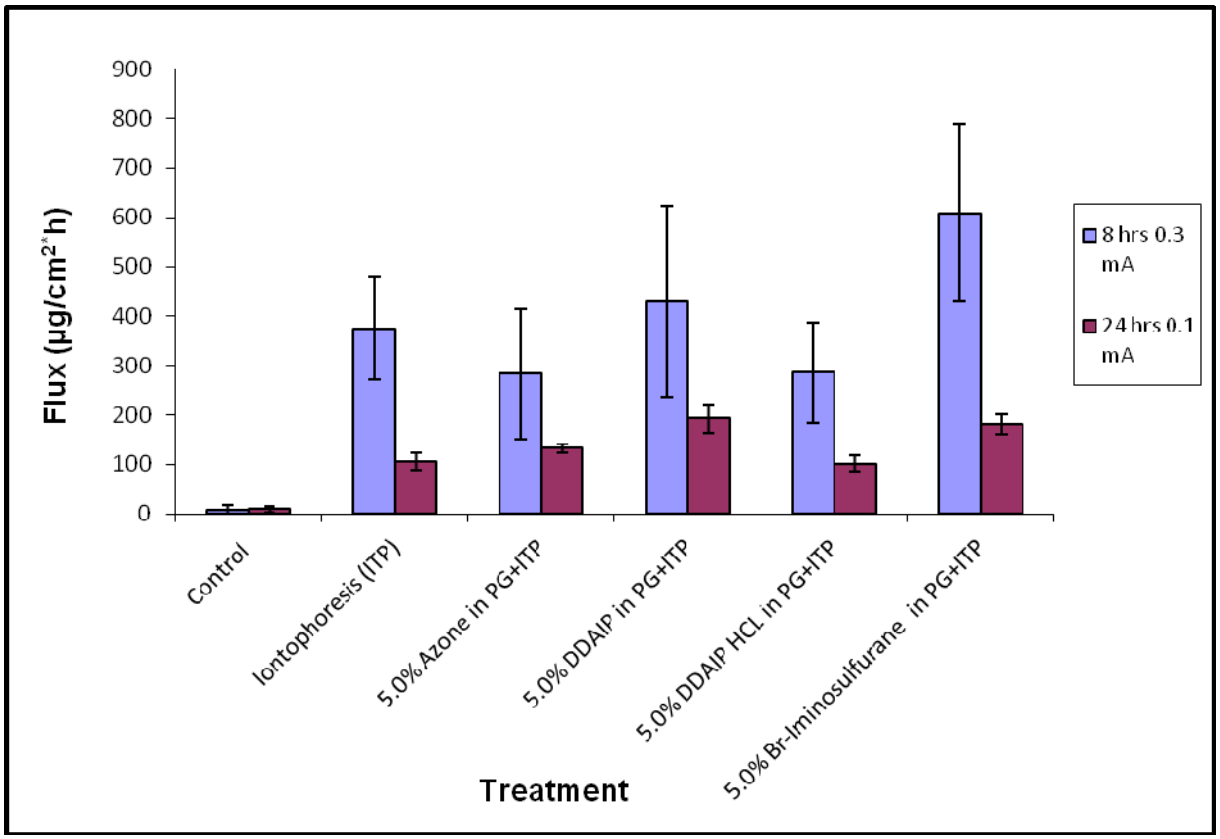

Figure 20. Flux comparison between 0.1 mA 24 hr vs 0.3 mA 8 hr treatment. ITP – iontophoresis

4.6.2 Nicotine Hydrogen Tartrate Transdermal Drug Delivery

4.6.2.1 Enhancement Using Iontophoresis

Table 13. Effect of current on transdermal delivery of NHT [a]

Iontophoresis (mA)	Flux ($\mu g/cm^2*h$)	Q_8 ($\mu g/cm^2$)	ER
Control	1.3±1.9	9.9±14.6	1
0.1	56.1±11.4[b]	433.2±85.4	39.8
0.3	138.4±72.3[b, c]	1326.6±186.2	106.5

[a] Data are presented as means ± S.D. ($3 \leq N \leq 8$).

[b] Statistically significantly better than control ($p < 0.05$).

[c] Statistically significantly better than that control and 0.1 mA ($p < 0.05$).

Effect of iontophoresis at 0.1 and 0.3 mA on transdermal delivery of NHT through porcine skin was performed using *in vitro* Franz cell diffusion model. Table 13 showed that when compared to control, significant enhancement effect was achieved using iontophoresis for 8 h at 0.1 and 0.3 mA and increasing current intensity linearly increased the enhancement effects (Figure 21). 0.3 mA iontophoresis had significantly higher enhancement effect than control and 0.1 mA. Also drug cumulative amount permeated significantly increased with the use of iontophoresis when compared to control. When a 10 cm^2 patch is used for 24 h, 0.3 mA iontophoresis can potentially deliver 3 x Q_8 x 10 = 3 x 1326 x 10 = 39.8 mg of NHT per day, i.e., an equivalent therapeutic level of 13 mg of nicotine per day can be achieved.

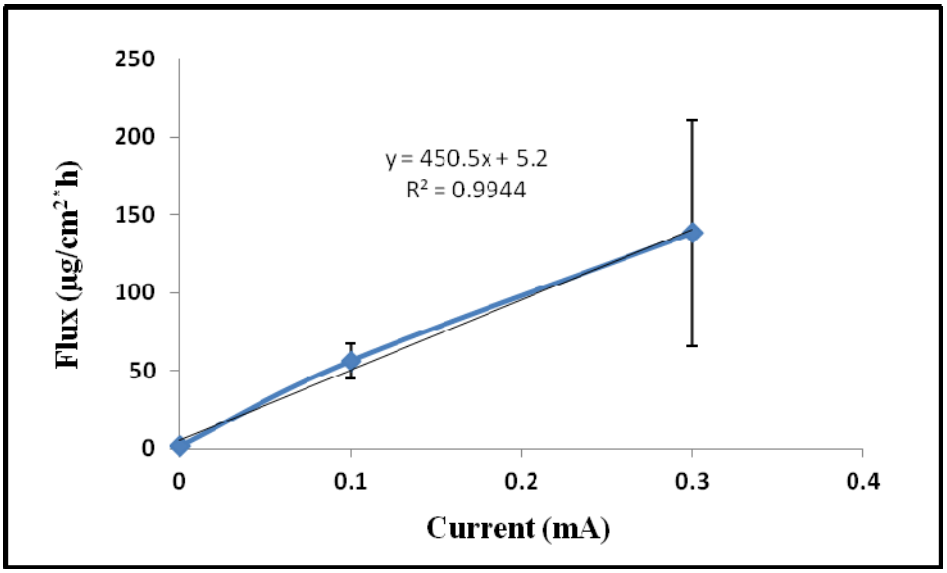

Figure 21. The effect of current intensity on flux of NHT through porcine skin

4.6.2.2 Enhancement Using Chemical Enhancer

The effect of enhancer pretreatment was evaluated using *in vitro* Franz cell diffusion model on porcine skin. Results from Table 14 and 15 demonstrated that compared to Control, none of the tested enhancers at concentration of 2.5% or 5.0% w/v provided significant enhancement effect on transdermal delivery of NHT. It may be due to the fact that NHT is a big molecular with molecular weight of 462 Da. It is very close to the threshold of 500 Da which was not recommended for passive transdermal delivery [5]. Furthermore, it indicated that iontophoresis was a much more effective approach for enhancing transdermal delivery of NHT than chemical enhancer.

Table 14. Effect of 1.0 hr enhancer pretreatment on transdermal delivery of NHT at 8 h [a]

Enhancer	Flux ($\mu g/cm^2*h$)	Q_8 ($\mu g/cm^2$)	ER
Control	1.3±1.9	9.9±14.6	1
PG	1.5±3.7	10.9±26.8	1
2.5% Azone in PG	0.9±1.4	7.7±12.4	1
5.0% Azone in PG	0.2±0.6	2.3±5.5	1
2.5% DDAIP in PG	1.4±2.5	10.9±18.5	1
5.0% DDAIP in PG	1.3±0.6	9.7±4.9	1
5.0% DDAIP HCl in Water	2.2±5.3	11.3±33.9	1
5.0% DDAIP HCl in PG	0.6±0.7	4.7±5.8	1
2.5% Br-Iminosulfurane in PG	1.0±2.5	8.8±18.9	1
5.0% Br-Iminosulfurane in PG	0.6±1.4	4.4±10.8	1

[a] Data are presented as means ± S.D. ($3 \leq N \leq 8$).

Table 15. Effect of 1.0 h enhancer pretreatment on transdermal delivery of NHT at 24 h [a]

Enhancer	Flux ($\mu g/cm^2*h$)	Q_{24} ($\mu g/cm^2$)	ER
Control	2.0±2.4	45.7±54.5	1
PG	2.5±3.3	60.6±77.2	1
2.5% Azone in PG	1.5±0.9	33.8±21.7	1
5.0% Azone in PG	0.7±0.9	17.8±17.2	1
2.5% DDAIP in PG	2.5±2.4	61.4±55.5	1
5.0% DDAIP in PG	0.8±0.4	19.8±10.6	1
5.0% DDAIP HCl in Water	3.4±5.6	78.7±133.7	1
5.0% DDAIP HCl in PG	0.7±0.9	17.9±21.7	1
2.5% Br-Iminosulfurane in PG	1.6±2.2	38.1±52.2	1
5.0% Br-Iminosulfurane in PG	0.4±0.9	9.2±22.4	1

[a] Data are presented as means ± S.D. ($3 \leq N \leq 8$).

4.6.2.3 Combination Enhancement Effect

Combined treatments of iontophoresis and chemical enhancers were conducted to investigate their synergistic enhancement effects on transdermal delivery of NHT using *in vitro* Franz cell diffusion model on porcine skin.

Table 16 and 17 demonstrated that combined treatment of iontophoresis (0.1 mA or 0.3 mA for 8.0 h) and chemical enhancer pretreatment (1.0 h) significantly enhanced transdermal delivery of NHT and iontophoresis was the dominated contributor for the combined enhancement effect. It was observed that the combined treatment of iontophoresis (0.1 mA or 0.3 mA 8.0 h) and chemical enhancer 2.5% (w/v) Azone or 5.0% (w/v) DDAIP or 5.0% (w/v) Br-iminosulfurane provided synergistic enhancement effects. It was also observed that except for Azone, increasing enhancer concentration of DDAIPand Br-iminosulfurane from 2.5% to 5.0% in combination with iontophoresis at least directionally increased their enhancement effects. Figure 8 shows that values for cumulative NHT permeated through skin transdermally exhibited the same trend as for flux values.

In addition, it was found (Table 17 and 18) that when the total iontophoresis "dosing" was the same: from Table 17, it was: 0.3 mA x 8 h = 2.4 mA*h; from Table 18, it was: 0.1 mA x 24 h = 2.4 mA*h, for all tested enhancers, 0.3 mA for 8 hrs iontophoresis always demonstrated significantly higher enhancement effect ($p<0.05$). However, combined treatment of 0.1mA for 24 h of iontophoresis and enhancer seemed to deliver higher total drug cumulative amount permeated than the combined treatment of 0.3 mA 8.0 h of iontophoresis and enhancer. Therefore, depending on purpose, higher current intensity can dramatically increase the mode of action while low current intensity can be more suitable for sustained drug release.

Table 16. Combined effect of iontophoresis 0.1 mA 8 h treatment and 1.0 h enhancer pretreatment [a]

Enhancer	Flux ($\mu g/cm^2*h$)	Q8 ($\mu g/cm^2$)	ER
Control	1.3±1.9	9.9±14.6	1
0.1 mA	56.1±11.4 [b]	433.2±85.4	43.2
PG+0.1 mA	59.1±9.5 [b]	456.0±77.9	45.5
2.5% Azone in PG+0.1 mA	66.7±11.2 [b, c]	521.3±88.5	51.3
5.0% Azone in PG+0.1 mA	42.7±12.7 [b]	277.9±162.4	32.8
2.5% DDAIP in PG+0.1 mA	39.6±7.0 [b]	312.2±56.4	30.5
5.0% DDAIP in PG+0.1 mA	68.2±7.7 [b, c]	529.9±58.2	52.5
5.0% DDAIP HCl in Water+0.1 mA	34.2±17.7 [b]	270.1±137.9	26.3
5.0% DDAIP HCl in PG+0.1 mA	53.9±65.7 [b]	413.5±497.5	41.5
2.5% Br-Iminosulfurane in PG+0.1 mA	44.1±11.9 [b]	349.3±93.2	33.9
5.0% Br-Iminosulfurane in PG+0.1 mA	92.6±34.9 [b, c]	744.7±324.8	71.2

[a] Data are presented as means ± S.D. ($3 \leq N \leq 8$).

[b] Statistically significantly better than Control ($p < 0.05$).

[c] Synergistic enhancement effects were achieved using iontophoresis and chemical enhancers.

Table 17. Combined effect of iontophoresis 0.3 mA 8 hrs treatment and 1.0 hr enhancer pretreatment [a]

Enhancer	Flux ($\mu g/cm^2*h$)	Q8 ($\mu g/cm^2$)	ER
Control	1.3±1.9	9.9±14.6	1
0.3 mA	138.4±72.3 [a]	1326.6±186.2	106.5
PG+0.3 mA	147.8±12.3 [b]	1149.09±99.3	113.7
2.5% Azone in PG+0.3 mA	205.4±31.0 [b, c]	1591.8±238.7	158.0
5.0% Azone in PG+0.3 mA	155.3±63.7 [b]	1214.7±493.4	119.5
2.5% DDAIP in PG+0.3 mA	136.7±45.2 [b]	1079.8±355.6	105.2
5.0% DDAIP in PG+0.3 mA	161.5±10.2 [b, c]	1253.5±58.2	124.2
5.0% DDAIP HCl in Water+0.3 mA	148.2±44.3 [b]	1158.4±341.8	114.0
5.0% DDAIP HCl in PG+0.3 mA	117.7±44.2 [b]	956.7±398.0	90.5
2.5% Br-Iminosulfurane in PG+0.3 mA	193.4±65.1 [b, c]	1521.5±489.0	148.8
5.0% Br-Iminosulfurane in PG+0.3 mA	203.5±38.9 [b, c]	1596.2±282.7	156.5

[a] Data are presented as means ± S.D. ($3 \leq N \leq 8$).

[b] Statistically significantly better than Control ($p < 0.05$).

[c] Synergistic enhancement effects were achieved using iontophoresis and chemical enhancers.

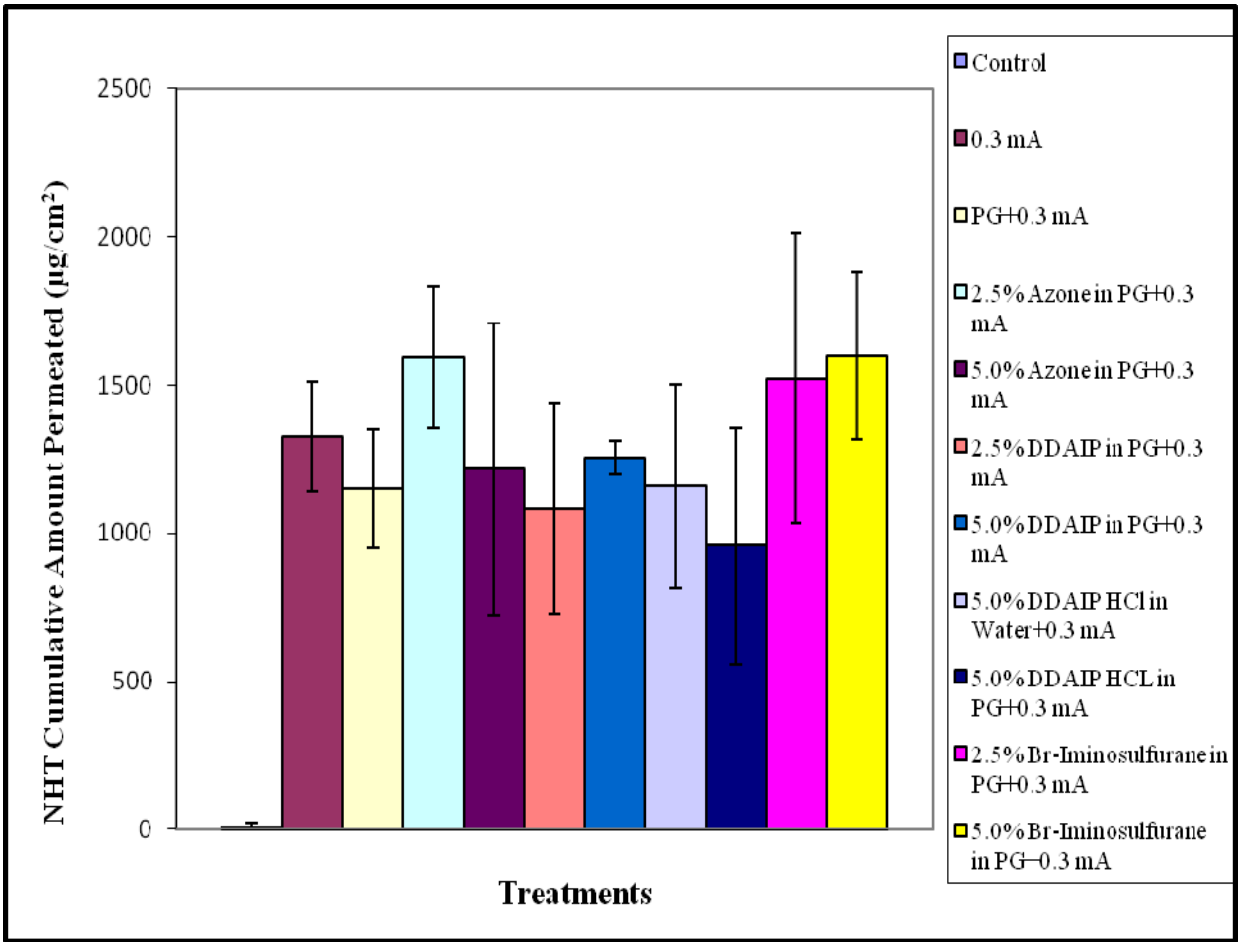

Figure 22. Combined effect of iontophoresis and enhancer on transdermal delivery of NHT

Table 18. Combined effect of iontophoresis 0.1 mA 24 hrs treatment and 1.0 hr enhancer pretreatment [a]

Enhancer	Flux ($\mu g/cm^2*hr$)	Q_{24} ($\mu g/cm^2$)	ER
Control	2.0±2.4	45.7±54.5	1
0.1 mA	58.1±9.6 [b]	1427.1±275.8	29.1
PG+0.1 mA	60.9±8.0 [b]	1453.3±195.4	30.5
2.5% Azone in PG+0.1 mA	78.6±11.7 [b]	1847.9±278.7	39.3
5.0% Azone in PG+0.1 mA	42.2±12.8 [b]	992.3±302.5	21.1
2.5% DDAIP in PG+0.1 mA	33.2±7.0 [b]	796.3±149.8	16.6
5.0% DDAIP in PG+0.1 mA	60.3±7.0 [b]	1405.7±168.0	30.2
5.0% DDAIP HCl in Water+0.1 mA	38.2±13.4 [b]	900.6±316.9	19.1
5.0% DDAIP HCl in PG+0.1 mA	32.1±18.0 [b]	784.8±481.8	16.0
2.5% Br-Iminosulfurane in PG+0.1 mA	49.8±4.4 [b]	1253.6±128.9	24.9
5.0% Br-Iminosulfurane in PG+0.1 mA	101.0±41.2 [b]	2396.9±953.2	50.5

[a] Data are presented as means ± S.D. ($3 \leq N \leq 8$).

[b] Statistically significantly better than Control ($p < 0.05$).

4.6.3 Diltiazem HCl (DHCl) Transdermal Delivery

4.6.3.1 Enhancement Using Iontophoresis

The passive permeation of DHCl through porcine skin was minimal (Table =19), which was similar to the results from murine skin obtained by Nolan [146]. Therefore, physical enhancement technique - iontophoresis at 0.1, 0.2 and 0.3 mA was applied to enhance transdermal delivery of DHCl through porcine skin using *in vitro* Franz cell diffusion model. Table 19 shows that when compared to control, significant enhancement effect was achieved using iontophoresis for 8 hrs at 0.1, 0.2 and 0.3 mA, respectively. While 0.3 mA iontophoresis had significantly higher enhancement effect than that of 0.1 and 0.2 mA, the correlation between current and flux was not linear but a S shape (Figure 23). Also drug cumulative amount permeated significantly increased with the use of iontophoresis when compared to control. It was also observed (Table 20) that even when iontophoresis was discontinued at 8 hrs, the post-iontophoretic effect on drug permeation continued to be statistically significant when compared to Control, indicating that iontophoresis increased the permeability of porcine skin for DHCl probably through first disrupting porcine stratum corneum and increasing intercellular space for enhancing transdermal drug delivery [163,164]. Furthermore, post-iontophoretic effect of 0.3 mA was significantly higher than that of 0.1 and 0.2 mA, but significantly reduced, indicating that the flux of the drug was predominantly electrically driven. This transport process was likely to involve the direct effect of the electrical field on the drug ion coupled with the indirect effect of electroosmosis. These results are in line with the hypothesis mentioned the literature [165,166,167,168], i.e. for the iontophoretic transdermal transport of low and intermediate molecular weight cations, the electroosmotic contribution is less significant than the effects of direct electrostatic repulsion and the increase in the permeability of the skin. When a 10 cm^2

patch is used for 24 h, 0.3 mA iontophoresis can potentially deliver Q_{24} x 10 = 1304 x 10 = 13.0 mg of DHCl which is about 13 x 1000 µg / 6000 ml of blood (average blood volume), i.e, 2.2 µg / ml. It is more than the required therapeutic dose of 200 ng/ml blood level of DHCl per day.

Table 19. Effect of current on transdermal delivery of DHCl (Stage I) [a]

Iontophoresis (mA)	Flux (µg/cm^2*h)	Q8 (µg/cm^2)	ER
Control	0.4±0.3	3.0±2.6	1.0
0.1	18.9±10.4[b]	154.1±83.5	47.3
0.2	29.3±5.6[b]	231.4±43.9	73.3
0.3	100.3±33.7[b, c]	796.8±276.6	250.8

[a] Data are presented as means ± S.D. (3≤N≤8).

[b] Statistically significantly higher than control ($p < 0.05$).

[c] Statistically significantly higher than 0.1 mA, 0.2 mA and control ($p < 0.05$).

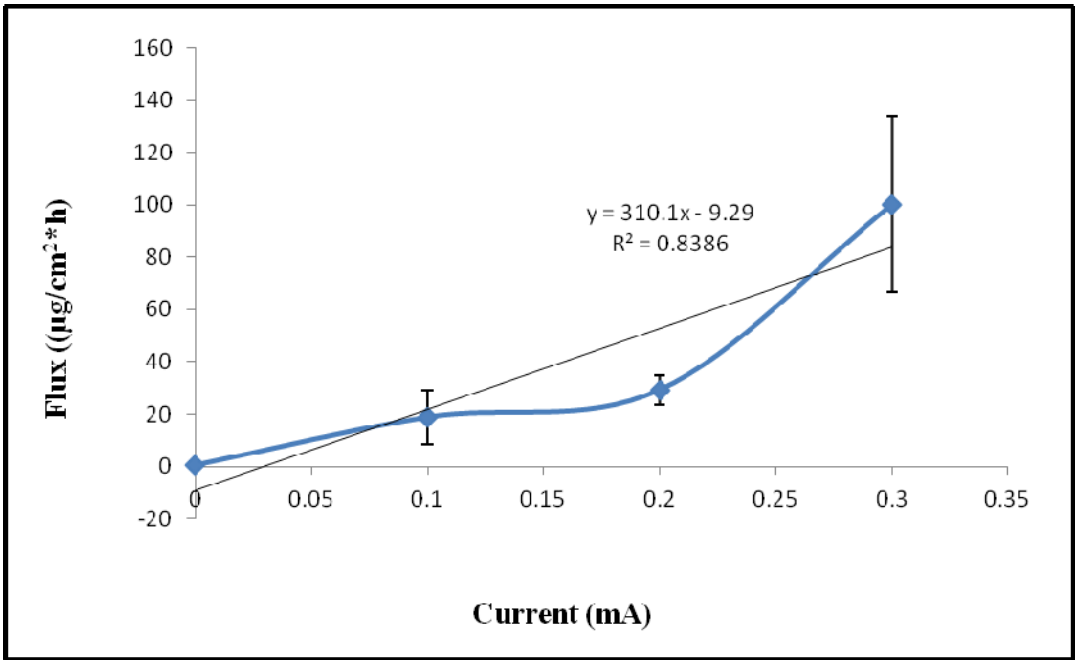

Figure 23. The effect of current on transdermal delivery of DHCl (Stage I)

Table 20. Effect of current on transdermal delivery of DHCl (Stage II) [a]

Iontophoresis (mA)	Flux ($\mu g/cm^2*h$)	Q_{24} ($\mu g/cm^2$)	ER
Control	0.9±0.9	17.9±16.4	1.0
0.1	10.3±5.5[b]	310.1±163.9	11.4
0.2	14.9±4.1[b]	458.9±57.9	16.5
0.3	33.4±1.6[b, c]	1304.3±254.8	37.1

[a] Data are presented as means ± S.D. ($3 \leq N \leq 8$).

[b] Statistically significantly higher than control ($p < 0.05$).

[c] Statistically significantly higher than 0.1 mA, 0.2 mA and control ($p < 0.05$).

4.6.3.2 Enhancement Using Chemical Enhancer

The effect of enhancer pretreatment was evaluated using *in vitro* Franz cell diffusion model on porcine skin. Results from Table 21 and 22 demonstrated that compared to Control, only 5.0% DDAIP in PG provided significant enhancement effect on transdermal delivery of DHCl throughout the entire 24 h period of permeation study. But its effect was still much less than that of iontophoresis even at a low current of 0.1 mA, indicating that iontophoresis was a much more effective approach for enhancing transdermal delivery of DHCl than tested chemical enhancers.

Table 21. Effect of 1.0 h enhancer pretreatment on transdermal delivery of DHCl (Stage I) [a]

Enhancer	Flux ($\mu g/cm^2*h$)	Q_8 ($\mu g/cm^2$)	ER
Control	0.4±0.3	3.0±2.6	1.0
PG	0.3±0.0	0.4±0.3	1.0
2.5% Azone in PG	0.8±0.1	5.6±1.3	2.0
5.0% DDAIP in PG	3.0±1.2[b]	25.2±10.4	7.5
5.0% DDAIP HCl in water	0.1±0.0	1.0±0.4	1.0
5.0% DDAIP HCl in PG	0.3±0.2	2.8±1.6	1.0
5.0% Br-Iminosulfurane in PG	0.3±0.1	2.5±0.7	1.0

[a] Data are presented as means ± S.D. ($3 \leq N \leq 8$).

[b] Statistically significantly higher than other enhancers and control ($p < 0.05$).

Table 22. Effect of 1.0 hr enhancer pretreatment on transdermal delivery of DHCl (Stage II) [a]

Enhancer	Flux ($\mu g/cm^2*h$)	Q_{24} ($\mu g/cm^2$)	ER
Control	0.9±0.9	17.9±16.4	1.0
PG	0.4±0.3	19.5±8.9	1.0
2.5% Azone in PG	1.4±0.3	28.8±5.6	1.6
5.0% DDAIP in PG	8.4±2.4[b]	161.1±48.8	9.3
5.0% DDAIP HCl in water	0.4±0.1	6.8±2.2	1.0
5.0% DDAIP HCl in PG	0.6±0.6	13.1±10.7	1.0
5.0% Br-Iminosulfurane in PG	1.0±0.4	18.6±6.7	1.0

[a] Data are presented as means ± S.D. ($3 \leq N \leq 8$).

[b] Statistically significantly higher than other enhancers and control ($p < 0.05$).

4.6.3.3 Combination Enhancement Effect

Combined treatments of iontophoresis and chemical enhancers were conducted to investigate their synergistic enhancement effects on transdermal delivery of DHCl using *in vitro* Franz cell diffusion model on porcine skin.

Table 23 and 24 demonstrated that 8 h of combined treatment of iontophoresis (0.3 mA for 8.0 h) and chemical enhancer pretreatment (1.0 h) significantly enhanced transdermal delivery of DHCl and iontophoresis was the dominated contributor for the combined enhancement effect. It was observed that only the combined treatment of iontophoresis (0.3 mA 8.0 h) and chemical

enhancer 2.5% (w/v) Azone provided synergistic enhancement effect. Figure 24 shows that values for cumulative DHCl permeated through skin transdermally exhibited the same trend as values for flux. It is also evidenced (Table 24) that even after iontophoresis was discontinued at 8 h, the enhancement effect of post-iontophoresis continued to be statistically significant when compared to control until 24 h. Again iontophoresis was the major contributor. However, there was no synergistic effect observed for all tested enhancers. In the case of DDAIP HCl in PG and DDAIP HCl in water, the combined effects were actually much lower than that of iontophoresis alone. It may be due to the fact that ions from DDAIP HCl may be competing with DHCl drug for iontophoresis.

Table 23. Combined effect of iontophoresis 0.3 mA 8 hrs treatment and 1.0 h enhancer Pretreatment (Stage I) [a]

Enhancer	Flux ($\mu g/cm^2*h$)	Q_8 ($\mu g/cm^2$)	ER
Control	0.4±0.3	3.0±2.6	1.0
0.3	100.3±33.7[b]	796.8±276.6	250.8
PG+0.3 mA	48.4±23.9[b]	319.7±118.9	121.0
2.5% Azone in PG+0.3 mA	106.0±59.5[b, c]	871.4±450.0	265.0
5.0% DDAIP in PG+0.3 mA	86.1±13.1[b]	692.3±103.6	215.3
5.0% DDAIP HCl in water+0.3 mA	48.0±14.0[b]	383.6±110.9	120.0
5.0% DDAIP HCl in PG+0.3 mA	26.2±9.7[b]	214.7±80.0	65.5
5.0% Br-Iminosulfurane in PG+0.3 mA	72.1±15.4[b]	577.5±117.5	180.3

[a] Data are presented as means ± S.D. ($3 \leq N \leq 8$).

[b] Statistically significantly higher than Control ($p < 0.05$).

[c] Statistically significantly higher than other enhancers and Control ($p < 0.05$).

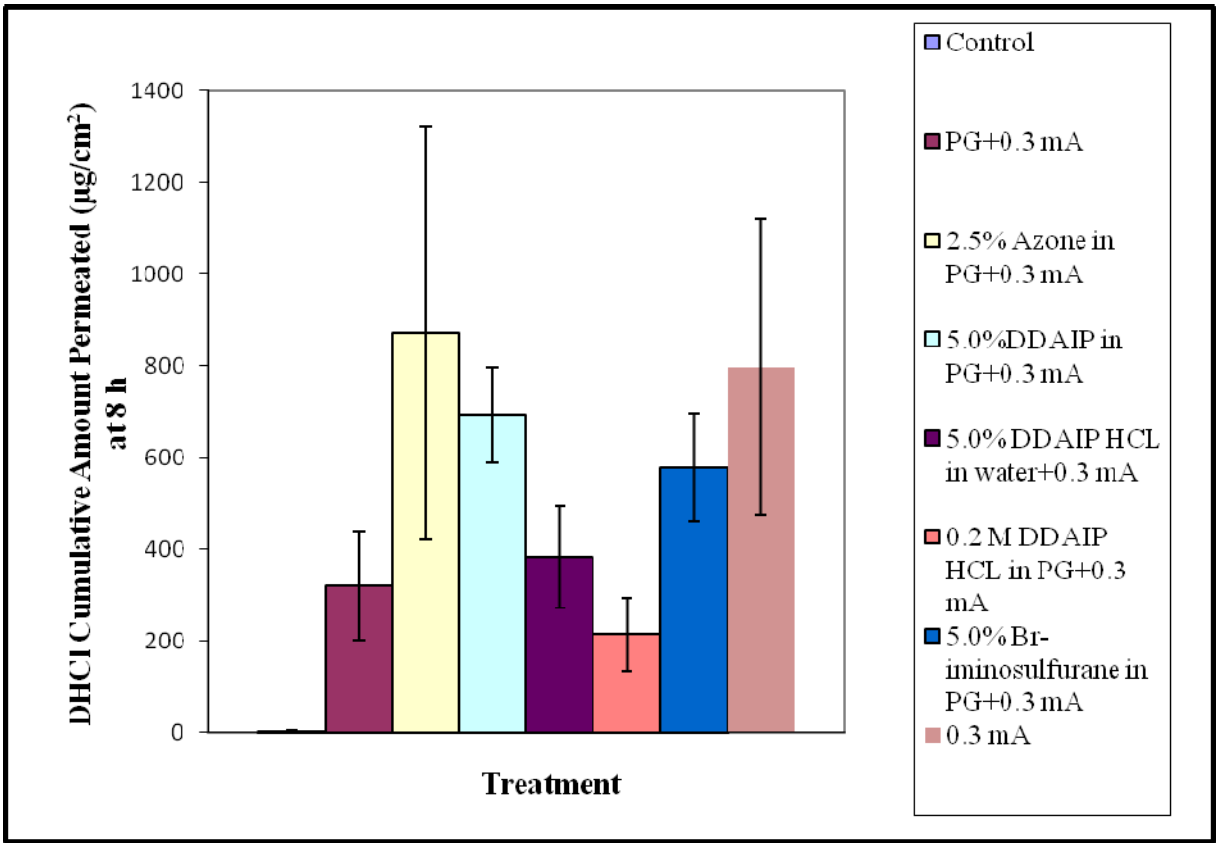

Figure 24. Combined effect of iontophoresis and enhancer on transdermal delivery of DHCl

Table 24. Combined effect of iontophoresis 0.3 mA 8 h treatment and 1.0 h enhancer pretreatment (Stage II) [a]

Enhancer	Flux ($\mu g/cm^2*h$)	Q_{24} ($\mu g/cm^2$)	ER
Control	0.9±0.9	17.9±16.4	1
0.3	33.4±1.6[b]	1304.3±254.8	37.1
PG+0.3 mA	14.6±3.1[b]	389.5±44.2	16.0
2.5% Azone in PG+0.3 mA	33.7±6.7[b]	1387.7±529.4	37.4
5.0% DDAIP in PG+0.3 mA	35.1±9.3[b]	1227.4±154.8	39.0
5.0% DDAIP HCl in water+0.3 mA	17.6±5.9[b]	646.3±177.3	19.6
5.0% DDAIP HCl in PG+0.3 mA	13.3±7.7[b]	416.6±177.2	14.8
5.0% Br-Iminosulfurane in PG+0.3 mA	25.2±l.6[b]	973.2±158.3	28.0

[a] Data are presented as means ± S.D. ($3 \leq N \leq 8$).

[b] Statistically significantly higher than control ($p < 0.05$).

4.6.4 Ondansetron HCl Transdermal Delivery

The passive permeation of ODAN HCl through porcine skin was minimal (Table 25) which. Therefore, physical enhancement technique - iontophoresis at 0.1, 0.2 and 0.3 mA was applied to enhance transdermal delivery of ODAN HCl through porcine skin using *in vitro* Franz cell diffusion model. Table 25 shows that when compared to control, significant enhancement effect

was achieved using iontophoresis for 8 h at 0.1, 0.2 and 0.3 mA, respectively. While 0.3 mA iontophoresis had significantly higher enhancement effect than that of 0.1mA, the correlation between current and flux was linear (Figure 25). Also drug cumulative amount permeated significantly increased with the use of iontophoresis when compared to control. It was also observed (Table 26) that even when iontophoresis was discontinued at 8 h, the post-iontophoretic effect on drug permeation continued to be statistically significant when compared to control, indicating that iontophoresis increased the permeability of porcine skin for ODAN HCl probably through first disrupting porcine stratum corneum and increasing intercellular space for enhancing transdermal drug delivery [163,164]. Furthermore, post-iontophoretic effect of 0.3 mA was significantly higher than that of 0.1 mA, but significantly reduced, indicating that the flux of the drug was predominantly electrically driven.

4.6.4.1 Enhancement Using Iontophoresis

Table 25. Effect of current on transdermal delivery of ODAN HCl (Stage I) [a]

Iontophoresis (mA)	Flux ($\mu g/cm^2*h$)	Q8 ($\mu g/cm^2$)	ER
Control	0.1±0.1	1.2±0.9	1
0.1	3.1±1.5[b]	24.6±12.2	31
0.2	8.3±2.5[b]	67.0±21.4	83
0.3	9.9±2.2[b, c]	79.0±18.2	99

[a] Data are presented as means ± S.D. ($3 \leq N \leq 8$).

[b] Statistically significantly higher than control ($p < 0.05$).

[c] Statistically significantly higher than 0.1 mA and control ($p < 0.05$).

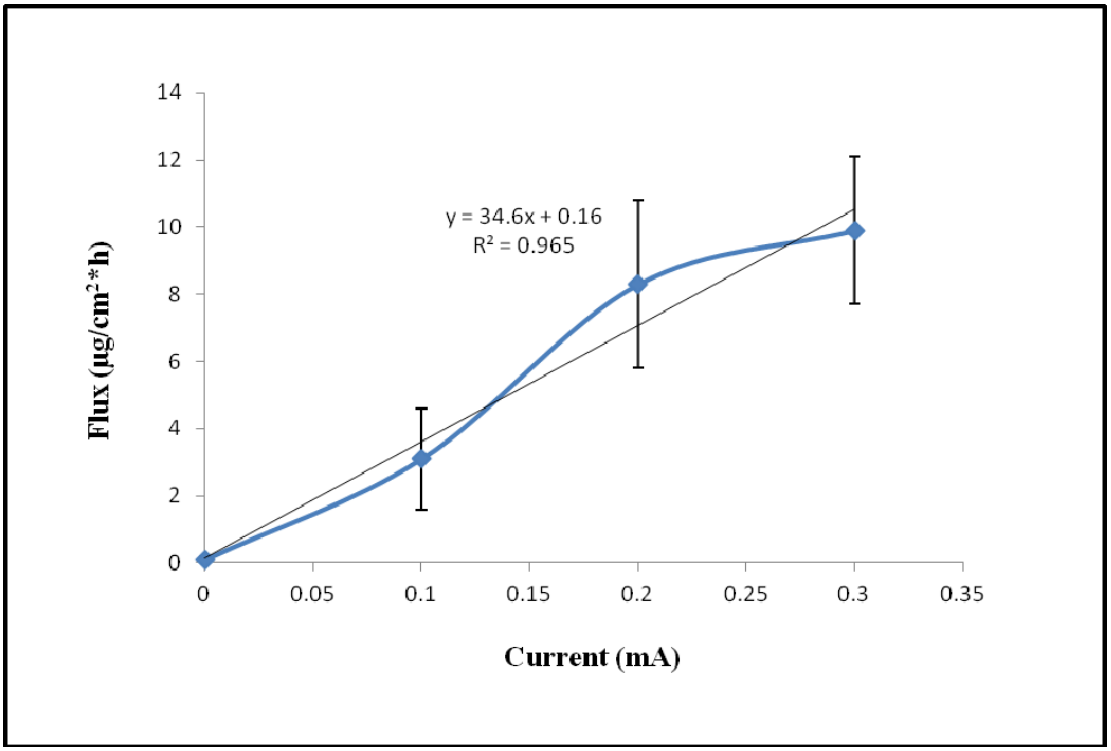

Figure 25. The effect of current on transdermal delivery of ODAN HCl (Stage I)

Table 26. Effect of current on transdermal delivery of ODAN HCl (Stage II) [a]

Iontophoresis (mA)	Flux (µg/cm²*h)	Q_{24} (µg/cm²)	ER
Control	0.1±0.1	1.2±1.0	1
0.1	1.8±0.4[b]	53.2±15.1	18
0.2	4.2±1.9[b]	135.6±31.6	42
0.3	5.5±1.5[b, c]	162.3±38.0	55

[a] Data are presented as means ± S.D. ($3 \leq N \leq 8$).

[b] Statistically significantly higher than control ($p < 0.05$).

[c] Statistically significantly higher than 0.1 mA and control ($p < 0.05$).

4.6.4.2 Enhancement Using Chemical Enhancer

Table 27 and 28 showed that no enhancement effect was observed from enhancer pretreatments.

Table 27. Effect of 1.0 hr enhancer pretreatment on transdermal delivery of ODAN HCl (Stage I) [a]

Enhancer	Flux ($\mu g/cm^2*h$)	Q_8 ($\mu g/cm^2$)	ER
Control	0.1±0.1	1.2±0.9	1
PG	0.1±0.1	0.2±0.02	1
2.5% Azone in PG	0.1	0.5±0.1	1
5.0% DDAIP in PG	0.1	0.7±0.3	1
5.0% DDAIP HCl in water	0.1±0.1	0.6±0.6	1
5.0% DDAIP HCl in PG	0.1±0.1	0	1
5.0% Br-Iminosulfurane in PG	0.1±0.1	0.6±0.3	1

Table 28. Effect of 1.0 hr enhancer pretreatment on transdermal delivery of ODAN HCl (Stage II) [a]

Enhancer	Flux ($\mu g/cm^2*h$)	Q_{24} ($\mu g/cm^2$)	ER
Control	0.1±0.1	1.2±1.0	1
PG	0	0.80±0.3	1
2.5% Azone in PG	0.2±0.1	3.1±1.5	1
5.0% DDAIP in PG	0.3±0.1	6.3±2.4	3
5.0% DDAIP HCl in water	0.1±0.1	1.6±1.6	1
5.0% DDAIP HCl in PG	0.1±0.1	0.6±0.4	1
5.0% Br-Iminosulfurane in PG	0.2±0.1	3.5±1.2	1

4.6.4.3 Combined Enhancement Effect

Combined treatments of iontophoresis and chemical enhancers were conducted to investigate their synergistic enhancement effects on transdermal delivery of ODAN HCl using *in vitro* Franz cell diffusion model on porcine skin.

Table 29 and 30 demonstrated that 8 h of combined treatment of iontophoresis (0.3 mA for 8.0 h) and chemical enhancer pretreatment (1.0 h) significantly enhanced transdermal delivery of ODAN HCl and iontophoresis was the dominated contributor for the combined enhancement effect. It was observed that the combined treatment of iontophoresis (0.3 mA 8.0 h) and chemical enhancer 2.5% (w/v) Azone, 5% DDAIP and 5% Br-iminosulfurane provided synergistic enhancement effect. Figure 26 shows that values for cumulative ODAN HCl permeated through skin transdermally exhibited the same trend as values for flux. It is also evidenced (Table 30) that even after iontophoresis was discontinued at 8 h, the enhancement effect of post-iontophoresis continued to be statistically significant when compared to control until 24 h. Again iontophoresis was the major contributor. However, DDAIP HCl in PG and DDAIP HCl in water, the combined effects were actually much lower than that of iontophoresis alone. It may be due to the fact that ions from DDAIP HCl may be competing with ODAN HCl drug for iontophoresis.

Table 29. Combined effect of iontophoresis 0.3 mA 8 hrs treatment and 1.0 h enhancer Pretreatment (Stage I) [a]

Enhancer	Flux ($\mu g/cm^2*h$)	Q_8 ($\mu g/cm^2$)	ER
Control	0.1±0.1	1.2±0.9	1
0.3	9.9±2.2[b, c]	79.0±18.2	99
PG+0.3 mA	15.2±3.6[b]	119.7±28.9	152.5
2.5% Azone in PG+0.3 mA	16.5±2.0[b, c]	133.1±21.6	165
5.0% DDAIP in PG+0.3 mA	16.7±2.2[b, c]	143.2±18.3	167
5.0% DDAIP HCl in water+0.3 mA	5.0±0.5[b]	40.7±4.1	50
5.0% DDAIP HCl in PG+0.3 mA	3.1±1.2[b]	25.0±9.7	31
5.0% Br-Iminosulfurane in PG+0.3 mA	14.1±3.4[b]	110.8±27.2	141

[a] Data are presented as means ± S.D. ($3 \leq N \leq 8$).

[b] Statistically significantly higher than control ($p < 0.05$).

[c] Statistically significantly higher than the other combined treatments and control ($p < 0.05$).

Table 30. Combined effect of iontophoresis 0.3 mA 8 h treatment and 1.0 h enhancer Pretreatment (Stage II) [a]

Enhancer	Flux ($\mu g/cm^2*hr$)	Q_{24} ($\mu g/cm^2$)	ER
Control	0.1±0.1	1.2±1.0	1
0.3	5.5±1.5[b]	162.3±38.0	55
PG+0.3 mA	4.6±1.1[b]	189.5±44.2	46
2.5% Azone in PG+0.3 mA	5.5±3.0[b]	216.6±27.5	55
5.0% DDAIP in PG+0.3 mA	8.1±0.9[b,c]	267.6±18.3	81
5.0% DDAIP HCl in water+0.3 mA	4.3±0.4[b]	106.1±9.6	43
5.0% DDAIP HCL in PG+0.3 mA	1.5±0.5[b]	48.3±17.8	15
5.0% Br-Iminosulfurane in PG+0.3 mA	6.3±2.7[b]	48.3±17.8	63

[a] Data are presented as means ± S.D. ($3 \leq N \leq 8$).

[b] Statistically significantly higher than control ($p < 0.05$).

[c] Statistically significantly higher than the other combined treatments and control ($p < 0.05$).

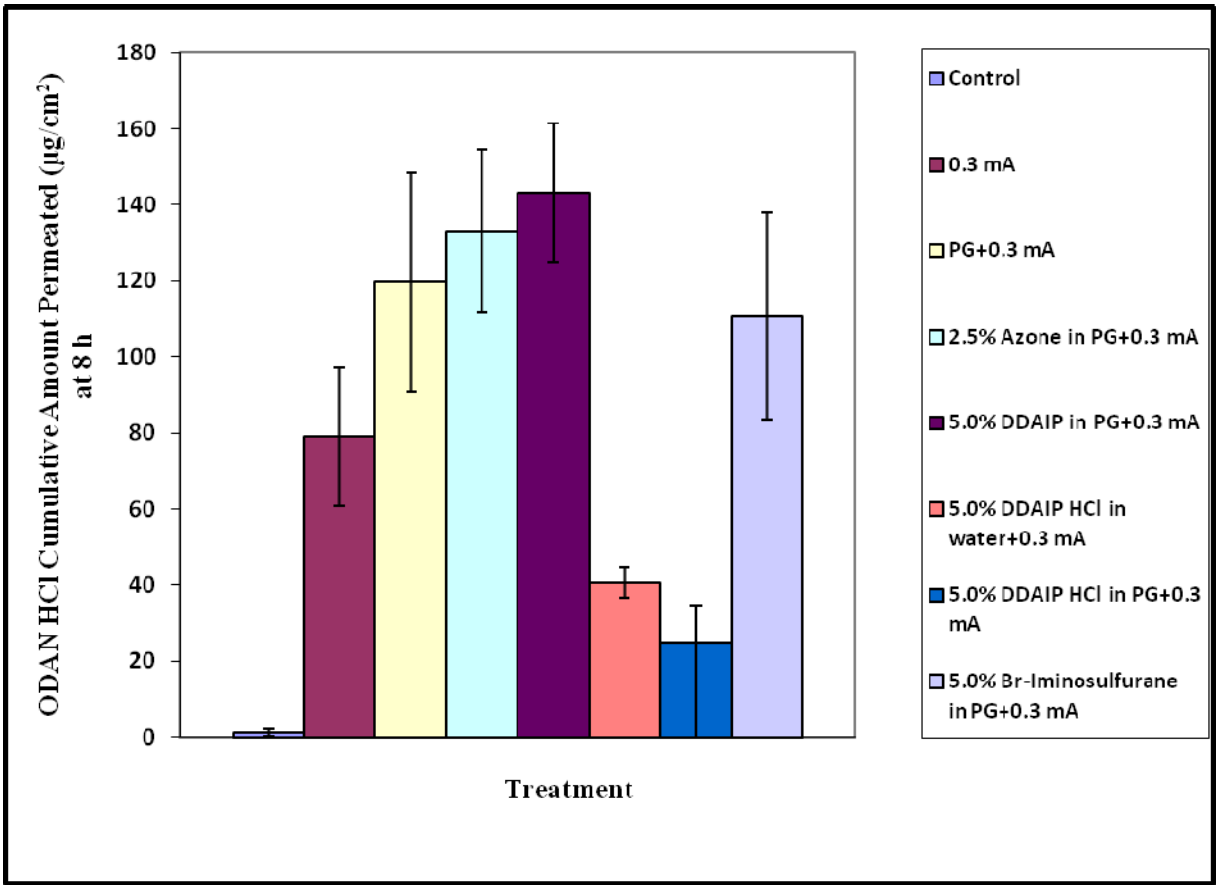

Figure 26. Combined effect of iontophoresis and enhancer on transdermal delivery of ODAN HCl

4.6.5 Skin Integrity Evaluation

4.6.5.1 Scanning Electron Microcopy

SEM was utilized to evaluate the integrity of skin surface and cross sections of untreated and various treated skin samples. Figure 27 and 28 were the images for the surface and cross section of untreated skin. Figure 29 and 30 were the images for the surface and cross section of 3 h of 2.5% Azone + 0.3 mA 8 h treated skin. Figure 31 and 32 were the images for the surface and cross section of 3 h of 5% DDAIP + 0.3 mA 8 h treated skin. Figure 33 and 34 were the images

for the surface and cross section of 3 h of 5% DDAIP HCl + 0.3 mA 8 h treated skin. Figure 35 and 36 were the images for the surface and cross section of 3 h of 5% Br-iminosulfurane+0.3 mA 8 h treated skin. Figure 37 and 38 were the images for the surface and cross section of 0.3 mA 8 h treated skin. Figure 39 and 40 were the images for the surface and cross section of 10% oleic acid + 0.3 mA8 h treated skin.

It was observed that no major morphology changes were observed on the surfaces of the untreated and various treated skin samples (Figures 28, 30, 32, 34, 36, 38 and 40). However, compared to untreated (Figure 27), cross section of 10% oleic acid +0.3 mA 8 h treated skin (Figure 39) showed more detacched corneocytes which was in agreement with the observation in the literature [130]. Cross section of 5% DDAIP + 0.3 mA 8 h treated skin (Figure 31) and 2.5% Azone + 0.3 mA 8 h treated skin (Figure 29) showed some detached corneocytes, too.

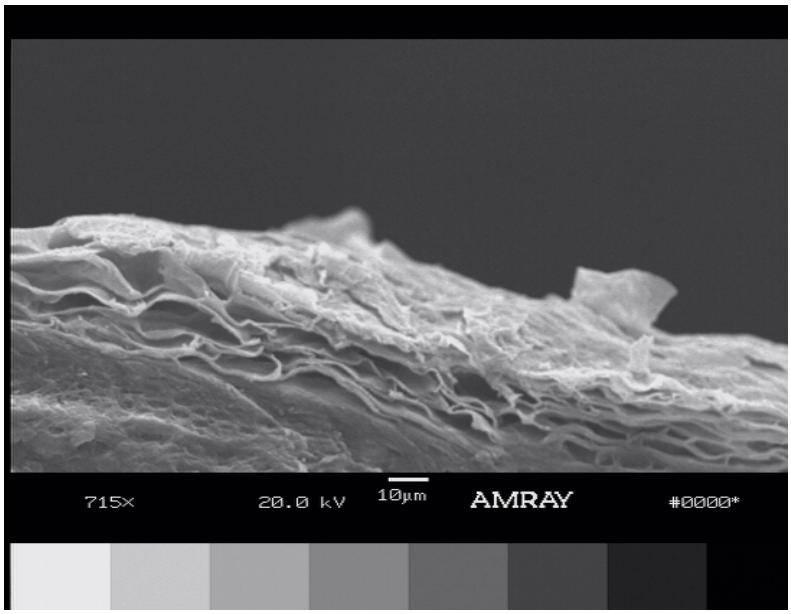

Figure 27. Cross section of untreated pig skin

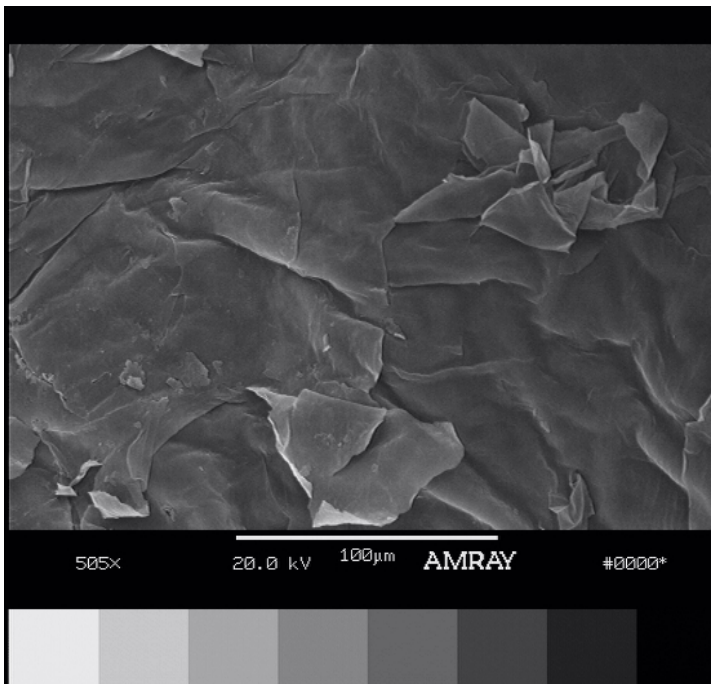

Figure 28. Surface of untreated pig skin

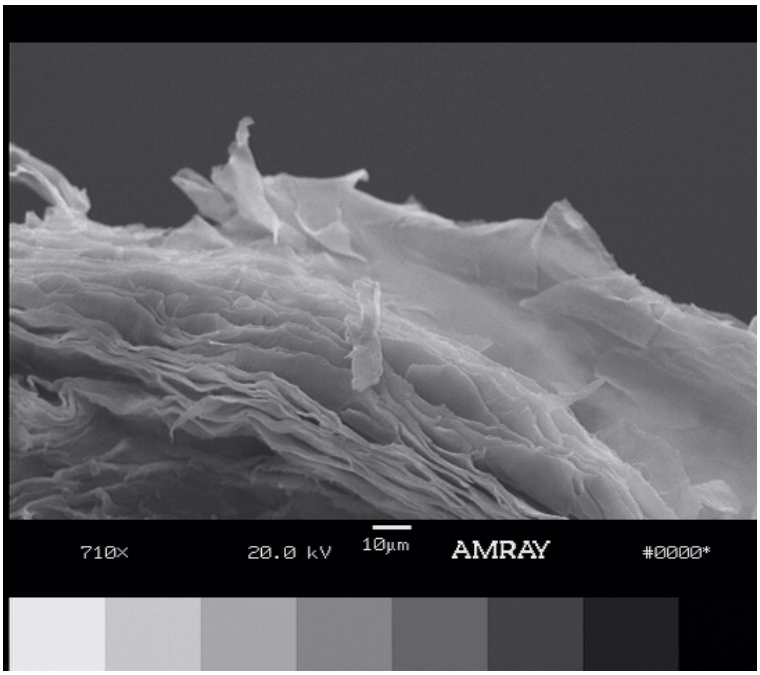

Figure 29. Cross section of 5% Azone + 0.3 mA 8 h treated skin

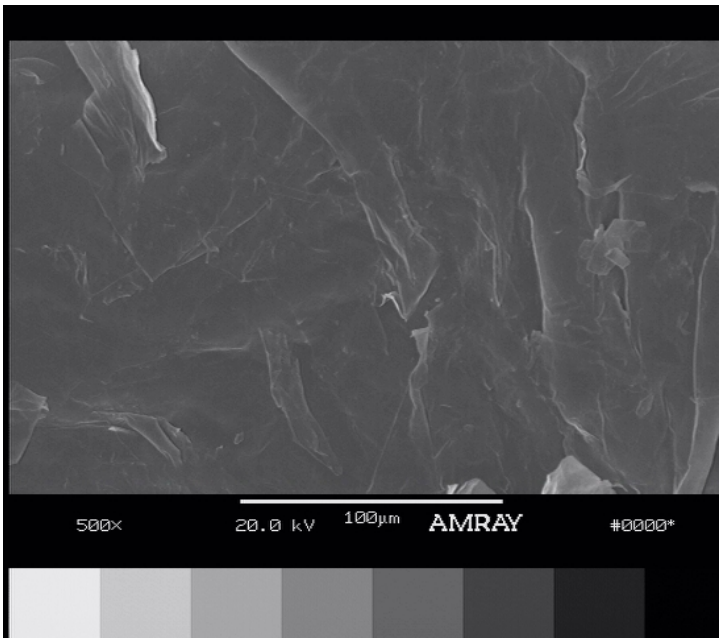

Figure 30. Surface of 5% Azone + 0.3 mA 8 h treated skin

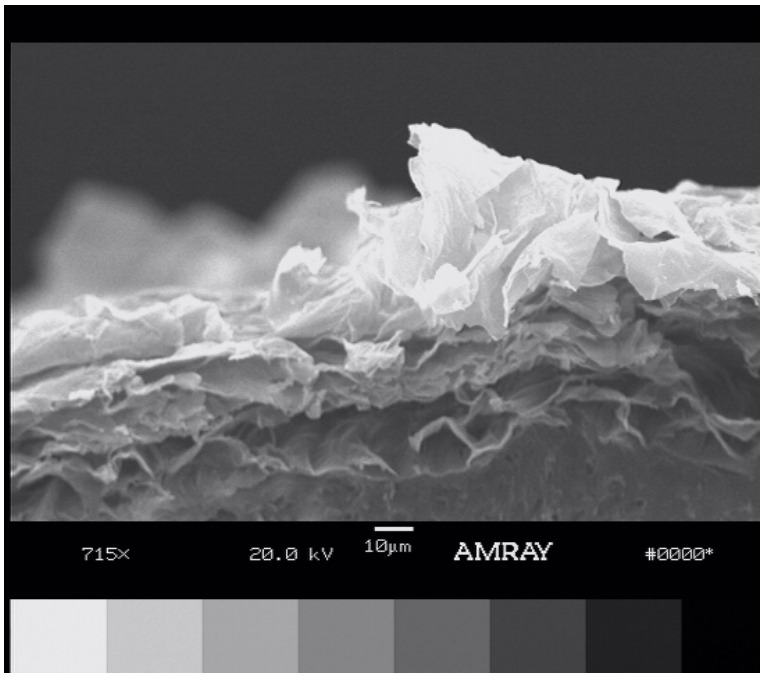

Figure 31. Cross section of 5% DDAIP + 0.3 mA 8 h treated skin

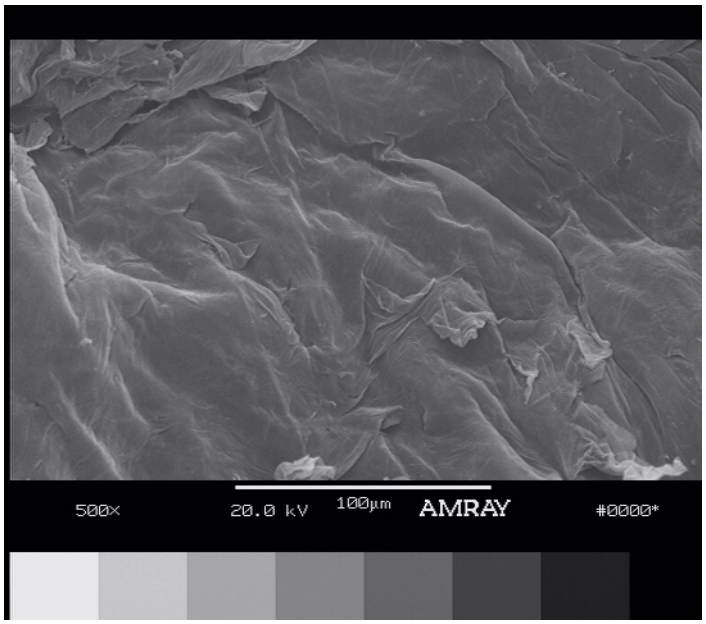

Figure 32. Surface of 5% DDAIP + 0.3 mA 8 h treated skin

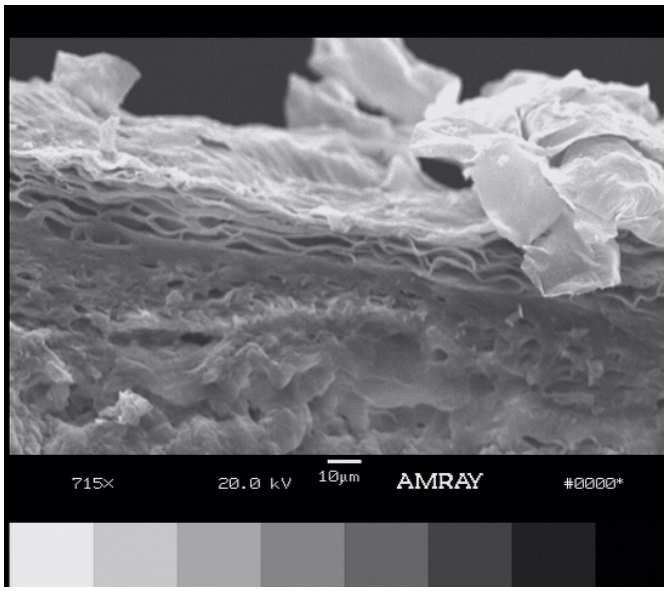

Figure 33. Cross section of 5% DDAIP HCl+ 0.3 mA 8 h treated skin

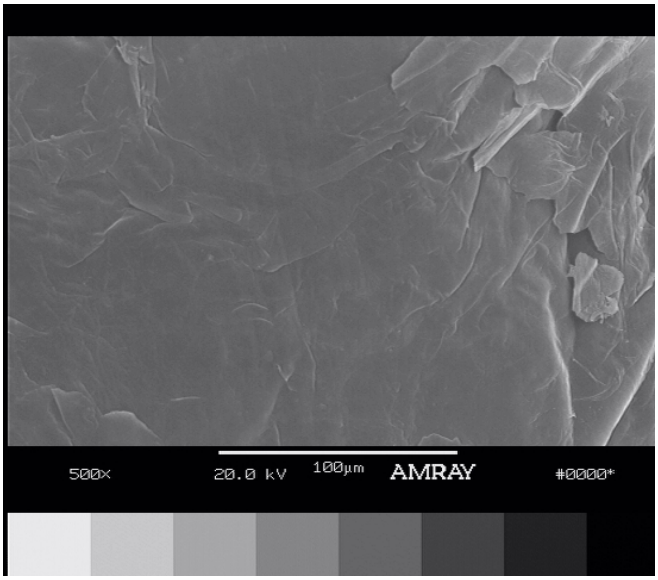

Figure 34. Surface of 5% DDAIP HCl+ 0.3 mA 8 h treated skin

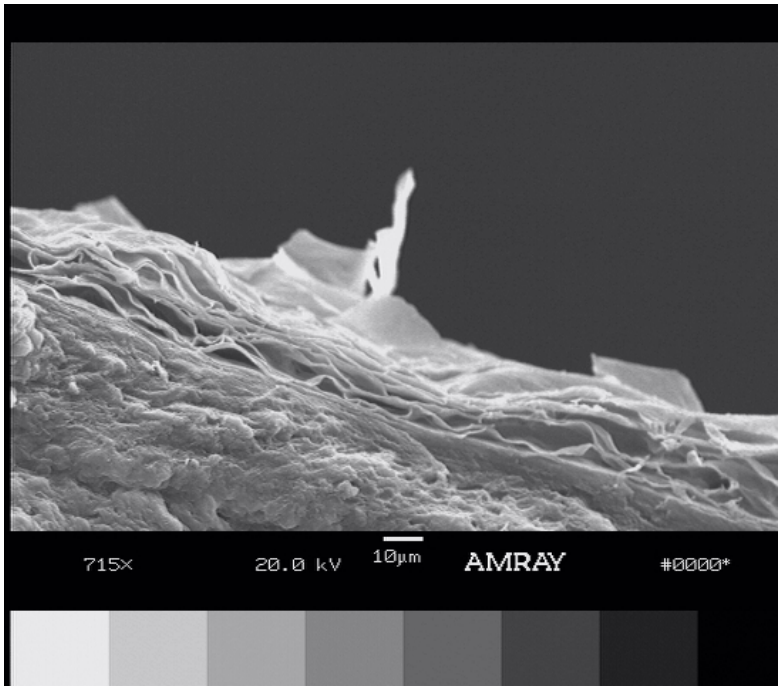

Figure 35. Cross section of 5% Br-iminosulfurane + 0.3 mA 8 h treated skin

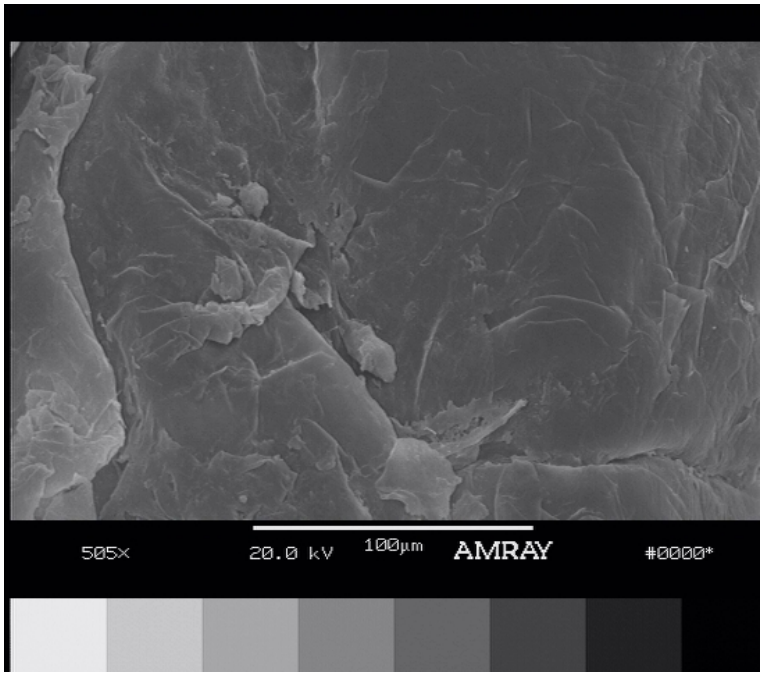

Figure 36. Surface of 5% Br-iminosulfurane + 0.3 mA 8 h treated skin

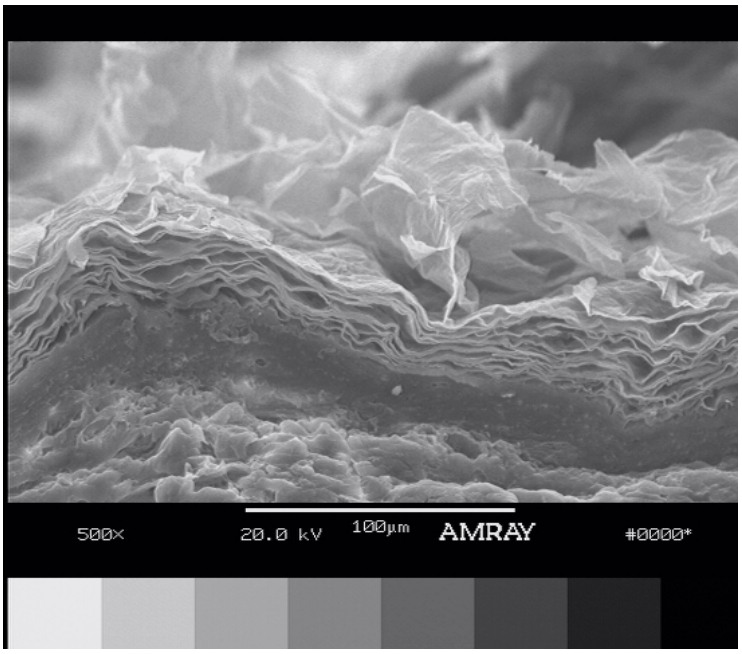

Figure 37. Cross section of 0.3 mA 8 h treated skin

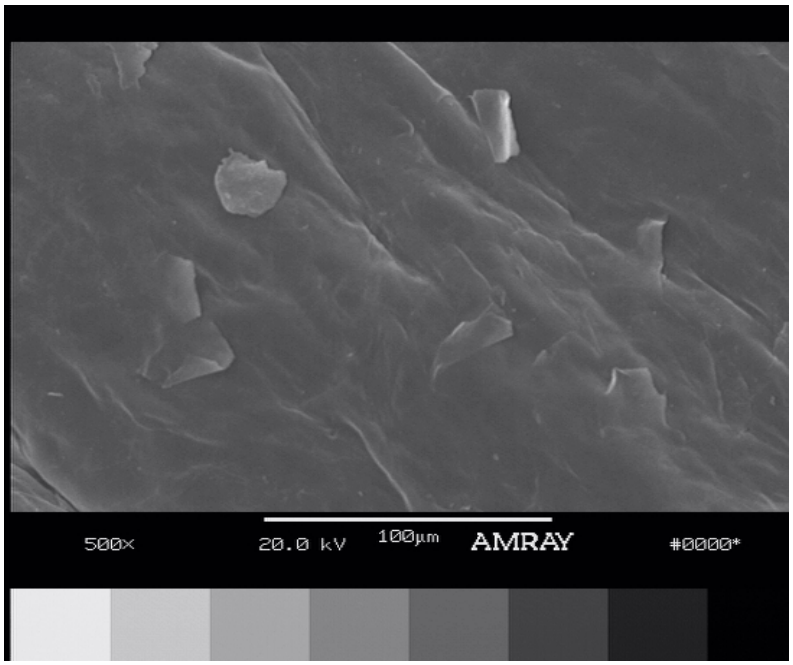

Figure 38. Surface of 0.3 mA 8 h treated skin

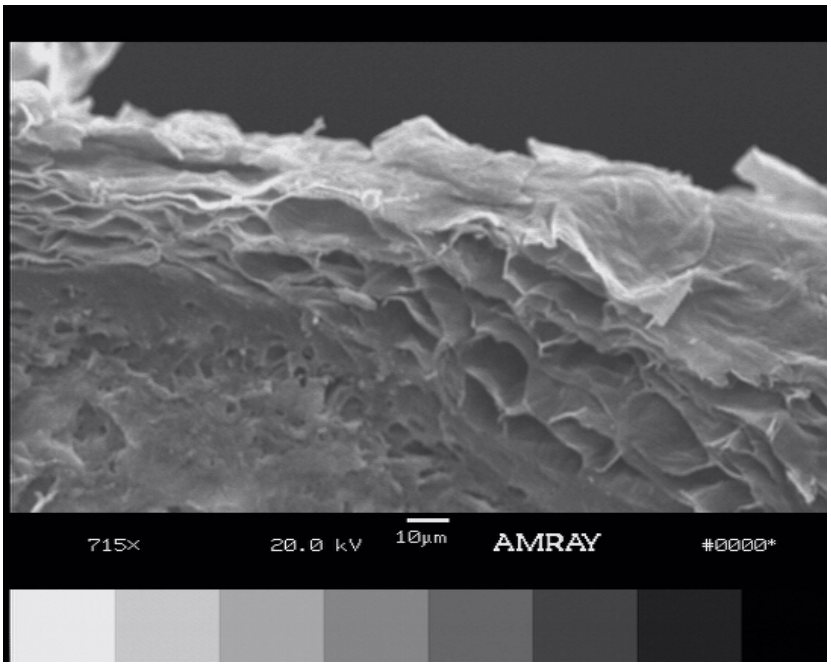

Figrue 39. Cross section of 10% Oleic acid + 0.3 mA 8 h treated skin

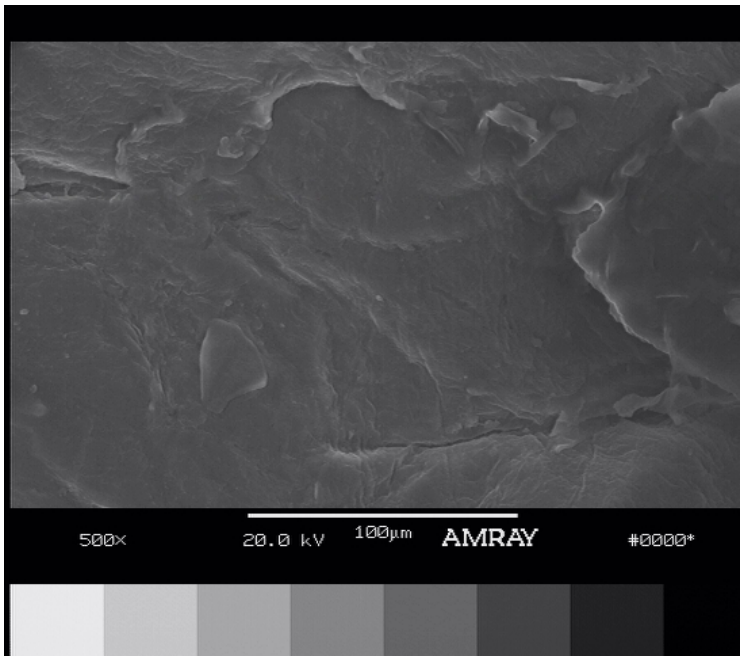

Figrue 40. 10% Oleic acid + 0.3 mA 8 h treated skin

4.6.5.2 Differential Scanning Calorimetry

DSC was performed on control sample, and samples treated with/without iontophoresis and chemical enhancers or their combination treatment. A typical thermogram (25 to 250 °C, heating rate 10 °C/min) of pig SC was demonstrated in Figure 41. There were five transition temperatures observed for all samples.

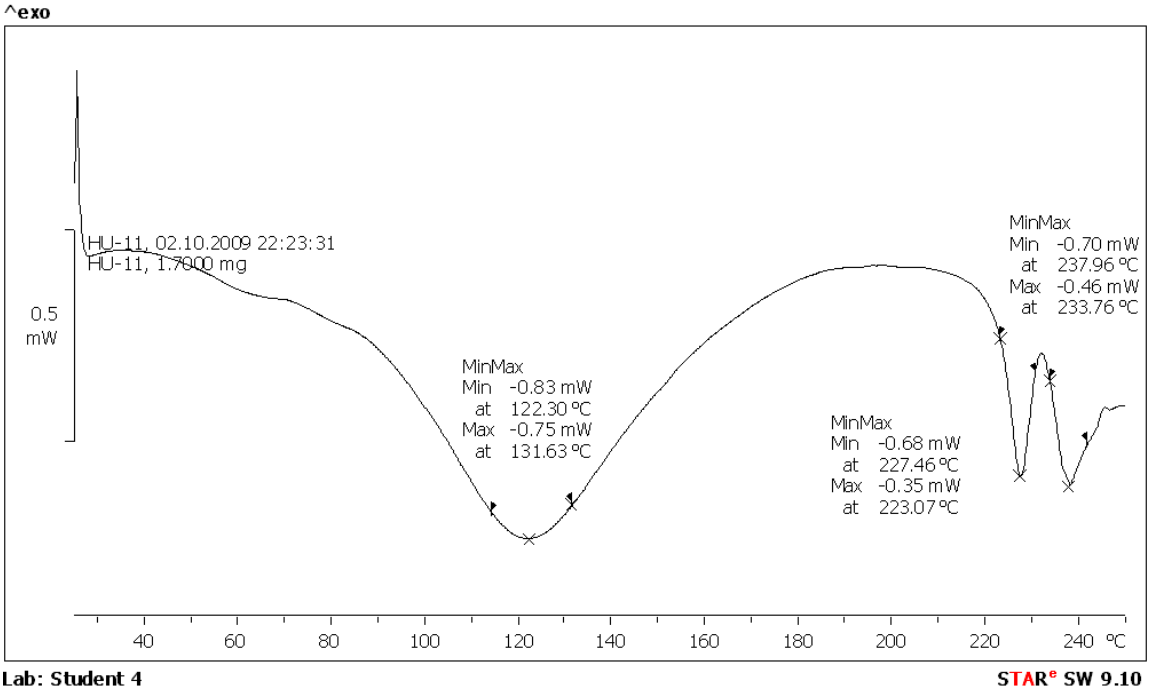

Figure 41. DSC Thermograms of Pig Stratum Corneum

T1 (105-130°C) represents changes in stratum corneum protein conformation [169]. T2 and T3 occured when stratum corneum was totally burned out.

Table 31 demonstrated that there were no significant differences in T1, T2, and T3 among SC control (untreated) sample, iontophoresis and chemical enhancer treated samples, especially for T1, T2, and T3, indicating that iontophoresis and chemical enhancer treatments did not

significantly alter or denature SC lipids, or if there was any initial alteration or damage to SC lipids, SC could restorer itself later.

Table 31. Transition Temperatures of SC Control, Iontophoresis and Chemical Enhancer Treated Samples (N=2)

Transition Temp. (°C)	Control	Current Only	Chemical Enhancer Pretreatment for 3 hours											
			PG		0.2 M Azone in PG		0.2 M BR in PG		0.2 M DDAIP in PG		0.2 M DDAIP HCL in PG		0.2 M DDAIP HCL in Water	
		0.3	0	0.3	0	0.3	0	0.3	0	0.3	0	0.3	0	0.3
T1	117	118	124	118	108	102	103	103	115	118	108	95	125	132
T2	225	227	227	229	226	228	229	227	228	228	228	228	227	229
T3	238	237	238	243	246	243	241	240	243	241	240	245	243	242

Note: 0.3 represents 0.3 mA current iontophoresis; 0 represent no iontophoresis

4.6.6 Skin Cytotoxicity Study

MTS 3-(4, 5-dimethylthiazol-2-yl)-5-(3-carboxymethoxyphenyl)-2-(4-sulfophenyl)-2H-tetrazolium, inner salt) assay was used to evaluate enhancer cytotoxicity in skin cells.

The results of DDAIP in PG and DDAIP HCl in water at different concentrations are shown in Figure 42 and 43. The results indicate that DDAIP at a concentration of less than 0.016 μm and DDAIP HCl at a concentratin of less than 0.18 μm had no detrimental effect on skin cells. However, NexMed – the supplier of DDAIP and DDAIP HCl conducted acute, repeated dose

toxicity, sensitization, genotoxicity, reproductive and developmental toxicity, absorption distribution, metabolism, and excretion (ADME), and carcinogenicity studies. The in vivo study results showed that DDAIP and DDAIP HCl had a low acute toxicity (mouse and rat LD50 > 5.0 g/kg) are rapidly metabolized to n-dodecanol and *N, N*-dimethylalanine by esterase enzymes in skin, plasma and microsomes, are well tolerated on skin of rats and mice at ≤ 5% in repeat dose studies, were negative for sensitization, genotoxicity, reproductive effects and carcinogenicity in a 2-year rat SC study [170].

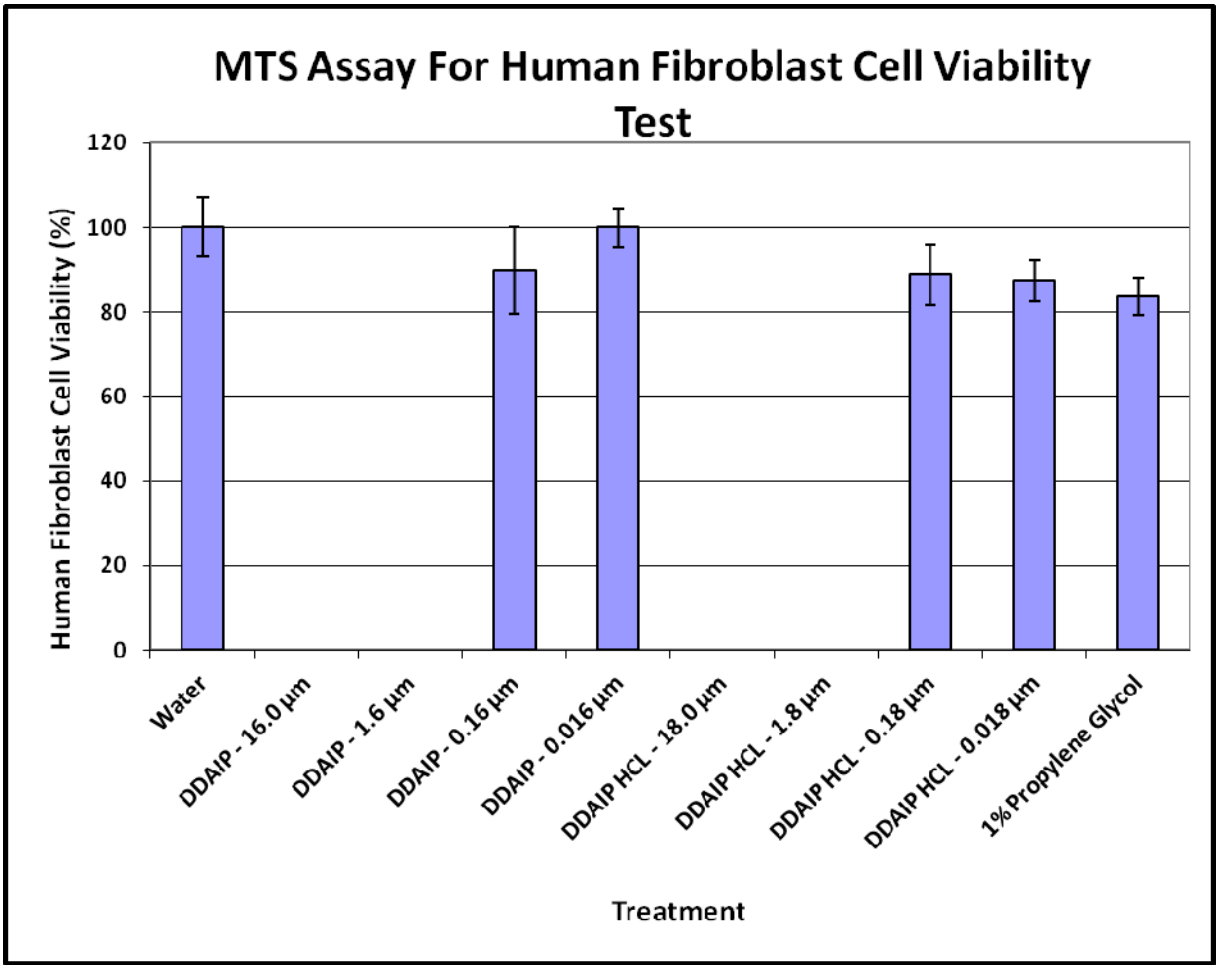

Figure 42. Human fibroblast cell viability vs DDAIP and DDAIP HCl treatments

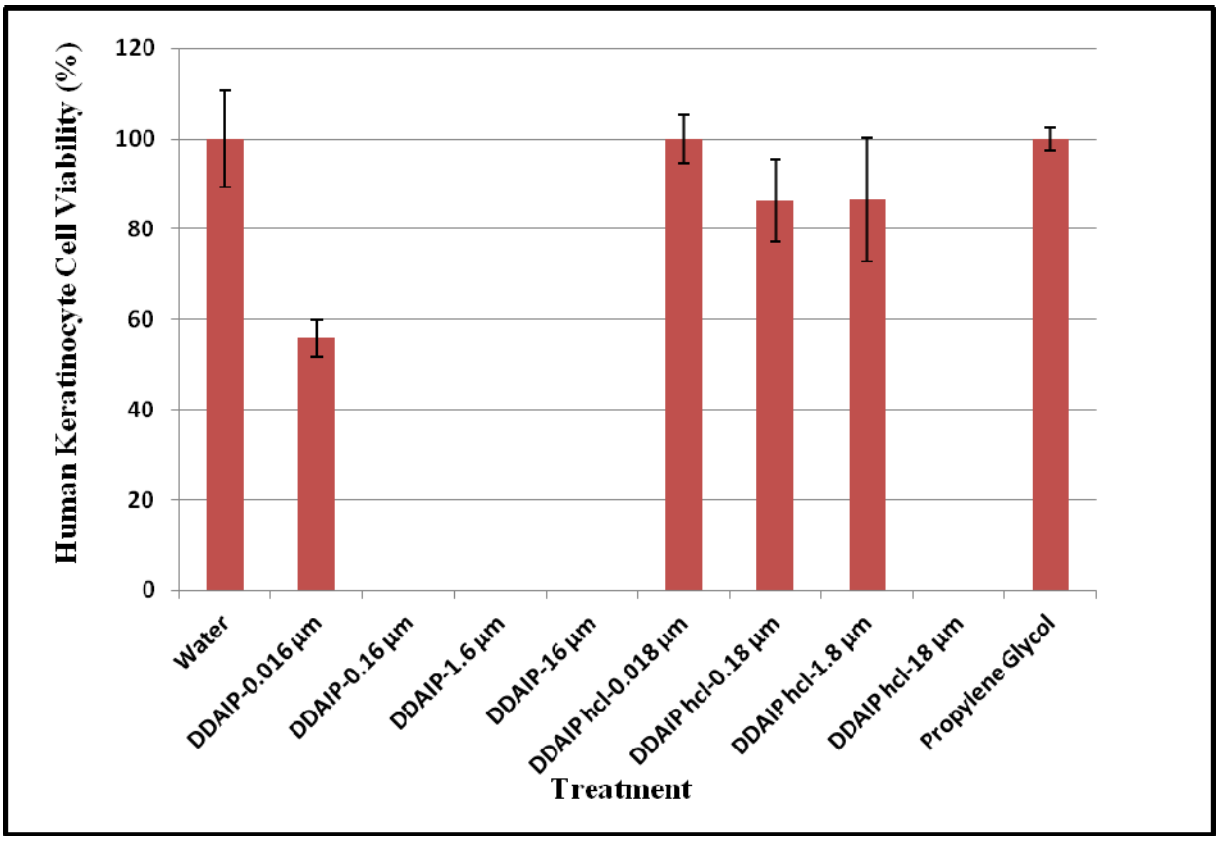

Figure 43. Human keratinocyte cell viability vs DDAIP and DDAIP HCl treatments

4.7 Summary

Transdermal Drug Delivery of LHCl, NHT, DHCl and ODAN HCl

Enhancement effects of iontophoresis or chemical enhancers (Azone, DDAIP, DDAIP HCl and Br-iminosulfurane) and their combination treatment on transdermal delivery of LHCl, NHT, DHCl and ODAN HCl were studied using *in vitro* Franz cell diffusion model on porcine skin. The results demonstrated that none of the tested enhancers alone could not enhance transdermal delivery of either one of four drugs to reach a therapeutic dose level, howev
er iontophoresis alone or its combination with one of the four enhancers could potentially delivery therapeutic doses of LHCl, DHCl, NHT and ODAN HCl into blood stream.

It was found that increasing current intensity from 0.1 mA to 0.3 mA significantly enhanced transdermal delivery of LHCl, NHT, DHCl and ODAN HCl. Higher current intensity of 0.3 mA could provide faster mode of enhancement action while low current intensity of 0.1 mA could be used to provide sustained enhancement effect.

Increasing enhancer concentration from 2.5% to 5.0% w/v at least directionally increased the LHCl amount permeated except for Azone. It was also found that increasing enhancer pretreatment duration from 1.0 hr to 3.0 hrs did increase enhancement effect directionally, but not statistically significant. Br-iminosulfurane was the most effective enhancer and DDAIP was the second most effective enhancer in enhancing transdermal delivery of LHCl. All the four enhances were not effective in enhancing transdermal delivery of NHT and ODAN HCl. However, DDAIP was effective in enhancing transdermal delivery of DHCl. DDAIP HCl was not effective in delivering the four drugs transdermally.

When combined treatments were performed, it was found that while iontophoresis was always the dominating driving force to provide enhancement effect, Br-iminosulfurane and iontophoresis provided synergistic effects for transdermal delivery of LHCl and NHT, and DDAIP and iontophoresis provided syngergistic effects for NHT and ODAN HCl.

When "iontophoresis dosing" was at the same level (2.4 mA*h) on transdermal delivery of LHCl and NHT, it was observed that 0.3 mA 8 h (iontophoresis dose = 0.3 x 8 h) of iontopohoresis can provide higher enhancement effect than 0.1 mA 24 h (iontophoresis dose = 0.1 x 24 h), i.e. fast mode of action. However, 0.1 mA for 24 hrs can provide higher and more sustained LHCl and NHT permeability.

Skin Integrity and Cytotoxicity Study

SEM and DSC data suggested that neither iontophoreis and chemical enhancer nor their combination caused detrimental effects on skin. NexMed's in vivo data [170] and cytotoxicity data for Br-iminosulfurane [15] further confirmed that DDAIP, DDAIP HCl and Br-iminosulfurane at this use level of 5% are safe to be used as chemical enhancers for enhancing transdermal drug delivery.

CHAPTER 5 *IN VITRO* TRANSBUCCAL EXPERIMENTAL METHODOLOGY

5.1 Materials and Equipment

All materials and equipment used have been described in Section 4.1, except for the following: EpiOral™ Tissue (ORL-202) was purchased from MatTek Corporation Ashland, MA and Nikon Eclipse E 800 light microscope and Nikon Digital Camera (Model DXM 1200) (Micro Optics, Cedar Knolls, NJ) were used for all histological studies. Microplate Power Wave X Scanning Spectrophotometer (Bio-TEK Instruments, Inc., Winooski, VT, USA) was used for the buccal tissue cytotoxicity study.

5.2 Methodology

Buccal Tissue Preparation

Buccal mucosa samples with underlying connective tissue were surgically removed from the pig cheek area (Barton's Farms and Biologicals, Great Meadows, NJ) and stored under – 30 ^{o}C for future use. Prior to use, the samples were thawed at room temperature for at least 3 hours. Then the underlying connective tissue was removed using a scalpel blade and the remaining buccal mucosa was then carefully trimmed using surgical scissors to a thickness of about 300 - 400 μm. The buccal tissues were placed in phosphate buffered saline (PBS) with pH = 7.5 for 1.0 hour prior to use.

In Vitro Transbuccal Permeation Study

Franz diffusion cells (PermeGear, PA, USA) were used for all i*n vitro* permeation studies using buccal tissue under varying conditions: passive (control), 1.0 hr enhancer pretreatment, 8.0 hrs iontophoresis (0.1, 0.2 and 0.3 mA), and combined treatment of 1.0 hr enhancer pretreatment and 8.0 hrs iontophoresis at 0.3 mA, and then passive only up to 24 hrs. All experiments were performed at 37°C.

For the passive permeation study, Franz cell receptor compartment was filled with PBS solution and stirred at 600 rpm. The buccal tissue was placed in between the donor and receptor compartments with the side of connective tissue facing the donor compartment. The available diffusion area was 0.64 cm^2. 0.3 ml of the drug formulation was added into the donor compartment at the beginning of the experiment. At different time points (0.0, 0.5, 1.0, 3.0, 5.0, 8.0, 12, 20.0, 24.0 hrs), 300 µl sample was withdrawn from receptor compartment for HPLC analysis and immediately replaced with 300 µl of PBS (pH =7.5).

For enhancer pretreatment, the same procedures described above for passive permeation were followed except that the buccal tissue was pretreated for 1 hr by adding 30 µl of chemical enhancer solution on top of buccal tissue in the donor compartment prior to the application of 0.3 ml drug formulation.

For iontophoresis, Phoresor II Auto (Model PM 850) provided 0.1, 0.2 and 0.3 mA for 8 hrs of treatment. The anodal electrode (Ag) was placed in the gel formulation in the donor compartment about 2 mm above the buccal tissue membrane. The cathode (AgCl) was inserted into the receptor compartment. After 8 hours, iontophoresis was discontinued and then the passive-only permeation experiment continued for 16 hrs. The sampling method and time points were the same as for passive and chemical enhancer pretreatment permeation experiments.

5.3 Data Analyses

The steady state flux at time t (J, μg cm $^{-2}$) was calculated from the slope of the linear portion of the profile of cumulative drug amounts permeated *vs*. time. The cumulative drug amount in the receptor compartment after 8 hrs and 24 hrs was defined as Q_8 and Q_{24} (μg cm $^{-2}$), respectively. The enhancement ratio (ER) for flux was calculated as follows:

$$ER = \frac{\text{Flux for treated buccal tissue with enhancer or iontophoresis or their combination}}{\text{Flux for untreated buccal tissue}}$$

Results were presented as mean±standard error (n) where n represented the number of replicates. Data analysis of ER was performed for treated tissue against control by the unpaired Student's t-test. ANOVA was used to compare ERs among different treated tissues. A probability of less than 5% ($p<0.05$) was considered significant.

5.4 Evaluation of Buccal Integrity

Histology of Tissues

The morphological changes in both untreated and treated buccal tissues were evaluated using light microscopy. Buccal membrane samples were sectioned carefully and fixed in 10% buffered formalin for 1 day at room temperature. Tissue samples were successively dehydrated with 50%, 75%, 95% and 100% alcohol for one hour each. This was followed by immersing in xylene at least three times, and finally embedding in Tissue-Tek O.C.T. compound under dry ice. Using a microtome (Leica Model CM 1850, Leica Microsystems, Inc. Bannockburn, IL, USA), 7 μm thin slices were prepared and then stained with Mayer's Harris Hematoxylin and Eosin Y (H&E). The stained slices were examined under a Nikon Eclipse E 800 light microscope (Micro Optics, Cedar Knolls, NJ) at 40 X. A Nikon Digital Camera (Model DXM 1200) was used to capture

images. Images were processed by SPOT ^{TM} Imaging Software, Version 5.0 (Diagnostic Instrument, Inc., Sterling Heights, MI, USA).

5.5. Buccal Cytotoxicity Study

EpiOral ™ tissue (ORL-200) from MatTek Corp. was used and this is a multilayered tissue mainly composed of an organized basal layer and multiple non-cornified layers analogous to native human buccal tissue. A 24-well plate containing ORL-200 (cell culture inserts) was stored in the refrigerator (4 ^{o}C) prior to use. Under sterile forceps, the cell culture inserts were transferred into four 6-well plates containing pre-warmed assay medium (37 ^{o}C). The 6-well plates containing the tissue samples were then placed in a humidified 37 ^{o}C and 5% CO_2 incubator for 1 hour prior to dosing. Tissues were exposed to 20, 60, and 240 minutes of enhancer solution dosed in duplicate. Two inserts were left untreated to serve as a Negative Control (sterilized water) and another two inserts served as a Positive Control (1% Triton X-100 - a nonionic surfactant, polyethylene glycol p-(1,1,3,3-tetramethylbutyl)-phenyl ether). Exposure time for the Positive and Negative Controls was 60 minutes as per EpiOral 200 Protocol from MatTek Corp. [171]. After 1 hour incubation, the assay media was removed from the wells and replaced with 0.9 ml of pre-warmed fresh media, then 40 µl of 1:1 diluted enhancer solution (5% DDAIP HCl in water) in sterilized water were added into the cell culture inserts atop the EpiOral™ tissue. 40 µl of sterilized water as negative control and 100 µl of 1% Triton -100 as positive control were added in separate wells. Then the well plates containing the dosed EpiOral™ tissues were returned to the incubator for 20, 60, and 240 minutes. After the exposures, each tissue insert was gently removed, rinsed with PBS solution at least twice and transferred into a 24-well plate containing premixed MTS solution (ratio of MTS reagent : assay

medium = 1:4) The 24-well plate was then returned to 37 ^{o}C, 5% CO_2 incubator for 3 hours. After this, 100 µl of the reacted MTS solutions from each well was pipetted into a marked 96-well microtiter plate for spectrophotometer reading (SPR) at 490 nm using Microplate Power Wave X Scanning Spectrophotometer (Bio-TEK Instruments, Inc., Winooski, VT, USA). 100µl of assay medium was used as a blank. The EpiOral tissue % viability at each of the dosed concentrations was calculated using the following formula:

% Viability = 100 x [SPR for Treated Sample/ SPR for Negative Control]

Dose response curve was established using a semi-log scale to plot % viability (linear y axis) vs. the dosing time (log x axis). ET-50 value - the time required for the % viability of EpiOral™ tissue to fall to 50 was obtained through interpolation. All the SPR were deducted from blank readings for viability and ET-50 value final calculations.

5.6. Results and Discussion

5.6.1 Lidocaine HCl (LHCl) Transbuccal Delivery

5.5.1.1 Enhancement Using Iontophoresis

The physical enhancement technique - iontophoresis was applied to enhance transbuccal delivery of LHCl through porcine buccal tissue using *in vitro* Franz cell diffusion model. Table 32 shows that when compared to control, significant enhancement effects were achieved using iontophoresis for 8 hrs at 0.1, 0.2 and 0.3 mA, respectively. 0.3 mA iontophoresis provided significantly higher enhancement effect than that of 0.1, but not significantly than 0.2 mA. The correlation between current and flux was linear (Figure 44). It was observed (Table 33) that when iontophoresis was discontinued at 8 h, the post-iontophoretic effect on drug permeation

continued to be statistically significant when compared to control, indicating that iontophoresis increased the permeability of the buccal tissue.

It was also observed that flux values for 0.1, 0.2 and 0.3 mA treatments were not significantly reduced, indicating that the flux of the drug may be not predominantly electrically driven (electrorepulsion) and instead the direct effect of electroosmosis may be important as well during iontophoretic transbuccal transport of LHCl. When a 10 cm^2 patch is used for 24 hrs, 0.3 mA iontophoresis can potentially deliver 3 x Q_8 x 10 = 3 x 1910 x 10 = 57.3 mg / day, i.e., a therapeutic level: an epidural dose of LHCl can be delivered into blood circulation.

Table 32. Effect of current on transbuccal delivery of LHCl (Stage I) [a]

Iontophoresis (mA)	Flux ($\mu g/cm^2*h$)	Q8 ($\mu g/cm^2$)	ER
Control	44.7±9.6	345.6±74.3	1.0
0.1	137.1±13.1[b]	1085.2±92.1	3.1
0.2	184.0±30.3[b]	1431.7±229.5	4.1
0.3	241.7±60.5[b]	1910.2±454.7	5.4

[a] Data are presented as means ± S.D. ($3 \leq N \leq 8$).

[b] Statistically significantly higher than control ($p < 0.05$) (Student's t-test).

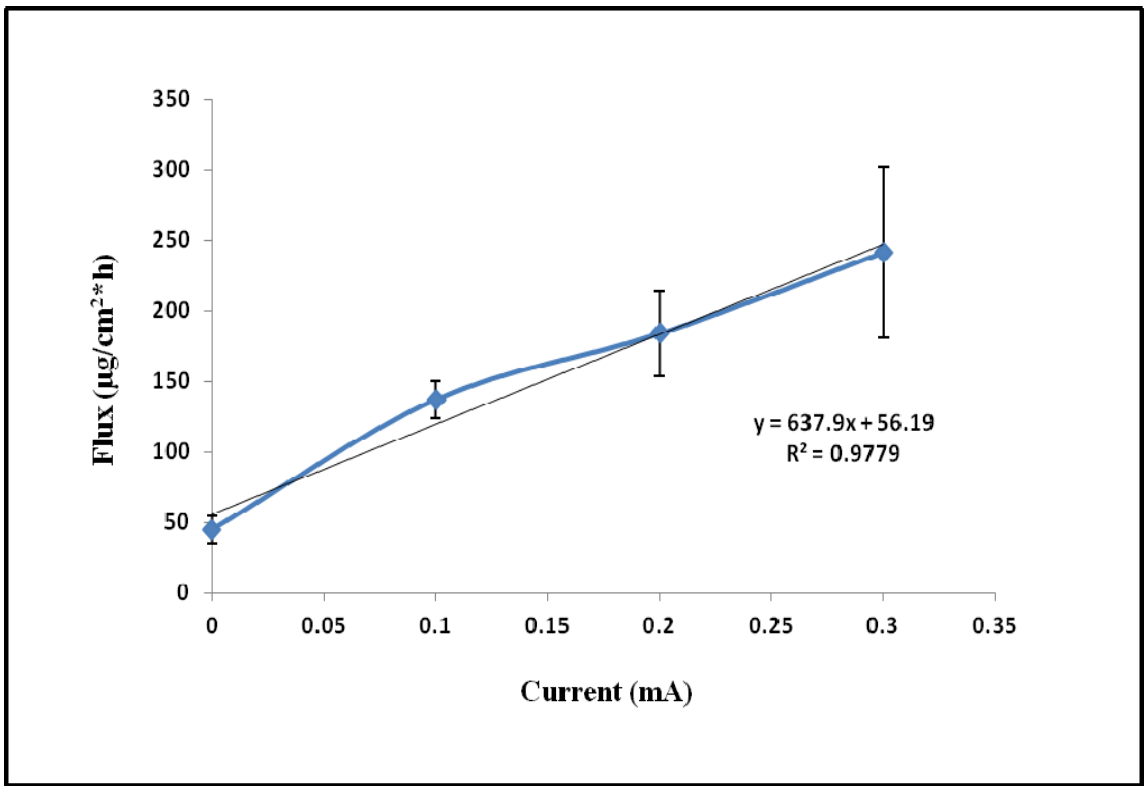

Figure 44. Effect of current on flux of LHCl transbucal delivery at 8 h.

Data are presented as means ± S.D. (3≤N≤8).

Table 33. Effect of current on transbuccal delivery of LHCl (Stage II) [a]

Iontophoresis (mA)	Flux (µg/cm²*h)	Q_{24} (µg/cm²)	ER
Control	72.4±24.4	1486.1±452.2	1.0
0.1	125.9±11.6	3106.2±219.8[b]	1.7
0.2	110.9±26.4	3222.9±468.8[b]	1.5
0.3	175.6±63.9[b]	4702.7±1426.0[b]	2.4

[a] Data are presented as means ± S.D. (3≤N≤8).

[b] Statistically significantly higher than control ($p < 0.05$) (Student's t-test).

5.5.1.2 Enhancement Using Chemical Enhancer

The enhancement effects of various 1 h enhancer pretreatments (Azone, DDAIP and DDAIP HCl and Br-iminosulfurane) on transbuccal delivery of LHCl were evaluated using *in vitro* Franz cell diffusion model on porcine buccal tissue. Table 34 and 35 show that compared to control, DDAIP HCl significantly enhanced transbuccal delivery of LHCl while DDAIP, Azone and Br-iminosulfurane demonstrated marginal enhancement effect. It is of interest to note that DDAIP HCl in water exhibited higher permeability than DDAIP HCl in PG, indicating that PG actually acted as a penetration "retardant" when used as a vehicle for DDAIP HCl. Table also shows that using 5% DDAIP HCl in water treatment alone, transbucal delivery of LHCl (Q_{24}) could reach 6926 ($\mu g/cm^2$) within 24 h, i.e. potentially when a small patch of 10 cm^2 containing only 2.5% LHCl is used, this particular enhanced drug delivery system could deliver 69.3 mg/day – a therapeutic epidural dose into blood circulation through buccal route.

It was also interesting to find that DDAIP HCl in water pretreatment alone (Table 28 and 29) provided significantly higher enhancement of transbuccal delivery of LHCl than iontophoresis at 0.3 mA during the first 8 h and the following 16 h of the study ($p<0.05$) (1 and 2). It is most probable that iontophoresis enhanced transbuccal drug delivery through disordering of the outer epithelial cell layers, i.e. more of the paracellular route [68] similar to disrupting porcine stratum corneum and increasing intercellular space for enhancing transdermal drug delivery [163,164]. In addition, buccal tissues contain a lot of polar lipids which can compete with LHCl for iontophoresis, thus reduce the enhancement effect of iontophoresis. However, hydrophilic DDAIP HCl was more potent in enhancing transbuccal delivery of a hydrophilic drug through both intercellular (paracellular) and intracellular (transcellular) pathways due to the fact that

buccal tissue is non-keratinized, lacks the organized intercellular lipid lamellae and contains large amount of polar lipids [47] that allow more interaction with hydrophilic compounds.

Table 34. Effect of 1.0 hr enhancer pretreatment on transbuccal delivery of LHCl (Stage I) [a]

Enhancer	Flux ($\mu g/cm^2*h$)	Q_8 ($\mu g/cm^2$)	ER
Control	44.7±9.6	345.6±74.3	1.0
PG	39.1±7.3	299.4±59.9	1.0
2.5% Azone in PG	92.8±62.5	754.2±543.7	2.1
5.0% DDAIP in PG	91.6±34.4	716.5±281.8	2.0
5.0% DDAIP HCl in water	368.5±111.5[b]	2902.0±853.1	8.2
5.0% DDAIP HCl in PG	217.7±54.0[b]	1703.9±419.2	4.9
5.0% Br-Iminosulfurane in PG	92.4±26.9	749.7±216.8	2.1

[a] Data are presented as means ± S.D. ($3 \leq N \leq 8$).

[b] Statistically significantly higher than other enhancers and control ($p < 0.05$) (Student's t-test).

Table 35. Effect of 1.0 h enhancer pretreatment on transbuccal delivery of LHCl (Stage II) [a]

Enhancer	Flux ($\mu g/cm^2*h$)	Q_{24} ($\mu g/cm^2$)	ER
Control	72.4±24.4	1486.1±452.2	1.0
PG	46.7±6.8	1002.3±168.6	1.0
2.5% Azone in PG	141.9±34.2	2989.1±1065.6	2.0
5.0% DDAIP in PG	113.7±35.8	2548.1±874.5	1.7
5.0% DDAIP HCl in water	262.6±72.2	6926.6±2028.8 [b]	4.7
5.0% DDAIP HCl in PG	289.5±34.8	6086.3±1057.1 [b]	4.1
5.0% Br-Iminosulfurane in PG	189.5±46.2	3794.4±942.2	2.6

[a] Data are presented as means ± S.D. ($3 \leq N \leq 8$).

[b] Statistically significantly higher than other enhancers and control ($p < 0.05$) (Student's t-test).

5.5.1.3 Combined Enhancement Effect

Combined treatments using iontophoresis and chemical enhancers were conducted to investigate their potential synergistic enhancement effects on transbuccal delivery of LHCl using *in vitro* Franz cell diffusion model and porcine buccal tissue. Table 36 shows that the combined treatments of iontophoresis (0.3 mA for 8 h) and chemical enhancers (Azone, DDAIP, DDAIP HCl and Br-iminosulfurane) provided significant enhancement effects on transbuccal delivery of LHCl when compared to control. However, there were no synergistic enhancement effects

observed. It was also observed that the combination of DDAIP HCl in water and iontophoresis (0.3 mA) was the most effective treatment in enhancing transbuccal delivery of LHCl (Figure 45). However, with DDAIP HCl in water pretreatment, the flux value (431.1 μg/cm^2*h) from the combined treatment was much less than the sum of the flux values of DDAIP HCl in water (368.5 μg/cm^2*h) and iontophoresis (241.7 μg/cm^2*h) during the 24 h of the study (Table 37). The same trend was recorded for DDAIP HCl in PG. It can be explained by the fact that DDAIP HCl – the salt form of DDAIP contained ions that competed with LHCl for iontophoresis, thus the enhancement effect of iontophoresis was reduced.

Table 36. Combined effect of iontophoresis 0.3 mA 8 hrs treatment and 1.0 hr enhancer pretreatment (Stage I) [a]

Treatment	Flux ($\mu g/cm^2*h$)	Q_8 ($\mu g/cm^2$)	ER
Control	44.7±9.6	345.6±74.3	1.0
0.3 mA	241.7±60.5[b]	1910.2±454.7	5.4
PG+0.3 mA	250.7±41.3[b]	2014.5±313.2	5.6
2.5% Azone in PG+0.3 mA	250.4±15.8[b]	1977.7±126.4	5.6
5.0% DDAIP in PG+0.3 mA	275.9±42.9[b]	2195.6±320.1	6.2
5.0% DDAIP HCl in water+0.3 mA	431.1±27.5[b, c]	3373.0±190.9	9.6
5.0% DDAIP HCl in PG+0.3 mA	406.3±363.7[b]	2992.8±237.8	9.1
5.0% Br-Iminosulfurane in PG+0.3 mA	249.8±32.8[b]	2028.9±255.5	5.6

[a] Data are presented as means ± S.D. ($3 \leq N \leq 8$).

[b] Statistically significantly higher than control ($p < 0.05$) (Student's t-test).

[c] Statistically significantly higher than Azone, Br-iminosulfurane, DDAIP and control ($p < 0.05$) (Student's t-test).

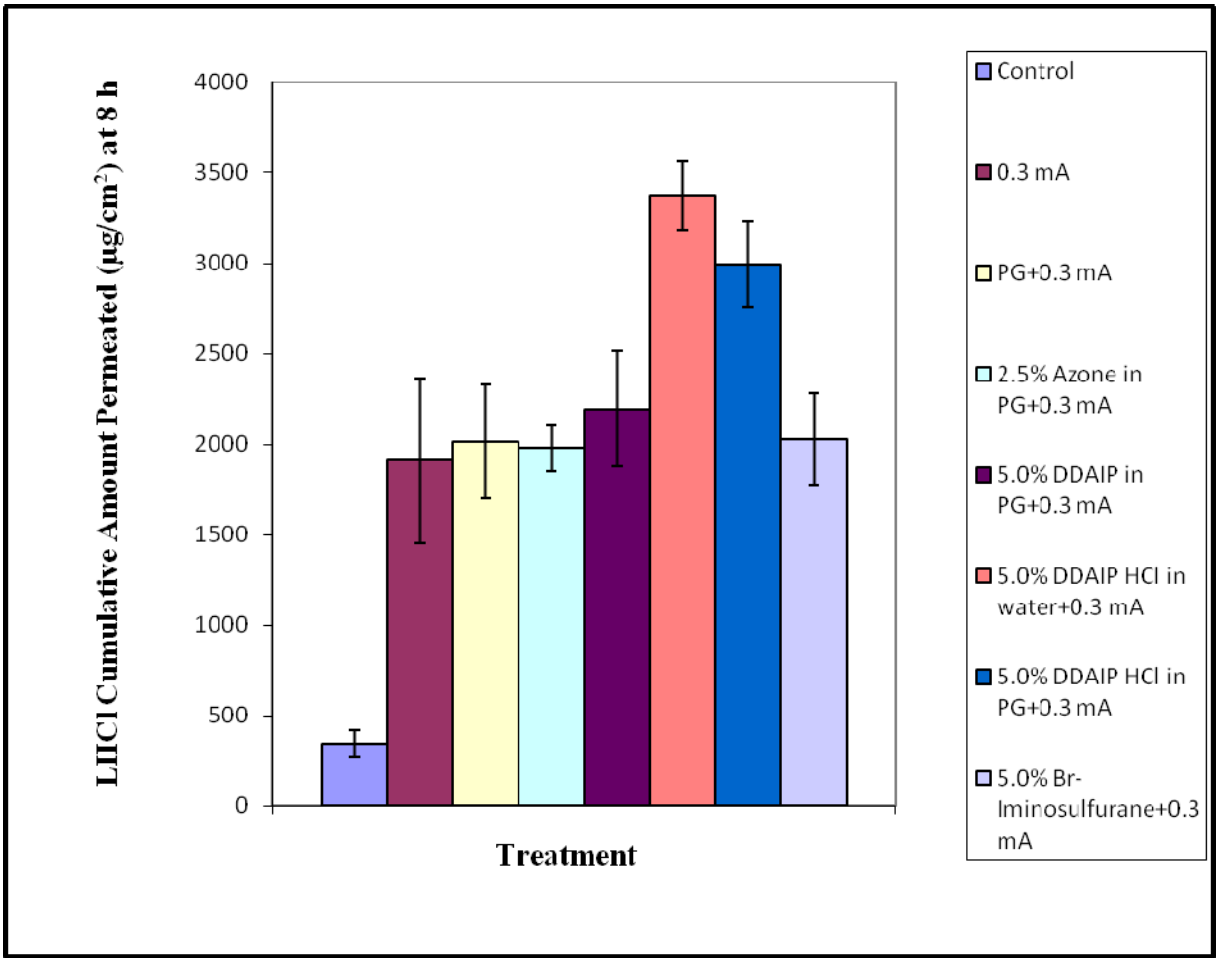

Figure 45. Combined effect of iontophoresis and enhancer on transbuccal delivery of LHCl

Table 37. Combined effect of iontophoresis 0.3 mA 8 hrs treatment and 1.0 hr enhancer pretreatment (Stage II) [a]

Treatment	Flux ($\mu g/cm^2*hr$)	Q_{24} ($\mu g/cm^2$)	ER
Control	72.4±24.4	1486.1±452.2	1.0
0.3 mA	175.6±63.9[b]	4702.7±1426.0	2.4
PG+0.3 mA	88.0±7.6	3432.2±375.6	1.1
2.5% Azone in PG+0.3 mA	168.9±18.9[b]	4697.1±214.4	2.3
5.0% DDAIP in PG+0.3 mA	164.6±42.8[b]	5010.5±670.3	2.3
5.0% DDAIP HCl in water+0.3 mA	303.5±42.7[b, c]	8079.8±786.1	4.2
5.0% DDAIP HCL in PG+0.3 mA	185.4±15.8[b]	5846.9±2270.5	2.6
5.0% Br-Iminosulfurane in PG+0.3 mA	192.8±34.4[b]	5177.5±662.1	2.7

[a] Data are presented as means ± S.D. ($3 \leq N \leq 8$).

[b] Statistically significantly higher than control ($p < 0.05$).

[c] Statistically significantly higher than Azone, Br-iminosulfurane, DDAIP and control ($p < 0.05$) (Student's t-test).

5.6.2 Nicotine Hydrogen Tartrate Transbuccal Delivery (NHT)

5.5.2.1 Enhancement Using Iontophoresis

Iontophoresis was applied to enhance transbuccal delivery of NHT through porcine buccal tissue using *in vitro* Franz cell diffusion model. Table 38 shows that when compared to control, significant enhancement effect was achieved using iontophoresis for 8 hrs at 0.1, 0.2 and 0.3 mA, respectively. 0.3 mA iontophoresis provided significantly higher enhancement effect than that of 0.1 and 0.2 mA and the correlation between current and flux was linear (Figure 46). It was observed (Table 39) that when iontophoresis was discontinued at 8 h, the post-iontophoretic effect on drug permeation continued to be statistically significant when compared to Control, indicating that iontophoresis increased the permeability of the buccal tissue. It was also observed that flux values for 0.1, 0.2 and 0.3 mA treatments were significantly reduced, indicating that the flux of the drug may be predominantly electrically driven (electrorepulsion) and the effect of electroosmosis may not be significant during iontophoretic transbuccal transport of NHT. When a 10 cm^2 patch is used for 24 hrs, 0.3 mA iontophoresis can potentially deliver 3 x Q_8 x 10 = 3 x 629 x 10 = 18.9 mg / day, i.e., a therapeutic level of NHT can be delivered into blood circulation.

Table 38. Effect of current on transbuccal delivery of NHT (Stage I) [a]

Iontophoresis (mA)	Flux ($\mu g/cm^2*h$)	Q8 ($\mu g/cm^2$)	ER
Control	0.9±0.4	6.9±2.6	1.0
0.1	17.6±6.9[b]	141.5±58.6	19.5
0.2	27.0±16.7[b]	207.4±143.2	30.0
0.3	81.7±35.9[b, c]	629.5±276.8	90.7

[a] Data are presented as means ± S.D. ($3 \leq N \leq 8$).

[b] Statistically significantly higher than control ($p < 0.05$) (Student's t-test)..

[c] Statistically significantly higher than 0.1 mA, 0.2 mA and control ($p < 0.05$) (Student's t-test).

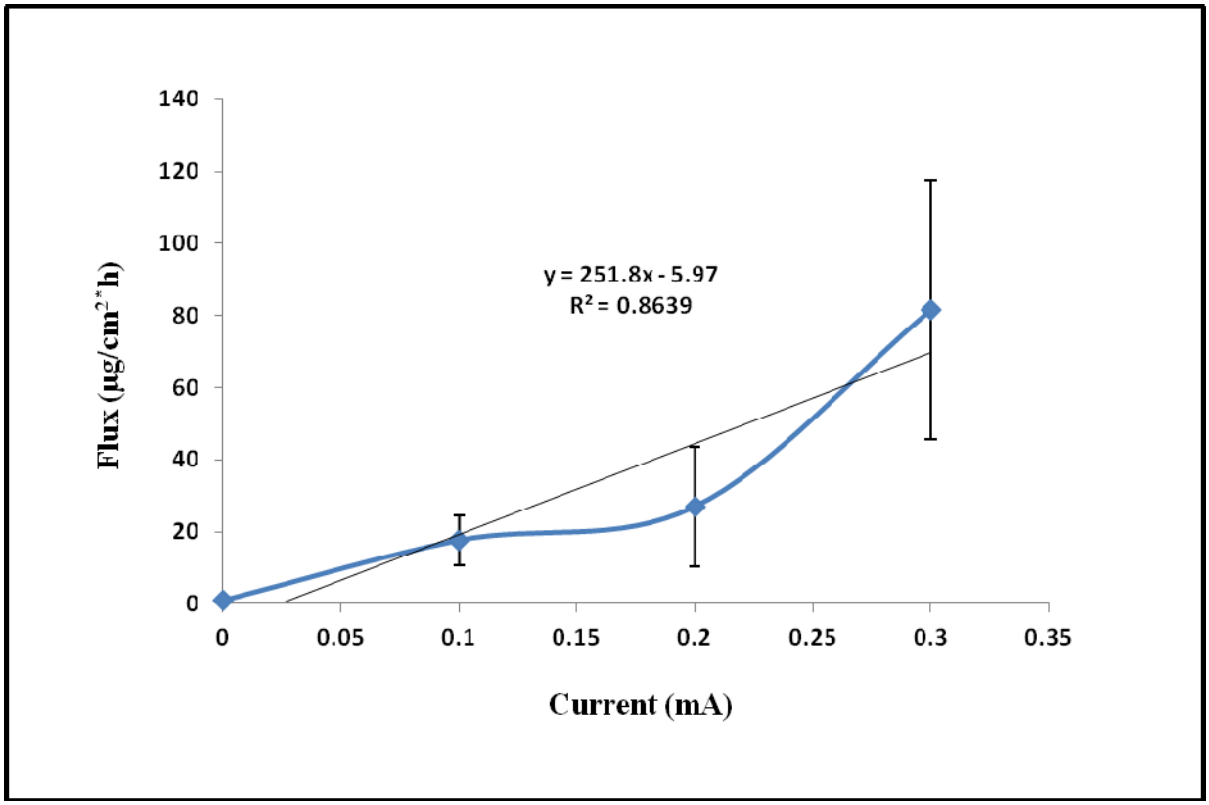

Figure 46. NHT Flux (µg/cm^2*h) vs Current (mA)

Table 39. Effect of current on transbuccal delivery of NHT (Stage II) [a]

Iontophoresis (mA)	Flux (µg/cm^2*h)	Q_{24} (µg/cm^2)	ER
Control	1.6±0.4	33.2±5.4	1.0
0.1	25.2±9.0[b]	582.8±237.6	15.8
0.2	26.6±18.1[b]	615.1±284.4	16.6
0.3	28.7±22.7[b]	1053.7±597.2	17.9

[a] Data are presented as means ± S.D. (3≤N≤8).

[b] Statistically significantly higher than control ($p < 0.05$) (Student's t-test).

5.5.2.2 Enhancement Using Chemical Enhancer

The enhancement effects of various 1 h enhancer pretreatments (Azone, DDAIP and DDAIP HCl and Br-iminosulfurane) on transbuccal delivery of NHT were evaluated using *in vitro* Franz cell diffusion model on porcine buccal tissue. During 8 h of permeation study, Table 40 shows that DDAIP HCl and DDAIP significantly enhanced transbuccal delivery of NHT while Azone and Br-iminosulfurane did not provide enhancement effect. During 24 h of permeation study, the results suggested (Table 40) that all tested enhancers exhibited enhancement effects and DDAIP HCl was clearly the most effective enhancer in promoting transbuccal delivery of NHT.

It is of interest to note that DDAIP HCl in water provided higher permeability than DDAIP HCl in PG, indicating that PG actually acted as a penetration "retardant" when used as a vehicle for DDAIP HCl. Table 40 also shows that using 5% DDAIP HCl in water treatment alone, transbucal delivery of NHT (Q_{24}) could reach 9255 ($\mu g/cm^2$) within 24 h, i.e. potentially when a small patch of 10 cm^2 containing only 20 mg/ml of NHT gel is used, this particular enhanced drug delivery system could deliver 92 mg/day – a therapeutic dose into blood circulation through buccal route. It was also interesting to find that DDAIP HCl in water pretreatment alone (Table 34 and 35) provided significantly higher enhancement of transbuccal delivery of NHT than iontophoresis at 0.3 mA during the first 8 h and the following 16 h of the study ($p<0.05$) (Table 38 and 39). It is most probable that iontophoresis enhanced transbuccal drug delivery through disordering of the outer epithelial cell layers, i.e. more of the paracellular route [68] similar to disrupting porcine stratum corneum and increasing intercellular space for enhancing transdermal drug delivery [163,164]. In addition, buccal tissues contain relatively high amounts of polar lipids that can compete with NHT during the iontophoretic process, thus reducing the enhancement effect of iontophoresis. However, hydrophilic DDAIP HCl was more potent in

enhancing transbuccal delivery of a hydrophilic drug through both intercellular (paracellular) and intracellular (transcellular) pathways due to the fact that buccal tissue is non-keratinized, lacks the organized intercellular lipid lamellae and contains large amount of polar lipids [47] that allow more interaction with hydrophilic compounds.

Table 40. Effect of 1.0 hr enhancer pretreatment on transbuccal delivery of NHT (Stage I) [a]

Enhancer	Flux ($\mu g/cm^2*h$)	Q_8 ($\mu g/cm^2$)	ER
Control	0.9±0.4	6.9±2.6	1.0
PG	1.0±1.0	1.0±1.0	1.0
2.5% Azone in PG	1.0±1.0	1.0±1.0	1.0
5.0% DDAIP in PG	70.3±60.3[b, c]	579.8±490.21	78.1
5.0% DDAIP HCl in water	335.2±104.5[b, c]	2768.0±789.0	372.4
5.0% DDAIP HCl in PG	171.1±58.9[b]	1304.6±415.4	190.1
5.0% Br-Iminosulfurane in PG	1.0	9.6±19.0	1.0

[a] Data are presented as means ± S.D. ($3 \leq N \leq 8$).

[b] Statistically significantly higher than control ($p < 0.05$) (Student's t-test).

[c] Statistically significantly higher than Azone, Br-iminosulfurane, DDAIP and control ($p < 0.05$) (ANOVA).

Table 41. Effect of 1.0 h enhancer pretreatment on transbuccal delivery of NHT (Stage II) [a]

Enhancer	Flux ($\mu g/cm^2*h$)	Q_{24} ($\mu g/cm^2$)	ER
Control	1.6±0.4	33.2±5.4	1.0
PG	3.1±2.2	40.2±26.4	2.0
2.5% Azone in PG	34.7±21.8[b]	505.9±310.8	21.7
5.0% DDAIP in PG	122.7±62.2[b]	2566.7±1463.3	76.7
5.0% DDAIP HCl in water	405.5±88.6[b, c]	9255.6±1471.4	253.4
5.0% DDAIP HCl in PG	401.3±36.9[b, c]	7609.4±528.9	250.8
5.0% Br-Iminosulfurane in PG	17.7±10.2[b]	324.7±186.2	11.1

[a] Data are presented as means ± S.D. ($3 \leq N \leq 8$).

[b] Statistically significantly higher than control ($p < 0.05$) (Student's t-test)..

[c] Statistically significantly higher than Azone, Br-iminosulfurane, DDAIP and control ($p < 0.05$) (ANOVA).

5.5.2.3 Combined Enhancement Effect

Combined treatments of iontophoresis and chemical enhancers were conducted to investigate their synergistic enhancement effects on transbuccal delivery of NHT using *in vitro* Franz cell diffusion model on porcine buccal tissue. Table 42 shows that the combined treatments of iontophoresis (0.3 mA for 8 h) and chemical enhancer pretreatment 1 h (Azone, DDAIP, DDAIP HCl and Br-iminosulfurane) provided significant enhancement effects on transbuccal delivery of NHT when compared to control. During the 8 h of combined treatments, there were no synergistic enhancement effects observed, and only additive enhancement effects were observed for iontophoresis and DDAIP HCl or DDAIP. It was also observed that the combination of DDAIP HCl in water and iontophoresis (0.3 mA) was the most effective treatment (Figure 47). However, with DDAIP HCl in water pretreatment, the flux value (400.5 $\mu g/cm^2*h$) from the combined treatment was much less than the sum of the flux values of DDAIP HCl in water (335.5$\mu g/cm^2*h$) and iontophoresis (81.7 $\mu g/cm^2*h$) during the 24 h of the study (Table 43). The same trend was recorded for DDAIP HCl in PG. It can be explained by the fact that DDAIP HCl – the salt form of DDAIP contained ions that competed with NHT during the iontophoretic process, thus reducing the enhancement effect of iontophoresis.

Table 42. Combined effect of iontophoresis 0.3 mA 8 hrs treatment and 1.0 hr enhancer pretreatment (Stage I) [a]

Treatment	Flux ($\mu g/cm^2*h$)	Q_8 ($\mu g/cm^2$)	ER
Control	0.9±0.4	6.9±2.6	1.0
0.3 mA	81.7±35.9[b]	629.5±276.8	90.7
PG+0.3 mA	53.1±20.9[b]	394.0±157.9	59.0
2.5% Azone in PG+0.3 mA	48.5±18.1[b]	374.3±159.1	53.9
5.0% DDAIP in PG+0.3 mA	215.3±136.7[b, c]	1683.9±1022.8	239.2
5.0% DDAIP HCl in water+0.3 mA	400.5±41.4[b, c]	3158.1±323.1	445.0
5.0% DDAIP HCl in PG+0.3 mA	376.0±87.4[b, c]	2942.3±667.5	417.8
5.0% Br-Iminosulfurane in PG+0.3 mA	51.1±15.9[b]	406.7±121.7	56.8

[a] Data are presented as means ± S.D. ($3 \leq N \leq 8$).

[b] Statistically significantly higher than control ($p < 0.05$) (Student's t-test)..

[c] Statistically significantly higher than Azone, Br-iminosulfurane, DDAIP and control ($p < 0.05$) (ANOVA).

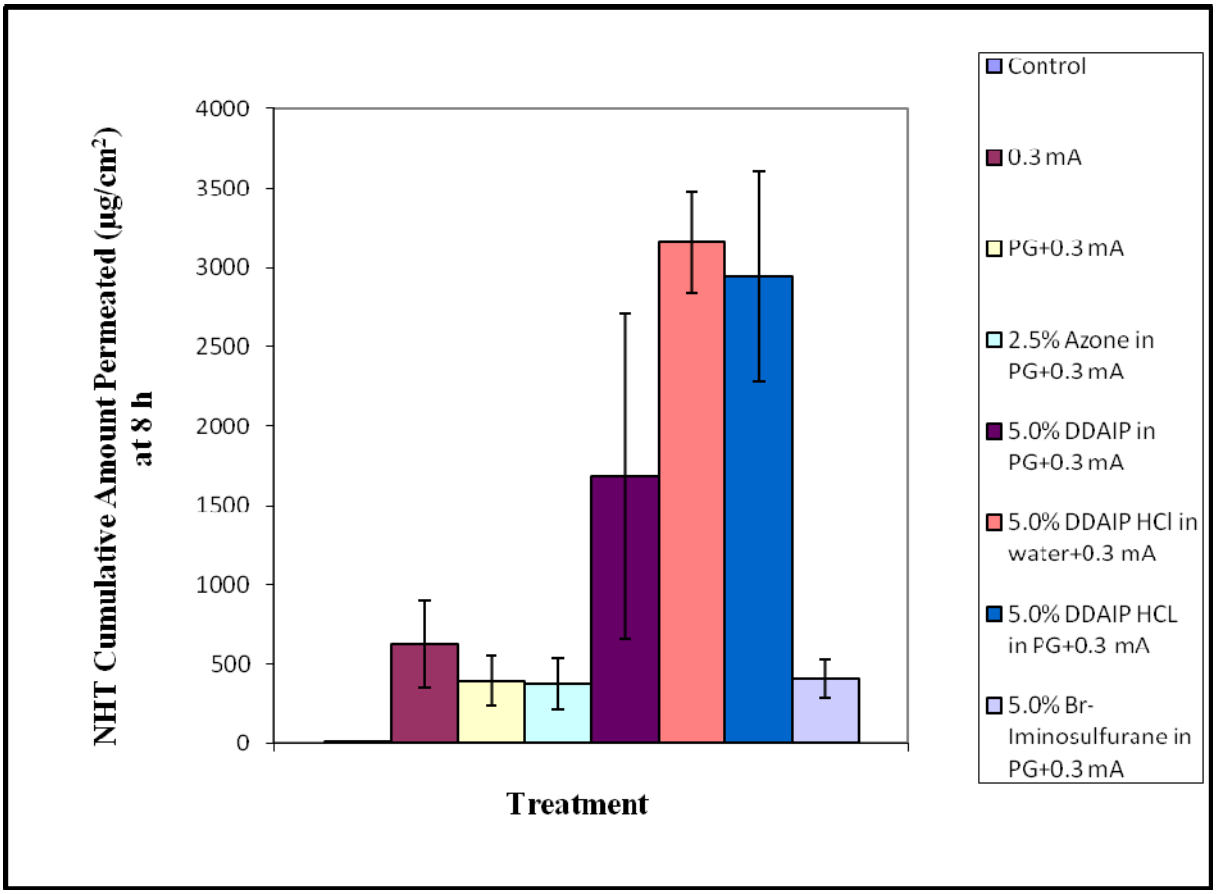

Figure 47. Combined effect of iontophoresis and enhancer on transbuccal delivery of NHT

Table 43. Combined effect of iontophoresis 0.3 mA 8 hrs treatment and 1.0 hr enhancer pretreatment (Stage II) [a]

Treatment	Flux ($\mu g/cm^2*hr$)	Q_{24} ($\mu g/cm^2$)	ER
Control	1.6±0.4	33.2±5.4	1
0.3 mA	28.7±22.7[b]	1053.7±597.2	17.9
PG+0.3 mA	28.20±28.5[b]	899.2±609.6	17.6
2.5% Azone in PG+0.3 mA	37.6±25.7[b]	974.7±562.5	23.5
5.0% DDAIP in PG+0.3 mA	113.0±49.8[b]	3493.1±1343.3	70.6
5.0% DDAIP HCl in water+0.3 mA	236.6±72.1[b, c]	6916.2±1238.7	147.9
5.0% DDAIP HCL in PG+0.3 mA	281.5±46.8[b, c]	7410.8±1333.7	175.9
5.0% Br-Iminosulfurane in PG+0.3 mA	45.4±26.5[b]	1132.0±469.9	28.0

[a] Data are presented as means ± S.D. ($3 \leq N \leq 8$).

[b] Statistically significantly higher than control ($p < 0.05$) (Student's t-test).

[c] Statistically significantly higher than other enhancers and control ($p < 0.05$) (ANOVA).

5.6.3 Diltiazem HCl Transbuccal Delivery (DHCl)

5.5.3.1 Enhancement Using Iontophoresis

Iontophoresis was applied to enhance transbuccal delivery of DHCl through porcine buccal tissue using *in vitro* Franz cell diffusion model. Table 44 shows that when compared to control, significant enhancement effect was achieved using iontophoresis for 8 hrs at 0.1, 0.2 and 0.3 mA, respectively. 0.3 mA iontophoresis provided significantly higher enhancement effect than that of 0.1, but not significantly than 0.2 mA. The correlation between current and flux was linear (Figure 48). It was observed (Table 45) that when iontophoresis was discontinued at 8 h, flux values for 0.1, 0.2 and 0.3 mA treatments were significantly reduced, indicating that the flux of the drug was predominantly electrically driven (electrorepulsion) and electroosmosis was not a significant contributor to iontophoretic transbuccal transport of DHCl and iontophoresis treatment did not increase permeability of buccal tissue. When a 10 cm^2 patch is used for 24 hrs, 0.3 mA iontophoresis can potentially deliver 3 x Q_8 x 10 = 3 x 650.9 x 10 = 19.0 mg / day, i.e., a therapeutic dose of DHCl can be delivered into blood circulation.

Table 44. Effect of current on transbuccal delivery of DHCl (Stage I) [a]

Iontophoresis (mA)	Flux ($\mu g/cm^2*h$)	Q8 ($\mu g/cm^2$)	ER
Control	32.6±9.5	258.3±73.6	1
0.1	54.5±2.6	430.0±18.7	1.7
0.2	72.5±16.7[b]	574.8±118.6	2.2
0.3	80.7±18.0[b]	650.9±139.1	2.5

[a] Data are presented as means ± S.D. ($3 \leq N \leq 8$).

[b] Statistically significantly higher than control ($p < 0.05$) (Student's t-test).

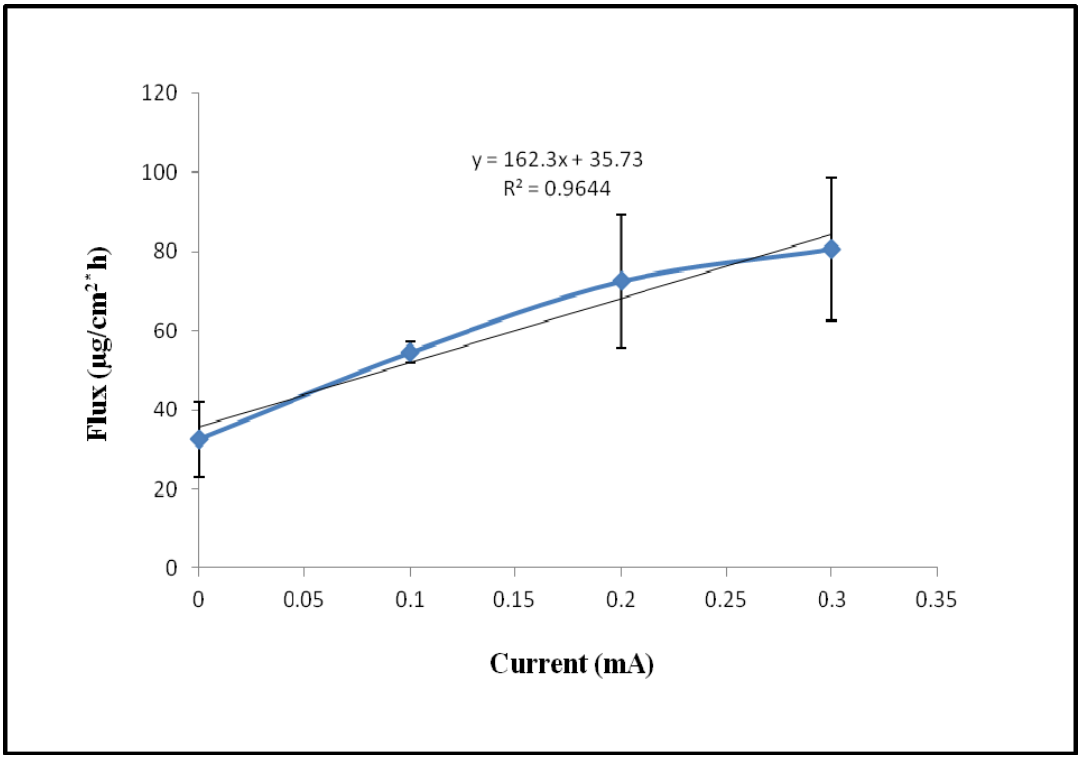

Figure 48. DHCl Flux ($\mu g/cm^2*h$) vs current (mA)

Table 45. Effect of current on transbuccal delivery of DHCl (Stage II) [a]

Iontophoresis (mA)	Flux ($\mu g/cm^2*h$)	Q_{24} ($\mu g/cm^2$)	ER
Control	56.4±18.0	1160.9±370.8	1.0
0.1	62.5±2.7	1426.7±45.2	1.4
0.2	71.8±16.7	1720.1±361.9	1.4
0.3	52.8±36.2	1513.9±667.1	1.0

[a] Data are presented as means ± S.D. ($3 \leq N \leq 8$).

6.3.1.2 Enhancement Using Chemical Enhancer

The enhancement effects of various 1 h enhancer pretreatments (Azone, DDAIP and DDAIP HCl and Br-iminosulfurane) on transbuccal delivery of DHCl were evaluated using *in vitro* Franz cell diffusion model and porcine buccal tissue. Table 46 shows that at 8 h compared to control, all tested enhancers demonstrated only marginal enhancement effect. However, at 24 h DDAIP HCl in water provided significant enhancement effect (Table 47) while other enhancers only provided marginal enhancement effects. It is of interest to note that DDAIP HCl in water exhibited higher permeability than DDAIP HCl in PG, indicating that PG actually acted as a penetration "retardant" when used as a vehicle for DDAIP HCl. It was also interesting to find that at 24 h DDAIP HCl in water pretreatment alone (Table 47) provided significantly higher transbuccal permeability of DHCl than iontophoresis (0.3 mA 8 h). It is most probable that iontophoresis enhanced transbuccal drug delivery through disordering of the outer epithelial cell layers, i.e. more of the paracellular route [68] similar to disrupting porcine stratum corneum and increasing

intercellular space for enhancing transdermal drug delivery [163,164]. However, hydrophilic DDAIP HCl was more potent in enhancing transbuccal delivery of a hydrophilic drug through both intercellular (paracellular) and intracellular (transcellular) pathways due to the fact that buccal tissue is non-keratinized, lacks the organized intercellular lipid lamellae and contains large amount of polar lipids [47] that allow more interaction with hydrophilic compounds.

Table 46. Effect of 1.0 h enhancer pretreatment on transbuccal delivery of DHCl (Stage I) [a]

Enhancer	Flux ($\mu g/cm^2*h$)	Q_8 ($\mu g/cm^2$)	ER
Control	32.6±9.5	258.3±73.6	1
PG	96.4±26.9	757.5±212.2	3
2.5% Azone in PG	83.8±27.4	662.6±218.3	2.5
5.0% DDAIP in PG	54.9±11.2	428.0±83.9	1.7
5.0% DDAIP HCl in water	58.9±14.5	485.1±113.3	1.8
5.0% DDAIP HCl in PG	37.2±29.6	299.7±236.1	1.1
5.0% Br-Iminosulfurane in PG	66.2±22.4	532.2±179.7	2

[a] Data are presented as means ± S.D. ($3 \leq N \leq 8$).

Table 47. Effect of 1.0 h enhancer pretreatment on transbuccal delivery of DHCl (Stage II) [a]

Enhancer	Flux ($\mu g/cm^2*h$)	Q_{24} ($\mu g/cm^2$)	ER
Control	56.4±18.0	1160.9±370.8	1
PG	59.7±39.4	1678.9±822.4	1
2.5% Azone in PG	104.2±37.1	2362.9±806.9	1.8
5.0% DDAIP in PG	72.1±12.0	1591.9±254.7	1.3
5.0% DDAIP HCl in water	141.9±28.3[b]	2798.8±605.9	2.5
5.0% DDAIP HCl in PG	97.8±2.8	1957.9±281.2	1.7
5.0% Br-Iminosulfurane in PG	128.5±48.2	2573.0±942.5	2.3

[a] Data are presented as means ± S.D. ($3 \leq N \leq 8$).

[b] Statistically significantly higher than control ($p < 0.05$) (Student's t-test).

6.3.1.3 Combined Enhancement Effect

Combined treatments of iontophoresis and chemical enhancers were conducted to investigate their potential synergistic enhancement effects on transbuccal delivery of DHCl using *in vitro* Franz cell diffusion model and porcine buccal tissue. Table 48 shows that the combined treatments of iontophoresis (0.3 mA for 8 h) and chemical enhancers (DDAIP, DDAIP HCl and Br-iminosulfurane) provided significant enhancement effects on transbuccal delivery of DHCl when compared to Control. However, combined treatments of Azone and iontophoresis only

provided marginal enhancement effects. No synergistic enhancement effects were noted. It was also observed that the combination of DDAIP HCl in water and iontophoresis (0.3 mA) was the most effective treatment in enhancing transbuccal delivery of DHCl (Figure 49). However, with DDAIP HCl in water pretreatment, the flux value (111.3 $\mu g/cm^2*h$) from the combined treatment was much less than the sum of the flux values of DDAIP HCl in water (58.9 $\mu g/cm^2*h$) and iontophoresis (80.7 $\mu g/cm^2*h$) during the 8 h of the study. The same trend was recorded for DDAIP HCl in PG. It can be explained by the fact that DDAIP HCl – the salt form of DDAIP contained ions that competed with DHCl during the iontophoretic process, thus the overall enhancement effect was reduced.

Table 48. Combined effect of iontophoresis 0.3 mA 8 h treatment and 1.0 h enhancer pretreatment (Stage I) [a]

Treatment	Flux ($\mu g/cm^2*h$)	Q_8 ($\mu g/cm^2$)	ER
Control	32.6±9.5	258.3±73.6	1
0.3 mA	80.7±18.0[b]	650.9±139.1	2.5
PG+0.3 mA	96.4±27.0[b]	757.5±212.3	3
2.5% Azone in PG+0.3 mA	46.8±8.1	379.0±67.7	1.4
5.0% DDAIP in PG+0.3 mA	157.0±49.7[b]	1233.6±375.7	4.8
5.0% DDAIP HCl in water+0.3 mA	111.3±37.3[b]	885.2±281.7	3.4
5.0% DDAIP HCl in PG+0.3 mA	62.3±20.0[b]	509.7±199.9	1.9
5.0% Br-Iminosulfurane in PG+0.3 mA	88.2±11.0[b]	699.4±96.7	2.7

[a] Data are presented as means ± S.D. ($3 \leq N \leq 8$).

[b] Statistically significantly higher than control ($p < 0.05$) (Student's t-test)..

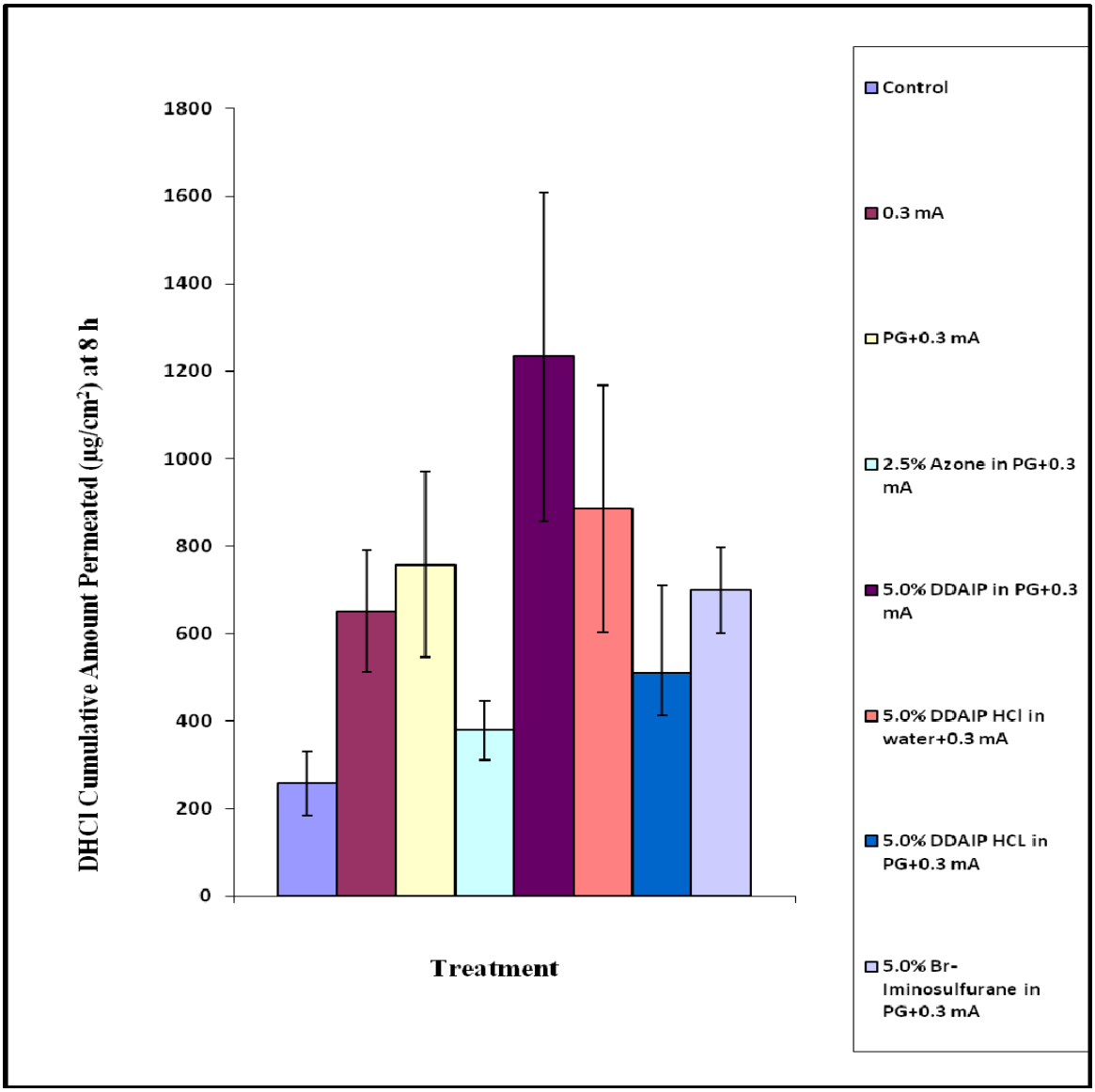

Figure 49. Combined effect of iontophoresis and enhancer on transbuccal delivery of DHCl

Table 49. Combined effect of iontophoresis 0.3 mA 8 h treatment and 1.0 h enhancer pretreatment (Stage II) [a]

Treatment	Flux ($\mu g/cm^2*h$)	Q_{24} ($\mu g/cm^2$)	ER
Control	56.4±18.0	1160.9±370.8	1
0.3 mA	52.8±36.2	1513.9±667.1	1
PG+0.3 mA	59.7±39.4	1678.9±822.4	1.1
2.5% Azone in PG+0.3 mA	139.2±27.3[b]	2609.7±468.1	2.5
5.0% DDAIP in PG+0.3 mA	111.5±18.5	3072.1±646.3	2
5.0% DDAIP HCl in water+0.3 mA	190.3±33.3[b]	3813.6±706.2	3.4
5.0% DDAIP HCl in PG+0.3 mA	139.4±31.2[b]	2742.0±388.9	2.5
5.0% Br-Iminosulfurane in PG+0.3 mA	70.3±33.6	1862.8±630.3	1.2

[a] Data are presented as means ± S.D. ($3 \leq N \leq 8$).

[b] Statistically significantly higher than control ($p < 0.05$) (Student's t-test).

6.3.2 Ondansetron HCl (ODAN HCl)

6.3.2.1 Enhancement Using Iontophoresis

Anodal iontophoresis at 0.1, 0.2, and 0.3 mA was applied to buccal tissue for 8 h and then discontinued to allow passive permeation of drug for another 16 h. The flux, cumulative amount of drug permeated and ER are shown in Tables 50 and 51 for Stage I (0 to 8 h) and Stage II (8 to 24 h). Iontophoresis (0.1, 0.2 and 0.3 mA) provided significantly higher flux of ODAN HCl when compared to control. The transbuccal flux linearly increased as current increased from 0.1 to 0.3 mA (Figure 50). Furthermore, the enhancement ratio increased as current increased during Stage I. The enhancement ratio at Stage II leveled off, but was still significantly higher than that of Control. It indicates that the enhancement effect of iontophoresis was significant not only during the 8 h of treatment but throughout the 24 h of the study. It also indicates that the flux of the drug was predominantly electrically driven (electrorepulsion) and electroosmosis was not a significant contributor to iontophoretic transbuccal transport of ODAN HCl, and iontophoretic treatment did increase permeability of buccal tissue. When a 10 cm^2 patch with 0.5% ODAN HCl is used for 24 h, 0.3 mA iontophoresis can potentially deliver $3 \times Q_8 \times 10 = 3 \times 190.4 \times 10 = 5.7$ mg daily dose of ODAN HCl can be delivered into blood circulation.

Table 50. Effect of current on transbuccal delivery of ODAN HCl at Stage I [a]

Iontophoresis (mA)	Flux ($\mu g/cm^2*h$)	Q8 ($\mu g/cm^2$)	ER
Control	3.2±0.7	25.5±5.1	1
0.1	10.6±4.5[b]	83.3±33.5	3.3
0.2	16.5±6.5[b]	132.7±50.1	5.2
0.3	22.8±4.6[b]	190.4±42.7	7.1

[a] Data are presented as means ± S.D. (4≤N≤5).

[b] Statistically significantly higher than control ($p < 0.05$) (Student's t-test).

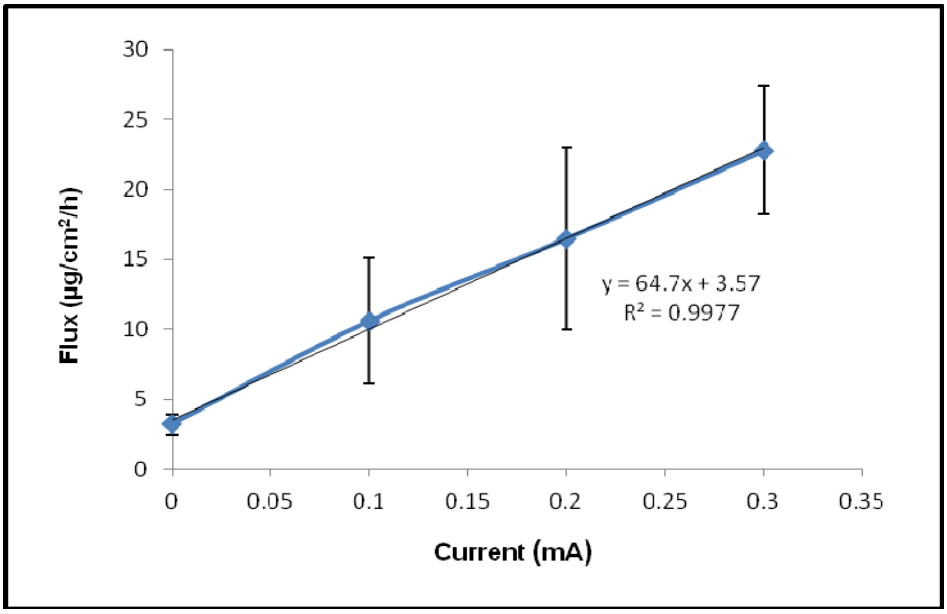

Figure 50. Effect of current on flux of transbuccal delivery of ODAN HCl.

Data are presented as means ± S.D. (4≤N≤5).

Table 51. Effect of current on transbuccal delivery of ODAN HCl (Stage II) [a]

Iontophoresis (mA)	Flux ($\mu g/cm^2*h$)	Q_{24} ($\mu g/cm^2$)	ER
Control	4.9±1.1	104.7±22.8	1
0.1	13.7±4.3[b]	296.9±90.1	2.8
0.2	12.7±5.3[b]	337.4±130.5	2.6
0.3	11.9±2.3[b]	380.4±68.1	2.4

[a] Data are presented as means ± S.D. ($4 \leq N \leq 5$).

[b] Statistically significantly higher than control at $p < 0.05$ (Student's t-test).

6.3.2.2 Enhancement Using Chemical Enhancer

Azone in PG, DDAIP HCl in water, DDAIP HCl in PG, DDAIP in PG, Br-iminosulfurane in PG or PG alone was applied (30 µl) to the buccal tissue for 1 h prior to the permeation experiment. After the 1 h enhancer pretreatment, 0.3 ml of 0.5% ODAN HCl gel formulation was applied. Samples were taken at different time points from 0 to 24 h. Tables 52 and 53 provide comparisons between flux and ER of passive transport of ODAN HCl through enhancer pretreated and untreated (control) tissues. The passive flux of ODAN HCl was significantly greater in all enhancer treated tissues in comparison to Control. DDAIP HCl in water resulted in significantly higher flux and ER than did DDAIP in PG, Azone in PG and Br-iminosulfurane in PG. It shows that compared to Control, the enhancement effect of chemical enhancers was significant throughout the 24 h of the study. It is of interest to note that DDAIP HCl in water exhibited significantly higher permeability than DDAIP HCl in PG, indicating that PG actually acted as a penetration "retardant" when used as a vehicle for DDAIP HCl. The enhancement

differences among the four enhancers may be due to their different physico-chemical properties and mechanisms of action. Azone is a hydrophobic enhancer which is reported to increase membrane lipid fluidity and enhances mainly intercellular drug diffusion [102]. Hydrophobic enhancer Br-iminosulfurane is believed to be more effective in enhancing hydrophobic drug permeation through lipid membranes [15]. DDAIP enhances drug transport by interacting with the polar region of the phospholipid bilayer and promoting the motional freedom of lipid hydrocarbon [122]. However, buccal tissue is non-keratinized, lacks the organized intercellular lipid lamellae and contains large amount of polar lipids [47] that allow more interaction with hydrophilic compounds. Therefore, hydrophilic DDAIP HCl was more potent in enhancing transbuccal delivery of a hydrophilic drug through both intercellular (paracellular) and intracellular (transcellular) pathways than hydrophobic enhancers Azone, DDAIP and Br-iminosulfurane. Furthermore, it was also interesting to find that DDAIP HCl pretreatment alone provided significantly higher enhancement of transbuccal delivery of ODAN HCl than iontophoresis at 0.3 mA during the first 8 h and the following 16 h of the study. It is most probable that iontophoresis enhanced transbuccal drug delivery through disordering of the outer epithelial cell layers, i.e. more of the paracellular route [68] similar to disrupting porcine stratum corneum and increasing intercellular space for enhancing transdermal drug delivery [163,164]. Table 53 shows that using 5% DDAIP HCl in water treatment, transbuccal delivery of ODAN HCl (Q_{24}) could reach 920.3 ($\mu g/cm^2$) within 24 h, i.e. potentially when a small patch of 10 cm^2 containing only 0.5% ODAN HCl is used, this particular enhanced drug delivery system could deliver 9.2 mg/day into blood circulation through buccal route.

Table 52. Effect of 1.0 h enhancer pretreatment on transbuccal delivery of ODAN HCl

Stage I[a]

Enhancer	Flux ($\mu g/cm^2*h$)	Q_8 ($\mu g/cm^2$)	ER
Control	3.2±0.7	25.5±5.1	1.0
PG	10.7±2.6[b]	83.4±19.3	3.3
2.5% Azone in PG	11.3±2.9[b]	88.7±23.1	3.5
5.0% DDAIP in PG	5.1±1.1	41.5±8.1	1.6
5.0% DDAIP HCl in water	29.3±8.0[c]	231.2±62.7	9.2
5.0% DDAIP HCl in PG	12.4±7.0[b]	100.7±56.4	3.9
5.0% Br-Iminosulfurane in PG	9.2±3.6[b]	73.1±27.8	2.8

[a] Data are presented as means ± S.D. (N=4).

[b] Statistically significantly higher than control at $p < 0.05$ (Student's t-test).

[c] Statistically significantly higher than the other enhancer treated and control at $p < 0.05$ (ANOVA)

Table 53. Effect of 1.0 h enhancer pretreatment on transbuccal delivery of ODAN HCl Stage II [a]

Enhancer	Flux ($\mu g/cm^2*h$)	Q_{24} ($\mu g/cm^2$)	ER
Control	4.9±1.1	104.7±22.8	1
PG	10.9±0.8[b]	257.1±31.9	2.2
2.5% Azone in PG	15.8±3.1[b]	340.7±70.0	3.2
5.0% DDAIP in PG	11.3±0.8[b]	221.0±15.6	2.3
5.0% DDAIP HCl in water	41.6±7.6[c]	920.3±169.1	8.5
5.0% DDAIP HCl in PG	24.5±3.8[b]	490.8±107.2	5.0
5.0% Br-Iminosulfurane in PG	14.8±4.1[b]	309.5±83.1	3.0

[a] Data are presented as means ± S.D. (N=4).

[b] Statistically significantly higher than control at $p < 0.05$ (Student's t-test).

[c] Statistically significantly higher than the other enhancer treated and control at $p < 0.05$ (ANOVA)

5.5.4.3 Combined Enhancement Effect

Azone in PG, DDAIP HCl in water, DDAIP HCl in PG, DDAIP in PG, Br-iminosulfurane in PG and vehicle PG was applied (30 µl) to the top of buccal tissue for 1 h prior to the anodal iontophoretic permeation experiment. After 1 h enhancer pretreatment, 0.3 ml of 0.5% ODAN HCl gel formulation was applied to the top of buccal tissues, and then 0.3 mA iontophoresis was applied for 8 h. At the end of 8 h of 0.3 mA iontophoresis treatment, iontophoresis was ceased to

allow passive permeation to continue for another 16 h. Samples were taken at different time points from 0 to 24 h. Data in Tables 54 and 55 provide evidence that combined treatment of enhancer with iontophoresis resulted in no synergistic only additive enhancement effect in the case of Azone, DDAIP and Br-iminosulfurane. The combined treatments did provide significantly higher permeability than that of control ($p<0.05$) and the combination of DDAIP HCl in water and iontophoresis (0.3 mA) was the most effective treatment in enhancing transbuccal delivery of ODAN HCl (Figure 51). However, with DDAIP HCl in water pretreatment, the flux (30.2 $\mu g/cm^2/h$) from the combined treatment was much less than the sum of the fluxes of DDAIP HCl in water (41.6 $\mu g/cm^2/h$) and iontophoresis (11.9 $\mu g/cm^2/h$) during the 24 h of the study. The same trend was recorded for DDAIP HCl in PG. It can be explained by the fact that DDAIP HCl – the salt form of DDAIP contained ions that competed with ODAN HCl during the iontophoretic process, thus the enhancement effect of iontophoresis was reduced.

Table 54. Combined effect of iontophoresis 0.3 mA 8 h treatment and 1.0 hr enhancer pretreatment (Stage I) [a]

Treatment	Flux ($\mu g/cm^2*h$)	Q_8 ($\mu g/cm^2$)	ER
Control	3.2±0.7	25.5±5.1	1.0
0.3 mA	22.8±4.6[b]	190.4±42.7	7.1
PG+0.3 mA	19.7±1.2[b]	133.9±10.8	4.6
2.5% Azone in PG+0.3 mA	34.1±6.0[b]	267.9±42.2	10.7
5.0% DDAIP in PG+0.3 mA	23.5±1.6[b]	196.3±9.1	7.3
5.0% DDAIP HCl in water+0.3 mA	43.0±14.6[b]	336.7±110.7	13.4
5.0% DDAIP HCl in PG+0.3 mA	26.1±4.2[b]	210.8±52.8	8.2
5.0% Br-Iminosulfurane in PG+0.3 mA	24.0±3.6[b]	188.6±25.1	7.5

[a] Data are presented as means ± S.D. ($3 \leq N \leq 5$).

[b] Statistically significantly higher than control at $p < 0.05$ (Student's t-test).

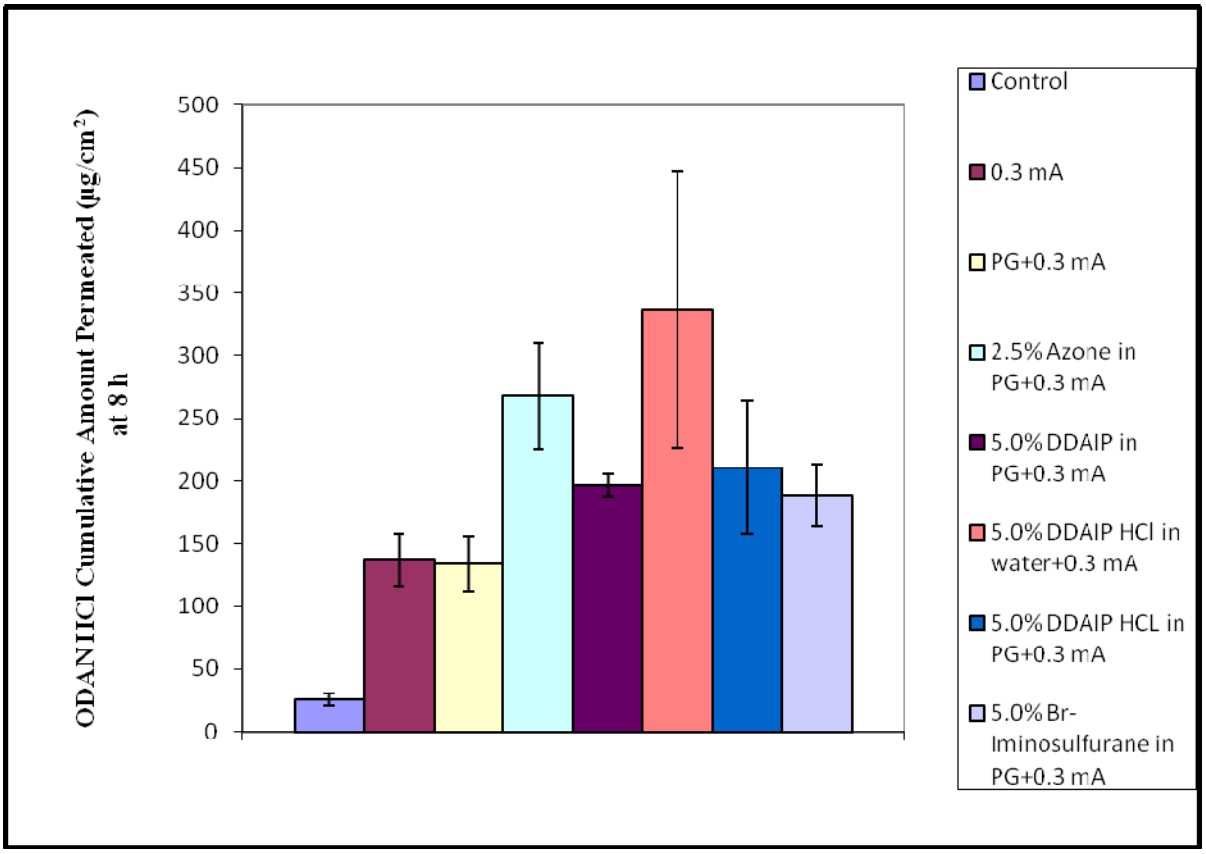

Figure 51. Combined effect of iontophoresis and enhancer pretreatment 1.0 h on ODAN HCl cumulative amount permeated at 8 h.

Table 55. Effect of combined treatment of current and chemical enhancers on transbuccal delivery of ODAN HCl at Stage II [a]

Treatment	Flux ($\mu g/cm^2*hr$)	Q_{24} ($\mu g/cm^2$)	ER
Control	4.9±1.1	104.7±22.8	1
0.3 mA	11.9±2.3[b]	309.8±68.1	2.4
PG+0.3 mA	10.7±1.5[b]	306.9±15.0	2.0
2.5% Azone in PG+0.3 mA	15.1±0.5[b]	520.9±52.7	3.1
5.0% DDAIP in PG+0.3 mA	12.5±3.1[b]	405.0±46.2	2.6
5.0% DDAIP HCl in water+0.3 mA	30.2±7.7[b]	833.5±214.4	6.2
5.0% DDAIP HCL in PG+0.3 mA	20.5±5.2[b]	538.8±131.	4.2
5.0% Br-Iminosulfurane in PG+0.3 mA	13.0±2.5[b]	405.3±22.7	2.7

[a] Data are presented as means ± S.D. ($3 \leq N \leq 5$)

[b] Statistically significantly higher than control at $p < 0.05$ (Student's t-test).

5.6.5 Buccal Integrity Evaluation

5.6.5.1 Histological Study

A histological study was performed to evaluate the integrity of treated and untreated porcine tissues using standard H&E methodology. Treated tissues included those following 0.3 mA iontophoresis for 8 h and combined treatment of 0.3 mA iontophoresis for 8 h plus 1 h enhancer pretreatment: DDAIP HCl in water and DDAIP HCl in PG. Light micrographs (40 X) (Figure. 52 –57) show the morphology of treated and untreated buccal tissues. Compared to untreated (Figure. 52), no major morphological changes were observed after 0.5% ODAN HCl passive permeation (Figure. 53), 0.3 mA for 8 h (Figure. 54), 0.3 mA for 8 h + 5% DDAIP HCl in water treatment (Figure. 55), and 0.3 mA for 8 h + 5% DDAIP HCl in PG treatment (Figure. 56). 10% Oleic acid in PG pretreatment was used as a positive control since it was reported to cause detachment of keratinocytes in stratum corneum of skin [13]. Thus a similar approach was taken and 1 h 10% oleic acid in PG pretreatment was used as a positive control and integrity of the treated tissue was recorded. The micrograph showed significant damage in the buccal epithelial layers – the white arrow pointed area (Figure. 57).

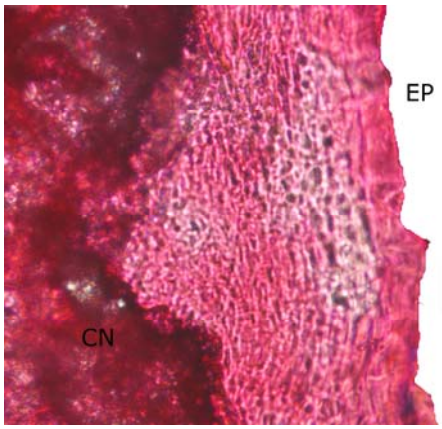

Figure. 52. Untreated porcine buccal tissue (EP – epithelium; CN – connective tissue.)

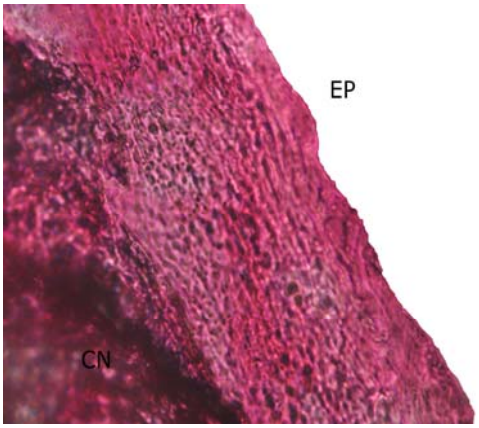

Figure. 53. 0.5% ODAN HCl passive permeation (EP – epithelium; CN – connective tissue.)

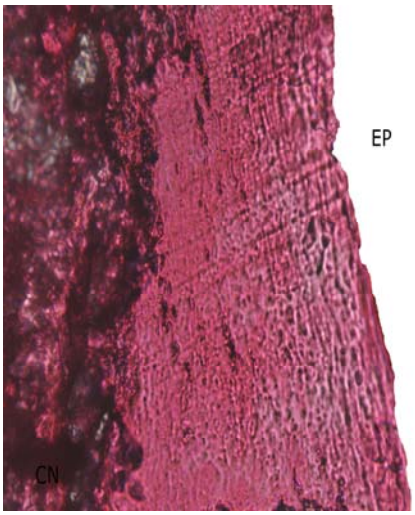

Figure. 54. Iontophoresis 0.3 mA for 8 h (EP – epithelium; CN – connective tissue.)

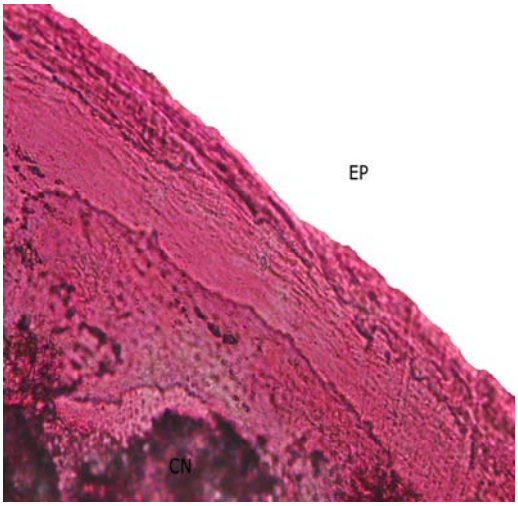

Figure. 55. Combined treatment of iontophoresis 0.3 mA for 8 h + 5% DDAIP HCl in water 1 h pretreatment (EP – epithelium; CN – connective tissue.)

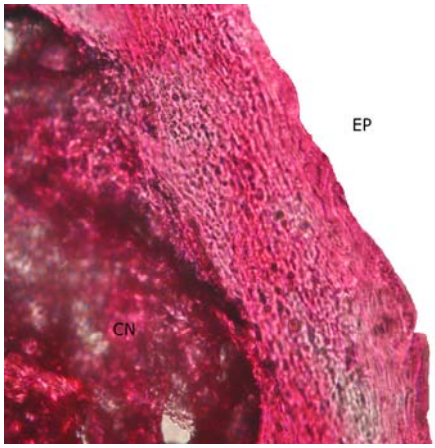

Figure. 56. Combined treatment of iontophoresis 0.3 mA for 8 h + 5% DDAIP HCl in PG 1 h pretreatment (EP – epithelium; CN – connective tissue.)

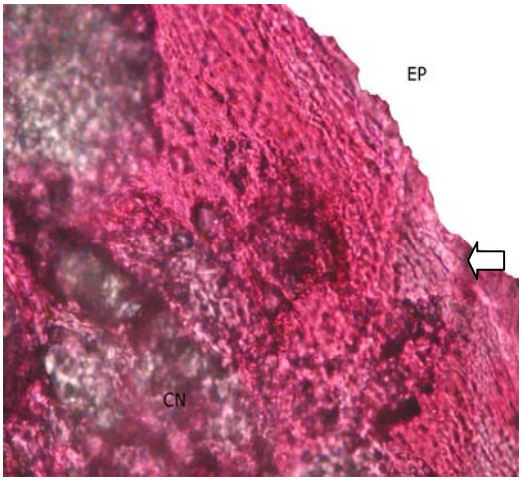

Figure. 57. Combined treatment of iontophoresis 0.3 mA for 8 h + 10% oleic acid in PG 1 h pretreatment (EP – epithelium; CN – connective tissue.)

5.6.5.2. Buccal Differential Scanning Calorimetry (DSC) Study

DSC was performed on control sample, and samples treated with/without iontophoresis and chemical enhancers or their combination treatment. A typical thermogram (25 to 150 °C, heating rate 10 °C/min) of untreated and treated porcine buccal tissue was demonstrated in Figure 58. There was only one transition temperature at about 130 °C observed for all samples. This temperature represents changes in buccal tissue protein conformation [169]. The results indicated that iontophoresis and chemical enhancer treatments did not significantly alter or denature lipids within buccal tissue.

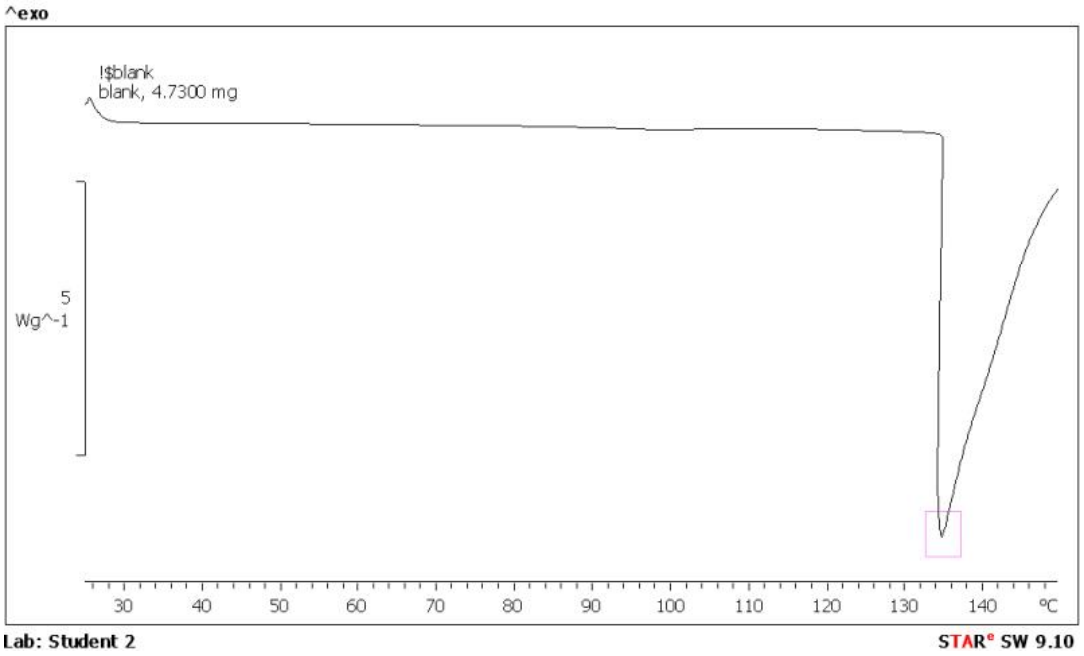

Figure 58. DSC Thermograms of Porcine Buccal Tissue

5.6.5.3. Buccal Cytotoxicity Study

EpiOral™ Study

Cytotoxicity evaluation (MTS assay) was conducted using EpiOral™ tissue in duplicate using 5% DDAIP HCl in water should this read DDAIP HCl in water – the best performing chemical enhancer from this study. Sterilized water treated tissue was used as negative control and 1% Triton – 100 treated tissue as positive control. At the end of the experiments, cell viability was evaluated by measuring the mitochondrial dehydrogenase activities according to the MTS assay [162]. The mean optical density (OD) of the untreated control tissues was set to represent 100% of viability (MTS test, n = 2, OD = 0.999) and the results were quantified as percentage of the negative controls. (Figure 59) demonstrated that DDAIP HCl treatment in a concentration range of 0.05% to 5% in water for 4 h did not reduce the viability of EpiOral™ tissue compared to water - the negative control, and viability (100%) of 5% DDAIP HCl in water treated EpiOral tissue was significantly higher than that (49%) of positive control. The DDAIP HCl in water dose response curve obtained from MTS EpiOral™ tissue (Figure 58) indicated that ET-50 value of 5% DDAIP HCl in water was greater than 1000 min, significantly more than the 49 min for the positive control, indicating that DDAIP HCl at less than 5% (w/v) in water did not have significant detrimental effects on the cells.

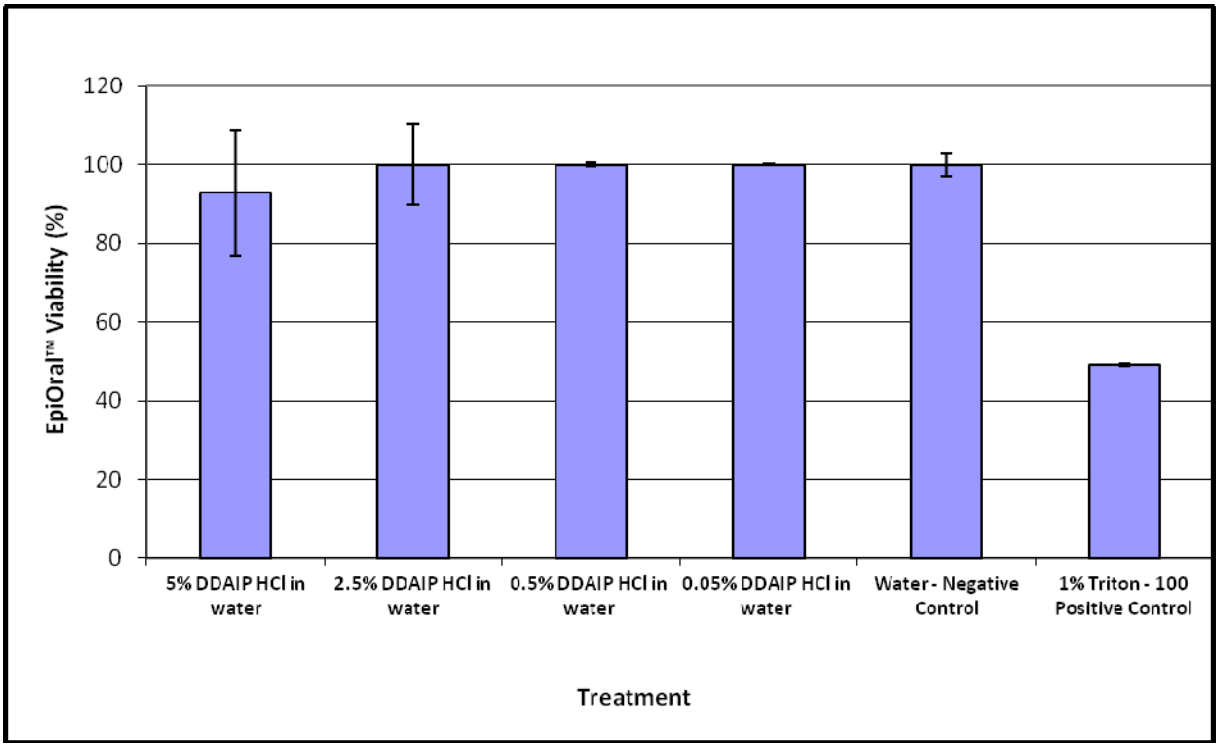

Figure. 59. EpiOral™ tissue viability (%) of different treatments for 4 h. Data are presented as means ± S.D. (N=2)

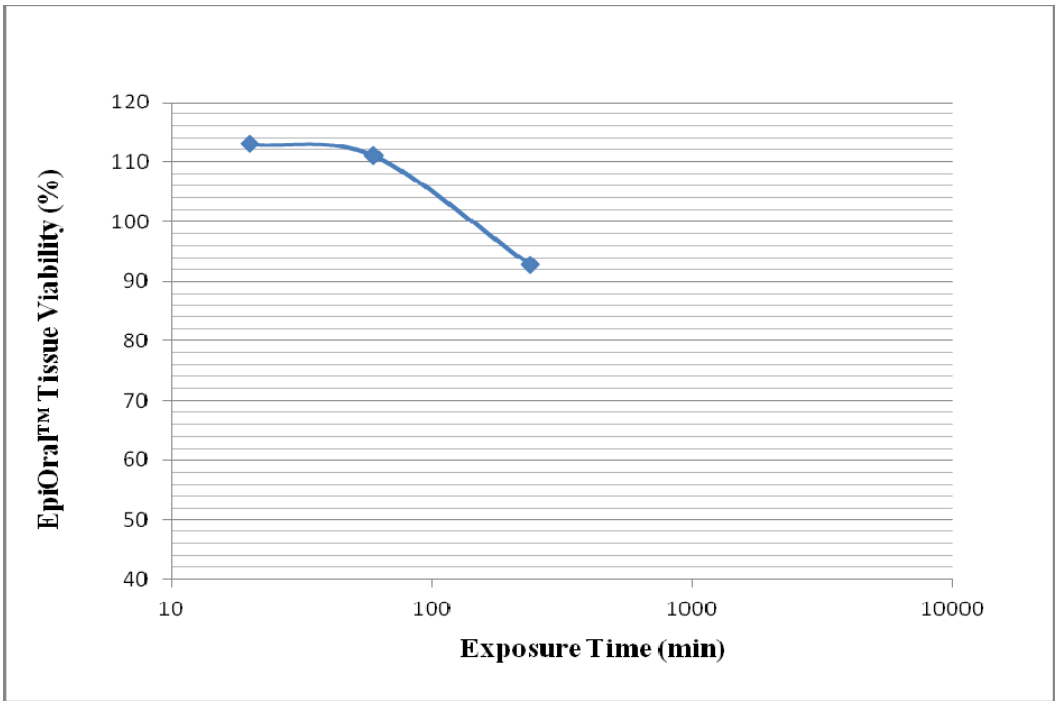

Figure. 60. ET value of 5% DDAIP HCl in water in a dose response curve from EpiOral™ tissue

5.6.6 Comparison Between Transbuccal and Transdermal Drug Delivery

During the same 8 h period of permeation study, LHCl passively diffused through porcine buccal tissue much more effectively than through porcine skin which was in agreement with the published literature: the permeability of the buccal mucosa is 4-4000 times greater than that of the skin [172]. The effect of iontophoresis (0.1, 0.2, 0.3 mA) on transdermal and transbuccal delivery of LHCl, NHT, DHCl and ODAN HCl was compared (Table 56, 57, 58 and Table 59 and Figure 61, 62, 63 and Figure 64). It was observed that enhancement ratio (ER) from iontophoresis treatment (0.1, 0.2 and 0.3 mA) with transbuccal delivery of these four drugs was much less than with transdermal delivery. This may be explained by the fact that the major barrier of skin - SC has pores in hair shaft and eccrine gland areas which exhibit less resistance to ionized molecules. Meanwhile, compared to SC of skin, the major barrier of buccal tissue –

epithelium- contains small amounts of neutral lipids but 10 times more water and 8 times more polar lipids, mainly cholesterol sulfate and glucosylceramides [33], which allow more passive diffusion for hydrophilic compounds LHCl, NHT, DHCl and ODAN HCl and compete for iontophoresis, thus reduce the effect of iontophoresis on transbuccal delivery. As a result, when iontophoresis is applied, ionized compounds such as LHCl, NHT, DHCl and ODAN HCl may be transferred through hair shafts and eccrine glands more easily through skin, i.e. the impact of iontophoresis on transderml delivery of LHCl, NHT, DHCl and ODAN HCl was higher than on transbuccal delivery.

Table 56. Enhancement effect of iontophoresis on transbuccal and transdermal delivery of LHCl at 8 h

Iontophoresis (mA)	ER for Transbuccal	ER for Transdermal
Control	1.0	1.0
0.1	3.1	8.3
0.2	4.1	33.9
0.3	5.4	50.8

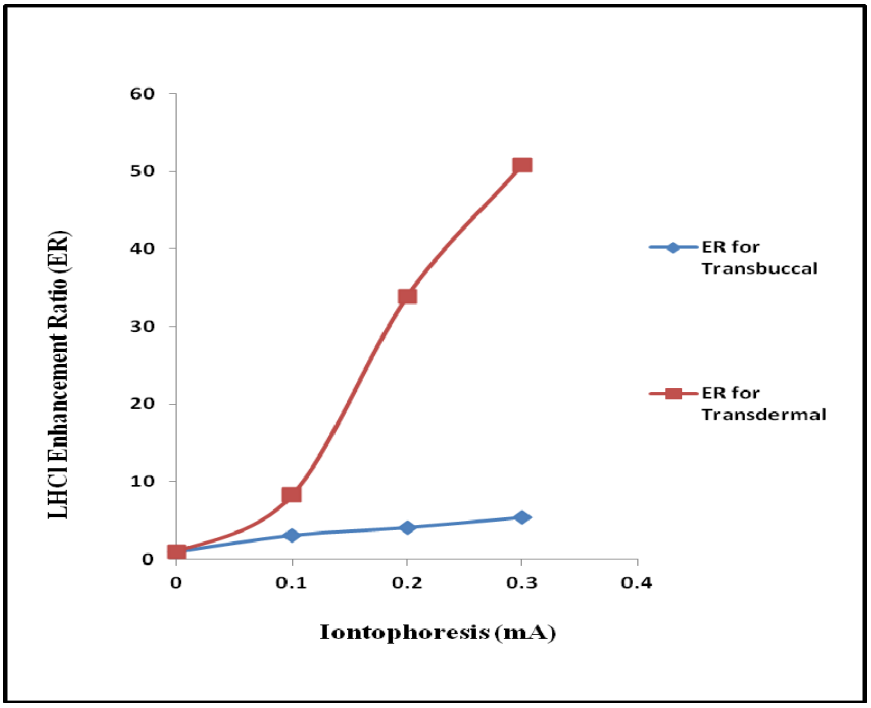

Figure 61. Enhancement effect of iontophoresis on transdermal and transbuccal delivery of LHCl at 8 h

Table 57. Enhancement effect of iontophoresis on transbuccal and transdermal delivery of NHT at 8 h

Iontophoresis (mA)	ER for Transbuccal	ER for Transdermal
0	1	1
0.1	19.5	39.8
0.2	30	70.5
0.3	90.7	106.5

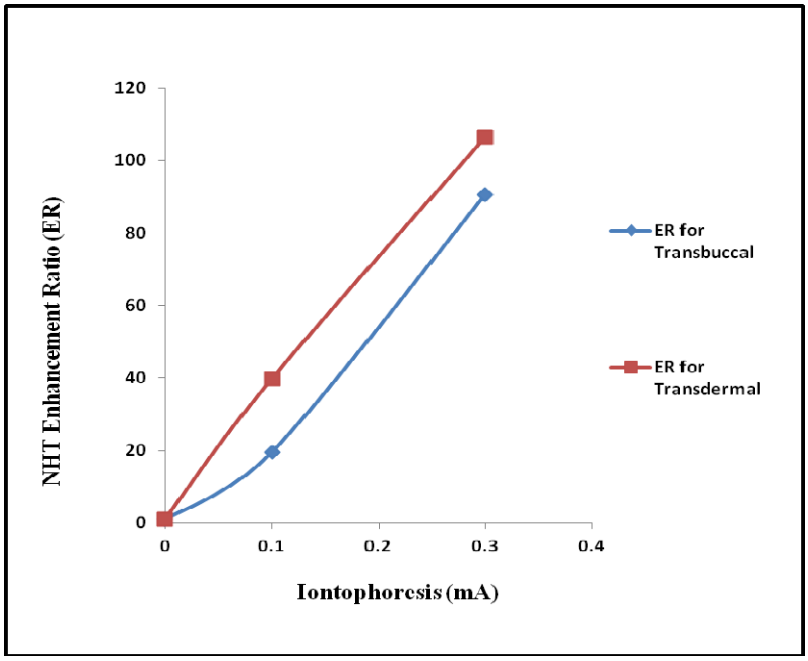

Figure 62. Enhancement effect of iontophoresis on transdermal and transbuccal delivery of NHT at 8 h

Table 58. Enhancement effect of iontophoresis on transbuccal and transdermal delivery of DHCl at 8 h

Iontophoresis (mA)	ER for Transbuccal	ER for Transdermal
0	1	1
0.1	1.7	47.3
0.2	2.2	73.3
0.3	2.5	250.8

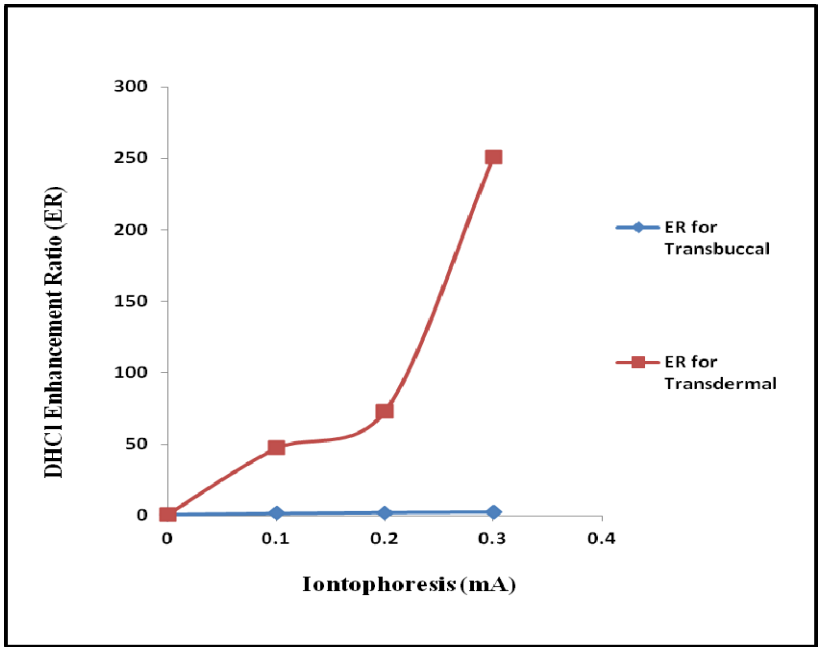

Figure 63. Enhancement effect of iontophoresis on transdermal and transbuccal delivery of DHCl at 8 h

Table 59. Enhancement effect of iontophoresis on transbuccal and transdermal delivery of ODAN HCl at 8 h

Iontophoresis (mA)	ER for Transbuccal	ER for Transdermal
0	1	1
0.1	3.3	18
0.2	5.2	42
0.3	7.1	55

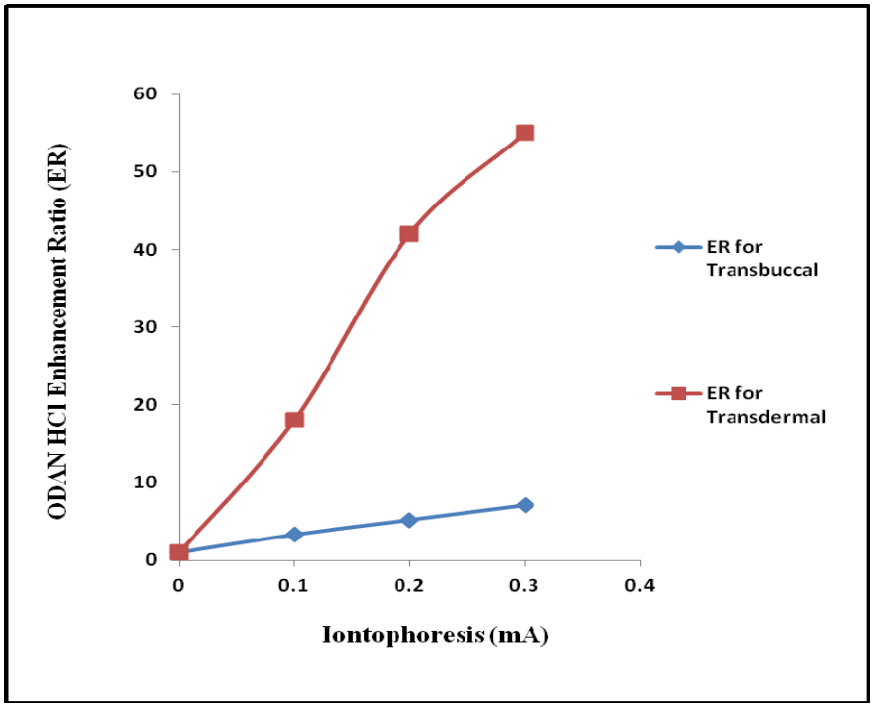

Figure 64. Enhancement effect of iontophoresis on transdermal and transbuccal delivery of ODAN HCl at 8 h

Effect of enhancers

Tables 60 - 63 and Figures 65 - 68 provide data that enhancement effects of different enhancer pretreatments (1 h) on transbuccal and transdermal delivery of LHCl, NHT, DHCl and ODAN HCl were different. Hydrophobic enhancers Azone and DDAIP had similar marginal enhancement effects on both transdermal and transbuccal delivery of LHCl, NHT, DHCl and ODAN HCl. When compared to control, hydrophobic enhancers Br-iminosulfurane and DDAIP had higher enhancement effect on transdermal delivery than on transbuccal delivery of LHCl. DDAIP also had directionally higher transdermal flux of DHCl than the control. However, hydrophilic enhancer DDAIP HCl had much higher enhancement effect on transbuccal delivery than on transdermal delivery of LHCl, NHT, DHCl and ODAN HCl. The enhancement

differences among the four enhancers may be due to their different properties and mechanisms of action. Azone is a hydrophobic enhancer which is reported to increase lipid fluidity and enhances only intercellular drug diffusion [102]. Hydrophobic enhancer Br-iminosulfurane is believed to be more effective in enhancing hydrophobic drug permeation through lipid membranes [15]. DDAIP enhances drug transport by interacting with the polar region of the phospholipid bilayer and promoting the motional freedom of lipid hydrocarbon [122]. However, buccal tissue is non-keratinized, lacks the organized intercellular lipid lamellae and contains large amount of polar lipids [47] that allow more interaction with hydrophilic compounds. Therefore, hydrophilic DDAIP HCl was more potent in enhancing transbuccal delivery of a hydrophilic drug through both intercellular (paracellular) and intracellular (transcellular) pathways than hydrophobic enhancers Azone, DDAIP and Br-iminosulfurane.

Table 60. Enhancement effect of enhancer pretreatment (1 h) on transbuccal and transdermal delivery of LHCl at 8 h

Enhancer	ER for Transbuccal	ER for Transdermal
Control	1	1
PG	1	1.1
2.5% Azone in PG	2.1	1.4
5.0% DDAIP in PG	2	2.1
5.0% DDAIP HCl in water	8.2	1.3
5.0% DDAIP HCl in PG	4.9	1
5.0% Br-Iminosulfurane in PG	2.1	4.8

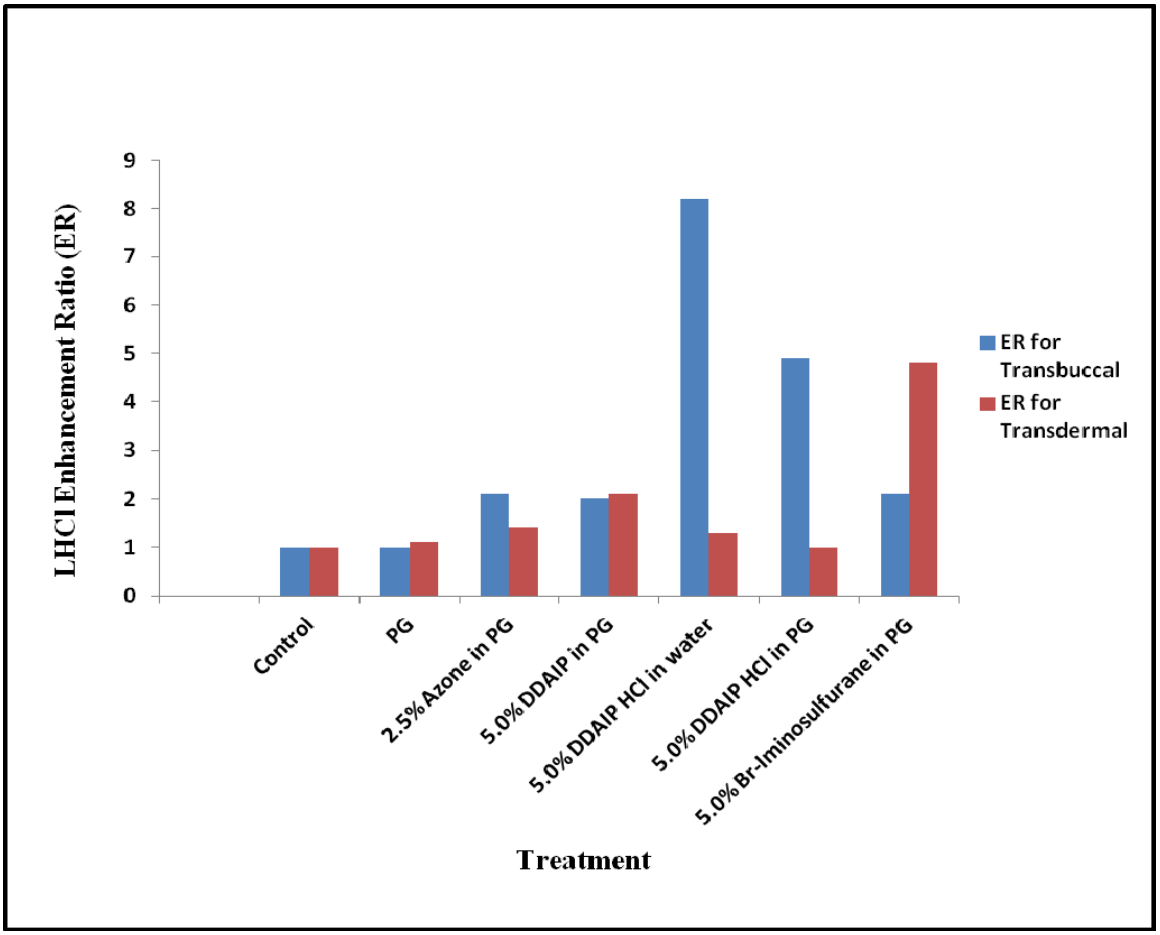

Figure 65. Enhancement effect of enhancer on transbuccal and transdermal delivery of LHCl at 8 h

Table 61. Enhancement effect of enhancer pretreatment (1 h) on transbuccal and transdermal delivery of NHT at 8 h

Enhancer	ER for Transbuccal	ER for Transdermal
Control	1	1
PG	1	1
2.5% Azone in PG	1	1
5.0% DDAIP in PG	78.1	1
5.0% DDAIP HCl in water	372.4	1
5.0% DDAIP HCl in PG	190.1	1
5.0% Br-Iminosulfurane in PG	1	1

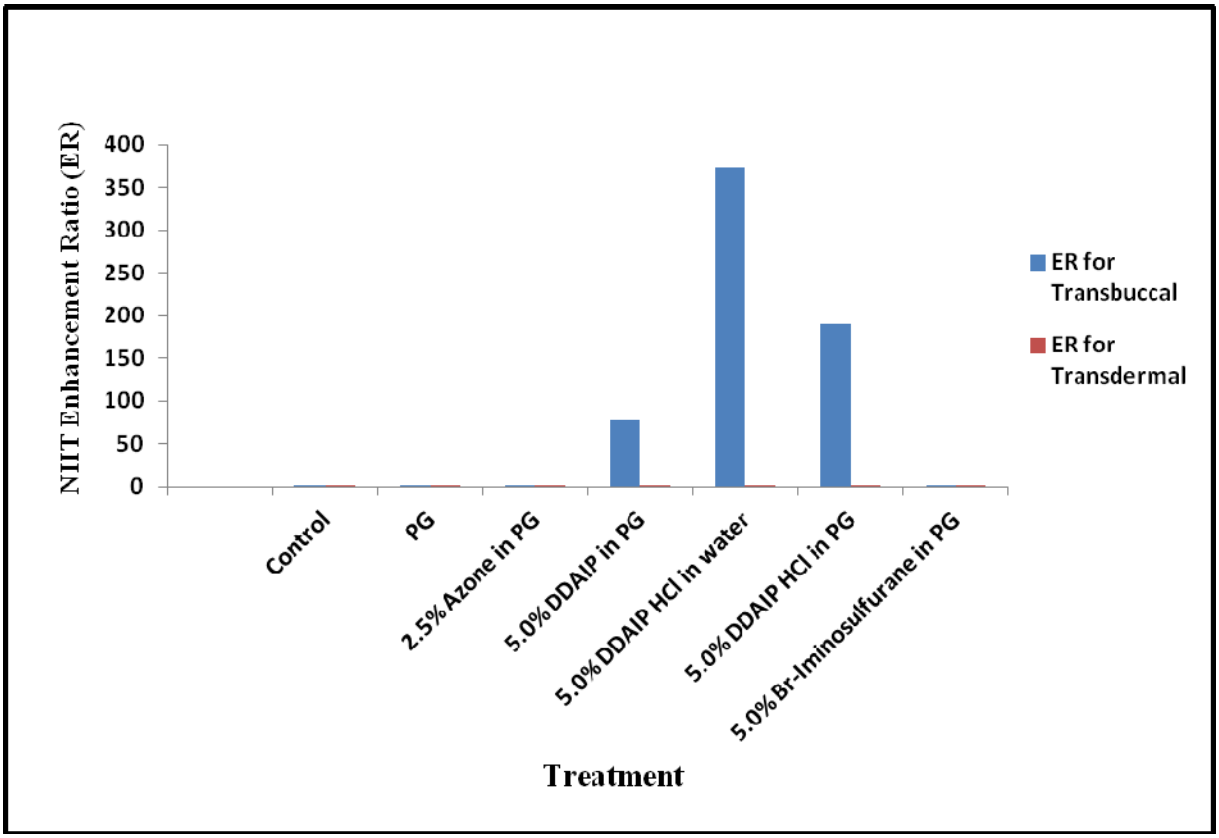

Figure 66. Enhancement effect of enhancer on transbuccal and transdermal delivery of NHT at 8 h

Table 62. Enhancement effect of enhancer pretreatment (1 h) on transbuccal and transdermal delivery of DHCl at 8 h

Enhancer	ER for Transbuccal	ER for Transdermal
Control	1	1
PG	3	1
2.5% Azone in PG	2.5	2
5.0% DDAIP in PG	1.7	7.5
5.0% DDAIP HCl in water	1.8	1
5.0% DDAIP HCl in PG	1.1	1
5.0% Br-Iminosulfurane in PG	2	1

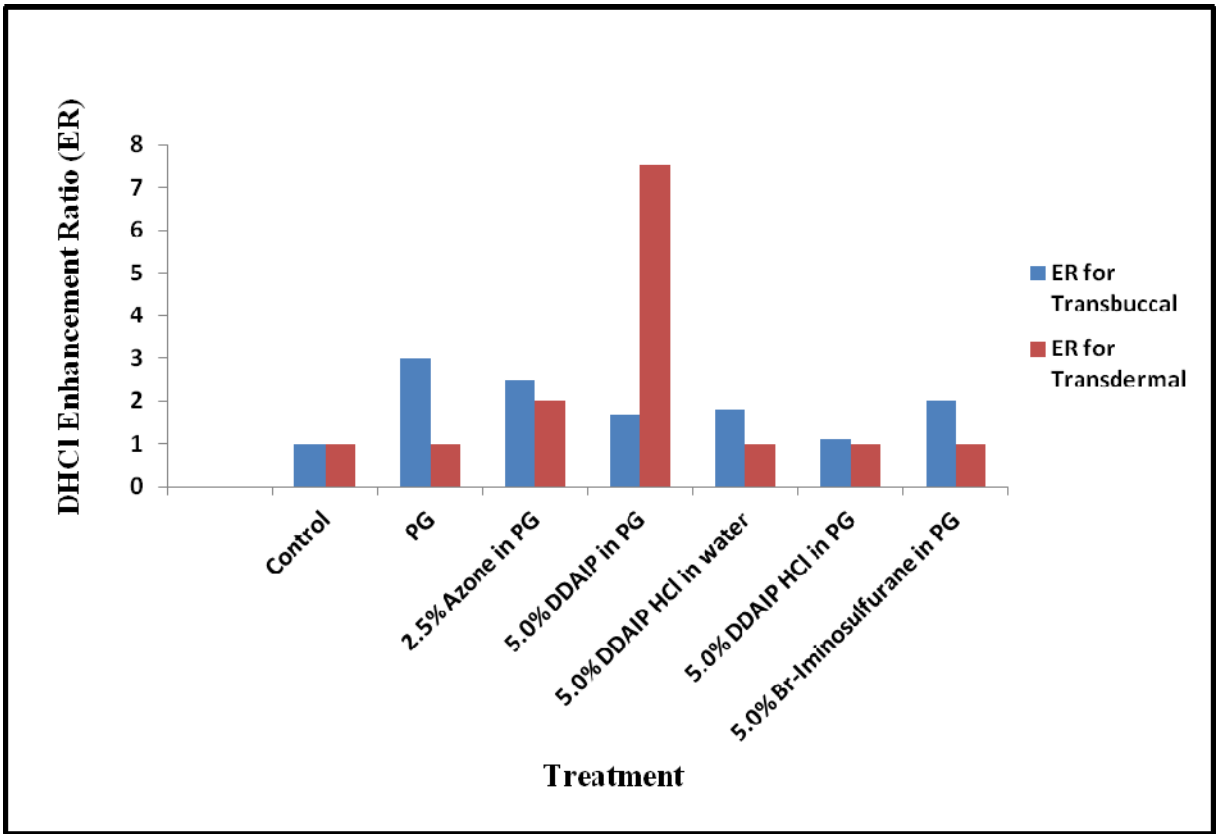

Figure 67. Enhancement effect of enhancer on transbuccal and transdermal delivery of DHCl at 8 h

Table 63. Enhancement effect of enhancer pretreatment (1 h) on transbuccal and transdermal delivery of ODAN HCl at 8 h

Enhancer	ER for Transbuccal	ER for Transdermal
Control	1	1
PG	3.3	1
2.5% Azone in PG	3.5	1
5.0% DDAIP in PG	1.6	1
5.0% DDAIP HCl in water	9.2	1
5.0% DDAIP HCl in PG	3.9	1
5.0% Br-Iminosulfurane in PG	2.8	1

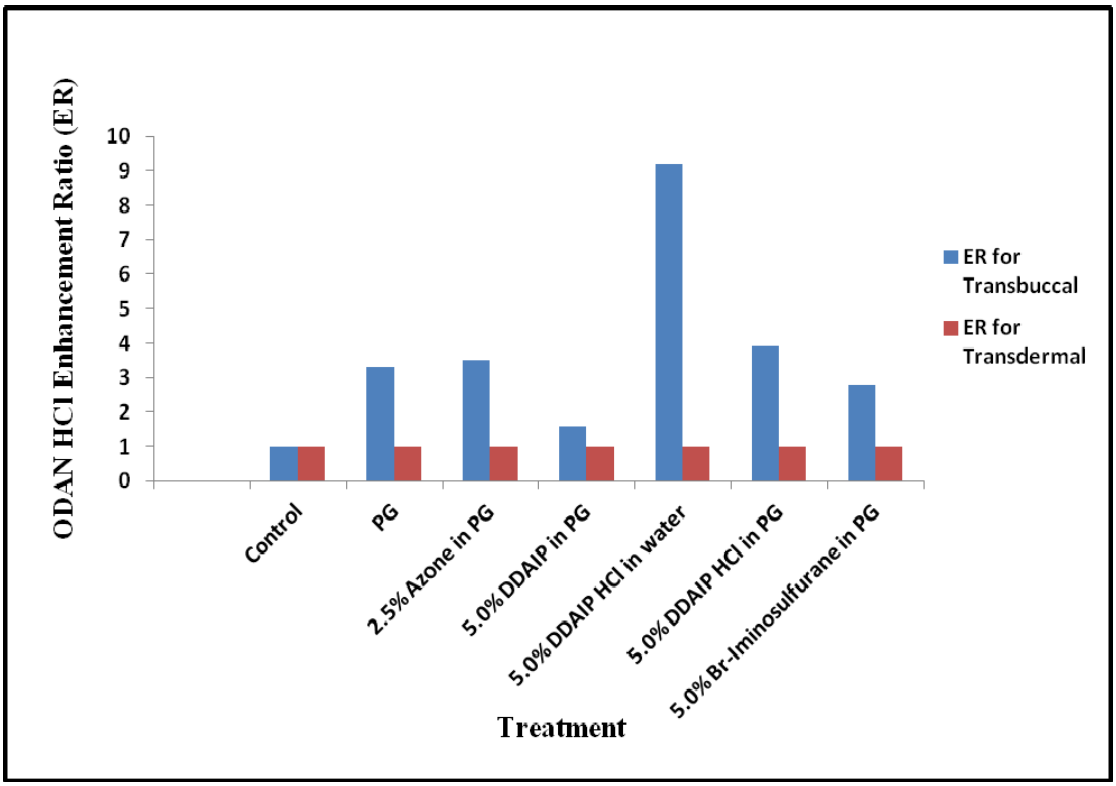

Figure 68. Enhancement effect of enhancer on transbuccal and transdermal delivery of ODAN HCl at 8 h

Effect of combined treatment of enhancer and iontopohoresis

Tables 64 – 67 and Figures 69 -72 show the results of enhancement effect of combined treatment of iontophoresis (0.3 mA for 8 h) and enhancer pretreatment (1 h) on transbuccal and transdermal delivery of LHCl, NHT, DHCl, and ODAN HCl at 8 h. The results demonstrated that combined effects of enhancer and iontophoresis on transdermal delivery were much higher than on transbuccal delivery and iontophoresis was the major contributor of the combined enhancement effect. Synergistic enhancement effect was only observed on transdermal delivery of LHCl and DHCl from the combined treatment of iontophoresis and Br-iminosulfurane and DDAIP. In the case of DDAIP HCl, the enhancement effect of combined treatment was actually less than the sum of enhancement effect of DDAIP HCl and iontophoresis due to the fact that hydrophilic DDAIP HCl may be competing with LHCl.

Table 64. Enhancement effect of combined treatment of iontophoresis and enhancer pretreatment on transbuccal and transdermal delivery of LHCl at 8 h

Treatment	ER for Transbuccal	ER for Transdermal
Control	1	1
0.3 mA	5.4	50.8
PG+0.3 mA	5.6	61.5
2.5% Azone in PG+0.3 mA	5.6	61.5
5.0% DDAIP in PG+0.3 mA	6.2	50.8
5.0% DDAIP HCl in water+0.3 mA	9.6	39.7
5.0% DDAIP HCl in PG+0.3 mA	9.1	25.3
5.0% Br-Iminosulfurane in PG+0.3 mA	5.6	85.2

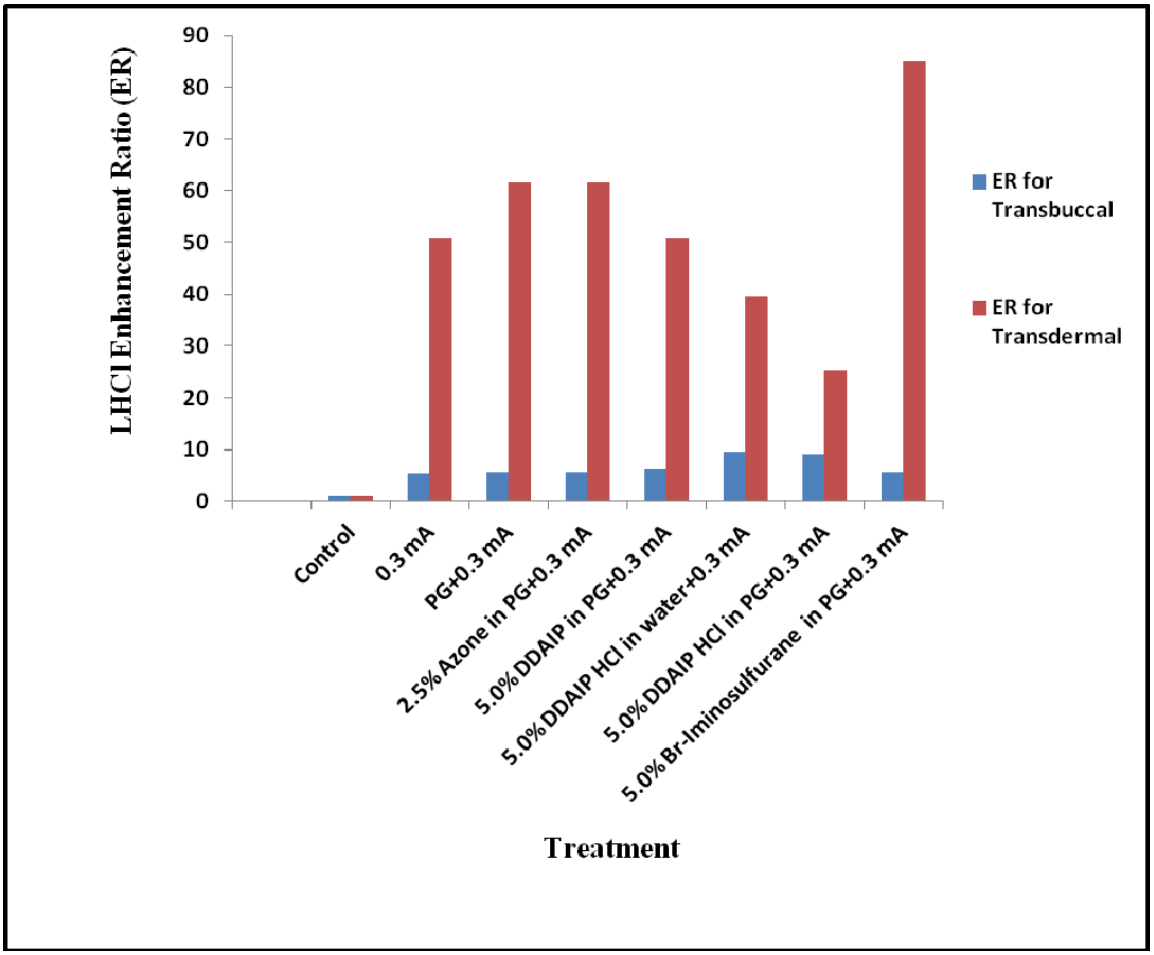

Figure 69. Enhancement effect of combined treatment of iontophoresis and enhancer on transbuccal and transdermal delivery of LHCl at 8 h

Table 65. Enhancement effect of combined treatment of iontophoresis and enhancer pretreatment on transbuccal and transdermal delivery of NHT at 8 h

Treatment	ER for Transbuccal	ER for Transdermal
Control	1	1
0.3 mA	90.7	106.5
PG+0.3 mA	59	113.7
2.5% Azone in PG+0.3 mA	53.9	158
5.0% DDAIP in PG+0.3 mA	239.2	124.2
5.0% DDAIP HCl in water+0.3 mA	445	89.5
5.0% DDAIP HCl in PG+0.3 mA	417.8	90.5
5.0% Br-Iminosulfurane in PG+0.3 mA	56.8	156.5

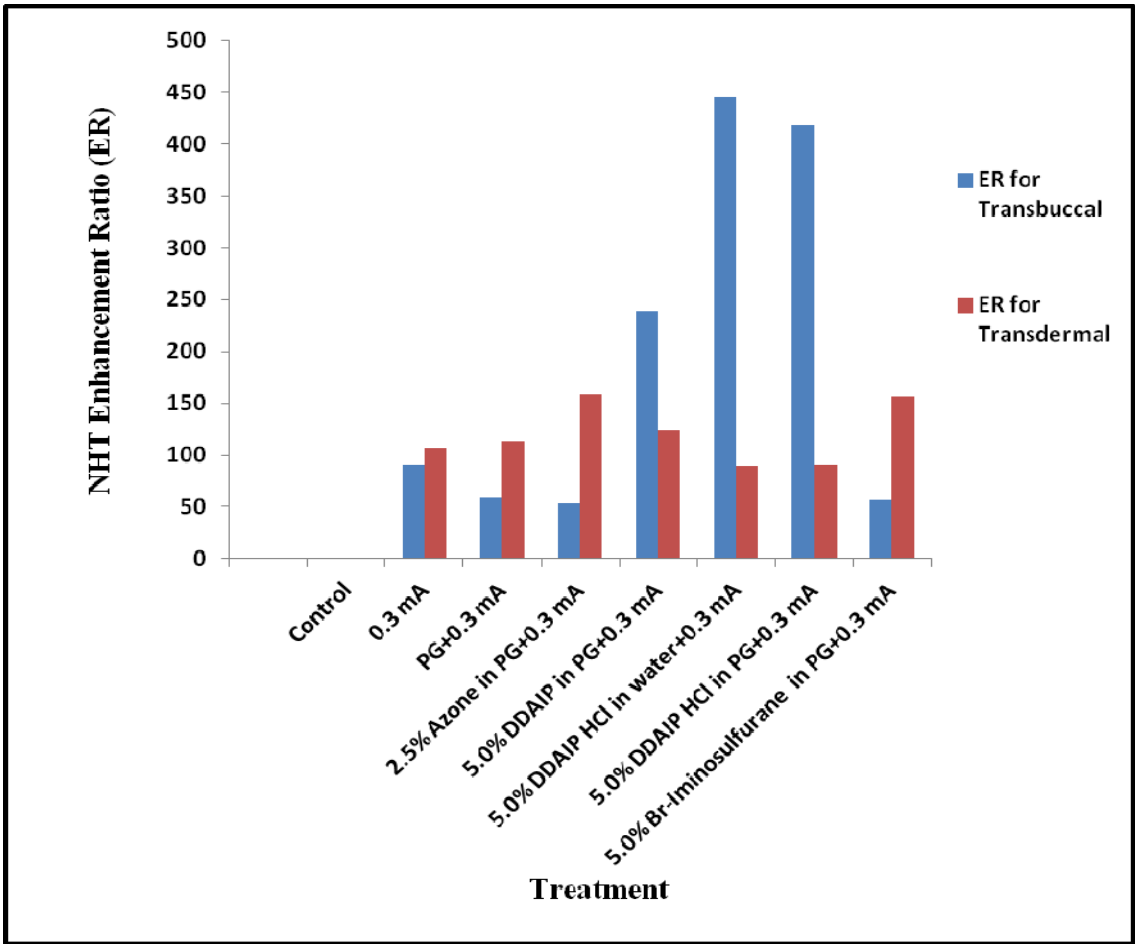

Figure 70. Enhancement effect of combined treatment of iontophoresis and enhancers on transbuccal and transdermal delivery of NHT at 8 h

Table 66. Enhancement effect of combined treatment of iontophoresis and enhancer pretreatment on transbuccal and transdermal delivery of DHCl at 8 h

Treatment	ER for Transbuccal	ER for Transdermal
Control	1	1
0.3 mA	2.5	250.8
PG+0.3 mA	3	121
2.5% Azone in PG+0.3 mA	1.4	265
5.0% DDAIP in PG+0.3 mA	4.8	215.3
5.0% DDAIP HCl in water+0.3 mA	3.4	120
5.0% DDAIP HCl in PG+0.3 mA	1.9	65.5
5.0% Br-Iminosulfurane in PG+0.3 mA	2.7	180.3

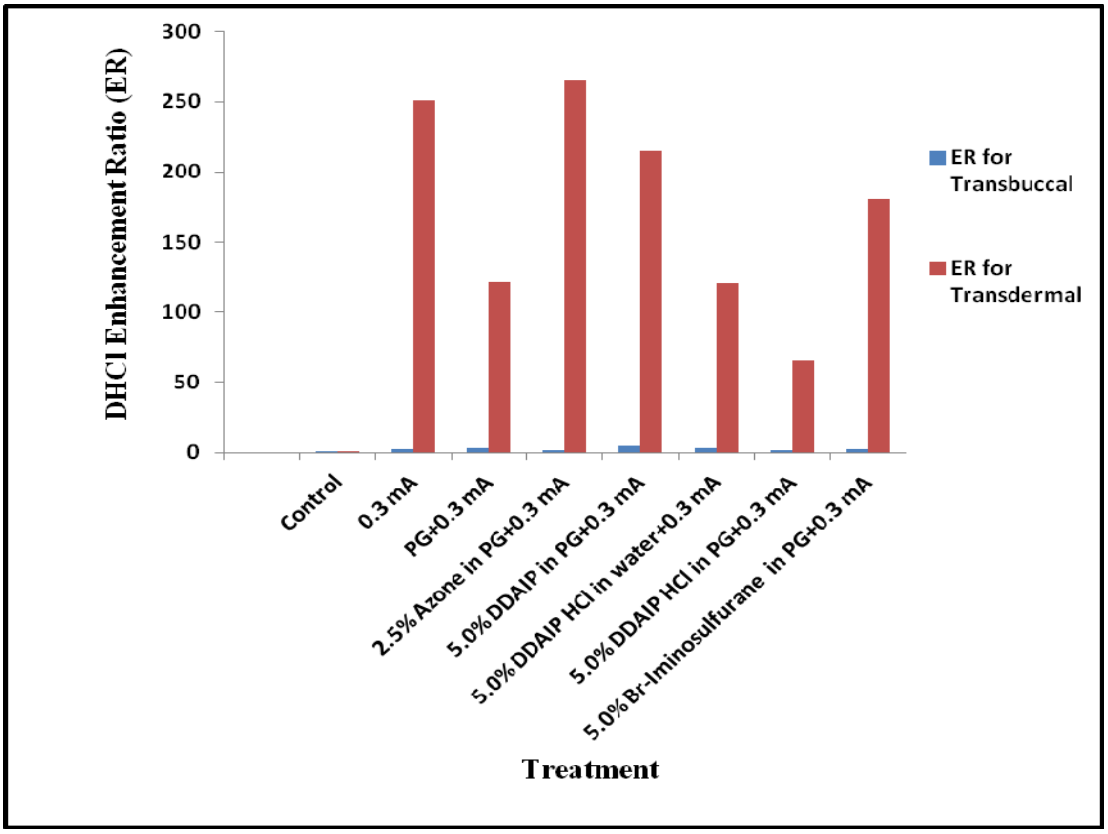

Figure 71. Enhancement effect of combined treatment of iontophoresis and enhancer on transbuccal and transdermal delivery of DHCl at 8 h

Table 67. Enhancement effect of combined treatment of iontophoresis and enhancer pretreatment on transbuccal and transdermal delivery of ODAN HCl at 8 h

Treatment	ER for Transbuccal	ER for Transdermal
Control	1	1
0.3 mA	7.1	99
PG+0.3 mA	4.6	152.5
2.5% Azone in PG+0.3 mA	10.7	165
5.0% DDAIP in PG+0.3 mA	7.3	167
5.0% DDAIP HCl in water+0.3 mA	13.4	50
5.0% DDAIP HCl in PG+0.3 mA	8.2	31
5.0% Br-Iminosulfurane in PG+0.3 mA	7.5	141

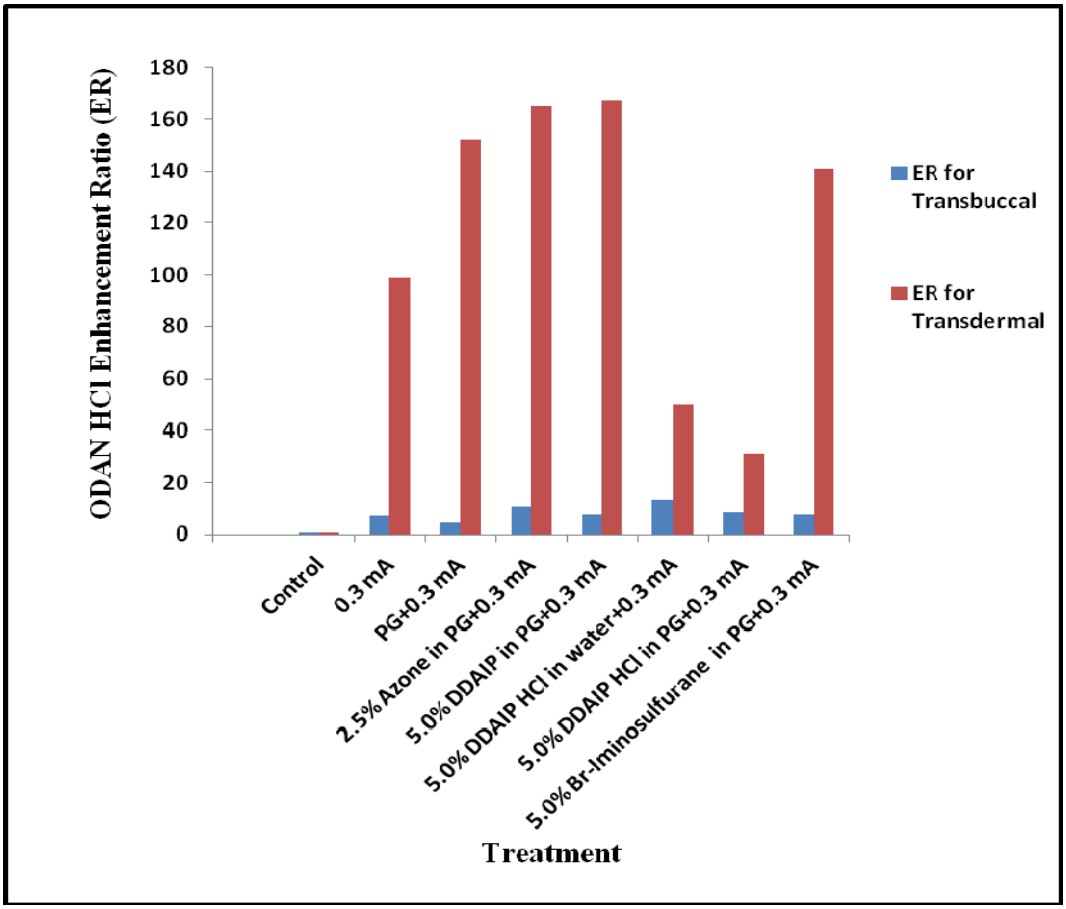

Figure 72. Enhancement effect of combined treatment of iontophoresis and enhancer on transbuccal and transdermal delivery of ODAN HCl at 8 h

5.7 SUMMARY

The buccal mucosa offers several advantages for controlled drug delivery for extended periods of time. The mucosa is well supplied with both vascular and lymphatic drainage and first-pass metabolism in the liver and pre-systemic elimination in the gastrointestinal tract are avoided. The area is well suited for a retentive device and appears to be acceptable to the patient. With the right dosage form design and formulation, the permeability and the local environment of the mucosa can be controlled and manipulated in order to accommodate drug permeation. Buccal drug delivery is a promising area for continued research with the aim of systemic delivery of orally inefficient drugs as well as a feasible and attractive alternative for non-invasive delivery of potent peptide and protein drug molecules. However, the need for safe and effective buccal permeation/absorption enhancers is a crucial component for a prospective future in the area of buccal drug delivery.

In conclusion, for the four hydophilic drugs studied, iontophoresis (0.3 mA) was effective in enhancing both transdermal and transbuccl drug delivery. Enhancement effect of iontophoresis on transdermal drug delivery was much higher than on transbuccal drug delivery. Chemical enhancers (5% w/v of DDIP, DDAIP HCl and Br-iminosulfurane) were more effective in enhancing transbuccal drug delivery than transdermal drug delivery. In the case of DDAIP HCl, its enhancement effect on transbuccal drug delivery was even higher than iontophoreis (0.3 mA). The combined treatment of iontophoresis and chemical enhancer provided limited synergistic effect on transdermal drug delivery, but no synergistic effect on transbuccal drug delivery.

CHAPTER 6.

PATCH FORMULATION AND ITS PERMEATION STUDY

6.1 Drug Patch Formulation

One of the most popular dosage forms for transdermal and transbuccal delivery is the patch. Transdermal / transbuccal patches consist of a reservoir or matrix that contain drug(s) designed to release the active ingredient at a constant rate over a period of several hours to days after after placing the system on the skin or buccal tissue. The patches may also include a rate controlling membrane that controls the drug release rate. A typical "general" patch formulation consists of the following main components [173]:

- Liner which protects the patch during storage. This liner is removed prior to use.
- Drug: Drug solution or saturated solution/gel in direct contact with release liner.
- Pressure sensitive adhesive that provides adherence to the skin and may also be the matrix in which the drug may be incorporated.
- Rate controlling membrane that regulates the release of the drug from the reservoir and multi-layer patches
- Backing laminate that protects the patch from the outer environment.

There are four main types of transdermal patches:

1. Single-layer Drug-in-Adhesive: The drug is included directly within the skin/buccal contacting adhesive. The adhesive layer is responsible making sure the patch adheres to the skin/buccal tissue as well as acts as a drug reservoir and releases the active into the

skin/buccal membrane. The adhesive layer is sandwiched by a temporary liner and a removable backing.

2. Multi-layer Drug-in-Adhesive: This type of system is similar to the Single-layer Drug-in-Adhesive in that the drug is incorporated directly into the adhesive. The multi-layer system adds another layer of drug-in-adhesive, usually separated by a membrane. This patch is also sandwiched by a temporary liner-layer and a permanent backing.
3. Reservoir: The reservoir transdermal system design includes a liquid compartment containing a drug solution or suspension or gel separated from the release liner by a semi-permeable membrane and adhesive. The adhesive component of the product can either be as a continuous layer between the membrane and the release liner or as a concentric configuration around the membrane.
4. Matrix: The matrix system has a drug layer of a semisolid matrix containing a drug solution or suspension or gel, which is in direct contact with the release liner and the adhesive layer which is attached to the backing layer. Some patches may have a rate controlling membrane and examples of such systems have been commercialized in Europe for fentanyl and buprenorphine.

In this study, for the purpose of proof of concept, the simple matrix formulation approach was selected to make patch formulations for diltiazem HCl and ondansetron HCl (Figure 73).

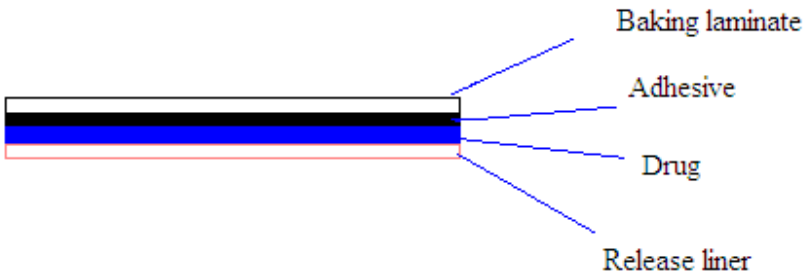

Figure 73. Patch formulation components

6.1.1 Diltiazem HCl

a) Preparation of 3% DHCl Gel Formulations with and without enhancer

- 3% DHCl gel formulation without enhancer: 4% hydroxylpropyl methylcellulose (Methocel K15M premium grade – HPMC) was uniformly dispersed in deionized water to form a clear gel. Then a 3% DHCl was added into the 4% HPMC gel and then mix until uniform using lightning mixer to form a 3% DHCl gel formulation (pH = 6.0; viscosity (RV/E/2 min) = 400,000 cps).

- 3% DHCl gel formulation with 5% DDAIP enhancer: 4% hydroxylpropyl methylcellulose (Methocel K15M premium grade – HPMC, Dow Chemicals, Inc., Auburn Hills, MI) was uniformly dispersed in 88% deionized water to form a clear gel. 5% DDAIP enhancer was dispersed into the HPMC gel and mixed until uniform. Then a 3% DHCl was added into the 4% HPMC gel and then mix until uniform using lightning mixer to form a 3% DHCl gel formulation with 5% DDAIP enhancer (pH = 5.5; viscosity (RV/E/2 min) = 400,000 cps).

- 3% DHCl gel formulation with 5% DDAIP HCl enhancer: 4% w/w hydroxylpropyl methylcellulose (Methocel K15M premium grade – HPMC) was uniformly dispersed in 88% deionized water to form a clear gel. 5% DDAIP HCl enhancer was dispersed into the HPMC gel and mixed until uniform. Then a 3% w/v DHCl was added into the 4% HPMC gel and mixed until uniform using lightning mixer to form a 3% DHCl gel formulation with 5% DDAIP HCl enhancer (pH = 5.8; viscosity (RV/E/2 min) = 400,000 cps).

b) Preparation of adhesive and backing layer: add 10 grams of adhesive (Ethyl acetate, GMS3080 from Cytec Gelva (Springfield, MA)) to a 20 x 30 cm^2 of backing laminate roll (3M Scotchpak™ 9732 Backing Polyester Film Laminate, Saint Paul, MN), then use a Drawdown machine (lab scale, Accu-lab™ JR from Industry Tech., Inc., Oldsmar, FL) to roll on the adhesive on the baking laminate roll to form a thickness of 0.058" uniformed layer of adhesive on the backing laminate.

c) Patch completion: About 0.3 ml of 3% DHCl gel formulation from Step 1 was added uniformly on the side of adhesive layer attached on backing laminate (1 x 1 cm^2), then a release liner (2 x 2 cm^2) (Fluoropolymer Coated Polyester Film, 3M Scotchpak™ 1020) was placed on top of the DHCl gel formulation from Step 1. Finally, a configuration 1 x 1 cm^2 of 3% DHCl patch was obtained by using a punching machine (F-2000MB Cartoning machine, Bloomington, MN) to punch through the DHCl gel sandwiched by baking laminate and release liner.

6.1.2 Ondansetron HCl

a) Preparation of 2% ODAN HCl Gel Formulation with / without enhancer

- 2% ODAN HCl gel formulation without enhancer: 0.02% citric acid was dissolved in 93.98% deionized water and then 4% hydroxylpropyl methylcellulose (Methocel K15M premium grade – HPMC) was added and mixed well to form a uniformed clear gel. Finally 2% ODAN HCl was added into the gel and mixed until uniform using lightning mixer to form a 2% ODAN HCl gel formulation (pH = 3.6; viscosity (RV/E/2 min) = 500,000 cps).

- 2% ODAN HCl gel formulation with DDAIP enhancer: 0.02% citric acid was dissolved in 88.98% deionized water and then 4% hydroxylpropyl methylcellulose (Methocel K15M premium grade – HPMC) was added and mixed well to form a uniformed clear gel. Then 5% DDAIP enhancer was added and mixed uniformly. Finally 2% ODAN HCl was added into the gel and mixed until uniform using lightning mixer to form a 2% ODAN HCl gel formulation with 5% DDAIP enhancer (pH = 3.6; viscosity (RV/E/2 min) = 500,000 cps).

- 2% ODAN HCl gel formulation with DDAIP enhancer: 0.02% citric acid was dissolved in 88.98% deionized water and then 4% hydroxylpropyl methylcellulose (Methocel K15M premium grade – HPMC) was added and mixed well to form a uniformed clear gel. Then 5% DDAIP HCl enhancer was added and mixed uniformly. Finally 2% ODAN HCl was added into the gel and mixed until uniform using lightning mixer to form a 2% ODAN HCl gel formulation with 5% DDAIP HCl enhancer (pH = 3.8; viscosity (RV/E/2 min) = 500,000 cps).

Steps b and c were the same as described in Section 7.1.1.

6.2 Transderml and Transbuccal Delivery Systems

In vitro passive transdermal and transbuccal delivery permeation studies of several 3% DHCl and 2% ODAN HCl formulations were performed using Franz cell diffusion model using porcine skin and buccal tissues. Enhancement effects of iontophoresis (0.3 mA for 8 h) was also evaluated on transdermal and transbuccal delivery of 3% DHCl and 2% ODAN HCl patches with and without DDAIP and DDAIP HCl as enhancers. The methodology was the same as described in Chapters 4 and 5 for transdermal and transbuccal permeation studies of 2% DHCl gel and 0.5% ODAN HCl gel.

6.3 Results and Discussion

6.3.1 Diltiazem HCl

6.3.1.1 *In Vitro* Transdermal permeation study

Tables 68 and 69 show that the 3% DHCl patch provided skin with exclusivity which possibly resulted in higher transbuccal permeation than 3% DHCl gel. When compared to passive patch permeation, 5% DDAIP provided only marginal enhancement effect during 8 h but significant enhancement effect at 24 h. Iontophoresis (0.3 mA for 8 h) provided significant higher enhancement effect than DHCl patch with 5% DDAIP during 8 h of iontophoresis and post-iontophoresis from 8 to 24 h. It was observed that enhancement effect from post- iontophoresis (Stage II) was significantly reduced after iontophoresis was discontinued at 8 h (Stage I), indicating that iontophoretic enhancement effect was primarily electrorepulsion driven and the contribution from electroosmosis was not significant. The cumulative amount permeated during Stage II from post-iontophoresis was significantly higher than that of DHCl patch, DHCl patch with 5% DDAIP, indicating that iontophoresis increased the permeability of skin possibly

through disrupting porcine stratum corneum lipids and increasing intercellular space for transdermal drug delivery [163,164]. It was also observed that no synergistic effect was observed when using combined treatment of DDAIP and iontophoresis throughout 24 h period of study.

Table 68. 3% DHCl transdermal permeation study (0 - 8 h) (Stage I [a])

Formulation	Flux ($\mu g/cm^2*h$)	Q_8 ($\mu g/cm^2$)	ER
Gel	0.5±0.3	7.6±5.5	1.0
Patch	2.1±1.2[b]	13.7±8.4	4.2
Patch + 0.3 mA	71.1±7.7[b, c]	608.5±81.8	142.2
Patch + 5% DDAIP	2.8±2.1	20.4±16.3	5.6
Patch + 5% DDAIP + 0.3 mA	30.2±27.5[b, c]	247.2±224.2	60.4

[a] Data are presented as means ± S.D. ($3 \leq N \leq 8$).

[b] Statistically significantly higher than gel ($p < 0.05$) (Student's t-test).

[c] Statistically significantly higher than gel, patch and patch + 5% DDAIP ($p < 0.05$) (ANOVA).

Table 69. 3% DHCl transdermal permeation study (8 - 24 h) (Stage II [a])

Formulation	Flux ($\mu g/cm^2*h$)	Q_{24} ($\mu g/cm^2$)	ER
Gel	0.7±0.4	18.3±11.6	1.0
Patch	3.3±1.7[b]	64.8±32.6	4.7
Patch + 0.3 mA	17.3±9.9[b, c]	993.2±141.1	24.7
Patch + 5% DDAIP	4.0±2.3[b]	80.7±50.9	5.7
Patch + 5% DDAIP + 0.3 mA	11.5±9.6[b, c]	472.8±401.1	16.4

[a] Data are presented as means ± S.D. ($3 \leq N \leq 8$).

[b] Statistically significantly higher than gel ($p < 0.05$) (Student's t-test).

[c] Statistically significantly higher than gel, patch and patch + 5% DDAIP ($p < 0.05$) (ANOVA).

6.3.1.2 *In Vitro* Transbuccal Permeation Study

Tables 70 and 71 show that 3% DHCl patch provided skin with exclusivity which possibly resulted in higher transbuccal permeation than 3% DHCl gel. When compared to passive patch permeation, both iontophoresis (0.3 mA for 8 h) and 5% DDAIP HCl provided significantly higher permeability of DHCl via porcine buccal tissue during 24 h study period. It was observed that 5% DDAIP HCl even provided higher enhancement effect that iontophoresis (0.3 mA for 8 h) during the entire 24 h period of the study. It was observed that enhancement effect from post-iontophoresis (Stage II) was not significantly reduced after iontophoresis was discontinued at 8 h (Stage I), indicating that iontophoretic enhancement effect was not primarily electrorepulsion driven and contribution from electroosmosis may be significant as well. It was also observed that no synergistic effect was observed when using combined treatment of DDAIP HCl and

iontophoresis throughout 24 h period of study. It may be due to the fact that the ions from hydrophilic DDAIP HCl competed for iontophoresis with DHCl, thus reduced the enhancement effect of iontophoresis.

Table 70. 3% DHCl transbuccal permeation study (0 – 8 h) (Stage I [a])

Formulation	Flux ($\mu g/cm^2*h$)	Q_8 ($\mu g/cm^2$)	ER
Gel	24.1±8.16	170.3±58.20	1.0
Patch	41.0±3.8[b]	290.8±42.3	1.7
Patch + 0.3 mA	160.1±100.3[b, c]	1344.5±611.4	6.6
Patch + 5% DDAIP HCl	185.9±101.1[b, c]	1212.5±911.7	7.7
Patch + 5% DDAIP HCl + 0.3 mA	266.4±59.5[b, c]	1945.0±642.3	11.1

[a] Data are presented as means ± S.D. ($3 \leq N \leq 8$).

[b] Statistically significantly higher than gel ($p < 0.05$) (Student's t-test).

[c] Statistically significantly higher than patch and gel ($p < 0.05$) (ANOVA).

Table 71. 3% DHCl transbuccal permeation study (8 - 24 h) (Stage II [a])

Formulation	Flux ($\mu g/cm^2*h$)	Q_{24} ($\mu g/cm^2$)	ER
Gel	51.7±11.5	941.2±210.0	1.0
Patch	61.4±4.3	1230.8±63.6	1.2
Patch + 0.3 mA	143.9±52.3[b]	3535.1±1704.9	2.8
Patch + 5% DDAIP HCl	208.6±17.1[b]	4634.2±1186.0	4.0
Patch + 5% DDAIP HCl + 0.3 mA	176.4±13.2[b]	5149.4±608.23	3.4

[a] Data are presented as means ± S.D. ($3 \leq N \leq 8$).

[b] Statistically significantly higher than patch and gel ($p < 0.05$) (ANOVA).

6.3.2 Ondansetron HCl

6.3.2.1 *In Vitro* Transdermal Permeation Study

Tables 72 and 73 show that cumulative amount permeated from 2% ODAN HCl patch was comparable to 2% ODAN HCl gel during the 24 h period of study. When compared to passive patch permeation, 5% DDAIP HCl provided no enhancement effect during the 24 h period of study. Iontophoresis (0.3 mA for 8 h) provided significant higher enhancement effect than ODAN HCl patch with 5% DDAIP during 8 h of iontophoresis and post-iontophoresis from 8 to 24 h. It was observed that enhancement effect from post- iontophoresis (Stage II) was significantly reduced from ER = 106 to 41 after iontophoresis was discontinued at 8 h (Stage I), indicating that iontophoretic enhancement effect was primarily electrorepulsion driven and

contribution from electroosmosis was not significant. The cumulative amount permeated during Stage II from post-iontophoresis was significantly higher than that of ODAN HCl patch, ODAN HCl patch with 5% DDAIP, indicating that iontophoresis increased the permeability of skin possibly through disrupting porcine stratum corneum and increasing intercellular space for enhancing transdermal drug delivery [163,164]. It was also observed that no synergistic effect was observed when using combined treatment of DDAIP and iontophoresis throughout 24 h period of study. It may be due to the fact that the dispersion of lipophilic DDAIP in ODAN HCl gel increased the resistance of drug layer, thus reduced the enhancement effect of iontophoresis.

Table 72. 2% ODAN HCl transdermal permeation study (0 - 8 h) Stage I [a]

Formulation	Flux ($\mu g/cm^2*h$)	Q_8 ($\mu g/cm^2$)	ER
Gel	0.1±0.1	0.9±0.8	1.0
Patch	0.1±0.1	1.6±0.4	1.0
Patch + 0.3 mA	10.6±2.7[b]	69.7±21.6	106.0
Patch + 5% DDAIP	0.1±0.1	0	1.0
Patch + 5% DDAIP + 0.3 mA	8.0±2.7[b]	70.5±31.2	80.0

[a] Data are presented as means ± S.D. ($3 \leq N \leq 8$).

[b] Statistically significantly higher than gel, patch and patch + DDAIP ($p < 0.05$) (ANOVA).

Table 73. 2% ODAN HCl transdermal permeation study (8 - 24 h) Stage II [a]

Formulation	Flux ($\mu g/cm^2*h$)	Q_{24} ($\mu g/cm^2$)	ER
Gel (Control)	0.1±0.1	1.9±1.7	1.0
Patch	0.2±0.1	5.0±2.7	2.0
Patch + 0.3 mA	4.1±1.2[b]	173.6±36.9	41.0
Patch + 5% DDAIP	0.1±0.1	1.7±1.3	1.0
Patch + 5% DDAIP + 0.3 mA	3.5±1.7[b]	128.6±48.2	35.0

[a] Data are presented as means ± S.D. ($3 \leq N \leq 8$).

[b] Statistically significantly higher than gel, patch and patch + DDAIP ($p < 0.05$) (ANOVA).

6.3.2.2 *In Vitro* Transbuccal permeation study

Tables 74 and 75 show that cumulative amount permeated from 2% ODAN HCl patch was comparable to 2% ODAN HCl gel during the 24 h period of study. When compared to passive patch permeation, both iontophoresis (0.3 mA for 8 h) and 5% DDAIP HCl provided significantly higher permeability of ODAN HCl via porcine buccal tissue during 24 h study period. It was observed that 5% DDAIP HCl even provided higher enhancement effect that iontophoresis (0.3 mA for 8 h) during the entire 24 h period of the study. This result was in line with transbuccal delivery of 0.5% ODAN HCl in Chapter 6. It was also observed that enhancement effect from post- iontophoresis (Stage II) was not significantly reduced after iontophoresis was discontinued at 8 h (Stage I), indicating that iontophoretic enhancement effect was not primarily electrorepulsion driven and contribution from electroosmosis may be significant as well. It was also observed that no synergistic effect was observed when using

combined treatment of DDAIP HCl and iontophoresis throughout 24 h period of study. It may be due to the fact that the ions from hydrophilic DDAIP HCl competed for iontophoresis with ODAN HCl, thus the enhancement effect of iontophoresis was reduced.

Table 74. 2% ODAN HCl transbuccal permeation study (0 – 8 h) Stage I [a]

Formulation	Flux ($\mu g/cm^2*h$)	Q_8 ($\mu g/cm^2$)	ER
Gel	10.3±2.7	67.4±20.9	1.0
Patch	9.7±2.1	71.2±22.1	1.0
Patch + 0.3 mA	34.9±13.2[b]	296.6±90.8	3.4
Patch + 5% DDAIP HCl	144.0±30.6[b, c]	1153.6±383.5	14.0
Patch + 5% DDAIP HCl + 0.3 mA	129.3±36.6[b, c]	1059.2±441.1	12.6

[a] Data are presented as means ± S.D. ($3 \leq N \leq 8$).

[b] Statistically significantly higher than gel and patch ($p < 0.05$) (ANOVA).

[c] Statistically significantly higher than patch, gel and patch + 0.3 mA ($p < 0.05$) (ANOVA).

Table 75. 2% ODAN HCl transbuccal permeation study (8 - 24 h) Stage II [a]

Formulation	Flux ($\mu g/cm^2*h$)	Q_{24} ($\mu g/cm^2$)	ER
Gel	15.8±3.9	310.1±75.2	1.0
Patch	17.6±2.1	330.5±52.4	1.1
Patch + 0.3 mA	30.9±13.7[b]	756.4±310.4	2.0
Patch + 5% DDAIP HCl	43.3±25.8[b]	2048.8±130.1	2.7
Patch + 5% DDAIP HCl + 0.3 mA	44.2±24.7[b]	1982.2±116.2	2.8

[a] Data are presented as means ± S.D. ($3 \leq N \leq 8$).

[b] Statistically significantly higher than gel and patch ($p < 0.05$) (ANOVA).

6.4 SUMMARY

The 3% DHCl patch formulation delivered higher amount of DHCl through both porcine skin and buccal tissue when compared to the gel formulation at the same drug concentration. Iontophoresis (0.3 mA for 8 h) significantly enhanced transdermal and transbuccal delivery of DHCl. It was of interest to note that mechanisms of iontophoretic enhancement effect on transdermal and transbuccal delivery of DHCl were different. It seemed to be that for transdermal delivery of DHCl electrorepulsion was the primarily driving force, but in the case of transbuccal delivery of DHC, electroosmosis may be also important. DHCl patch formulation with DDAIP enhancer provided higher transdermal permeability of DHCl when compared to DHCl patch. DHCl patch formulation with DDAIP HCl enhancer provided significantly higher transbuccal delivery of DHCl when compared to DHCl patch. There were no synergistic

enhancement effects observed from combined treatment of enhancers (DDAIP and DDAIP HCl) and iontophoresis for transdermal and transbuccal delivery of DHCl. However, it was interesting to observe that DDAIP HCl treatment alone provided higher enhancement effect than iontophoreis alone. It was also noticed that transbuccal route of DHCl delivery using patch formulations seemed to be more effective than transdermal route.

Iontophoresis (0.3 mA for 8 h) significantly enhanced transdermal and transbuccal delivery of ODAN HCl in gel and patch formulations. It was of interest to note that mechanisms of iontophoretic enhancement effect on transdermal and transbuccal delivery of ODAN HCl were different. It seemed to be that for transdermal delivery of ODAN HCl electrorepulsion was the primarily driving force, but in the case of transbuccal delivery of ODAN HCl, electroosmosis may be also important. ODAN HCl patch formulation with DDAIP enhancer provided higher transdermal permeability of ODAN HCl when compared to ODAN HCl patch. ODAN HCl patch formulation with DDAIP HCl enhancer provided significantly higher transbuccal delivery of ODAN HCl when compared to ODAN HCl patch and iontophoresis treatment. There were no synergistic enhancement effects observed from combined treatment of enhancer (DDAIP or DDAIP HCl) and iontophoresis for transdermal and transbuccal delivery of ODAN HCl. However, it was interesting to observe that DDAIP HCl treatment alone provided higher enhancement effect than iontophoreis alone.

Patch formulation was a feasible dosage form for the delivery of DHCl and ODAN HCl transdermally and transbuccally. Iontophoresis was more effective in enhancing transdermal delivery of DHCl and ODAN HCl in patch formulations. DDAIP HCl was more effective in enhancing transbuccal delivery of DHCl and ODAN HCl in patch formulations. Overall, the

transbuccal route was proved to be more effective in delivering DHCl and ODAN HCl in patch formulations than the transdermal route.

CHAPTER 7. Thesis Study Conclusions

The studies reported in this thesis demonstrated that chemical enhancers, iontophoresis as well as their combined treatment can significantly enhance both transdermal and transbuccal drug delivery. The mechanisms of these enhancement effects have not yet been completely elucidated and were not the main focus of this work. However, we need to realize that the impact of additional important factors such as pH, ionic strength, resistance changes in skin and buccal tissue during iontophoresis still have to be fully investigated. The transport pathways and the molecular ionic interactions between the drug and the chemical enhancers during transdermal and transbuccal drug delivery are not clearly understood. These need to be further investigated. In the reported work for this thesis, DSC was used to investigate the impact of chemical enhancers on lipid integrity of skin and buccal tissue. However, limited differences in phase transition temperatures of lipids in SC and buccal epithelium were observed between untreated and chemical enhancer treated skin and buccal. Therefore, confocal Raman microscopy [15] should be utilized to investigate the impact of chemical enhancers on lipid and protein integrity and the penetration process and possible mechanisms of action of the enhancers as well as interaction between the enhancer and lipids and protein in the SC and buccal epithelium.

In this thesis, a simple matrix patch formulation approach was used to successfully conduct proof-of-concept experiment in transdermal and transbuccal drug delivery with and without incorporating chemical enhancers in the formulations. The flux of passive permeation was rather low indicating that chemical or physical enhancement approaches are required for delivery of therapeutic amounts of drug across the membranes. An optimal patch should be designed through selecting a multifunctional bioadhesive polymer [174]. Bioadhesive polymer-related

factors such as molecular weight, concentration, swelling capability, adhesion force, and initial contact time between polymer and mucus layer should be investigated to ensure fast and sustained drug release profile for both oil and water soluble drugs. A more advanced membrane matrix hybrid type patch [175] may be designed to allow improved drug release rate control using solid polymer matrix to replace the semi-solid drug reservoir.

This thesis demonstrated that the combined treatment of chemical enhancers and iontophoresis significantly enhanced transdermal and transbuccal drug delivery. However, no synergistic enhancement effects were observed. To achieve this objective, two key approaches should be further investigated. Firstly, the patch formulation should be investigated to ensure improved transdermal and transbuccal passive permeation by optimizing drug concentrations within the polymer gel and adhesion forces of the adhesive. Secondly, combined treatment of chemical enhancers and other physical enhancement methods should be investigated. These physical methods may be selected form the following: iontophoresis, electroporation, sonophoresis and microneedles. With the optimized dosage form design and formulation, the permeability and the local environment of the SC and buccal mucosa can be controlled and manipulated in order to achieve the therapeutic levels of drug permeation.

In this thesis, porcine skin and buccal tissues were utilized for all the *in vitro* drug delivery studies. It has been established in the literature that porcine skin and buccal membranes are the closest models to human skin and buccal tissue. Future studies should utilize pig to conduct *in vivo* drug delivery, pharmacokinetic and pharmacodynamic experiments to study the enhancement effects of various factors: formulation, drug concentration, ionic strength, chemical enhancers, and iontophoresis, etc.. Also an *in vivo* pig study can provide useful data to evaluate skin and buccal irritation potential from drug formulation as well as the different treatments.

Ideally, for optimization of the patch with so many variables, modeling work should be conducted prior to actual experimental work. This computing work will provide ranges for the parameters for iontophoretic transdermal and transbuccal drug-delivery systems. Furthermore, this work will mainly involve an analytical solution for transdermal and transbuccal iontophoresis models [176], which will be used to estimate the diffusion coefficient (D), the surface concentration (Cs), the time delay (td) and the electromigration/convection factor (γ). The drug diffusion coefficient in the diffusion cell donor cell will be determined in the absence of an electric field. This value will be then used to graphically estimate Cs and γ from iontophoretic experiments. The model parameters will be refined by orthogonal collocation-based regression procedures written in Mathematica (Wolfram Research Inc.). The correlation will be demonstrated between experimental and predicted values. From this study, the factors that will impact most on the drug-permeation rate will be identified based on data regression analysis.

Data from the thesis has already been provided to Dr. Simon Laurent at the New Jersey Institute of Technology (NJIT), Newark, NJ and work has begun on the correlations and computational modeling.

REFERENCES

[1] Scheindlin, S. *Molecular Interventions* 2004, *4*, 308
[2] Segal, M. *http://www.fda.gov/bbs/topics/consumer/CON00112.html*. 2007.
[3] Langer, R. *Advanced Drug Delivery Reviews* 2004, *56*, 557.
[4] Scheindlin, S. *Molecular Interventions* 2004, *4*, 308.
[5] Naik, A.; Kalia, Y. N.; Guy, R. H. *Pharmaceutical Science & Technology Today* 2000, *3*, 318.
[6] Prausnitz, M. R.; Mitragotri, S.; Langer, R. *Nat Rev Drug Discov* 2004, *3*, 115.
[7] Thomas, B. J.; Finnin, B. C. *Drug Discovery Today* 2004, *9*, 697.
[8] Birudaraj R, M. R., Li X, Jasti BR. *Crit Rev Ther Drug Carrier Syst.* . 2005, *22*, 295
[9] http://www.essortment.com/all/chewinggumhis_rdjz.htm.
[10] Conaghey, O. M.; Corish, J.; Corrigan, O. I. *International Journal of Pharmaceutics* 1998, *170*, 225.
[11] Hoogstraate, J. A. J.; Wertz, P. W. *Pharmaceutical Science & Technology Today* 1998, *1*, 309.
[12] Hassan, N.; Ahad, A.; Ali, M.; Ali, J. *Expert Opinion on Drug Delivery* 2010, *7*, 97.
[13] Wang, Y.; Fan, Q.; Song, Y.; Michniak, B. *Effects of fatty acids and iontophoresis on the delivery of midodrine hydrochloride and the structure of human skin*, 2003; Vol. 20.
[14] Femenía-Font, A.; Balaguer-Fernández, C.; Merino, V.; López-Castellano, A. *International Journal of Pharmaceutics* 2006, *323*, 125.
[15] Song, Y.; Xiao, C.; Mendelsohn, R.; Zheng, T.; Strekowski, L.; Michniak, B. *Pharmaceutical Research* 2005, *22*, 1918.
[16] D. Frank, M. L., W. Pfister *Poster Presentation, 2006 AAPS Annual Meeting and Exposition, San Antonio, TX, USA* 2006.
[17] Holbrook, K. A. *McGraw Hill, New York* 1993.
[18] Holbrook, K. A. 1993.
[19] T.J. Franz, P. A. L. *CRC Press, New York* 2000.
[20] K.A. Holbrook, G. F. O. *J Invest Dermatol.* 1974, *62*, 415.
[21] Pierre G. Agache, P. A., Philippe Humbert, Howard I. Maibach *Springer pubisher, Inc.* 2004, 113.
[22] Marjukka Suhonen, T.; A. Bouwstra, J.; Urtti, A. *Journal of Controlled Release* 1999, *59*, 149.
[23] Bouwstra, J. A.; Dubbelaar, F. E. R.; Gooris, G. S.; Ponec, M. *Acta Dermato-Venereologica* 2000, *80*, 23
[24] Brod, J. *International Journal of Dermatology* 1991
30, 84.
[25] P.W. Wertz, B. v. d. B. *Chemistry and Physics of Lipids* 1998, *91*, 85.
[26] L. Coderch, O. L., A. de la Maza, J.L. Parra, *American Journal of Clinical Dermatology* 2003, *4*, 107.
[27] Bowser, P. A.; Nugteren, D. H.; White, R. J.; Houtsmuller, U. M. T.; Prottey, C. *Biochimica et Biophysica Acta (BBA) - Lipids and Lipid Metabolism* 1985, *834*, 419.
[28] WERTZ, P. W. *Acta Derm Venereol Supp* 2000, *208*, 7
[29] L. Coderch, O. L., A. de la Maza, J.L. Parra, *American Journal of Clinical Dermatology*

2003, *4*, 107.
[30] Fluhr JW, K. J., Jain M, Ahn SK, Feingold KR, Elias PM. *J. Invest Dermatol.* 2001, *117*, 44
[31] Kessner, D.; Brezesinski, G.; Funari, S. S.; Dobner, B.; Neubert, R. H. H. *Chemistry and Physics of Lipids* 2010, *163*, 42.
[32] Bouwstra, J. A.; Gooris, G. S.; Dubbelaar, F. E. R.; Ponec, M. *J. Lipid Res.* 1999, *40*, 2303.
[33] Wertz, P. W. a. D. D. *J Lipid Res* 1983, *24*, 759.
[34] DAVIES, H. W.; TROTTER, M. D. *British Journal of Dermatology* 1981, *104*, 649.
[35] Schmook, F. P.; Meingassner, J. G.; Billich, A. *International Journal of Pharmaceutics* 2001, *215*, 51.
[36] Mowafy, M.; Cassens, R. G. *J. Anim Sci.* 1975, *41*, 1281.
[37] Coderch L, L. O., de la Maza A, Parra JL. *Am J Clin Dermatol.* 2003, *4*, 107.
[38] Barbero AM, F. H. *Toxicol In Vitro* 2009, *23*, 1.
[39] Akomeah, F. K.; Martin, G. P.; Brown, M. B. *Journal of Pharmaceutical Sciences* 2007, *96*, 824.
[40] PD, F. *Adv Biol Skin* 1969, *9*, 419.
[41] Gandhi, R. E. a. R. *Ind. J. Pharm. Sci.* 1988. , *50*, 142.
[42] Smart, J. D. *Advanced Drug Delivery Reviews* 1993, *11*, 253.
[43] Mitra A. K, A. H. H., Johnston *Encyclopedia of Pharmaceutical technology, Marcel Dekker Inc.* 2002, 2081.
[44] C.A. Squier, N. W. J., R.M. Hopps, *Blackwell Scientific Publications, Oxford,* 1976, 7.
[45] Galey, W. R., Lonsdale, H.K., and Nacht, S. *J. Invest. Dermat.* 1976, *67*, 713.
[46] Garza, J. e. a. *J. Dent. Res.* 1998, *77*, 293.
[47] C. A. Squier, P. C., and P. W. Wertz *J Invest Dermatol* 1991, *96*, 123.
[48] Wertz, P. W. a. S., C.A. *Marcel Dekker, Inc., New York, NY, USA* 1996, *(Rathbone, M.J., ed.)*, 1.
[49] Prausnitz, M. R.; Langer, R. *Nat Biotech* 2008, *26*, 1261.
[50] Brown, M. B., et al. *Drug Deliv, 2006. 13(3): p. 175-87.* 2006, *13*, 175.
[51] Barry, B. W. *Drug Discovery Today* 2001, *6*, 967.
[52] Brown, M. B.; Martin, G. P.; Jones, S. A.; Akomeah, F. K. *Drug Deliv* 2006, *13*, 175.
[53] Cross, S. E.; Roberts, M. S. *Curr Drug Deliv* 2004, *1*, 81.
[54] Kanikkannan, N. *BioDrugs* 2002, *16*, 339.
[55] Pillai, O.; Borkute, S. D.; Sivaprasad, N.; Panchagnula, R. *Int J Pharm* 2003, *254*, 271.
[56] Raiman, J.; Koljonen, M.; Huikko, K.; Kostiainen, R.; Hirvonen, J. *Eur J Pharm Sci* 2004, *21*, 371.
[57] L.M.C. Collins, C. D. *J. Dent. Res.* 1987, *66*, 1300.
[58] J.W. Lee, J. H. P., J.R. Robinson *J. Pharm. Sci.* 2000, *89*, 850.
[59] M.E. de Vries, H. E. B., J.C. Verhoef, H.E. Junginger *Crit. Rev. Ther. Drug Carr. Syst.* 1991, *8*, 271.
[60] Veuillez, F.; Kalia, Y. N.; Jacques, Y.; Deshusses, J.; Buri, P. *European Journal of Pharmaceutics and Biopharmaceutics* 2001, *51*, 93.
[61] Peppas, N. A. a. B., P.A. *J. Control. Rel.* 1985, *2*, 257.
[62] Ch'ng, H. S., Park, H., Kelly, P., and Robinson, J.R. *J. Pharm. Sci.* 1985, *74*, 399.

[63] Sanzgiri, Y. D., Topp, E.M., Benedetti, L., and Stella, V.J. *Int. J. Pharm.* 1994, *107*, 91.
[64] Lehr, C. M., Bouwstra, J.A., Schact, E.H., and Junginger, H.E. *Int. J. Pharm.* 1992, *78*, 43.
[65] Anders, R. a. M., H. *Int. J. Pharm.* 1989, *49*, 231.
[66] Veillard, M. M., Longer, M.A., Martens, T.W., and Robinson, J.R. *J. Control. Rel.* 1987, *6*, 123.
[67] Giannola, L. I.; De Caro, V.; Giandalia, G.; Siragusa, M. G.; Tripodo, C.; Florena, A. M.; Campisi, G. *European Journal of Pharmaceutics and Biopharmaceutics* 2007, *67*, 425.
[68] Jacobsen, J. *Journal of Controlled Release* 2001, *70*, 83.
[69] Banga, A. K. a. C., Y.W. *Journal of controlled Release* 1988, *7*, 1.
[70] Chien, Y. W.; Banga, A. K. *J Pharm Sci* 1989, *78*, 353.
[71] Rai, R.; Srinivas, C. R. *Indian J Dermatol Venereol Leprol* 2005, *71*, 236.
[72] Chesnoy, S.; Durand, D.; Doucet, J.; Couarraze, G. *J Control Release* 1999, *58*, 163.
[73] van der Geest, R.; Danhof, M.; Bodde, H. E. *Pharm Res* 1997, *14*, 1798.
[74] van der Geest, R.; van Laar, T.; Gubbens-Stibbe, J. M.; Bodde, H. E.; Danhof, M. *Pharm Res* 1997, *14*, 1804.
[75] Meidan, V. M.; Al-Khalili, M.; Michniak, B. B. *Int J Pharm* 2003, *264*, 73.
[76] Zakzewski, C. A.; Wasilewski, J.; Cawley, P.; Ford, W. *J Control Release* 1998, *50*, 267.
[77] Burnette, R. R.; Marrero, D. *J Pharm Sci* 1986, *75*, 738.
[78] Tiwari, S. B.; Udupa, N. *Int J Pharm* 2003, *260*, 93.
[79] Burton, H. S., Jr. *Percutaneous Penetration Enhancers. CRC Press, Boca Raton, Florida* 1995, 351.
[80] Ledger, P. *Advanced drug delivery reviews* 1992, *9*, 289.
[81] Kalia, Y. N.; Naik, A.; Garrison, J.; Guy, R. H. *Adv Drug Deliv Rev* 2004, *56*, 619.
[82] Guy, R. H.; Delgado-Charro, M. B.; Kalia, Y. N. *Skin Pharmacol Appl Skin Physiol* 2001, *14 Suppl 1*, 35.
[83] Guy, R. H.; Kalia, Y. N.; Delgado-Charro, M. B.; Merino, V.; Lopez, A.; Marro, D. *J Control Release* 2000, *64*, 129.
[84] Merino, V.; Lopez, A.; Kalia, Y. N.; Guy, R. H. *Pharm Res* 1999, *16*, 758.
[85] Panchagnula, R.; Pillai, O.; Nair, V. B.; Ramarao, P. *Curr Opin Chem Biol* 2000, *4*, 468.
[86] Turner, N. G.; Guy, R. H. *J Investig Dermatol Symp Proc* 1998, *3*, 136.
[87] Regnier, V.; Preat, V. *Pharm Res* 1998, *15*, 1596.
[88] Singh, P.; Maibach, H. I. *Crit Rev Ther Drug Carrier Syst* 1994, *11*, 161.
[89] Siddiqui, O.; Roberts, M. S.; Polack, A. E. *J Pharm Pharmacol* 1985, *37*, 732.
[90] Wearley, L. L. a. C., Y.W. *International Journal of Pharmaceutics* 1990, *59*, 87.
[91] Singh, P.; Boniello, S.; Liu, P.; Dinh, S. *Int J Pharm* 1999, *178*, 121.
[92] Kasting, G. B.; Keister, J. C. *Journal of Controlled Release* 1989, *8*, 195.
[93] Cazares-Delgadillo, J.; Naik, A.; Ganem-Rondero, A.; Quintanar-Guerrero, D.; Kalia, Y. N. *Pharm Res* 2007, *24*, 1360.
[94] Pacini, S.; Punzi, T.; Gulisano, M.; Cecchi, F.; Vannucchi, S.; Ruggiero, M. *Pharm Res* 2006, *23*, 114.
[95] Yoshida, N. H. a. R., M.S. *Journal of controlled Release* 1993, *25*, 177.
[96] Roberts, M. S.; Lai, P. M.; Anissimov, Y. G. *Pharm Res* 1998, *15*, 1569.
[97] Lai, P. M.; Roberts, M. S. *J Control Release* 1999, *58*, 323.
[98] Williams, A. C.; Barry, B. W. *Advanced Drug Delivery Reviews* 2004, *56*, 603.
[99] A.C. Watkinson, D. M. G., K.R. Brain, V.J. James, K.A. Waters, S. Azri-Meehan, R. Sharma, W. Dressler *STS Publishing, Cardiff* 1998, *5b*, 54.

[100] M. Goodman, B. W. B. *Int. J. Pharm.* 1989, *57*, 29.
[101] P.P. Sarpotdar, J. L. Z. *Drug Dev. Ind. Pharm.* 1986, *12*, 1625.
[102] BW, B. *J Control Release* 1987, *6*, 85.
[103] Shin SC, L. H. *Int. J. Pharm.* 2002, *54*, 201.
[104] Aungst BJ, R. N., Shefter E. *Int J Pharm.* 1986, *33*, 244.
[105] BJ., A. *Pharm. Res.* 1989, *6*, 244.
[106] William AC, B. B. *Int. J. Pharm.* 1989, *57*, R7.
[107] Cornwell PA, B. B. *J. Pharm. Pharmacol.* 1994, *46*.
[108] Bu¨yu¨ktimkin, N., Bu¨yu¨ktimkin, S., Rytting, J.H. *CRC Press, Boca Raton, FL* 1995, 91.
[109] P.P. Sarpotdar, J. L. Z. *J. Pharm. Sci.* 1986, *75*, 176.
[110] Aungst, B. J.; Rogers, N. J. *International Journal of Pharmaceutics* 1989, *53*, 227.
[111] Senel, S., Hoogstraate, A.J., Spies, F., Verhoef, J.C., Bos-van Geest, A., Junginger, H.E., and Bodde, H.E. *J. Control. Rel.* 1994, *32*, 45.
[112] Aungst, B. J. a. R., N.J. *Int. J. Pharm.* 1989, *53*, 227.
[113] Siegel, I. A. a. G., H.P. *Arch. Oral Biol.* 1985, *30*, 43.
[114] Shojaei, A. H. a. L., X. *Proceedings of International Symposium on Controlled Release of Bioactive Materials* 1996, *23*, 507.
[115] Manganaro, A. M. a. W., P.W. *Mil. Med.* 1996, *161*, 669.
[116] Gandhi, R. a. R., J. *Int. J. Pharm.* 1992, *85*, 129.
[117] Nakane, S., Kakumoto, M., Yulimatsu, K., and Chien, Y.W. *Pharm. Dev. Tech.* 1996, *1*, 251.
[118] Hoogstraate, A. J., Verhoef, J.C., Tuk, B., Pijpers, A., van leengoed, L.A.M.G., Vheijden, J.H.M., Junjinger, H.E., and Bodde, H.E. *J. Control. Rel.* 1996, *41*, 77.
[119] S. Sharma, J. K., A. P. Pawar *Pharmazie* 2006, *61*, 495.
[120] Büyüktimkin, S.; Büyüktimkin, N.; Rytting, J. H. *Pharmaceutical Research* 1993, *10*, 1632.
[121] Bu¨yu¨ktimkin, S., Bu¨yu¨ktimkin, N., Rytting, J.H. *Int. J. Pharm.* 1996, *127*, 245.
[122] Wolka, A. M.; Rytting, J. H.; Reed, B. L.; Finnin, B. C. *International Journal of Pharmaceutics* 2004, *271*, 5.
[123] Bu¨yu¨ktimkin, S., Bu¨yu¨ktimkin, N., Rytting, J.H. *Pharm. Res.* 1993, *10*, 1632.
[124] Ghannoum, M. A.; Long, L.; Pfister, W. R. *Mycoses* 2009, *52*, 35.
[125] Fujii M, B. S., Büyüktimkin N, Rytting JH. *Int J Pharm.* 2002, *2*, 121.
[126] N. Kim, M. E.-K., M. M. Henary, L. Strekowski *Int. J. Pharm.* 1999, *187*, 219.
[127] Amnon C. Sintov, P. J. Z., Bozena B. Michniak-Kohn *Journal of Controlled Release* 2009, *133*, 44.
[128] Longsheng Hu, P. B., Victor Meidan, Bozena B. Michniak-Kohn *Handbook of Non-Invasive Drug Delivery Systems* 2010, 95.
[129] Choi, E. H., Lee, S.H., Ahn, S.K., Hwang *Skin Pharmacol. Appl. Skin Phys.* 1999, *12*, 326.
[130] Wang, Y., Michniak, B. *Pharm. Res.* 2003, *20*, 1612.
[131] http://www.rxlist.com/xylocaine-drug.htm.
[132] http://www.mayoclinic.com/health/drug-information/dr601515.
[133] http://www.drugs.com/pro/lidocaine.html.
[134] http://www.lidoderm.com/.
[135] www.vyteris.com/Our_Products/Lidosite.php.

[136] Sintov, A. C.; Brandys-Sitton, R. *International Journal of Pharmaceutics* 2006, *316*, 58.
[137] Lee, P. J.; Ahmad, N.; Langer, R.; Mitragotri, S.; Prasad Shastri, V. *International Journal of Pharmaceutics* 2006, *308*, 33.
[138] http://www.rcplondon.ac.uk/pubs/books/nicotine/1-overview.htm.
[139] Ziedalski, T. M.; Ruoss, S. J. *Thoracic Surgery Clinics* 2005, *15*, 189.
[140] http://www.sigmaaldrich.com *Sigma Aldrich*.
[141] C. Dollery, E. *Churchill Livingstone, Edinburgh, UK* 1999, *(2nd Edition ed.)*.
[142] http://www.stopsmoking.net/nicorette.html.
[143] http://www.medicinenet.com/nicotine_gum/article.htm.
[144] http://www.nicorette.co.uk/stop-smoking/products/patch.aspx.
[145] Cheng, Y.-H.; Watts, P.; Hinchcliffe, M.; Hotchkiss, R.; Nankervis, R.; Faraj, N. F.; Smith, A.; Davis, S. S.; Illum, L. *Journal of Controlled Release* 2002, *79*, 243.
[146] Nolan, L. M. A.; Corish, J.; Corrigan, O. I.; Fitzpatrick, D. *International Journal of Pharmaceutics* 2007, *341*, 114.
[147] http://www.rxlist.com/tiazac-drug.htm.
[148] Lee, P. J.; Langer, R.; Shastri, V. P. *Pharmaceutical Research* 2003, *20*, 264.
[149] Limpongsa, E.; Umprayn, K. *AAPS PharmSciTech* 2008, *9*, 464.
[150] http://www.webmd.com/drugs.
[151] Hye Sun Gwak, I. S. O., In Koo Chun *Drug Development and Industrial Pharmacy* 2004, *30*, 187
[152] Ding, P. L., Wei; Zheng, Junmin *Journal of Chinese Pharmaceutical Sciences* 1999, *8*, 73.
[153] PermeGear *http://www.permegear.com/franz.htm*.
[154] www.uspnf.com/uspnf/pub/data/v29242/usp29242.
[155] Kaustubh R. Tambwekar, R. B. K., et al. *Journal of Pharmaceutical and Biomedical Analysis* 2003, *32*, 441.
[156] Najma Sultana, M. S. A., Nighat Shafi *Pakistan Journal of Pharmaceutical Sciences* 2001, *14*, 1.
[157] Zheng, H. P., Wei; Wang, Yan, et al. *Zhongguo Yiyao Gongye Zazhi Bianjibu* 2002, *33*, 603.
[158] Golden, G. M.; Guzek, D. B.; Kennedy, A. E.; McKie, J. E.; Potts, R. O. *Biochemistry* 1987, *26*, 2382.
[159] Valenta, C.; Nowak, M.; Hadgraft, J. *International Journal of Pharmaceutics* 2001, *217*, 79.
[160] Knutson, K.; Potts, R. O.; Guzek, D. B.; Golden, G. M.; McKie, J. E.; Lambert, W. J.; Higuchi, W. I. *Journal of Controlled Release* 1985, *2*, 67.
[161] Bouwstra, J.; Gooris, G.; Cheng, K.; Weerheim, A.; Bras, W.; Ponec, M. *J. Lipid Res.* 1996, *37*, 999.
[162] Promega Corp., M., WI, USA *Technical Bulletin* 2009.
[163] K.S. Bhatia, S. G., T.P. Freeman, J. Singh, *J. pharm. sci.* 1997, *86*, 1011.
[164] S. Singh, M. B., S.B. A. Jayaswal, Jj. Singh *int. J. Pharm.* 1998, *166*, 157.
[165] Srinivasan, V.; Higuchi, W. I.; Su, M.-H. *Journal of Controlled Release* 1989, *10*, 157.
[166] Sims, S. M.; Higuchi, W. I.; Srinivasan, V. *Pharmaceutical Research* 1992, *9*, 1402.
[167] Banga, A. K.; Bose, S.; Ghosh, T. K. *International Journal of Pharmaceutics* 1999, *179*, 1.

[168] Burnette RR, O. B. *J Pharm Sci.* 1987, *10*, 765.
[169] C.S. Leopold, B. C. L. *Journal of Pharmacy and Pharmacology* 1995, *47*, 276.
[170] W. Pfister, M. L., D. Frank *http://www.aapsj.org/abstracts/AM_2006/AAPS2006-003184.pdf* 2006.
[171] MatTek, C. *MTT EFFECTIVE TIME-50 (ET-50) PROTOCOL MK-24-007-0003* 2009.
[172] Y. Rojanasakul, L.-Y. W., M. Bhat, D.D. Glover, C.J. Malanga, J.K.H. Ma, *Pharm. Res.* 1992, *9*, 1029.
[173] S, A. G. a. D. *http://www.pharmainfo.net* 2009, *7*.
[174] Lee JW, P. J., Robinson JR. *J Pharm Sci.* 2000, *89*, 850.
[175] Aggarwal, G. *www.PhamInfor.net* 2009, *7*.
[176] Simon, L., Weltner, A.W., Wang, Y. and Michniak, B. *Journal of Membrane Science* 2006, *278*, 124.

Curriculum Vita

Longsheng Hu

Education

B.S., Chemistry, Electronic University of Science and Technology, Chengdu, China,1981-1985

M.S., Chemical Engr., Sichuan University, Chengdu, China, 1985-1988

M.S., Chemical Engr., University of Cincinnati, OH, USA, 1992-1996

M.S., Pharmaceutical Sci., University of Cincinnati, OH, USA, 1994-1996

Ph. D, Pharmaceutical Sci., Rutgers, The State University of New Jersey, NJ, USA, Oct., 2010

Principle Occupations

Scientist, Skin and Hair Care R&D, Avlon Industries, Inc., Chicago, IL , USA, 1996-2002

Scientist, Skin and Hair R&D, Pfizer, Inc., Morris Plains, NJ, USA, 2002-2006

Staff Scientist, Topical HealthCare R&D, Johnson & Johnson, Morris Plains, NJ, USA, 2006-Present

Publications

L. Hu, Wally Habib, Ali N. Syed, Hair brightening system, USA Patent 6007585, 1998

P. Batheja, D. Kaushik, **L. Hu** and B.B Michniak-Kohn, Transdermal iontophoresis, Transdermal Delivery, Drug Delivery, Pages 46-48, 2007

L. Hu, P. Batheja, V. Meidan, B. B. Michniak-Kohn, Chapter 4, Iontophoretic Transdermal Drug Delivery, Handdbook of Non-Invasive Drug Delivery Systems, Elsevier, Page 95-114, 2010